The Marsupial Sperm Tail Cytoskeleton: A Morphological and Biochemical Study

MARIO RICCI
BHSc (Hons)

Thesis submitted for the degree of
Doctor of Philosophy
The University of Adelaide

August 2004

Department of Anatomical Sciences
Faculty of Health Sciences
THE UNIVERSITY OF ADELAIDE

THE UNIVERSITY OF ADELAIDE
AUSTRALIA
SUB CRUCE LUMEN

DECLARATION

This work contains no material which has been accepted for the award of any other degree or diploma in any university or other tertiary institution and, to the best of my knowledge and belief, contains no material previously published or written by another person, except where due reference has been made in the text.

I give consent to this copy of my thesis, when deposited in the University library, being available for loan and photocopying.

Mario Ricci

August 2004

ACKNOWLEDGMENTS

I wish to extend my deepest thanks to my supervisor Associate Professor William Breed for his encouragement, guidance, assistance and intellectual input throughout this doctoral degree. Your support and advice was, and continues to be, very much appreciated.

For their excellent technical assistance and patience, I thank Mr Chris Leigh, Mrs Gail Hermanis, Mrs Nadia Gagliardi and staff of Adelaide Microscopy, in particular Ms Lyn Waterhouse. For proof reading this manuscript I again thank Mrs Hermanis.

To all my colleagues in the Department of Anatomical Sciences Reproductive Biology Group, but especially Dr Eleanor Peirce and Dr Jamie Chapman. I feel privileged to have been able to work, and to continue to work, with such intelligent, enthusiastic and supportive people, and count you as very good friends.

On a final note, I wish to sincerely thank my family for their love and unwavering confidence in my abilities.

PUBLICATIONS ARISING FROM THIS THESIS

Refereed Scientific Journals:

Ricci M and Breed WG (2001) Isolation and partial characterization of the outer dense fibres and fibrous sheath from the sperm tail of a marsupial: the brush-tail possum (*Trichosurus vulpecula*). *Reproduction* 121: 373-388

Refereed Conference Presentations:

Ricci M and Breed WG (2001) Immunocytochemical investigation of fibrous sheath morphogenesis in a marsupial: the brush-tail possum. Society for the Study of Fertility Annual Conference, p 34, University of Cambridge, England, July 2001.

Ricci M and Breed WG (2000) Isolation and partial characterisation of the outer dense fibres and fibrous sheath from the sperm tail of a marsupial. *Journal of Reproduction and Fertility Abstract Series 25*, Fertility 2000 Meeting, pp 86, Edinburgh, Scotland

Ricci M and Breed WG (1999) Isolation of the outer dense fibres and fibrous sheath from brush-tail possum spermatozoa. *Proceedings of the Thirtieth Annual Australian Society of Reproductive Biology Conference*, pp 109, Melbourne, Victoria, Australia

Copies of these publications can be found at end of thesis.

TABLE OF CONTENTS

LIST OF TABLES

LIST OF FIGURES

ABSTRACT

The motile apparatus of the sperm tail contains, like that of flagella and cilia, an axoneme composed of microtubules. However, unlike cilia and flagella, it also contains additional, unique, cytoskeletal structures which are thought to play important roles in sperm motility and stability. In eutherian mammals, these cytoskeletal structures, the outer dense fibres and fibrous sheath, are composed of multiple, highly insoluble, proteins. Marsupials diverged from eutherians over 100 million years ago and their sperm tails appear to have morphologically similar cytoskeletal structures, however almost nothing is known of their chemical composition or morphogenesis. For my PhD, I have investigated the formation, and protein composition, of the outer dense fibres and fibrous sheath of a model marsupial species, the brush-tail possum (*Trichosurus vulpecula*). Twelve spermatid steps of spermiogenesis were identified in the possum by transmission electron microscopy. Outer dense fibre and fibrous sheath morphogenesis were found to be lengthy, multi-step, processes extending over a large part of spermiogenesis. The major proteins in the outer dense fibres and fibrous sheath were determined by first developing procedures for isolating and solubilizing the proteins, whose molecular weights were then determined by SDS-PAGE. The outer dense fibres were found to have seven major proteins of kDa 73, 58, 55, 54, 52, 41 and 16, whereas the fibrous sheath had twelve major proteins of kDa 106, 76, 66, 62, 55, 53, 52, 46, 40, 30, 28 and 16. A polyclonal antibody was prepared against a major protein fraction of the fibrous sheath and, with this antibody, the morphogenesis of the fibrous sheath was found to be restricted to steps 7-12 of spermiogenesis. This antiserum did not react with the proteins extracted from the outer dense fibres thus indicating little homology between proteins of these two structures.

Nevertheless, this antibody showed strong cross-reactivity with the 76 and 62 kDa proteins of the fibrous sheath of several other species of marsupials from three other families, as well as with those from the laboratory rat, therefore indicating conservation of at least these two proteins across marsupial and eutherian subclasses. Furthermore, antisera obtained from an overseas laboratory prepared against the eutherian (laboratory mouse) GAPDS (47.5 kDa) fibrous sheath protein was found to label the possum fibrous sheath by immunofluorescence and immunogold electron microscopy, further indicating conservation of fibrous sheath proteins across both infraclasses of mammals. In addition, an antibody to a laboratory rat outer dense fibre protein, ODF2 (84 kDa), was found to cross-react with the possum outer dense fibre proteins of molecular weights 55 and 28 kDa, suggesting that proteins of this cytoskeletal structure may be similarly conserved, albeit of different molecular weights. The results of this study, thus indicate that, despite over 100 million years of divergence between marsupials and eutherians, there is conservation of several major proteins across these two extant infraclassess of mammals even though differences in their molecular weights occur. These findings indicate that, prior to divergence into the two major lineages of extant mammals, an increased complexity of the cytoskeleton of the sperm tail evolved that included incorporation of several additional proteins over and above those that make up the axoneme.

Chapter 1

LITERATURE REVIEW AND RESEARCH PROPOSAL

1.1 INTRODUCTION

The mammalian sperm tail contains unique cytoskeletal structures, not present in unicellular flagella and cilia, that are thought to play important, but as yet undefined, roles in sperm integrity, durability and/or motility. These structures, the outer dense fibres, which surround the axoneme, and the fibrous sheath, which surrounds the outer dense fibres, are composed of multiple proteins and are highly insoluble. Most of what is known of these cytoskeletal structures in mammalian sperm has been obtained from studies of these elements in eutherian species, particularly the laboratory rat. Very little is known of the outer dense fibres and fibrous sheath in marsupials. Therefore, for my PhD studies, I have attempted to morphologically, immunocytochemically, and biochemically characterize the outer dense fibres and fibrous sheath of spermatozoa from a model Australian marsupial species, the brush-tail possum, *Trichosurus vulpecula*.

1.2 THE MAMMALIAN SPERMATOZOON

The spermatozoon is a highly polarised, haploid cell, whose primary function is to contribute the male's genes to the embryo, thereby activating the oocyte to resume meiosis and development (Bedford and Hoskins, 1990). The mammalian spermatozoon has two main functional components, the head and the tail, or flagellum, which are joined at the neck. The head consists of an acrosome, nucleus and small amounts of cytoskeletal

material. The acrosome, which overlies the anterior part of the nucleus, is a membranous structure that contains hydrolytic enzymes. The sperm nucleus contains only one member of each chromosome pair and the chromatin is highly condensed (Eddy & O'Brien, 1994). The flagellum contains a central axoneme surrounded by at least two major cytoskeletal components, the longitudinally orientated outer dense fibres and the fibrous sheath. In addition, the anterior part of the flagellum contains mitochondria wrapped in a tight helix around the outer dense fibres. The flagellum, like the sperm head, is surrounded by a plasma membrane and contains little cytoplasm (Eddy & O'Brien, 1994). Although all mammalian sperm have these general characteristics, there are species-specific differences in the size and shape of the sperm head, and the length and relative size of the components of the flagellum.

The spermatozoon is the end product of the process of spermatogenesis in the male that occurs in the seminiferous tubules of the testis. Spermatogenesis involves mitotic divisions of spermatogonial stem cells, two meiotic divisions by spermatocytes, extensive morphological remodelling of spermatids during spermiogenesis, and the release of germ cells into the lumen of the seminiferous tubules by spermiation (Eddy & O'Brien, 1994). During spermiogenesis, as the spermatids differentiate, the acrosome forms, the nucleus condenses and changes shape, and the cells elongate and shed much of their cytoplasm (Eddy and O'Brien, 1994). The changing size and shape of these sperm components, particularly the acrosome, has enabled the developing spermatids to be precisely classified into "steps" based on their morphology (Russell *et al.,* 1990). Moreover, in transverse sections of the seminiferous tubules of the testis, spermatids, spermatogonia and spermatocytes, at specific phases of development, are always grouped together, and these groupings are termed "cell associations" or "stages" (Russell *et al.,* 1990). A

complete and ordered series of these stages, occurring in a given segment of the seminiferous tubule over time is known as a "cycle" or "cycle of seminiferous epithelium" (Russell *et al.*, 1990). In the laboratory rat, for which most information on staging has been published (e.g. Roosen-Runge and Giesel, 1950; Clermont and Percy, 1957; Leblond and Clermont, 1952a, b; Clermont and Rambourg, 1978; Russell *et al.*, 1990), 19 steps of spermatid development and 14 stages (I – XIV) (Leblond and Clermont, 1952a, b; Russell *et al.*, 1990) have been described.

1.3 THE SPERM HEAD

The mammalian sperm head contains the acrosome and nucleus, the latter of which is surrounded by moderate amounts of cytoskeletal material. The nucleus of the mature spermatozoon is characterized by highly condensed chromatin, and has a species-specific shape; sperm from most mammalian species have a spatulate shape, but those of rodents are usually falciform. The acrosome, whose contents originate from the Golgi Apparatus, is a membrane-bound vesicle that forms a cap over the anterior part of the nucleus and contains numerous hydrolytic enzymes that are released during the acrosome reaction to assist in the passage of sperm through the egg coats prior to fertilization (for reviews, see Bedford and Hoskins, 1990; Eddy and O'Brien, 1994; Curry and Watson, 1995).

1.3.1 Cytoskeletal Components of the Sperm Head

The major cytoskeletal element of the mammalian sperm head is the perinuclear theca, which covers the sperm nucleus and which is especially prominent in falciform spermatozoa (Courtens *et al.*, 1976). The perinuclear theca is a rigid capsule that can be subdivided into a subacrosomal layer, termed perforatorium in rodent sperm, that occupies the space between the acrosome and nucleus, and a postacrosomal layer that begins

More recently, it has been proposed that the perinuclear theca interacts with, and possibly activates, the oocyte at the time of fertilization (Sutovsky *et al.*, 2003)

where the acrosome ends and directly underlies the plasmalemma (Courtens *et al.*, 1976). The protein composition of the perinuclear theca has been analysed by sodium dodecyl sulfate-polyacrylamide gel electrophoresis (SDS-PAGE) and, although variable between species, is composed of numerous proteins of which a 15 kDa protein predominates in the laboratory rat (Oko and Clermont, 1988) and Australian plains rat (Breed *et al.*, 2000). Moreover, it has been shown that the protein composition of each of the two regions of the perinuclear theca is different, and that the 15 kDa laboratory rat protein is a major component of the perforatorium (Oko and Clermont, 1988; Oko, 1995). The full length nucleotide sequence of this 15 kDa protein, PERF 15, has been determined, and shown to bear resemblance to the sequence of a family of lipid-binding proteins, in particular myelin P2 (Oko and Morales, 1994), which is located between opposing membranes in the myelin sheath of Schwann cells in the peripheral nervous system and may have an important membrane-binding role (Kadlubowski *et al.*, 1980; Trapp *et al.*, 1983, 1984). The fact that PERF 15 and myelin P2 share sequence homology and intracellular location (between membranes) suggests that PERF 15 could also have a membrane-binding role in laboratory rat sperm by attaching the acrosome to the nucleus during sperm formation as well as contributing to the stability of the nuclear envelope during fertilization (Oko and Morales, 1994; Oko, 1995). A 15 kDa protein has also been identified from the subacrosomal space of bull spermatozoa (Oko and Maravei, 1994), however it bears no resemblance to the 15 kDa rat protein (Breed *et al.*, 2000), with sequence analysis demonstrating that the bull protein is a histone H2B variant that may assist in acrosome assembly and acrosome-nuclear binding (Aul and Oko, 2002).

1.4 THE SPERM FLAGELLUM

The flagellum of the mammalian spermatozoon consists of four distinct segments; the connecting piece (neck), the middle (mid) piece, the principal piece, and the end-piece. The main structural components within the flagellum are the axoneme, the mitochondrial sheath, the outer dense fibres, and the fibrous sheath. The kinetic apparatus of the flagellum is the axoneme which is composed of a '9 + 2' complex of microtubules that extends the full length of the flagellum. The outer dense fibres lie adjacent to the axoneme and extend longitudinally from the connecting piece to the posterior end of the principal piece, although the lengths of individual outer dense fibres vary. In addition, the mid-piece of the flagellum contains mitochondria which lie between the plasma membrane and outer dense fibres, whereas in the principal piece a fibrous sheath lies between the plasma membrane and the outer dense fibres.

The cytoskeletal components of the mammalian sperm flagellum include the axoneme, outer dense fibres and fibrous sheath.

1.4.1 Axoneme

The axoneme or, axial filament, runs the full length of the sperm flagellum and is composed of two central microtubules surrounded by nine evenly spaced outer microtubule doublets, thereby forming a '9 + 2' pattern (Fawcett, 1975). This structure is typical of most cilia and flagella and, with few exceptions, has been preserved over a long period of evolution from protozoa to mammals (Phillips, 1969; Baccetti and Afzelius, 1976). The nine outer doublets are numbered 1-9 in a clockwise direction with doublet number 1 being the only doublet situated in a plane perpendicular to that of the two central microtubules. Each of the outer doublets consists of a complete 'A' microtubule to which is

attached a C-shaped 'B' microtubule. The main structural component of these microtubules is tubulin, which is arranged in rows that form protofilaments aligned side-by-side to form microtubule walls (Farrell, 1982). The central and A microtubules are composed of 13 protofilaments whilst the incomplete B microtubule is made up of 10 protofilaments. Extending from the A microtubule towards the next doublet's B subfibre are two rows of dynein arms (outer and inner) (Satir, 1974, 1979; Gibbons, 1981; Gagnon, 1995). In addition, neighbouring outer doublets are linked to each other by nexin links, as well as to the central microtubules by radial spokes (Gagnon, 1995).

Flagellar movement is made possible by the active sliding of the nine outer microtubule doublets of the axoneme, and it is the dynein arms which are responsible for the sliding forces generated between adjacent doublets during flagella bending (Gagnon, 1995). This was confirmed by studies which demonstrated that sperm become immotile if the dynein arms are removed (Gibbons and Gibbons, 1973; Gibbons, 1981, 1989; Yano and Miki-Noumura, 1981), or if they are deleted by genetic mutation (Huang *et al.,* 1979). Dynein arms have ATPase activity, that is they bind and hydrolyse ATP, and the resultant conformational change of the dynein arms induces the sliding of outer doublets relative to each other. In effect the dynein arms "walk" along their neighbouring B tubule (Gagnon, 1995). Although the exact mechanisms by which the axoneme regulates its function remain unknown, factors such as calcium, phosphorylation and proteolysis are believed to regulate sperm motility (Gagnon, 1995).

1.4.2 Outer Dense Fibres

1.4.2.1 Location and Appearance of the Outer Dense Fibres

The flagella of most spermatozoa from species which practice external fertilization, for example the marine invertebrates, possess a simple '9 + 2' axoneme complex whereby nine pairs, or doublets, of microtubules surround two central tubules. In contrast, where internal fertilization has evolved in association with terrestrial life, the axoneme is surrounded by an accessory set of nine fibres so that the sperm tail has a '9 + 9 + 2' pattern (Baccetti *et al.*, 1973). These supplementary fibres can be short and thin, or thick and almost as long as the entire flagellum as is the case in Insecta and terrestrial vertebrates including reptiles and humans (Baccetti, 1982). In insects these structures are crystalloid or tubular, but in cephalopods and vertebrates they are filamentous (Baccetti, 1982; Afzelius, 1988). These filaments, frequently termed 'coarse fibres', differ in size and shape in the vertebrates, invertebrates and insects in which they are found, however they are most prominent in mammals. In mammalian sperm these accessory structures are termed outer dense fibres and they are often supplemented by additional cytoskeletal structures including the rigid fibrous sheath and the mitochondrial helix (Olson *et al.*, 1976). In insects other periaxonemal cytoskeletal structures are present including accessory bodies (Baccetti, 1972) and special mitochondria which contain crystals of a protein called crystallomitin (Baccetti *et al.*, 1977). The possible functional significance of the outer dense fibres and other accessory sperm tail cytoskeletal structures will be discussed later in this chapter.

The nine outer dense fibres are not only each paired to an outer microtubule doublet of the axoneme, but they are also attached to the striated columns of the connecting piece at the anterior end of the sperm flagellum (Fawcett, 1975). This connection is thought to provide

an anterior anchor for the outer dense fibres and therefore also the axoneme, by virtue of their linkage, which is necessary as the axoneme microtubules do not themselves terminate in a basal body, as is the case in cilia (Lindemann, 1996). Individual outer dense fibres are numbered 1-9 in a clockwise direction corresponding to the number assigned to the adjacent microtubule doublets to which the fibres are paired. Unlike the outer microtubule doublets, which are all identical in appearance, each outer dense fibre has a distinctive size and cross-sectional shape, although most have a teardrop profile with the rounded edge outermost and tapering towards the axoneme (Curry and Watson, 1995). Those outer dense fibres designated 1, 5 and 6, which are positioned in the plane of flagellar bending, are generally larger than the others (Fawcett, 1975).

The outer dense fibres are not all of equal length but instead extend posteriorly for varying distances into the principal piece of the sperm tail (Fawcett, 1975). In some species, such as the laboratory rat and hamster, the outer dense fibres are very thick and can extend most of the length of the principal piece, however in other species, such as the human and bull, the fibres are relatively slender and terminate about halfway down the principal piece (Fawcett, 1975; Serres *et al.,* 1983). In human sperm the outer dense fibres were initially thought to extend along the entire length of the flagellum (Burgos *et al.,* 1970) however subsequent studies showed that they gradually taper off once they pass from the middle piece to the principal piece so that they are only present in 60% of the principal piece (Holstein and Rososen-Runge, 1981; Serres *et al.,* 1983; Haidl and Becker, 1991). In comparison, in bull sperm the outer dense fibres occupy 66% of sections through the principal piece of the flagellum (Lindemann *et al.,* 1980). A detailed ultrastructural study, carried out to determine the lengths of each of the outer dense fibres in human sperm, showed that the fibres in this species can be assigned to three different groups with

respect to their length: short fibres (numbers 3 and 8; 6μm long), medium fibres (numbers 4, 2 and 7; 17-21 μm), and long fibres (numbers 9, 5, 6 and 1; 31-35μm) (Serres *et al.*, 1983). Outer dense fibres 3 and 8 are usually the first to terminate in sperm of most mammalian species, not just human, as their place is usually occupied in the principal piece by the inward extensions of the longitudinal columns of the fibrous sheath (Fawcett, 1975). In addition to their lengths, the order of termination of the outer dense fibres has also been determined for human sperm and it is relatively constant in this species: first fibres 3 and 8, then 4, 2 and 7, followed by 5 and 6, and finally 9 and 1, although fibres 5 and 6 can terminate either before or after fibre number 9 (Pedersen, 1974; Serres *et al.*, 1983). In comparison, in laboratory rat sperm, whilst the shortest outer dense fibres, also numbers 3 and 8, similarly extend almost the entire length of the middle piece (55 ± 11μm), the other fibres are all approximately the same length in the principal piece (108 ± 21μm) and occupy approximately 60% of the overall length of the sperm tail (Vera *et al.*, 1984).

By conventional transmission electron microscopy, the outer dense fibres usually appear homogenous, however ultrastructural studies employing selective staining techniques have shown that the fibres are in fact composed of two layers – a narrow, electron dense cortex, and a central medulla (Telkka *et al.*, 1961; Bawa, 1963; Gordon and Bensch, 1968; Fawcett, 1970; Olson and Sammons, 1980). The cortex is continuous on most of the fibre surface but is absent from the side facing the corresponding microtubule doublet of the axoneme (Fawcett, 1975). Subsequent surface replica studies in several mammalian species, including laboratory rat, bull and human, have demonstrated that the cortex of the outer dense fibres exhibits a regular pattern of oblique striations (Woolley, 1971; Pedersen, 1972; Baccetti *et al.*, 1973; Pihlaja and Roth, 1973; Phillips and Olson, 1974;

Espevik and Elgaester, 1978; Olson and Sammons, 1980). In the laboratory rat these striations are spaced approximately 40 nm apart and are orientated at an angle of 70-80° relative to the outer dense fibre long axis, the same angle as the mitochondrial helix in the middle piece (Woolley, 1971; Phillips and Olson, 1974; Olson and Sammons, 1980). However, in human sperm these striations are 16 nm apart (Pedersen, 1972), and in bull are either 20 nm (Philaja and Roth, 1973) or 50 nm (Baccetti *et al.*, 1973) apart. In the laboratory rat, the outer dense fibre striations appear to be composed of a single layer of 6-8 nm globular subunits which are located only in the cortex (Olson and Sammons, 1980) as opposed to both the cortex and medulla in sperm from human (Pedersen, 1972) and bull (Baccetti *et al.*, 1973).

In most mammalian species, small amounts of electron dense material are present between the outer dense fibres and axoneme in the middle and proximal principal regions of the sperm flagellum (Fawcett, 1975). These structures are known as satellite fibrils (Fawcett, 1975) and, although they appear granular in transverse sections, in laboratory rat sperm they are orientated longitudinally to the outer dense fibres (Fawcett, 1975; Olson and Sammons, 1980). The satellite fibrils share staining affinities with, and appear to arise from, the cortex of the outer dense fibres, however, it is still not known if and how the fibrils are attached to the fibres or axoneme (Fawcett, 1975). The satellite fibrils are most well developed, and therefore prominent, in sperm with very thick tails such as the ground squirrel (Fawcett, 1975).

1.4.2.2 Morphogenesis of the Outer Dense Fibres

The formation of the outer dense fibres, although noted anecdotally in several ultrastructural studies of spermiogenesis (Challice, 1952; Yasuzumi, 1956; de Krester,

1969; Fawcett and Phillips, 1969; Sapsford *et al.*, 1970; Fawcett *et al.*, 1971; Dooher and Bennett, 1973), was first described in detail, for the laboratory rat, by Irons and Clermont (1982a). In their study the data presented indicated that the formation of the outer dense fibres is a lengthy, multi-step procedure that extends from step 8-19 of spermiogenesis (Irons and Clermont, 1982a). Prior to these steps, the spermatid flagellum is composed simply of an axoneme surrounded by a sparse, electron-lucent, cytoplasm and delimited by the plasmalemma. In step 8 spermatids, nine very fine fibres, termed the anlagen of the outer dense fibres, develop adjacent to the outer microtubule doublets of the axoneme in the most proximal segment of the flagellum. During steps 9-14 of spermiogenesis, these fibres increase in length along the axoneme in a proximal-to-distal direction so that they are first observed in the distal segment of the middle piece of the flagellum and later along most of the principal piece (Irons and Clermont, 1982a). During steps 15 and 16, the rudimentary outer dense fibres rapidly increase in size and the largest fibres (1, 5 and 6) develop their characteristic tear-drop shape in sectional profile. During the remaining steps of spermiogenesis the outer dense fibres continue to grow, albeit slowly, until they assume their definitive, mature form, and the satellite fibrils also appear at this time (Irons and Clermont, 1982a). In addition to these findings, Irons and Clermont (1982a) also suggested, based on the results of an autoradiographic study using [^{3}H] proline and [^{3}H] cysteine, that the bulk of laboratory rat outer dense fibre proteins are synthesized in step 16 spermatids.

Subsequent investigations of outer dense fibre morphogenesis in the laboratory rat (Vera *et al.*, 1987; Oko and Clermont, 1989; Clermont *et al.*, 1990) have confirmed the above initial description and provided further insight into how these structures may be formed. Vera *et al.* (1987) analysed the radioactivity of laboratory rat outer dense fibre proteins from epididymal sperm collected at various time intervals after intratesticular sperm

injection with [^{3}H] leucine, and demonstrated that the proteins are synthesized in the second half of spermiogenesis. Subsequent light and electron microscopic immunocytochemical studies, using affinity-purified antibodies prepared against specific laboratory rat outer dense fibre proteins, were able to distinguish between the time of formation of the outer dense fibre proteins in the cytoplasm of the spermatids and their assembly along the axoneme (Oko and Clermont, 1989; Clermont *et al.*, 1990). In these studies, it was shown that outer dense fibre proteins are present in the entire cytoplasm of step 9-19 laboratory rat spermatids, but reach a peak in step 16-18, confirming earlier results (Oko and Clermont, 1989; Clermont *et al.*, 1990). Moreover, these immunocytochemical investigations also demonstrated that outer dense fibre staining is concentrated over specific 'granulated bodies' during spermiogenesis, these bodies forming adjacent to, and appearing to be associated with, the endoplasmic reticulum cisternae (Oko and Clermont, 1989; Clermont *et al.*, 1990). The granulated bodies are thought to arise from small 'puffs' of fuzzy, filamentous material in step 8-9 spermatids, which rapidly increase in number and size, and become granular and spherical, during steps 10-14 of spermiogenesis, decreasing in number thereafter (Clermont *et al.*, 1990). The intense immunoreactivity of the granulated bodies, and the fact that they develop in parallel with the outer dense fibres, which themselves continue to grow during spermiogenesis even though transcription has ceased (Monesi *et al.*, 1978; Hecht, 1987), has led to the hypothesis that these bodies serve as transitory storage sites for outer dense fibre proteins, although the mechanisms regulating the release of these proteins is not yet understood (Clermont *et al.*, 1990). This would explain why the granulated bodies are slowly resorbed in the final steps of spermiogenesis when the formation of the outer dense fibres is largely complete (Clermont *et al.*, 1990).

1.4.2.3 Protein Composition of the Outer Dense Fibres

In mammals the outer dense fibres account for approximately 30-40% of total sperm protein (Vera *et al.*, 1984), therefore it was imperative to develop techniques for isolating this structure. In laboratory rat (Olson and Sammons, 1980; Vera *et al.*, 1984; Oko, 1988; Kim *et al.*, 1999), bull (Baccetti *et al.*, 1973, 1976a,b; Brito *et al.*, 1986), and human (Henkel *et al.*, 1992; Haidl, 1993) sperm, the outer dense fibres have been isolated by a combination of mechanical separation, using sonication and density gradient centrifugation, and chemical dissection, employing selective solubilization by either the anionic detergent sodium dodecyl sulfate (SDS) with dithiothreitol (DTT), or the cationic detergent cetyltrimethylammonium bromide (CTAB) with mercaptoethanol or DTT. SDS has mostly been employed to isolate the outer dense fibres from laboratory rat sperm, whilst CTAB has been used for bull and human sperm. SDS-PAGE has subsequently been used to determine the number and molecular masses of the proteins comprising the outer dense fibres in these species. In the laboratory rat, the species that has been most studied, conflicting molecular weights of the protein compositions have been reported, but at least six major proteins occur (Olson and Sammons, 1980; Vera *et al.*, 1984; Oko, 1988; Kim *et al.*, 1999) (Table 1.1). In comparison, bull (Baccetti *et al.*, 1973, 1976b; Brito *et al.*, 1986) (Table 1.2), and human (Henkel *et al.*, 1992; Haidl, 1993) (Table 1.3) sperm outer dense fibres have been found to be composed of at least three and two major proteins each respectively. Furthermore, it has been shown that each of the major laboratory rat outer dense fibre proteins, as well as the 85 and 33 kDa bull proteins, but not the human fibre proteins, are phosphoproteins that are phosphorylated at serine residues (Vera *et al.*, 1984; Brito *et al.*, 1986; Henkel *et al.*, 1994).

TABLE 1.1

Comparison of Molecular Masses of Major‡ Outer Dense Fibre Proteins in Laboratory Rat Spermatozoa from Different Studies

Polypeptide	Olson and Sammons (1980)	Vera *et al.* (1984)	Oko (1988)	Kim *et al.* (1999)
a#	87	87	84	84
			80	79
b				66.2
c				57.2
d*	25	30.4	32	32
		26	26	29
				26
e	19	18.4	20	21.5
f		13		
g	12	11.5	14.4	15.5

a-g: Each line represents molecular masses, in kDa, of polypeptides that presumably correspond to each other.

‡Major being defined, by the respective authors, as the most prominent bands observable in SDS-gels stained with either Coomassie Blue or silver.

#Polypeptide 'a', first identified by Olson and Sammons (1980), was subsequently found to composed of two proteins by Oko (1988) and then Kim *et al.* (1999).

*Polypeptide 'd', first identified by Olson and Sammons (1980), was subsequently found to be composed of two proteins by Vera *et al.* (1984) and Oko (1988), and then three proteins by Kim *et al.* (1999).

Based on a table by Kim *et al.* (1999).

TABLE 1.2

Comparison of Molecular Masses of Major‡ Outer Dense Fibre Proteins in Bull Spermatozoa from Different Studies

Polypeptide	Baccetti *et al.* (1973)*	Baccetti *et al.* (1976b)*	Vera *et al.* (1984)#	Brito *et al.* (1986)
a	60	72	78	85
b	55	55	56	
c	30	31	33	33
d	15		11	11

a-d: Each line represents molecular masses, in kDa, of polypeptides that presumably correspond to each other.
‡Major being defined, by the respective authors, as the most prominent bands observable in SDS-gels stained with either Coomassie Blue or silver.
*In these studies the outer dense fibres were not isolated by detergent solubilization, but rather by intense sonication followed by density gradient centrifugation.
#Unpublished observations noted by Vera *et al.* (1984).

TABLE 1.3

Comparison of Molecular Masses of Major‡ Outer Dense Fibre Proteins in Human Spermatozoa from Different Studies

Polypeptide	Baccetti *et al.* (1976b)*	Henkel *et al.* (1992)	Haidl (1993)
a			105
b	72	67	67
c	57	55	55
d	31		
e	28		

a-e: Each line represents molecular masses, in kDa, of polypeptides that presumably correspond to each other.
‡Major being defined, by the respective authors, as the most prominent bands observable in SDS-gels stained with either Coomassie Blue or silver.
*In this study the outer dense fibres were not isolated by detergent solubilization, but rather by intense sonication followed by density gradient centrifugation.

1.4.2.4 Nucleotide and Amino Acid Sequences of the Major Outer Dense Fibre Proteins

Early biochemical studies of the proteins of the outer dense fibres sought to analyse their amino acid composition. In the laboratory rat, bull and human, it was found that cysteine and proline residues are largely confined to the low molecular weight proteins (Olson and Sammons, 1980; Vera *et al.,* 1984; Kim *et al.,* 1999), whereas the highest molecular weight protein (~84 kDa) contained large amounts of glutamic acid and leucine (Olson and Sammons, 1980; Vera *et al.,* 1984)

In order to gain further understanding of the biochemical properties of the major outer dense fibre proteins, the cloning and sequencing of genes encoding for these proteins has been undertaken. Progress in this regard had been hampered by the insoluble nature of the outer dense fibre proteins which makes it difficult to obtain amino terminal amino acid sequences by automated sequencing methods (Kim *et al.,* 1999). Nevertheless, to date, several key outer dense fibre proteins, as well as outer dense fibre-interacting proteins, have been sequenced (summarised in Table 1.4).

ODF1

The first outer dense fibre protein to be cloned and sequenced was the most prominent laboratory rat fibre protein. By SDS gel electrophoresis, the molecular weight of this protein was difficult to precisely assess and, therefore, it was deemed to be between 32 and 26 kDa in size. However, cloning of this protein has showed it to have a molecular weight of 27 kDa. The gene coding for this protein is now termed ODF1, however because the cDNAs originally cloned were independently sequenced in separate investigations, the gene was originally known as RT7 (van der Hoorn *et al.,* 1990), rts 5/1 (Burfeind and

Hoyer-Fender, 1991), and Odf27 (Morales *et al.*, 1994). The RT7 gene was sequenced, using differential cDNA cloning techniques, by van der Hoorn *et al.* (1990), although the exact location of the protein it synthesized was not known until a subsequent immunofluorescence study using a monoclonal antibody raised against it indicated that it was a structural component of the outer dense fibres (Higgy *et al.*, 1994). In contrast, the Odf27 cDNA was isolated by screening a rat testis cDNA library with an affinity-purified polyclonal antibody against the 27 kDa rat outer dense fibre protein (Morales *et al.*, 1994). Sequence analysis of the ODF1 cDNA revealed that the carboxy-terminal end contains tripeptide repeats of the amino acids Cysteine, Glycine and Proline (Cys-Gly-Pro), predicted that the protein most likely contains an extended rod-like structure (Shao and van der Hoorn, 1996), and demonstrated that the N-terminus folds as an amphipathic α-helix that resembles a leucine zipper (van der Hoorn *et al.*, 1990). (A leucine zipper consists of a stretch of amino acids with a leucine in every seventh position. A leucine zipper in one protein can interact with a leucine zipper in another protein to form a dimer (Lewin, 1997). The leucine zipper is thought to be responsible for the weak self-interaction of the ODF1 protein (Shao and van der Hoorn *et al.*, 1996).

The rts 5/1 cDNA codes for the full sequence of the 27 kDa rat outer dense fibre polypeptide which is 244 amino acids in length (Burfeind and Hoyer-Fender, 1991). Unlike RT7 and Odf27, the rts 5/1 cDNA was isolated by screening a rat testis cDNA library with the *Drosophila melanogaster* gene Mst(3)gl-9, used as a hybridisation probe to determine whether a homologous gene was also expressed in the mammalian testis (Burfeind and Hoyer-Fender, 1991). The Mst(3)gl-9 gene was originally cloned by Kuhn *et al.* (1988), and belongs to the Mst(3)CGP gene family, the proteins of which each contain high proportions of the repetitive Cys-Gly-Pro motifs in their carboxy-terminal ends (Schäfer *et al.*, 1993).

The proteins coded for by the Mst(3)CGP gene family have been detected in the *Drosophila* testis during spermiogenesis (Schäfer *et al.*, 1993), and it has been speculated, from immunofluorescent studies, that they are of specific accessory axonemal structures in the *Drosophila* sperm flagellum called satellite fibres. These structures are thought to be homologous to the outer dense fibres of mammalian sperm (Baccett et al., 1973; Kuhn *et al.*, 1988; Morales *et al.*, 1994). (NOTE: Satellite fibres are different to the mammalian satellite fibrils described in 1.4.2.1). Homologous sequences to that of the rat ODF1 cDNA have subsequently been identified in sperm from human (Gastmann *et al.*, 1993; Hofferbert *et al.*, 1993), mouse (Hoyer-Fender *et al.*, 1995), pig and bull (Kim *et al.*, 1995a).

ODF2

The second mammalian outer dense fibre protein to be sequenced was the 84 kDa laboratory rat protein. Originally termed 111-450, the ODF2 cDNA was isolated by utilizing the leucine zipper of the ODF1 protein as 'bait' in a yeast two-hybrid screening process (Shao *et al.*, 1997). The 84 kDa rat outer dense fibre protein is 519 amino acids in length and contains two C-terminal leucine zippers, the upstream one of which specifically interacts with the leucine zipper of ODF1 (Shao *et al.*, 1997). Western blotting, using antibodies raised against ODF2 fusion proteins, was used to demonstrate that the protein reacted to the 84 kDa rat outer dense fibre protein (Shao *et al.*, 1997). Moreover, two models have been proposed which attempt to describe the potential interaction of the ODF1 and ODF2 proteins by way of their leucine zippers (Shao *et al.*, 1997). In the favoured model it is hypothesized that the ODF2 protein acts as a structural link between two regions of the outer dense fibres (Shao *et al.*, 1997), a notion given credence by a subsequent immunocytochemical study which showed that the ODF2 protein is present

throughout the cortex and medulla of the rat outer dense fibres, as opposed to the exclusive medullary localization of the ODF1 protein (Schalles *et al.*, 1998).

ODF3

A laboratory rat cDNA, ODF3, was recently isolated and characterised and shown to encode for a putative outer dense fibre protein of approximately 110 kDa (Petersen *et al.*, 2002), although no such protein had previously been attributed to the rat by SDS gel electrophoresis. The secondary structure of this protein was predicted to consist mostly of coiled-coils with three leucine zipper regions. Furthermore, transcription of ODF3 was not restricted to the testis but was also found in the epididymis and brain suggesting that it may be involved in the general organization of the cellular cytoskeleton (Petersen *et al.*, 2002).

tpx-1, oppo1, OIP1 and Sak57

A 29 kDa laboratory rat outer dense fibre protein was cloned and sequenced by screening a rat testis expression library with an a polyclonal antibody raised against a whole rat outer dense fibre preparation (O'Bryan *et al.*, 1998). The isolated gene was designated tpx-1 by virtue of its homology with the mouse and human tpx-1 genes, the functions of which remain largely unknown (O'Bryan *et al.*, 1998).

Oppo 1 gene ('oppo' meaning 'tail' in Japanese), was isolated and cloned from a subtracted DNA library that was generated by subtracting the mRNA from 17-day-old mouse testes from the cDNA of 35-day-old mouse testes (Nakamura *et al.*, 2002). Interestingly, the predicted amino acid sequence of the oppo 1 protein has a 22-amino acid sequence common to the flagella of the *Salmonella typhimurium* bacteria, leading to the

suggestion that it may be concerned with flagella basal body formation in mammals (Nakamura *et al.*, 2002).

ODF1-interacting protein (OIP1) was isolated using a yeast two-hybrid library screen, and was found to interact with ODF1 via the evolutionarily conserved Cys-Gly-Pro repeats in the C-terminus (Zarsky *et al.*, 2003). OIP1 sequence analysis suggests that it is a member of the RING finger family of proteins. Moreover, deletion of the RING motif was found to significantly decrease OIP1-ODF1 binding, underscoring the apparent importance of this motif and providing additional information on how outer dense fibre proteins interact (Zarsky *et al.*, 2003).

A keratin-like protein termed Sak57 has been partially characterized in the laboratory rat and found to be associated first with the manchette early in spermiogenesis, before becoming a component of the outer dense fibres later in development (Kierszenbaum *et al.*, 1996).

SPAG2, SPAG4 and SPAG5

SPAG2 (sperm-associated antigen 2) was isolated and sequenced by screening a human cDNA library with sera from infertile and vasectomised men that contained antisperm antibodies (ASAs) (Diekman *et al.*, 1998). It was found to encode for a 56 kDa outer dense fibre protein that is expressed premeiotically during human spermatogenesis (Diekman *et al.*, 1998). SPAG4 (Shao *et al.* 1999) and SPAG5 (Shao *et al.*, 2001) were subsequently isolated by using the leucine zipper of ODF1 as bait in a yeast two-hybrid screen. Both were found to strongly interact with ODF1 presumably via the leucine zippers they contain, although interaction with ODF2 was not found to occur (Shao *et al.*, 2001).

TABLE 1.4

Proteins associated with the outer dense fibres

Name	Predicted MW (kDa)[1]	Actual MW (kDa)[3]	Species[4]	Location	Reference
ODF1	26.000	27	Lab rat	Medulla (EM)[5]	van der Hoorn *et al.*, (1990); Burfeind and Hoyer-Fender (1991); Morales *et al.*, (1994)
ODF2	72.000	84	Lab rat	Cortex and medulla (EM)	Shao *et al.*, (1997); Schalles *et al.*, (1998)
ODF3	113.522	100	Lab rat	Cortex and medulla (EM)	Petersen *et al.*, (2002)
tpx-1	29	ND	Lab rat	Outer dense fibres (IF)[6]	O'Bryan *et al.*, (1998)
oppo 1	ND[2]	33	Lab mouse	Outer dense fibres (IF)	Nakamura *et al.*, (2002)
OIP1	48.700*	70	Lab rat	Outer dense fibres (IF)	Zarsky *et al.*, (2003)
Sak57	ND	57	Lab rat	Outer dense fibres (IF)	Kierszbenbaum *et al.*, (1996)
Spag2	55.500	56	Human	Cortex and medulla (EM)	Diekman *et al.*, (1998)
Spag4	49.000	49	Lab rat	Cortex and medulla (EM)	Shao *et al.*, (1999)
Spag5	ND	200	Lab rat	Cortex and medulla (EM)	Shao *et al.*, (2001)

[1]Predicted molecular weight (MW) calculated from amino acid sequence
[2]Not determined
[3]Molecular weight calculated by SDS-PAGE
[4]Species in which protein was first sequenced
[5]Location determined by immunoelectron microscopy
[6]Location determined by immunofluorescence microscopy
*48.7 kDa predicted molecular weight based only on a partial cDNA sequence only

1.4.2.5 Possible Function(s) of the Outer Dense Fibres

Early histochemical and immunological studies indicated that the eutherian outer dense fibres possessed ATPase activity and were composed of proteins immunologically similar to muscle actin and myosin, suggesting that they may have an active role in flagellar movement (Nelson, 1958; 1962). However this was disproved in subsequent biochemical investigations which, together with structural studies demonstrating that flagellar

movement is caused by the sliding interactions of microtubule doublets, suggested that the outer dense fibres function instead as passive, stabilizing, elastic structures (Baccetti *et al.*, 1973; Price, 1973; Fawcett, 1975; Olson and Sammons, 1980). The outer dense fibre proteins, which are stabilized by disulphide-bonding (Calvin *et al.*, 1975), are thought to stiffen and/or provide elastic recoil for the axoneme, which may have become necessary to sustain the long flagella present in most mammalian sperm. Baltz *et al.*, (1990) demonstrated that species with very long sperm flagella, such as hamster, laboratory rat and guinea pig, have significantly thicker outer dense fibres than do sperm of human and bull which are proportionally shorter in length. It was argued that the increase in size of the outer dense fibres in longer sperm reflects the increased shearing forces which these sperm are subjected to during epididymal transit and especially ejaculation; the thicker outer dense fibres increase the tensile strength of the sperm and protect them against damage (Baltz *et al.*, 1990).

A working hypothesis was developed by Lindemann (1996) to explain the impact of the outer dense fibres on microtubule sliding and force production within the axoneme. The hypothesis is based on the fact that in mammalian sperm the outer microtubule doublets and central pair of microtubules of the axoneme do not penetrate into, and therefore are not anchored to, the connecting piece; therefore any forces produced by the sliding interactions of the outer doublets are ultimately transferred to the outer dense fibres which *are* anchored to the connecting piece at the flagellar base (Lindemann, 1996). In this proposed scheme, the outer dense fibres are thought to provide increased stiffness to the flagellum while at the same time increasing the bending torque to overcome the additional flexural rigidity of the flagellum (Lindemann, 1996). The increased stiffness reduces the maximum flagellar curvature, distributing each bend over a longer span of the axoneme

In addition, it is possible that a stiff flagellum increases the effective beat wavelength, and hence maximal attainable velocity, of a sperm cell. This may be an important strategy from the perspective of sperm competition theory.

and so consolidating the energy from a greater number of dynein cross-bridges into the production of a single flagellar bend. Consequently, the axoneme is able to generate the forces necessary to produce and propagate bends in large mammalian sperm flagella (Lindemann, 1996).

Recently, molecular characterization of some of the major outer dense fibre proteins has revealed details of its organisation and may eventually shed further light on its function. It has been demonstrated that the ODF1 protein is able to self-interact, as well as associate with ODF2, via its leucine zippers (Shao and van der Hoorn, 1996; Shao *et al.,* 1997). Furthermore, SPAG4 and SPAG5 bind to ODF1, but not ODF2 (Shao *et al.,* 1999). Secondary structure analysis of ODF3 has shown it to be a coiled-coil protein, leading to the hypothesis that it acts with ODF2 to form a scaffold onto which other outer dense fibre proteins may associate (Petersen *et al.,* 2002).

1.4.3 Fibrous Sheath

1.4.3.1 Location and Appearance of the Fibrous Sheath

The fibrous sheath is a tapering cylinder that extends from the annulus in the principal piece of the sperm flagellum. It immediately underlies, but is not attached to, the plasmalemma (Fawcett, 1970). Ultrastructural studies have suggested that it is present in not just mammals, but also some reptiles and birds (Eddy and O'Brien, 1994). Conclusions from early electron microscopic investigations suggested that the fibrous sheath was composed of a single fibre, wound in a helical fashion around the flagellum (Schnall, 1952; Anberg, 1957; Schultz-Larsen, 1958). However subsequent, more detailed studies demonstrated that it is composed of two structurally distinct segments, the dorsal and ventral 'longitudinal columns, which are connected by an array of circumferential ribs

(Fawcett, 1970, 1975). The longitudinal columns are positioned 180° apart and lie in the plane of the central pairs of axonemal microtubules. They run peripheral to outer microtubule doublets 3 and 8 of the axoneme in replacement of the two corresponding outer dense fibres which terminate at the annulus (Fawcett, 1970), thereby partitioning the flagellum into two unequal compartments. The longitudinal columns appear to be formed by longitudinally orientated, loosely packed filamentous structures, 15-20 nm in diameter, separated, or partially surrounded, by clear areas of similar dimensions (Fawcett, 1975). The size and shape of the longitudinal columns vary between species from narrow and inconspicuous in the guinea pig to prominent and elliptical in shape in the Chinese hamster (Fawcett, 1975).

The circumferential, or transverse, ribs of the fibrous sheath run perpendicular to, and make contact at their ends with, the longitudinal columns. The ribs are uniformly spaced and for the most part exist as separate elements, although in tangential sections they appear to occasionally bifurcate with one of the resulting branches joining the rib above or below (Fawcett, 1975). In some species, such as the laboratory mouse, the interconnection of the circumferential ribs is so extensive that the ribs fuse to form broad bands instead of remaining slender and separate (Fawcett, 1975). The thickness, as well as the extent of bifurcations, of the circumferential ribs gradually diminishes towards the distal end of the principal piece of the flagellum. In human sperm the ribs are 10-20 nm apart and about 50 nm thick (Baccetti, 1984). Negative staining techniques have demonstrated that the circumferential ribs are composed of parallel filaments which, in laboratory rat sperm, are approximately 5-6 nm in diameter, with each filament having a beaded substructure (Olson *et al.*, 1976).

1.4.3.2 Morphogenesis of the Fibrous Sheath

The formation of the eutherian fibrous sheath, although noted briefly in several ultrastructural studies of spermiogenesis (Nicander, 1962; Yasuzumi *et al.*, 1972; Einarsson and Nicander, 1968), was first described in detail for the laboratory rat by Irons and Clermont (1982b). In their electron microscope and radioautograhpic study using [^{3}H] proline, it was shown that the assembly of the fibrous sheath, like that of the outer dense fibres (see 1.4.4.2), is a lengthy, multistep procedure, in this case extending from steps 2 to 17 of spermiogenesis. However, unlike the dense fibres, which are laid down in a proximal-to-distal direction, development of the fibrous sheath proceeds in a distal-to-proximal direction along the axoneme (Irons and Clermont, 1982b). The longitudinal columns of the fibrous sheath appear first in step 2 spermatids as two thin rods of electron dense material in the flagellar cytoplasm between the plasmalemma and outer microtubule doublets 3 and 8 of the axoneme. During steps 2-10 of spermiogenesis these anlagen of the longitudinal columns increase in length, gradually extending along the principal piece of the flagellum (Irons and Clermont, 1982b). The rib anlagen first appear along the distal end of the flagellum of step 11 spermatids as a series of evenly spaced, circumferentially orientated, double striations underlying the plasmalemma, and are continuous at both ends with the anlagen of the longitudinal columns. The construction of this fibrous sheath framework continues gradually through steps 12-14 of spermiogenesis, however in step 15 there is a sudden increase in the electron density of the framework and neighbouring rib anlagen converge so that the ribs take on their definitive appearance (Irons and Clermont, 1982b). A gradual increase in thickness of the longitudinal columns in step 15-17 of spermiogenesis marks the completion of fibrous sheath morphogenesis in the laboratory rat. In addition to these results, the radioautographic studies carried out by Irons and Clermont (1982b) suggest that the longitudinal column proteins are gradually synthesized

and incorporated into the fibrous sheath over a 15 day period (steps 2-17). In comparison, the circumferential ribs are assembled along the length of the principal piece during a much shorter period, 4.5 days, between steps 11-15 of spermiogenesis from proteinaceous filaments synthesized in the cytoplasm of these spermatids. The fact that the timing and method of assembly of the longitudinal columns and circumferential ribs is different suggests that these two components are assembled by two independent mechanisms (Irons and Clermont, 1982b).

Subsequent light and electron microscopic immunocytochemical studies of laboratory rat fibrous sheath formation largely confirmed earlier findings. Using antibodies prepared against whole fibrous sheath preparations, as well as against individual fibrous sheath proteins, it was shown that the production of fibrous sheath proteins is exclusive to step 9-19 spermatids, although immunoreactivity is most intense in the cytoplasm of step 15-17 spermatids (Oko and Clermont, 1989; Clermont *et al.*, 1990). However, unlike the outer dense fibre proteins which appear to be concentrated in "granulated bodies" within the cytoplasm, dispersion of the fibrous sheath proteins is uniform and diffuse within the cytoplasm (Oko and Clermont, 1989; Clermont *et al.*, 1990). Moreover, the anlagen of the fibrous sheath is not immunoreactive to the anti-fibrous sheath antibodies suggesting that this 'framework' structure may serve as a trigger or organizer of fibrous sheath assembly rather than being an actual component of the mature fibrous sheath (Clermont *et al.*, 1990; Oko, 1998).

1.4.3.3 Protein Composition of the Fibrous Sheath

Early studies on the mammalian sperm flagellum noted that the fibrous sheath was resistant to solubilization by acid (Bradfield, 1955) and suggested that proteins of the

sheath are stabilized by disulphide bonds (Calvin and Bedford, 1971; Bedford and Calvin, 1974). Based on this finding, subsequent investigators developed techniques for isolating the fibrous sheath. The laboratory rat fibrous sheath was first isolated by detergent extraction using DTT and Urea, and it was shown to be composed predominantly of a single polypeptide with a molecular mass of 80 kDa (Olson *et al.*, 1976). Subsequent biochemical characterization of the rat fibrous sheath, however, demonstrated that additional proteins are present, although different authors reported varying numbers and molecular weights of proteins despite employing the same basic protocol developed by Olson *et al.* (1976). Three major proteins were reported each by Oko (1998) and Brito *et al.* (1989), although Kim *et al.* (1995b) reported 6 major proteins (Table 1.5). In each of these studies, however, additional minor proteins were revealed by SDS-PAGE; at least 20 proteins were found to be present in total in the rat fibrous sheath by Kim *et al.* (1995b). Nevertheless, the ~80 kDa fibrous sheath protein is most prominent and represents 35% of total fibrous sheath protein content (Brito *et al.*, 1989). The question of how these fibrous sheath proteins are assembled into the longitudinal columns and circumferential ribs of the fibrous sheath is yet to be determined, although it has been suggested that the other polypeptides present in the fibrous sheath might somehow direct the assembly of the ~80 kDa protein toward the formation of the ribs or columns (Olson *et al.*, 1976).

TABLE 1.5

Comparison of Molecular Masses of Major‡ Fibrous Sheath Proteins in Laboratory Rat Spermatozoa from Different Studies

Polypeptide	Olson *et al.* (1976)	Oko (1988)	Brito *et al.* (1989)	Kim *et al.* (1995b)
a#	80	75	80	87.5
				80.9
b				66.2
c				32.7
d		27.5	24	28.5
e		14.4	11.5	15.5

a-e: Each line represents molecular masses, in kDa, of polypeptides that presumably correspond to each other.
‡Major being defined, by the respective authors, as the most prominent bands observable in SDS-gels stained with either Coomassie Blue or silver.
#Polypeptide 'a', first identified by Olson *et al.* (1976), was subsequently subdivided into two bands Kim *et al.* (1995b).

The proteins of the fibrous sheath have also been isolated from other mammalian species (Table 1.6). In the laboratory mouse, the fibrous sheath is composed of two major (78 and 24 kDa) and four minor (112, 67, 63, 36 kDa) (Eddy *et al.,* 1991) bands. Human fibrous sheath preparations have been reported to contain either seven (97, 76, 62, 55, 33, 28 and 25 kDa) (Jassim *et al.,* 1992), or six (84, 72, 66.2, 57, 32 and 28.5 kDa) (Kim *et al.,* 1997) major proteins, although up to fourteen protein bands in total were detected by SDS-PAGE. In addition, at least eleven protein bands, of which the most intensely stained were 35, 32 and 28 kDa, were detected in the rabbit fibrous sheath (Kim *et al.,* 1997), whereas just three (80, 24, 11.5 kDa) were observed in gels of the hamster fibrous sheath (unpublished observations noted by Brito *et al.,* 1989) (Table 1.6). The fact that the fibrous sheath is composed, on average, of more proteins that the outer dense fibres from the

same species is not surprising given how much more structurally complex the fibrous sheath is compared to the outer dense fibres.

TABLE 1.6

Comparison of Molecular Masses (kDa) of Fibrous Sheath Proteins# From Laboratory Rat, Human, Mouse and Hamster Spermatozoa from Different Studies

[a]Laboratory Rat	[b]Human	[c]Rabbit	[d]Mouse	[e]Hamster
116	116	-	112	-
87	-	-	-	-
80	84	80	78	80
-	72	71	-	-
66	66	66	67	-
-	-	-	63	-
-	59	-	-	-
57	57	57	-	-
-	-	52	-	-
49	49	49	-	-
46	46	-	-	-
-	43	-	-	-
-	40	-	-	-
37	38	35	36	-
32	32	32	-	-
28	28	28	-	-
-	-	21	24	24
15	14	12	-	11

#Major and most minor fibrous sheath proteins.
[a]Data from Kim *et al.* (1995b).
[b,c]Data from Kim *et al.* (1997).
[d]Data from Eddy *et al.* (1991).
[e]Unpublished results reported by Brito *et al.* (1989)

Based on a table by Kim *et al.* (1997).

It has been suggested that some of the proteins of the mammalian fibrous sheath, and also to a lesser extent the outer dense fibres, are intermediate filaments or keratin-like in nature (Baccetti *et al.*, 1973; Bedford and Calvin, 1974; Calvin, 1975). This is mostly

because of their filamentous nature and relative insolubility due to extensive disulphide cross-linking (Calvin and Bedford, 1971; Bedford and Calvin, 1974; Calvin, 1975). Most immunocytochemical studies, using antibodies prepared against the major intermediate filament proteins, found no evidence of such proteins within the sperm flagellum (Franke *et al.*, 1979; van Vorstenbosch *et al.*, 1984; Kierszenbaum *et al.*, 1996; Longo *et al.*, 1987; Eddy *et al.*, 1991). However, a few antibodies directed against proteins of several classes of somatic intermediate filaments were found to react with the laboratory mouse fibrous sheath (Eddy *et al.*, 1991) and an anti-neurofilament antibody localizes to the cortex of the laboratory rat fibrous sheath (Jassim *et al.*, 1991b). Although this may appear to support the notion that at least some of the fibrous sheath proteins are intermediate filament-like in nature, it should be noted that characterization of the cDNAs coding for the major mammalian fibrous sheath proteins (see 1.4.3.4) has yet to reveal significant homology with any known intermediate filament proteins.

1.4.3.4 Nucleotide and Amino Acid Sequences of the Fibrous Sheath Protein

The amino acid composition of the laboratory rat fibrous sheath proteins was first examined by Brito *et al.* (1986) who demonstrated that the 80 kDa protein contained large amounts of lysine, aspartic acid, serine, glutamic acid and isoleucine. In comparison the 24 kDa protein contained a lower content of serine whereas the 11 kDa protein had more tyrosine (Brito *et al.*, 1989). Subsequent investigations largely confirmed these results (Kim *et al.*, 1995b) and showed similar findings for fibrous sheath proteins from human and rabbit sperm (Kim *et al.*, 1997).

As is the case for the outer dense fibre proteins, attempts at sequencing the major fibrous sheath proteins have been hampered by the insolubility of the proteins and the difficulty in obtaining the amino-terminal sequences of these proteins by automated microsequencing methods. Nevertheless, to date the gene sequences coding for at least eleven proteins localised to the fibrous sheath proteins are known. These proteins can be broadly divided into three groups: (1) A-kinase anchoring and associated proteins, which include AKAP4 (Carrera *et al.*, 1994; Fulcher *et al.*, 1995a), AKAP3 (Vijiyaraghaven *et al.*, 1999; Mandal *et al.*, 1999), TAKAP-80 (Mei *et al.*, 1997), rhophilin (Nakamura *et al.*, 1999), ropporin (Fujita *et al.*, 2000; Carr *et al.*, 2001) and ASP (Carr *et al.*, 2003), (2) glycolytic enzymes, which include GAPDS (Welch *et al.*, 1992; Bunch *et al.*, 1998), and HK1-S (Mori *et al.*, 1993, 1998; Travis *et al.*, 1998), and other fibrous sheath proteins, which include GSTM5 (Fulcher *et al.*, 1995a; Rowe *et al.*, 1998a, b) FS39 (Catalano *et al.*, 1997, 2001) and SPTRX-2 (Miranda-Vizuete *et al.*, 2003) (Table 1.7).

AKAP4

The most prominent laboratory mouse fibrous sheath protein, whose molecular weight was estimated by SDS-PAGE to be 78 kDa (Eddy *et al.*, 1991), was sequenced independently by two groups and the resultant cloned cDNAs were termed p82 and then AKAP82 (Carrera *et al.*, 1994; Johnson *et al.*, 1997), and Fsc1 (Fulcher *et al.*, 1995a). Carrera *et al.* (1994) isolated the cDNA by screening a mouse mixed germ cell cDNA expression library with an antibody raised against the 78 kDa mouse fibrous sheath protein. In addition, the N-terminal sequence of this fibrous sheath protein was also determined for comparison. Analyses of both sequences predicted that the protein is synthesized as a precursor protein of ~93 kDa (840 amino acids) that is proteolytically cleaved just prior to fibrous sheath assembly to form a mature ~73 kDa (661 amino acids) protein; by SDS-PAGE the molecular masses of these proteins were determined to be ~97 kDa for the precursor and

~82 kDa for the mature protein (Carrera *et al.*, 1994). Fulcher *et al.* (1995a) cloned their cDNA by using a peptide, obtained from a tryptic digest of fibrous sheath proteins, to construct primers which were used to amplify, from mouse testis first-strand cDNA by polymerase chain reaction, an 80 bp product which was in turn utilized as a probe to screen a mouse round spermatid cDNA library. Sequence analysis of the cloned mouse fibrous sheath protein indicated that it was rich in cysteine residues and potential phosphorylation sites, further suggesting that these proteins undergo extensive post-translational modifications, which may affect their migration on polyacrylamide gels, thereby explaining why the predicted and actual protein molecular weights differ slightly (Fulcher *et al.*, 1995a).

Whilst this fibrous sheath protein was shown to be sperm-specific (Fulcher *et al.*, 1995a), it was Carrera *et al.* (1994) who first noted that it had regional homologies, in particular in the N-terminal region, to domains within the A-Kinase anchoring protein (AKAP) group of polypeptides that are responsible for anchoring protein kinase A (PKA) to the cytoskeleton (Carrera *et al.*, 1994). Specifically, this fibrous sheath protein was found to bind to the regulatory subunit (RII) of PKA (Carrera *et al.*, 1994) and in a subsequent recombinant study the RII subunit-binding domain of this protein was mapped (Visconti *et al.*, 1997). As a result of these findings, this fibrous sheath protein was termed mAKAP82, and then recently renamed AKAP4 (Blake *et al.*, 2000).

Homologues of AKAP4 have been identified in sperm from human, laboratory rat and bull (Carrera *et al.*, 1996; Turner *et al.*, 1998; El-Alfy *et al.*, 1999; Moss *et al.*, 1999), and sequence analysis of the cDNAs indicates that these homologues are highly conserved. At the amino acid level, the mouse, human and bull proteins are at least 80% identical and

90% conserved (Moss *et al.*, 1999), whereas the rat and mouse proteins are approximately 93% identical (El-Alfy *et al.*, 1999). Furthermore, the specific RII-binding domain, as well as the precursor/mature AKAP4 cleavage site, are identical in all four species (El-Alfy *et al.*, 1999; Moss *et al.*, 1999).

AKAP3

As with AKAP4, two distinct groups also independently sequenced the AKAP3 fibrous sheath protein. One group solubilised bull sperm tails and isolated a ~110 kDa protein by 2D electrophoresis (Vijayaraghaven *et al.*, 1997b). This protein had earlier been shown to bind to the RII subunit of PKA (Horowitz *et al.*, 1984), and similar-sized proteins have also been found in the laboratory mouse (Lin *et al.*, 1995), rhesus monkey and human (Vijayaraghaven *et al.*, 1997b). Fragments of the 110 kDa peptide were sequenced and then utilised as probes to screen a mouse testis library. The isolated clone contains 864 amino acids and has a predicted molecular weight of ~96 kDa (Vijayaraghaven *et al.*, 1997b). Homologous clones from human and bovine testis libraries were subsequently obtained and 65% of the amino acids were conserved, with some regions, notably the C-terminal region, being much more conserved (Vijayaraghaven *et al.*, 1997b). The second group microsequenced a protein recognised by sera from infertile men and used PCR to clone the human cDNA (Mandal *et al.*, 1999). This protein was found to undergo tyrosine phosphorylation during in vitro capacitation of human sperm and has 40% amino acid similarity to AKAP4 (Mandal *et al.*, 1999).

TAKAP-80

The TAKAP-80 clone was isolated by screening a rat testis cDNA library with a radiolabeled RII probe (Mei *et al.*, 1997). An antibody against the recombinant TAKAP-80 protein recognised an 80 kDa protein in fibrous sheath extracts by western blotting,

however the deduced molecular weight of the 502 amino acid-long sequence was only ~56 kDa, indicating that this protein appears to migrate aberrantly high in SDS-PAGE gels (Mei *et al.,* 1997). A high affinity RII binding site was identified in the C-terminal domain of the protein (Mei *et al.,* 1997).

Rhophilin, Ropporin and ASP

In somatic cells, experimental data has shown that disruption of either PKA-AKAP interaction or PKA catalytic activity results in the loss of cAMP/PKA modulation of specific events, for example uterine smooth muscle contraction (Vijayaraghavan *et al.,* 1997b). In sperm, disruption of PKA-AKAP interaction inhibits sperm motility, however disruption of PKA catalytic activity does not appear to have any effect on sperm motility, suggesting that AKAPs can interact with proteins other than PKA (Vijayaraghavan *et al.,* 1997b). To isolate these proteins, a human testis library was screened with a fragment of the AKAP3 protein that contained the amphipathic helix domain onto which the RIIα subunit of PKA is thought to bind. Two proteins were identified: a human homolog of mouse ropporin and a novel protein with 39% sequence similarity to ropporin, termed AKAP-associated sperm protein (ASP) (Carr *et al.,* 2001). Both ropporin and ASP share strong sequence similarity with the RIIα domain of PKA suggesting that they interact with the amphipathic helix region of AKAPs.

Ropporin was also found to bind to a previously sequenced sperm protein, rhophilin. Rhophilin is a putative downstream target for Rho, a small GTPase that acts as a molecular switch to trigger reorganisation of the actin cytoskeleton and regulate cell-substrate adhesion, motility and cytokinesis (Bishop and Hall, 2000; Takai *et al.,* 2001). Immunogold electron microscopy has shown that rhophilin is restricted to the outer surface

of the fibrous sheath whereas ropporin is found throughout the entire fibrous sheath (Fujita *et al.*, 2000).

GAPDS

Glyceraldehyde 3-phosphate dehydrogenase (GAPD) is an essential enzyme in the main pathway of glycolysis in somatic cells (Nakamura *et al.*, 1986). For many years it was thought that this enzyme was involved in regulating glycolysis in spermatids, however the spermatogenic GAPD (GAPDS) version of this protein was first, unwittingly, isolated and cloned by Fenderson *et al.*, (1988) by screening a mouse spermatogenic cell expression library with a monoclonal antibody, ATC, obtained by immunising mice with dissociated rat testis cells. The mouse GAPDS gene encodes a protein of 438 amino acids and has 71% identity with the somatic GAPD (Welch *et al.*, 1992). Homologues of this protein have also been found in sperm from human (Welch *et al.*, 2000), boar (Westhoff and Kamp, 1997), rabbit, ram and rat (Welch *et al.*, 1995). Although the ATC antibody recognises a 67 kDa fibrous sheath protein by western blotting (Fenderson *et al.*, 1988), the predicted molecular weight of GAPDS is 47.5 kDa (Bunch *et al.*, 1998). It has been suggested that the proline-rich, N-terminus of GAPDS is responsible for this slower-than-expected migration in SDS gels (Bunch *et al.*, 1998).

HK1-S

Somatic type 1 hexokinase (HK1) is an enzyme, associated with the outer mitochondrial membrane, that catalyzes the conversion of glucose to glucose-6-phosphate in the initial step of glycolysis. Three germ cell specific splice variants of mouse sperm HK1 (HK1-S), Hk1-Sa, Hk1-Sb and Hk1-Sc, have been isolated and cloned by screening a mouse spermatogenic cell cDNA library with somatic HK1 (Mori *et al.*, 1993). Whilst somatic HK1 contains an N-terminal putative porin-binding domain (PPD) necessary for HK1 binding to

the outer mitochondrial membrane (Arora *et al.,* 1990; Griffin *et al.,* 1991), in HK1-S this domain is replaced with a unique, spermatogenic cell-specific sequence region (SSR) (Mori *et al.,* 1993). The lack of PPD suggested that HK1-S might have alternative locations in sperm, and immunostaining with sera prepared against each of the variants of HK1-S indicates that most of this protein in mature sperm is encoded by HK1-Sc and binds to the fibrous sheath (Travis *et al.,* 1998). Interestingly, some reactivity was also associated with the mitochondria, as well as in discrete clusters in the sperm head plasmalemma, suggesting potential novel functions for HK1-S in these locations.

Other Fibrous Sheath Proteins

A spermatogenic cell-specific member of the μ-class glutathione S-transferase (GST) protein, termed GSTM5, has been isolated from mouse sperm and sequenced (Fulcher *et al.,* 1995b). Somatic GSTs are a family of multifunctional proteins that catalyze the nucleophilic conjugation of glutathione (GSH) to a wide variety of electrophoretic compounds (Hayes and Pulford, 1995). Interestingly, this is the only fibrous sheath protein whose synthesis begins during the meiotic phase of spermatogenesis (Rowe *et al.,* 1998b). Rat and human homologues of GSTM5 have also been found (Rowe et al., 1998b). An additional ~39 kDa fibrous sheath protein, FS39, was reported by Catalano *et al.,* (1997). Secondary structure analysis of this protein indicates that it has structural similarities to intermediate filaments (Catalano *et al.,* 2001). Spermatid-specific thioredoxin-1 (SPTRX-1), a novel member of the thioredoxin family of proteins, has been identified as a fibrous sheath protein in the laboratory mouse and rat (Miranda-Vizuete *et al.,* 2003). Incorporation of SPTRX-1 into the fibrous sheath was found to lag behind fibrous sheath assembly, suggesting that it is required during the final stages of sperm tail development (Miranda-Vizuete *et al.,* 2003).

TABLE 1.7

Proteins associated with the fibrous sheath

Name	Predicted MW (kDa)[1]	Actual MW (kDa)[3]	Species[4]	Location	Reference
AKAP4	unprocessed: 92.870 (Carrera et al., 1994) 93.795 (Fulcher et al., 1995a) processed: 72.890	82	Lab mouse	Columns and ribs (EM)[5]	Carrera *et al.*, (1994); Fulcher *et al.*, (1995a)
AKAP3	95.578	110	Mouse; Human	Fibrous sheath (IF)[6]	Vijayaraghavan *et al.*, (1999); Mandal *et al.*, (1998)
TAKAP-80	55.800	80	Lab rat	Fibrous sheath (IF)	Mei *et al.*, (1997)
Rhophilin	71.000	71	Lab mouse	Most on outer surface of fibrous sheath (EM)	Nakamura *et al.*, (1999)
Ropporin	24.001	24	Lab mouse	Most on inner surface of fibrous sheath (EM)	Fujita *et al.*, (2000); Carr *et al.*, (2001)
GAPDS	47.455	69	Lab mouse	Columns and ribs (EM)	Welch *et al.*, (1992); Bunch *et al.*, (1998)
HK1-S	105.282	100	Lab mouse	Columns and ribs (EM)	Mori *et al.*, (1993, 1998); Travis *et al.*, (1998)
FS39	39.500	39	Lab mouse	Fibrous sheath (IF)	Catalano *et al.*, (1997)
GSTM5	26.600	26	Lab mouse	Fibrous sheath (IF)	Fulcher *et al.*, (1995b); Rowe *et al.*, (1998a, b)
SPTRX-2	66.900	68	Lab mouse and rat	Columns and ribs (EM)	Miranda-Vizuete *et al.*, (2003)
ASP	ND[2]	ND	Human	Testis specific	Carr *et al.*, (2001)

[1]Predicted molecular weight calculated from amino acid sequence
[2]Not determined
[3]Molecular weight calculated by SDS-PAGE
[4]Species in which protein was first sequenced
[5]Location determined by immunoelectron microscopy
[6]Location determined by immunofluorescence microscopy

(Adapted from Eddy *et al.*, 2003)

1.4.3.5 Possible Function(s) of the Fibrous Sheath

For many years, the fibrous sheath was largely viewed as a passive, mechanical component of the sperm flagellum, somehow involved in its bending (Fawcett, 1975). This notion was supported by the fact that defects in the assembly of the fibrous sheath result in immotile sperm and infertility (Serres *et al.*, 1986; Chemes *et al.*, 1987). The longitudinal columns of the fibrous sheath, by virtue of their inward projection and attachment to outer microtubule doublets 3 and 8 of the axoneme, are thought to restrict the participation of these microtubules in sliding and axoneme bending, thereby determining the plane of bending (Si and Okuno, 1993). Furthermore, it has been suggested that the presence of the fibrous sheath is essential in converting the non-progressive microtubular sliding into wavy movement (Jassim, 1995). This is achieved because the fibrous sheath, which is spring-like in shape, is located in a confined space; its anterior end starts at the annulus whereas its two longitudinal columns terminate posteriorly by attaching to outer microtubule doublets 3 and 8. Consequently any microtubular sliding will be transmitted to the fibrous sheath which, because of its location in a confined space and spring-like features, will cause the fibrous sheath, and therefore flagellum, to bend (Jassim, 1995). Moreover, during bending, the electrostatic repulsion caused by the proximity of the negatively charged phosphate groups on the major fibrous sheath proteins, which are phosphorylated, may lead to a reversal of the bending (Jassim, 1995).

Recently, as more and more individual fibrous sheath proteins have been isolated and sequenced, it has become clear that the fibrous sheath has additional functions. Chiefly, it may act as a scaffold for constituents of signalling cascades and for glycolytic enzymes. The presence of A-kinase anchoring proteins (AKAP4, AKAP3 and TAKAP-80) in the fibrous sheath of sperm from numerous eutherian species, including mouse, rat, human

and bull, provides strong evidence that it anchors protein kinase A (PKA), via its regulatory (RII) subunit, to the cytoskeleton. This is significant as sperm motility is thought to involve the cyclic-AMP (cAMP)-dependent phosphorylation of flagellar proteins by PKA (Tash and Means, 1983; Brokaw, 1987; Lindemann and Kanous, 1989; Tash and Bracho, 1994; Visconti *et al.,* 1997). The importance of AKAP-PKA tethering in sperm was emphasised in earlier studies demonstrating that fibrous sheath sliding along the axoneme is cAMP-dependent (Si and Okuno, 1993). The fibrous sheath proteins, ropporin and ASP, were also found to bind to AKAP3, and therefore might be involved in regulating sperm motility, albeit independently of PKA (Carr *et al.,* 2001). Ropporin also binds to another fibrous sheath protein, rhophilin, which in turn binds to Rho, a small GTPase. As Rho acts through effector molecules to induce the assembly of cytoskeletal components, it is has been hypothesized that the AKAPs of the fibrous sheath might also act as scaffolding proteins for the Rho-GTPase pathway and that Rho activates kinases to regulate sperm motility (Nakamura *et al.,* 1999; Fujita *et al.,* 2000; Carr *et al.,* 2001).

The mammalian fibrous sheath also anchors enzymes required for the glycolytic pathway that provide the energy required for sperm motility. Although lactate is the preferred energy substrate for round spermatids from numerous eutherian species, including rat (Grootegoed *et al.,* 1986), mouse (Grootegoed and Den Boer, 1989) and hamster (Mackenbach *et al.,* 1990), spermatozoa are able to utilise glucose effectively and it is required for in vitro hyperactivation and fertilisation (Fraser and Quinn, 1981). The GAPDS enzyme may be involved in sequestering glycolytic enzymes to the fibrous sheath, providing an important source of energy generation. The localisation of HK1-S to the fibrous sheath of eutherian sperm, when it normally is found only on the outer mitochondrial membrane in somatic cells, has also been interpreted to mean that in sperm

it may also be involved in extramitchondrial energy production, perhaps also acting in the glycolytic pathway (Travis *et al.*, 1998).

1.5 THE MARSUPIAL SPERMATOZOON

Marsupials account for approximately six percent of extant mammalian species, and are thought to have diverged from the most recent common ancestor with eutherian mammals over 100 million years ago. While the best known marsupials are Australian, for example the koala and kangaroo, approximately one-third are present in South or Central America where they are generally known as opossums (Rodger, 1991). Major families of marsupials have their own distinct sperm morphology, which has proven to be a useful phylogenetic character (Hughes, 1965; Harding *et al.*, 1987; Temple-Smith, 1987; Rodger, 1991). For example, sperm length varies dramatically between marsupial families, from about 90 µm in some phalangerids and macropodids, to more than 350 µm in the diminutive Western Australian honey possum, *Tarsipes rostratus* (Cummins and Woodall, 1985). Moreover, the structure of the marsupial sperm flagella, particularly that of the midpiece, as well as sperm head form, including nuclear shape and acrosome location, vary between marsupial families (Hughes, 1965; Harding *et al.*, 1987; Temple-Smith, 1987; Rodger, 1991). One of the most striking differences between eutherian and marsupial sperm is the manner of neck insertion into the sperm head, as well as the shape and location of the acrosome (Bedford, 1991; Mate and Rodger, 1991). These differences arise due to the manner of nuclear flattening during spermiogenesis. In eutherians the spermatid nucleus flattens laterally, i.e. in the same plane as the forming flagellum, and the acrosome forms a cap over the apical region of the nucleus. However, in most marsupials, the plane of nuclear flattening is dorsoventral, i.e. at right angles to the flagellum, so that the acrosome comes to lie on the dorsal side of the nucleus (Rodger, 1991). The marsupial

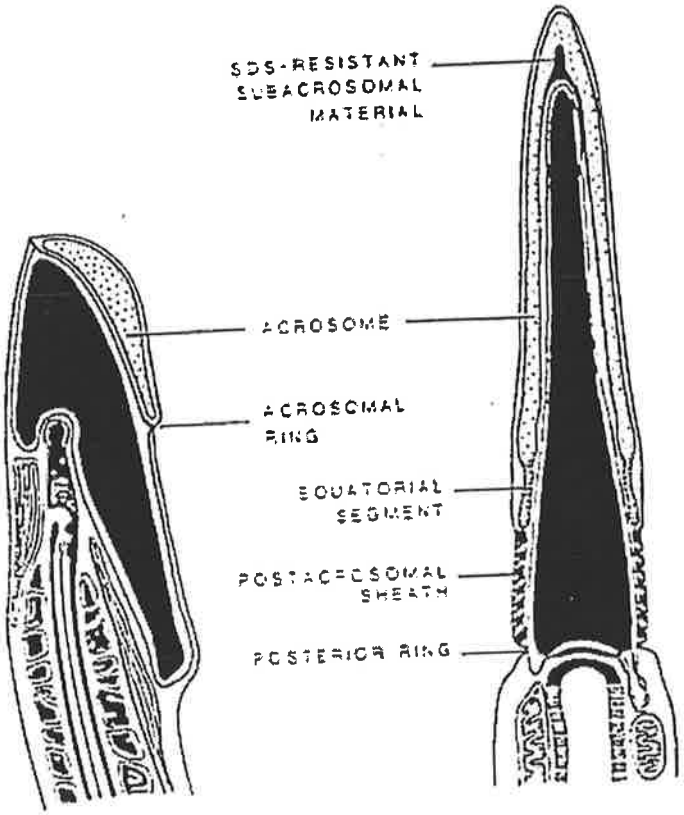

Comparison of the structural specialisations in generalised (a) marsupial and (b) eutherian sperm heads. In the marsupial sperm head the acrosome is located on the dorsal side of the nucleus and the flagellum inserts into the mid-ventral side of the nucleus. In comparison, in typical eutherian sperm the acrosome forms a cap that covers the anterior region of the sperm head.
(Temple-Smith, 1994)

sperm head then rotates approximately 90° as it passes down the epididymis so that its long axis comes to lie parallel to the flagellum; this rotation often begins in the testis but is completed during epididymal transit (Cummins, 1976).

1.5.1 The Marsupial Sperm Head

The marsupial sperm head varies in length from approximately 2 µm in the South American shrew possum, *Rhyncholestes raphanurus*, to 14 µm in the honey possum, *Tarsipes rostratus* (Harding *et al.*, 1982; Taggart and Temple-Smith, 1990; Temple-Smith, 1994). The marsupial sperm head is generally similar to that of eutherians, however there are some striking differences. In marsupials the location of the neck insertion into the nucleus, and the location and form of the acrosome, is unique (Hughes, 1965; Harding *et al.*, 1979). With the exception of koala and wombat sperm, all marsupial sperm are characterized by the insertion of the flagellum into one side of the sperm head nucleus, rather than to its trailing edge (Bedford, 1991). As a result, most marsupial sperm have a distinct dorsal-ventral orientation with the flagellum inserted into the ventral surface of the nucleus. Consequently, in most marsupials, the acrosome is restricted to the dorsal side of the nucleus and does not form a cap over the anterior region of the nucleus, as is the case in typical eutherian sperm (Harding *et al.*, 1979; Temple-Smith, 1994; Bedford, 1991). In addition, in contrast to the typical eutherian sperm head, the marsupial sperm head contains no perinuclear theca, although a very small amount of cytoskeletal material has been reported for the tammar wallaby, *Macropus eugenii* (Lin et al., 1998).

1.5.2 The Marsupial Sperm Flagellum

The marsupial sperm flagellum, like that of the eutherian, has been traditionally divided into four regions – the neck, middle piece, principal piece and endpiece. The basic

structure of the marsupial sperm flagellum appears to be similar to that of eutherians although there are some noticeable differences. For example, the mode of attachment of the connecting piece of the neck to the sperm head is unique to marsupials; the connecting piece is long and straight with an enlarged, rounded capitulum that typically has a 'ball-and-socket' type of connection with the articulation fossa of the nucleus (Temple-Smith and Bedford, 1976, 1980; Harding, 1977; Harding *et al.*, 1979; Temple-Smith, 1994). This type of articulation is thought to facilitate rotational movements of the sperm head on the flagellum during late spermiogenesis, epididymal maturation and passage through the female reproductive system (Harding *et al.*, 1979; Temple-Smith, 1994).

Unusual structural specializations are also present within the midpiece and principal piece of the marsupial sperm flagellum. The midpiece, which varies in length from approximately 4 µm in the caenolestid species to about 80 µm in the honey possum, is characterized by having a mitochondrial sheath and annulus. It varies considerably in shape in different marsupial species, from circular with a simple radial symmetry, which has been proposed as the ancestral condition for marsupial spermatozoa (Temple-Smith, 1987), to ovoid in appearance in the Dasyuridae and especially Tarsipedidae as a result of the extreme displacement of the outer dense fibres from the outer microtubule doublets of the axoneme (Harding *et al.*, 1979; Temple-Smith, 1994).

1.5.3 Cytoskeletal Components of the Marsupial Sperm Flagellum

The cytoskeletal components of the marsupial sperm flagellum include the axoneme, outer dense fibres and fibrous sheath, as well as a unique structure, present to varying degrees in most marsupial species, the midpiece and principal piece fibre network. Connecting

laminae are also sometimes present, particularly in sperm of Dasyurids, Peramelids and Tarsipidids where they are very prominent.

1.5.3.1 Midpiece and Principal Piece Fibre Network

Most marsupial species develop what are considered to be plasma membrane specializations in the posterior midpiece during their passage through the epididymis, with the exception of the koalas, wombats and bandicoots, termed the midpiece fibre network (Harding *et al.,* 1975, 1979; Olson, 1980; Olson *et al.,* 1977; Temple-Smith and Bedford, 1976, 1980; Temple-Smith, 1984, 1987, 1994). The midpiece fibre network consists, in its simplest form, of spirally arranged, parallel fibrous bands that surround the mitochondrial sheath and immediately underlie the midpiece plasmalemma (Harding *et al.,* 1975, 1979; Temple-Smith, 1994). It has been suggested that these fibres are derived from protein aggregations along the cytoplasmic surface of the plasma membrane (Olson *et al.,* 1977; Temple-Smith, 1981; 1994), and freeze-fracture studies have indicated that the fibres are associated with ordered aggregates of intramembranous particles which form parallel rows separated by particle-free spaces (Temple-Smith, 1981, 1994). The exact function of the midpiece fibre network remains unknown, however, on the basis of ultrastructural studies, it has been suggested that it serves a passive stiffening role, strengthening the sperm midpiece and thereby modifying flagellar bending (Harding *et al.,* 1976a, 1979). Another theory suggests that the midpiece fibre network may assist nutrient and energy transport across the unusually thick layer of peri-mitochondrial cytoplasm in the brush-tailed possum or along the exceptionally long flagellum of the honey possum (Temple-Smith, 1994). However, neither of these theories has been substantiated. The fate of the midpiece fibre network is not uniform in all marsupial families; while it is incorporated into the fertilized oocytes in the monodelphid and didelphid (Rodger and Bedford, 1982; Taggart *et al.,*

1993), that of *Sminthopsis crassicaudata* has been reported to be shed on or near the zona pellucida surface and/or within the perivitalline space at fertilisation (Breed and Leigh, 1998, 1992).

In addition to the midpiece fibre network, the principal piece of brush-tail possum spermatozoa also contains a fibrous network immediately beneath the plasmalemma, termed the principal piece fibre network. Unlike the midpiece fibre network, it is formed prior to spermiation and is less regular in its organization (Harding *et al.*, 1975).

1.5.3.2 Marsupial Outer Dense Fibres and Connecting Laminae

To date, very little is known about the marsupial outer dense fibres, with no studies carried out on determination of its protein composition in any species. However, it has been demonstrated that, during epididymal transit, the possum outer dense fibres, as well as midpiece fibre network and fibrous sheath, are stabilized, presumably by disulpide bonding, as evidenced by their greater resistance to disruption by SDS and DTT (Temple-Smith and Bedford, 1976). In addition, ultrastructural studies have demonstrated that, in dasyurid, tarsipedid and peramelid sperm, the midpiece outer dense fibres are radially displaced resulting in the flagella appearing ovoid in shape in cross-section (Harding *et al.*, 1979; Temple-Smith, 1994). In these sperm the outer dense fibres are connected to the axoneme by electron dense 'arms' termed connecting laminae. Connecting laminae were first described in detail for the bandicoot by Cleland and Rothschild (1959). In this species, all but the heart-shaped outer dense fibres 3 and 8 are joined to the axoneme by connecting laminae. Moreover, each lamina, except for the one associated with outer dense fibre 2, appears, in longitudinal section, as long, tenuous, but unbroken filaments (Cleland and Rothschild, 1959). In dasyurid sperm outer dense fibre 1 is also

characteristically displaced from the axoneme in the midpiece, as well as in the principal piece, of the sperm flagellum (Harding *et al.,* 1979). It had been suggested that the resultant outer dense fibre displacement in dasyurid and tarsipedid sperm might be associated with increased sperm length (250 –350 µm) in these marsupial families (Harding, 1977), however this appears unlikely given that the outer dense fibres of numbat (*Myrmecobius fasciatus*) sperm also exhibit radially displacement, yet are relatively shorter in length (140 µm) (Taggart *et al.,* 1995a, b). Instead, the outer dense fibre displacement may be associated with the unusual sinusoidal mode of forward progression of these sperm and/or their mode of sperm-egg interaction and penetration (Taggart and Temple-Smith, 1990; Taggart *et al.,* 1995a, b).

1.5.3.3 Marsupial Fibrous Sheath

In contrast to the outer dense fibres, several studies have examined the marsupial fibrous sheath. The presence of a fibrous sheath, or 'spiral' sheath as it was known at the time, in the marsupial flagellum was initially reported by Retzius (1906), but the first detailed ultrastructural studies of fibrous sheath morphology were carried out for the bandicoot, *Perameles nasuta*, by Cleland and Rothschild (1959) and Sapsford *et al.* (1970). In this species the longitudinal columns occupy the entire length of the principal piece and are joined by ribs that frequently branch and unite with other ribs. In transverse sections of the anterior principal piece of the bandicoot flagellum, the fibrous sheath is diamond-shaped with concave sides, with the thickened regions of the sheath composed of the extremities of the ribs which are unusually expanded (Cleland and Rothschild, 1959). Furthermore, large vacuoles are present within the rib extremities immediately adjacent to the longitudinal columns. Examination of these ribs at higher magnification suggested the presence of circularly orientated filamentous structures approximately 4-5 nm in width, with

similar, but less organized, structures of comparable width also present within the longitudinal columns in parallel with the long axis of the columns (Cleland and Rothschild, 1959; Sapsford *et al.*, 1970).

Recently a monoclonal antibody raised against possum acrosomal proteins and termed PSA-10, has been shown to bind predominantly to the midpiece fibre network and fibrous sheath of both possum and wallaby spermatozoa (Harris and Rodger, 1998). Western blotting of proteins selectively solubilized from marsupial sperm, subsequently suggested that two major possum and wallaby midpiece fibre network proteins have molecular masses of 158 and 182 kDa, whilst a 32 kDa polypeptide was associated with the principal piece network and/or fibrous sheath (Harris and Rodger, 1998). Furthermore, PSA-10 immunoreactivity with the principal piece of a number of mammalian and avian sperm suggests that the PSA-10 antigen may be a conserved fibrous sheath antigen (Harris and Rodger, 1998).

1.6 RESEARCH PROPOSAL

The cytoskeleton of all cells is more than just a structureless medium in which various organelles are suspended. In the sperm cell, cytoskeletal elements are especially unique and complex structures that consist of many proteins. As has been outlined above, the mammalian sperm flagellum contains three prominent cytoskeletal structures, the axoneme, outer dense fibres and fibrous sheath. Whilst the axoneme, via its sliding microtubules, is actively involved in sperm motility, the outer dense fibres and fibrous sheath are thought to play important, but as yet undefined, supportive roles. Most of what is known of the outer dense fibres and fibrous sheath, namely their structure, morphogenesis, protein composition, and most importantly, potential function, has been obtained from studies of these structures in eutherian species, particularly the laboratory rat. In marsupials, although some attempt has been made to isolate and characterize the proteins within the putative sperm head subacrosomal space, very little is known of the flagellar cytoskeletal structures despite the fact that, in some species, sperm movement patterns are distinctive, and additional unique elements like the midpiece fibre network and connecting laminae are present which may supplement and/or assist the outer dense fibres and fibrous sheath. Furthermore, whilst immunocytochemical and sequencing studies have demonstrated that some of the outer dense fibre and fibrous sheath proteins are conserved between eutherian species, it remains to be seen whether or not this evolutionary conservation extends from eutherians to marsupials which diverged from a common ancestor approximately 100 million years ago. Clearly, a detailed investigation of the basic structure and composition of these sperm flagellar cytoskeletal structures in a marsupial species is required if questions such as these are to be satisfactorily answered.

1.6.1 General Aims and Questions

The general aim of this thesis was to characterize morphologically, immunocytochemically and biochemically, the outer dense fibres and fibrous sheath of the marsupial sperm flagellum. The Australian marsupial species selected was the brush-tail possum, *Trichosurus vulpecula*, chiefly because it was the only marsupial species from which the quantity of tissue required for this investigation could be obtained. This study of outer dense fibre and fibrous sheath form and function was undertaken to try to determine:

- how they are formed during spermiogenesis.
- their protein composition.
- whether proteins identified are unique to the cytoskeletal structures and are conserved across both marsupials and eutherian mammals.

1.6.2 Specific Questions

To meet these aims, the objectives of the ensuing chapters of this thesis were to:

- describe the stages of spermiogenesis and germ cell associations in the possum seminiferous tubules so that the morphogenesis of the outer dense fibres and fibrous sheath can be described in detail.
- develop techniques to isolate, purify and solubilize the marsupial sperm outer dense fibres and fibrous sheath so that the protein composition of these cytoskeletal structures could then be determined by SDS-PAGE.
- raise antibodies against outer dense fibre and fibrous sheath proteins and use this antisera to determine whether, or not, proteins are unique to each cytoskeletal structure, and whether they are conserved across marsupial species, as well as between marsupials and eutherians.

- use antibodies prepared against eutherian outer dense fibre and fibrous sheath proteins to test for conservation of these proteins in marsupials.

Chapter 2

GENERAL MATERIALS AND METHODS

2.1 EXPERIMENTAL ANIMALS

The use of all animals for the research reported in this thesis was approved by the Animal Ethics Committee of The University of Adelaide. Furthermore, a South Australian National Parks and Wildlife Service permit was obtained for the collection of protected specimens. All research was conducted in the Department of Anatomical Sciences under ethics approval number 3/63/98.

The following Australian marsupial species were used: brush-tail possum (*Trichosurus vulpecula*), tammar wallaby (*Macropus eugenii*), koala (*Phascolarctus cinereus*), and fat-tailed dunnart (*Sminthopsis crassicaudata*). All of these animals, with the exception of the dunnarts, were obtained from wild populations. The possums were trapped locally and housed at the Central Animal House of The University of Adelaide where they were fed a diet of mixed cereal and fruit daily and water was available at all times. They were housed under regulated temperature conditions of 18-25°C and a lighting regime of 12 hours light: 12 hours dark. Animals required for experimentation were delivered to the Medical School Animal House of the University of Adelaide and utilized either immediately or within 24-48 hours; those that needed to be housed locally were kept in conditions identical to those described above. Wallaby tissue was obtained during licensed culls on a private property near Kingscote on Kangaroo Island in South Australia in 1997 and 1999, whilst koala

material was obtained from injured animals, for example due to road accidents, from the Adelaide Hills that were destined for euthanasia. Dunnart tissue was obtained from a colony bred and housed at the Central Animal House under a lighting regime identical to that for possums. The dunnarts were fed a diet of mouse cubes (Milling Industries, Mile End, SA) supplemented with mixed seed and fresh apple twice weekly and water was available at all times.

2.2 PREPARATION OF TISSUES FOR ROUTINE LIGHT AND TRANSMISSION ELECTRON MICROSCOPY

Possums were euthanased by CO_2, wallabies were shot, and koalas and dunnarts were killed by injection with an overdose of sodium pentobarbitone (koalas: ~20 ml of Lethabarb, Virbac, Peakhurst, NSW; dunnarts: ~200 µL of Nembutal, Rhone Merieux, Pinkenba, QLD). The epididymides were immediately dissected free, minced with scissors in 5 ml 0.2 M phosphate-buffered saline (PBS), pH 7.4, and incubated at room temp for 10 min to allow the spermatozoa to disperse into the buffer. The sperm suspension was washed twice in PBS by centrifugation at 700 *g* for 10 min and the resultant pellet was either first experimentally treated or otherwise immediately fixed for routine transmission electron microscopy in 3% glutaraldehyde / 3% paraformaldehyde made up in 0.2 M phosphate buffer, pH 7.4 for 2 h. The testes were also excised, cut into small pieces (~5mm^3), immersed in the above fixative for 2 h, cut into smaller cubes (~1-2 mm^3), and reimmersed in fixative for an additional 2 h. Occasionally it was necessary to obtain tissue from perfuse-fixed possums and, in these cases, animals were anaesthetized with isofluorane (4%, 1.5 L/min, DBL, Mulgrave, Victoria), and the testes and epididymides were fixed by vascular perfusion through the abdominal aorta. The vascular system was first rinsed with heparinized physiological saline containing 2.5% polyvinyl pyrolidone and 0.5% procaine hydrochloride until blood outflow had ceased, followed by perfusion with 3%

paraformaldehyde / 3% glutaraldehyde in 0.1 M phosphate buffer, pH 7.4, containing 2.5% polyvinyl pyrolidone for 5-10 min or until blood vessels visible in the testes had cleared. The testes and epididymides were dissected free, cut into small cubes (~1 mm^3), and immersed in the above fixative for 2 h. Immersion and perfusion fixed tissue was rinsed in two changes of 0.1 M phosphate buffer, pH 7.4, for 10 min each, and post-fixed in 1% osmium tetroxide in PBS, pH 7.4, for 1 h. Tissue was dehydrated by passing through a graded series of ethanols, cleared in two changes of propylene oxide, and infiltrated in a 1:1 ratio of propylene oxide:resin overnight. The tissue was embedded in pure resin (TAAB TK3, TAAB Laboratories, Berkshire) and blocks were polymerised at 60°C for at least 48 h. Thick (0.5-1.0µm) plastic sections were cut using a Reichert-Jung Ultracut ultramicrotome with a glass knife and stained with 0.25% toluidine blue in 0.5% sodium tetraborate prior to viewing under an Olympus BH-2 light microscope. Areas of interest were selected from the thick plastic sections, the blocks trimmed, and ultrathin sections of silver/gold interference colours (0.02-0.1 µm) were then cut using a diamond knife (Diatome Ltd, Bienne, Switzerland). Sections were collected onto copper/palladium grids (200 mesh), stained with uranyl acetate and lead citrate, and viewed with a Phillips CM100 transmission electron microscope at 80 kV.

For routine light microscopy tissues were prepared for paraffin embedding. Animals were euthanased as described above and testes and epididymides were dissected free, cut into cubes (~1cm^3) and immersion fixed in Bouin's solution for at least 24 h. Tissues were dehydrated by passing through a series of ethanols, cleared in Safsolv (Ajax Chemicals, Adelaide), and infiltrated with molten paraffin wax (Paraplast Plus, St Louis, Missouri) before embedding in fresh paraffin wax. Blocks were sectioned at 5-7 µm using a Reichert-Jung Biocut rotary microtome, sections were floated onto a warm water bath, collected

onto glass slides pre-coated with albumin, and dried in an oven at 37°C overnight. Sections required were subsequently dewaxed, rehydrated and experimentally treated (as described in subsequent chapters) if necessary, and stained with Haemtoxylin and Eosin (H&E) unless otherwise indicated.

Chapter 3

MORPHOGENESIS OF THE OUTER DENSE FIBRES AND FIBROUS SHEATH

3.1 INTRODUCTION

An important first step in characterising the outer dense fibres and fibrous sheath is to understand how they are formed during spermiogenesis. In eutherian mammals, early studies of spermiogenesis typically focussed on the development of components of the sperm head, rather than tail (e.g. Challice, 1952; de Krester, 1969). The first comprehensive investigation of outer dense fibre and fibrous sheath development was conducted for the laboratory rat by Irons and Clermont (1982a, b). In their ultrastructural studies, outer dense fibre formation was shown to proceed in a proximal-to-distal direction along the axoneme throughout most of spermiogenesis (Irons and Clermont, 1982a). In contrast, the longitudinal columns and circumferential ribs of the fibrous sheath were found to assemble independently of each other in a distal-to-proximal direction throughout most of spermiogenesis (Irons and Clermont, 1982b).

Prior to the current study, the morphogenesis of the outer dense fibres and fibrous sheath in marsupial species had only been examined for the long-nosed bandicoot (*Perameles nasuta*) (Sapsford *et al.*, 1967, 1969, 1970). Outer dense fibre and fibrous sheath formation in this species is similar to that for the rat. Aside from these early observations in a bandicoot species, there is virtually no published information on the morphogenesis of

either the outer dense fibres or fibrous sheath for any other marsupial species. Furthermore, considering how different in appearance sperm tails from bandicoot and possum are (see 1.5.3), one cannot presume that the assembly of these structures are similar between these species. Therefore, the aim of the current chapter is to describe, by transmission electron microscopy, the morphogenesis of the possum sperm outer dense fibres and fibrous sheath. In order to satisfactorily meet this objective, however, it will be necessary to first clearly define the individual stages of possum spermiogenesis so that the assembly of the outer dense fibres and fibrous sheath can be properly traced during this time.

3.2 MATERIALS AND METHODS

3.2.1 Transmission Electron Microscopy

Brush-tail possum testes were obtained, processed and stained for routine transmission electron microscopy (TEM) as described in detail in *Chapter 2: General Materials and Methods*. Briefly, testes from eight adult males were perfused and then immersion fixed in 3% glutaraldehyde/3% paraformaldehyde in 0.2 M phosphate buffer, tissue was cut into 2 mm^3 cubes, reimmersed in fixative for 2 h and embedded in epoxy resin. Thick (1 µm) plastic sections were cut with a glass knife on a microtome, stained with 0.025% toluidine blue in 0.5% sodium tetraborate and viewed under a phase light microscope. Thin (70-90 nm) sections of suitable regions of the testes were then cut on a diamond knife, placed on copper/palladium grids, stained with uranyl acetate and lead citrate and viewed on a Phillips CM 100 TEM at a voltage of 80 or 100 kV.

At least two different sections from each of six different possum testes were examined to ensure that results obtained were consistent and reproducible.

3.2.2 Criteria For Differentiating Possum Spermatids

In order to describe the assembly of the outer dense fibres and fibrous sheath throughout spermiogenesis, the different 'steps' of possum spermatid development will first be described based on the following criteria (Russell *et al.*, 1990):

(1) *Extent of acrosome development:*

Acrosomal material, which arises from the Golgi Apparatus, forms a vacuole that may, or may not, contain an electron dense granule. The acrosomal vacuole comes to lie in close contact with part of the outer nuclear envelope and may indent the nucleus. The acrosomal vacuole spreads over the anterior one-third to two-thirds of the nucleus, and condenses to form the acrosome.

(2) *Extent of chromatin condensation:*

During spermiogenesis, histones within the nucleus are gradually removed and replaced, initially by intermediate proteins, and then by protamines, which package the DNA extremely tightly. Associated with these changes in nuclear proteins, there is (a) a reduction in nuclear volume, and (b) condensation of the chromatin so that it appears increasingly electron dense by transmission electron microscopy. During this period, the nucleus also undergoes major shape changes.

(3) *Extent of manchette and nuclear ring development:*

The manchette typically appears from around mid-spermiogenesis near the lateral surface of the nuclear envelope. It steadily increases in size as the nucleus condenses and elongates. The manchette microtubules appear to emanate from the nuclear ring, which is a band of electron dense material that accumulates on the cytoplasmic side of

the plasma membrane. The manchette increases in prominence as spermiogenesis progresses but disappears prior to spermiation.

3.3 RESULTS

3.3.1 Steps of Possum Spermiogenesis

Low power light microscopic analysis of thick plastic sections of possum testes stained with Toluidine blue revealed nine, clearly distinguishable spermatid associations or 'stages' (Figure 3.1). Spermatid differentiation was subsequently classified into 12 unique 'steps' based on the extent of development of the acrosome, nucleus and manchette. In addition, the appearance of mature spermatozoa within the lumen of the seminiferous tubules at spermiation is described.

In the following description of spermiogenesis, the dorsal side of the nucleus refers to the side on which the acrosome resides, whereas the ventral side is that to which the flagellum attaches.

Step 1 spermatid:
(Figure 3.2a)

Spermatids were roughly spherical in shape and resided close to the lumen of the seminiferous tubules. The nuclei were round and contained fine granular chromatin spread evenly throughout the nucleus. Mitochondria and rough endoplasmic reticulum were uniformly distributed throughout the cytoplasm with a prominent Golgi Apparatus located adjacent the nucleus. In most of these spermatids, one to five small membrane bound proacrosomal vesicles were closely associated with, and presumably arose from, the Golgi Apparatus. These vesicles appeared devoid of material.

Step 2 spermatid:
(Figure 3.2b)

Nuclei remained spherical and composed of granular chromatin, and organelles, with the exception of the Golgi Apparatus, were uniformly distributed throughout the cytoplasm. Most of the small proacrosomal vesicles present in the Step 1 spermatids have fused into a single, large membrane bound acrosomal vesicle located adjacent the nucleus. This vesicle also appeared to be devoid of material. A distal centriole can be seen adjacent to the nucleus, almost directly opposite the site of the acrosomal vacuole in the cytoplasm (see insert). The axoneme of the flagellum extends away from this centriole (see insert).

Step 3 spermatid:
(Figure 3.3a)

The acrosomal vesicle became opposed to the outer nuclear envelope, indenting it slightly. The acrosomal and nuclear membranes in contact with one another are intensely stained. The nuclei remained roughly spherical, although the granular chromatin within began to accumulate in clumps rather than being uniformly dispersed as it had been in the previous steps.

Step 4 spermatid:
(Figure 3.3b)

The acrosomal vesicle, which still appeared devoid of material, had reached its maximal size and further depressed one side of the nucleus. The region of contact between the inner acrosomal membrane and nuclear envelope remained electron dense. The nucleus was still spherical in shape, however the chromatin was further condensed into larger, localised regions. The flagellum continued to extend away from the nucleus (not shown).

Step 5 spermatid:
(Figure 3.4.a)

This step was characterised by the collapse of the acrosomal vesicle and the associated dorsal protrusion of the nucleus towards the region of contact between the outer acrosomal membrane and the spermatid plasmalemma. The remainder of the nucleus was no longer circular in shape but instead had begun to bilaterally flatten so that it was ovoid-like in shape. The nuclear chromatin continued to condense in an irregular pattern throughout the entire nucleus although this was more prominent adjacent the acrosomal vesicle. Cytoplasm was sparse on the apical and lateral sides of the nucleus as most of the organelles had migrated to the region around the extending flagellum.

Step 6 spermatid:
(Figure 3.4b)

The acrosome had completely collapsed over the apical third of the nucleus. Microtubules appeared within the cytoplasm of the spermatid around the caudal half of the nucleus to form the manchette, which extended some distance into the infranuclear cytoplasm. Ectoplasmic specialisations, termed *Sertoli cell spurs* for marsupials by Sapsford *et al.*, (1969), first appeared as bilateral bands of electron dense material within the Sertoli cell cytoplasm overlying, and projecting away from, the acrosome. The extent of chromatin condensation was now uniform throughout the entire nucleus.

Step 7 spermatid:
(Figure 3.5a)

The dorsal surface of the nucleus projected further into the central portion of the acrosome, towards the Sertoli cell cytoplasm. The remainder of the nucleus had begun to flatten in a dorso-ventral, rather than bilateral, plane. Chromatin condensation was granular and homogeneous throughout most of the nucleus although several electron-lucent foci were evident. The proximal tips of the manchette microtubules were attached to

the nuclear ring, which, in longitudinal sections, formed a circular trough of electron dense material just lateral to the outer margins of the acrosome. The Sertoli cell spurs further extended into the Sertoli cell cytoplasm.

Step 8 spermatid:
(Figure 3.5b)

This step was characterised by the marked dorso-ventral flattening of the spermatid nucleus. Chromatin condensation continued, however it did not completely extend to the ventral margin of the nuclear envelope. This region, between the nuclear ring and connecting piece of the flagellum, was instead occupied by fine granular material. Several electron-lucent foci remained within the nucleus. The acrosome remained in close contact with the nucleus over most of its dorsal surface, and the nuclear ring increased in size and electron density.

Step 9 spermatid:
(Figure 3.6a)

From this stage onwards, the dorso-ventral flattening of the nucleus was uneven, resulting in the nucleus appearing somewhat triangular in shape. Moreover, the nucleus began to rotate so that its long axis approached that of the flagellum. Nuclear chromatin was almost completely condensed and electron lucent foci were no longer evident. The acrosome remained closely opposed to the dorsal surface of the nucleus with only a very narrow subacrosomal space present.

Step 10 spermatid:
(Figure 3.6b)

This step was characterised by the partial relocation of the acrosome to the apical region of the dorsal surface of the nucleus. It was associated with a considerable enlargement of

part of the underlying subacrosomal space. The nuclear ring migrated with the acrosome and the manchette remained attached to it.

Step 11 spermatid:
(Figure 3.7a):

The spermatid nucleus was now lying nearly parallel to the flagellum giving the cell a streamlined appearance. The anterior region of the acrosome projected away from the nucleus towards the Sertoli cell cytoplasm as the acrosome and nuclear rings migrated further towards the apical third of the dorsal side of the nucleus. The concave-shaped subacrosomal space migrated forward with the acrosome and contained some electron dense material. Mitochondria began to accumulate around the axoneme in the proximal segment of the flagellum. Sertoli cell spurs were no longer present.

Step 12 spermatid:
(Figure 3.7b):

Both the anterior and posterior regions of the acrosome now projected into deep concavities of the Sertoli cell plasma membrane. Consequently, the acrosome was markedly thinner in transverse section in these cells. The subacrosomal space was reduced and the nuclear ring was absent. Mitochondria completely surrounded the most proximal segment of the axoneme of the flagellum forming the mitochondrial sheath.

Spermatozoon at spermiation
(Figure 3.8):

Nuclei of spermatozoa in the process of being released from the seminiferous epithelium, had rotated 90 degrees to lie perpendicular to the flagella, resulting in cells having a 'T' shape. The anterior and posterior acrosomal extensions protruded further from the apical end of the dorsal surface of the nucleus, however the subacrosomal space was no longer discernable. The mitochondrial sheath was completely formed and a distinct cytoplasmic droplet was evident adjacent the connecting piece.

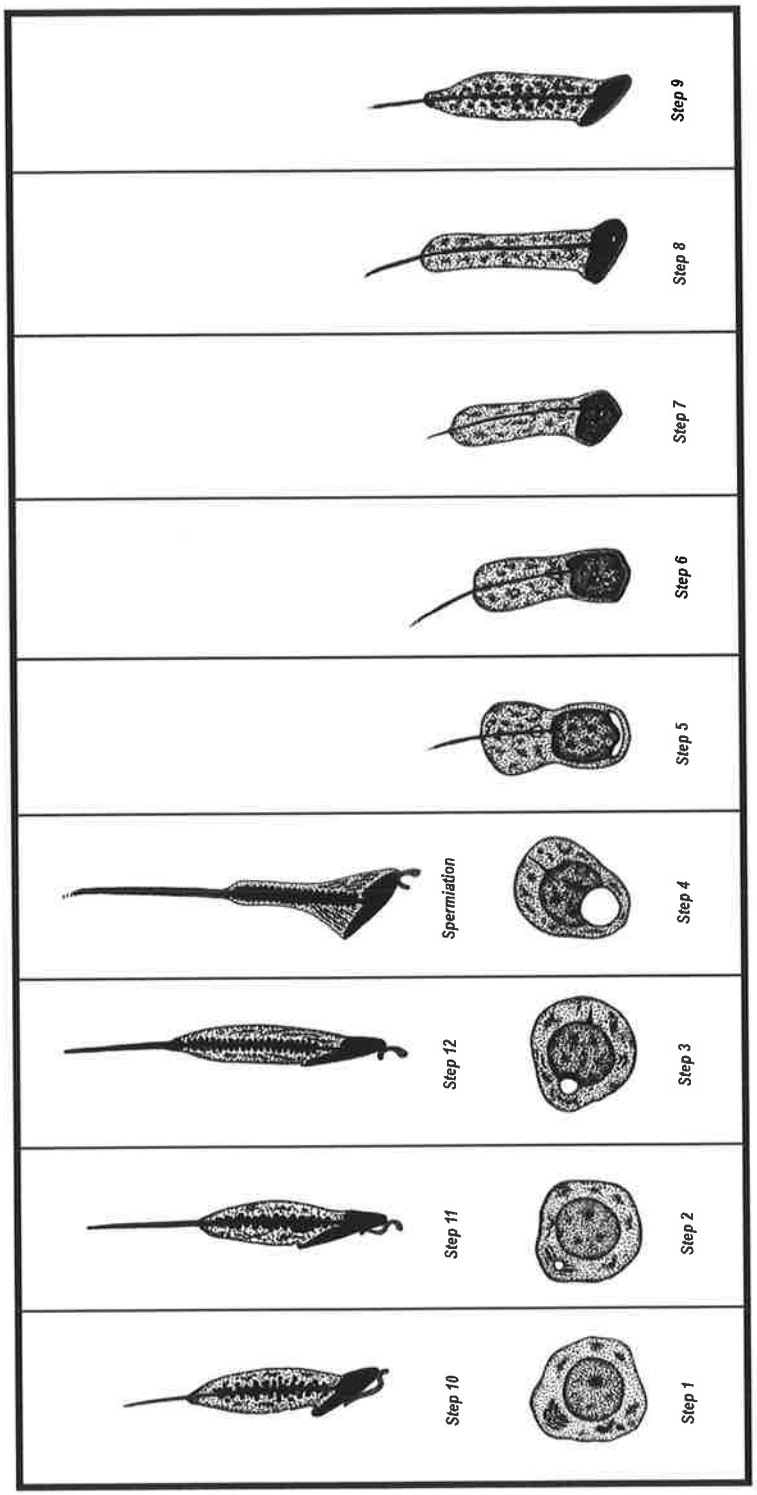

FIGURE 3.1 Diagrammatic illustration of the morphological changes of each of the 12 possum spermatid steps, and spermatozoon at spermiation, organised into 9 basic cellular associations.

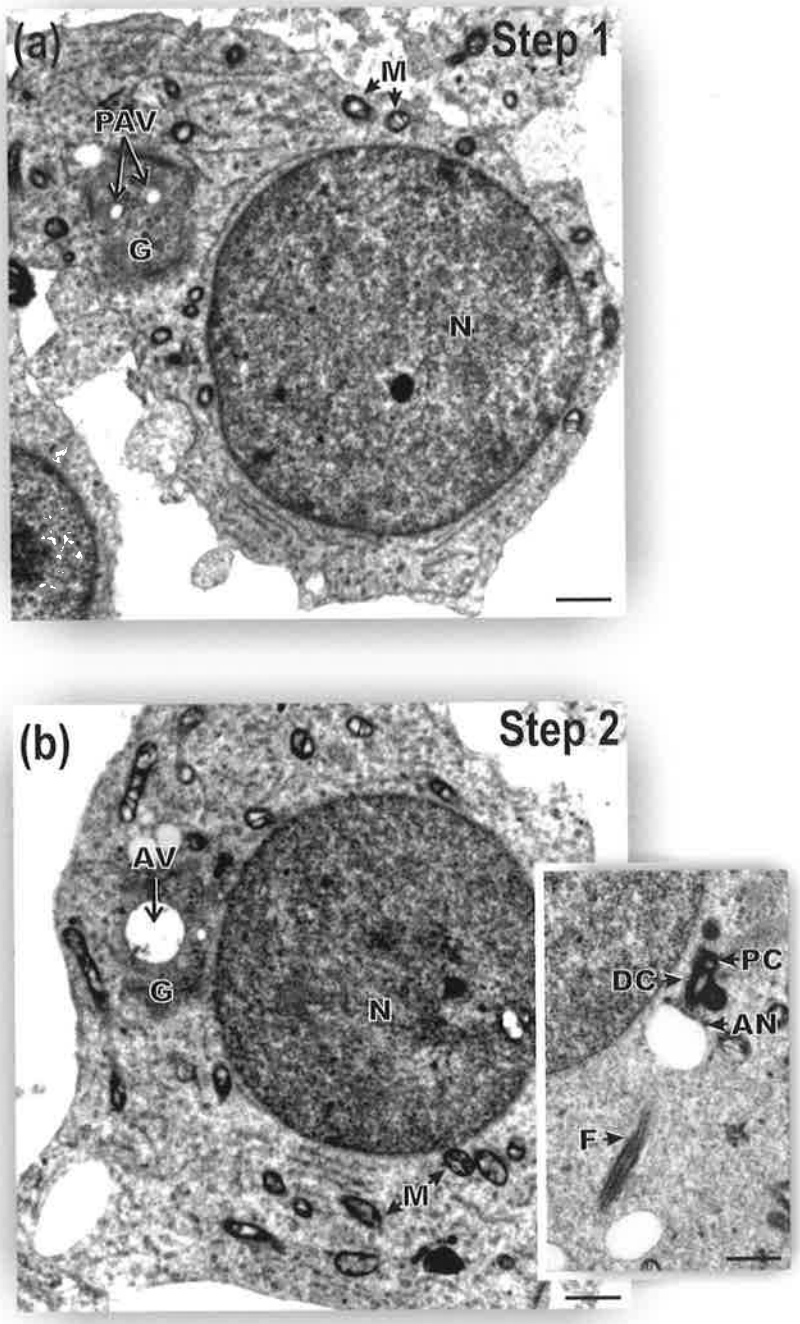

FIGURE 3.2 Electron micrographs showing (a) step 1 and (b) step 2 possum spermatids. (a) Several small proacrosomal vesicles (PAV) are present associated with the Golgi Apparatus (G). The nucleus (N) is circular and contains homogeneous chromatin. (b) A large, single acrosomal vesicle (AV) is present. (Insert) The proximal centriole (PC), distal centriole (DC) and early annulus (AN) of the developing flagellum (F) are evident.
Mitochondria (M).
Scale bars: (a) 0.8 μm, (b) 0.8 μm, (insert) 0.5 μm

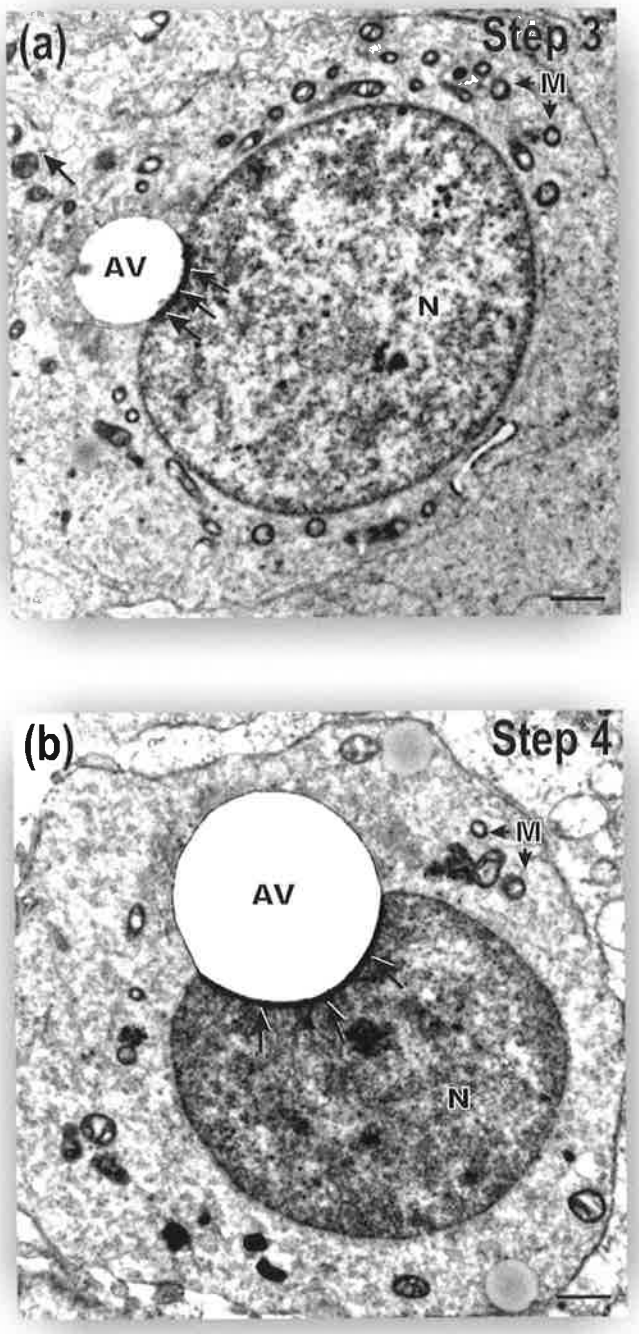

FIGURE 3.3 Electron micrographs showing (a) step 3 and (b) step 4 possum spermatids. (a) The acrosomal vesicle (AV) is apposed to the outer nuclear envelope and indents the nucleus (N) slightly. The regions of contact between the outer acrosomal and nuclear membranes is intensely stained (arrows). Major organelles, such as the mitochondria (M), are randomly distributed throughout the cytoplasm. (b) The acrosomal vesicle has reached its maximal size but appears devoid of material.
Scale bars: (a) 0.8 μm, (b) 0.8 μm

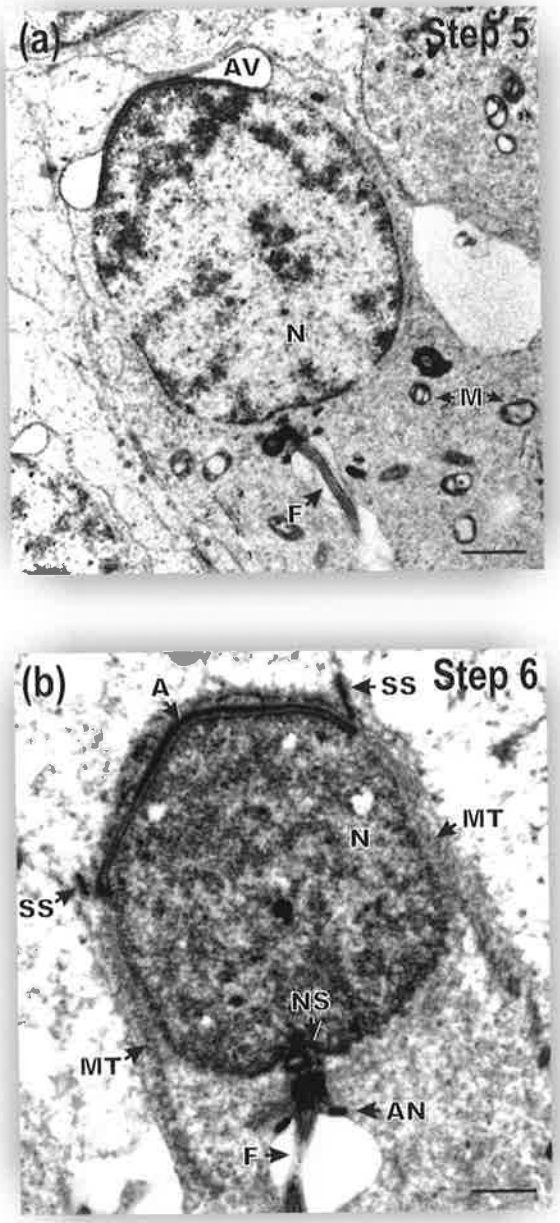

FIGURE 3.4 Electron micrographs showing (a) step 5 and (b) step 6 possum spermatids. (a) The acrosomal vesicle collapsed over the rostral surface of the spermatid nucleus (N), which appeared to migrate towards the region of contact between the outer acrosomal membrane and spermatid plasma membrane. The flagellum (F) extends further from the nucleus and is surrounded by most of the spermatid cytoplasm. Nuclear chromatin has begun to condense in irregular patches. (b) The acrosome (A) is completely flat over the dorsal third of the nucleus. Sertoli cell spurs (SS) appear lateral to the acrosome, and the manchette (MT) is present lateral to the nucleus. Condensation of nuclear chromatin is less irregular. Annulus (AN), Nuclear socket (NS).
Scale bars: (a) 1 μm, (b) 1.2 μm

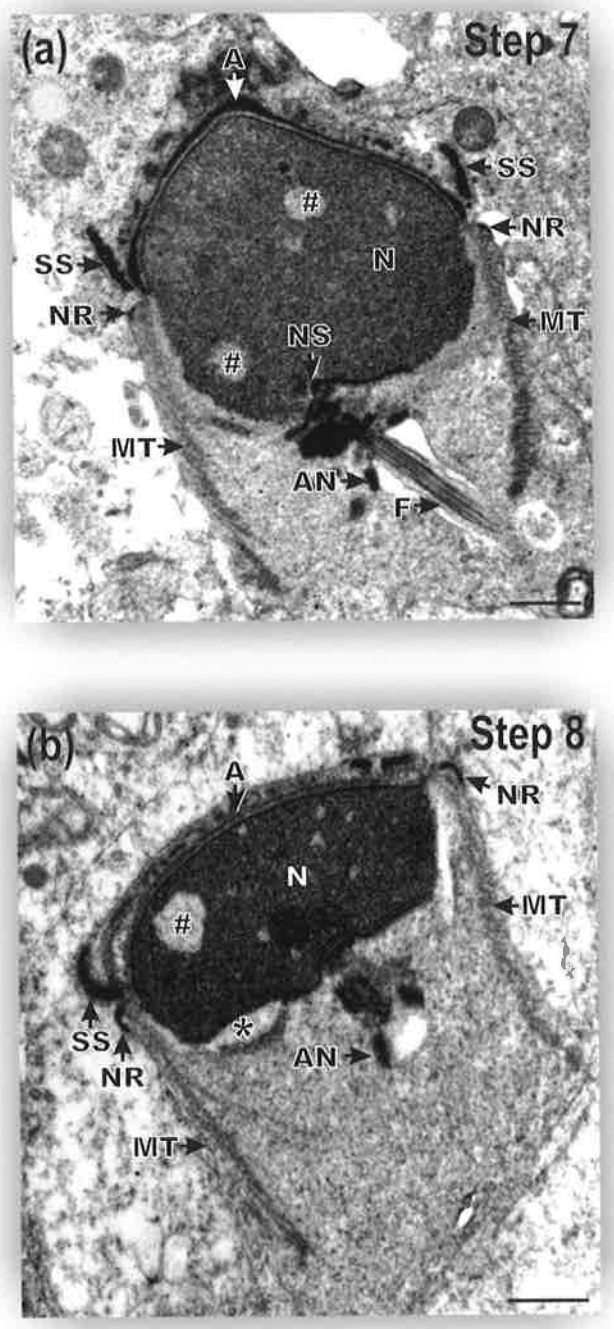

FIGURE 3.5 Electron micrographs showing (a) step 7 and (b) step 8 possum spermatids. (a) The dorsal side of the nucleus (N) is conical in shape. Chromatin condensation is fine and even throughout most of the nucleus although several less electron-dense foci (#) are present. Sertoli cell spurs (SS) and the manchette (MT) are prominent, and the nuclear ring (NR) is evident just caudal to the acrosome (A). Flagellum (F), Nuclear socket (NS). (b) The nucleus is dorso-ventrally flattened. A small portion of the nucleus adjacent to the nuclear socket remains uncondensed (*).
Scale bars: (a) 0.5 μm, (b) 0.6 μm

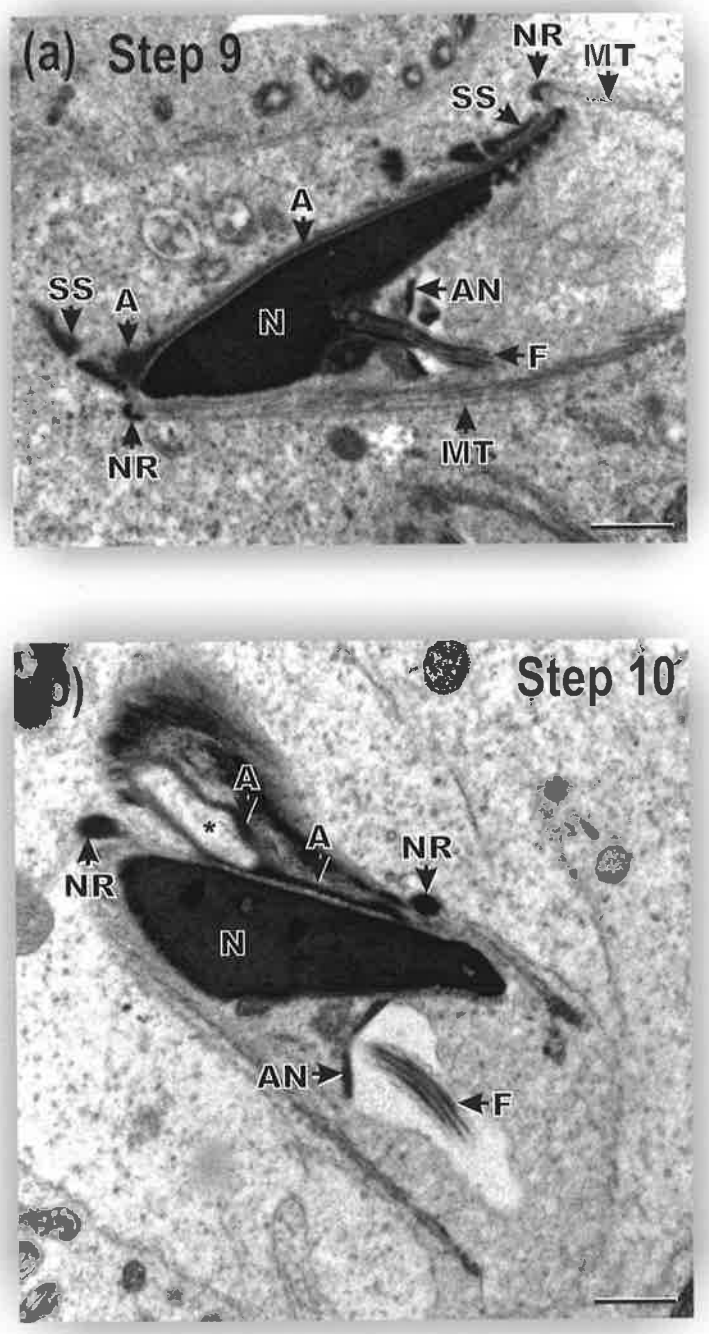

FIGURE 3.6 Electron micrographs showing (a) step 9 and (b) step 10 possum spermatids. (a) The nucleus (N) is almost triangular in shape and its long axis has begun to rotate towards that of the flagellum (F). The acrosome (A) is closely apposed to the entire dorsal surface of the nucleus. (b) The subacrosomal space (*) between the acrosome and nucleus is enlarged at the apical end of the dorsal side of the nucleus.
Annulus (AN), Flagellum (F), Nuclear ring (NR), Sertoli cell spurs (SS).
Scale bars: (a) 0.8 µm, (b) 0.8 µm

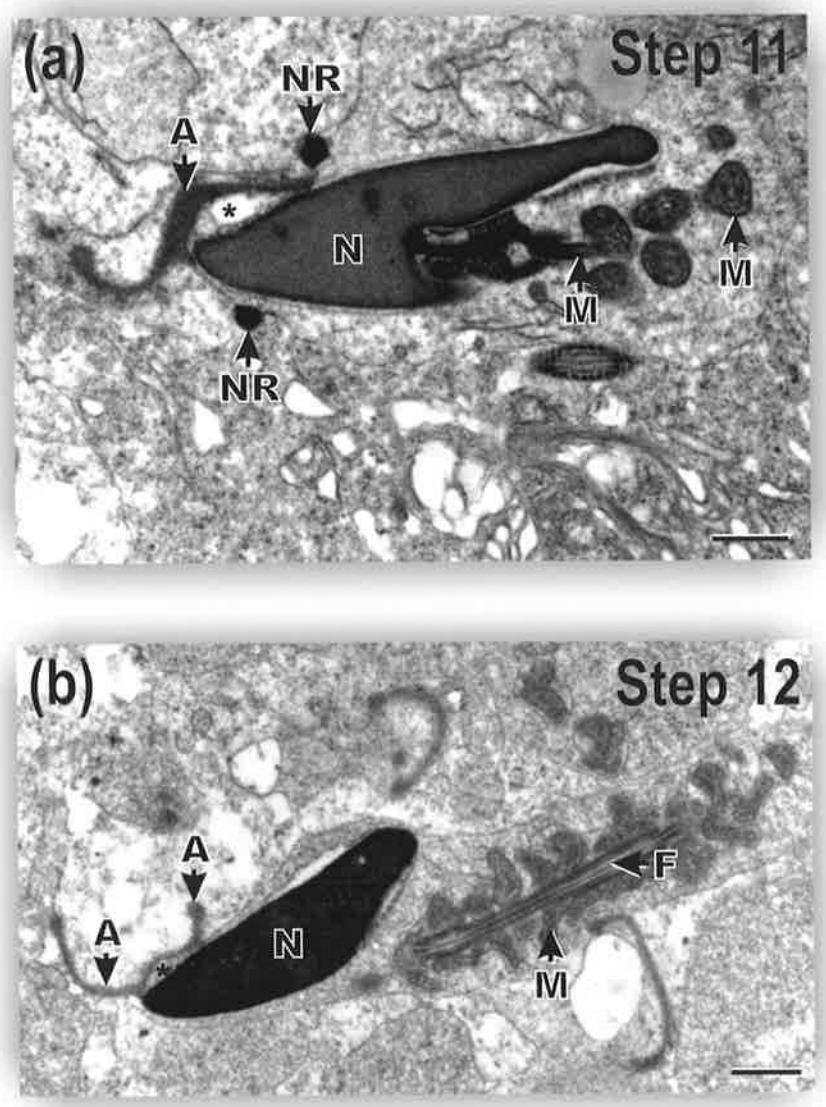

FIGURE 3.7 Electron micrographs showing (a) step 11 and (b) step 12 possum spermatids. (a) The nucleus (N) is now parallel to the flagellum. The apical end of the acrosome (A) projects away from the nucleus and toward the Sertoli cell membrane. Mitochondria (M) have now accumulated within the midpeice. (b) Both the anterior and posterior segments of the acrosome extend away from the dorsal side of the nucleus. The subacrosomal space (*) is reduced in size. Mitochondria completely surround the axoneme of the flagellum (F) within the midpiece.
Nuclear ring (NR).
Scale bars: (a) 0.5 μm, (b) 0.7 μm

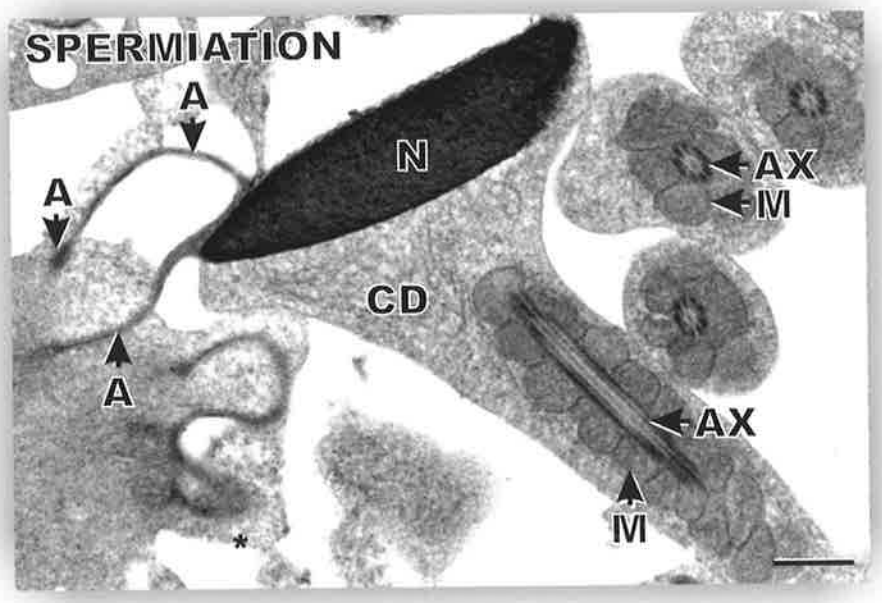

FIGURE 3.8 Electron micrographs of a spermatozoon being released from the seminiferous epithelium (spermiation). The long axis of the nucleus (N) is now perpendicular to that of the flagellum. The lateral extensions of the acrosome (A) remain embedded within the Sertoli cell cytoplasm. A cytoplasmic droplet (CD) is located adjacent the connecting piece of the flagellum.
Axoneme (AX), Mitochondria (M).
Scale bar: (a) 0.7 µm

3.3.2 Morphogenesis of the Outer Dense Fibres and Fibrous Sheath

During steps 1-3 of spermiogenesis, the axoneme of the flagellum had begun to develop from the distal centriole in the spermatid cytoplasm adjacent to the nucleus (Figure 3.2b insert). By the end of step 3, the '9+2' pattern of microtubules of the axoneme was present along the entire length of the extending flagellum (not shown). Although some electron dense material was found between the axoneme and plasmalemma at this stage, precursors to the outer dense fibres and fibrous sheath were not yet evident (Figure 3.9a).

The assembly of the fibrous sheath first began in step 4 spermatids at the distal end of the flagellum which was located within the lumen of the seminiferous tubule. In transverse sections of this part of the flagellum, electron dense material accumulated in the region between the plasmalemma and microtubule doublets 3 and 8 of the axoneme, forming the anlagen of the longitudinal columns (Figure 3.9b). In step 5 spermatids, the anlagen of the longitudinal columns had increased in length, extending in a proximal direction along the flagellum, however precursors to the outer dense fibres had not yet developed (not shown).

In step 6 spermatids a considerable amount of electron dense material had accumulated beneath the plasmalemma in the distal segment of the flagellum, and was attached to the margins of each of the thickening anlagen of the longitudinal columns (Figure 3.10a). In longitudinal sections, this electron dense material was found to be composed of a series of parallel, evenly spaced striations, which appeared to be circumferentially orientated and, therefore, are presumed to be the anlagen of the circumferential ribs of the fibrous sheath (Figure 3.10b, c).

Concurrent with the formation of the rib anlagen in step 6 spermatids, was the appearance, for the first time during spermiogenesis, of the anlagen of the outer dense fibres in the proximal segment of the flagellum (Figure 3.11). They appeared intermittent along this segment of the axoneme as electron dense masses immediately adjacent the outer microtubule doublets (Figure 3.11). In step 7 spermatids, the anlagen of the outer dense fibres extended distally along the flagellum, in the opposite direction to the anlagen of the fibrous sheath which extended proximally (Figure 3.12).

In step 8 spermatids, electron dense material accumulated between adjacent pairs of the rib anlagen along the developing principal piece of the flagellum (Figure 3.13a). Subsequently, these structures thickened and began to resemble mature ribs for the first time. During step 9, there was additional coalescence of adjacent rib anlagen to form the larger, definitive ribs of the fibrous sheath (Figure 3.13b). The number of rib anlagen that fused at this stage ranged from 2-3 in the most distal segment of the developing principal piece of the flagellum, to 6-12 in the most proximal segment, so that the developing fibrous sheath was considerably larger in the latter region. These ribs were united at each of their ends to the longitudinal columns which simultaneously thickened and grew in a distal-to-proximal direction adjacent to the axoneme (Figure 3.13b).

During step 10, the rib anlagen appeared to have been laid down in advance of the anlagen of the longitudinal columns and fibrous sheath within the proximal segment of the flagellum (Figure 3.14a, b). Consequently, the rib anlagen appeared 'zipper-like' in longitudinal section (Figure 3.14b). Completion of fibrous sheath assembly in this segment of the flagellum was brought about by the gradual growth of the longitudinal columns and

further thickening and coalescence of adjacent rib anlagen during the subsequent steps of spermiogenesis.

During steps 10 (not shown) and 11, the outer dense fibres continued to assemble in a distal direction along the axoneme of the developing principal piece of the flagellum (Figure 3.15a). Furthermore, the longitudinal columns of the fibrous sheath appeared considerably larger than in previous steps, although the newly formed circumferential ribs were conspicuously electron lucent, perhaps reflecting their early state of development (Figure 3.15a). These ribs projected away from the axoneme giving the flagellum an ovoid cross-sectional shape. In longitudinal sections, adjacent ribs were found to continue to coalesce and thicken (Figure 3.15b). In the proximal segment of the developing principal piece of step 11 spermatids, fusion of adjacent rib anlagens associated with the appearance of small, electron-lucent spaces within the longitudinal columns of the fibrous sheath (Figure 3.16).

Step 12 of spermiogenesis was characterised by the rapid enlargement of the outer dense fibres. This was especially pronounced within the midpiece of the flagellum where each outer dense fibre became approximately equal in size (Figure 3.17a). In contrast, in the principle piece, outer dense fibres 1, 5 and 6 were most developed and assumed a kidney-like shape in transverse section (3.17c). The remaining outer dense fibres were significantly smaller, but nevertheless still discernable (Figure 3.17c), although fibre 4 was indistinguishable from the outer microtubules of the axoneme in the distal segment of the principle piece (not shown). During this period, the fibrous sheath continued its gradual increase in size (Figure 3.17b). Growth of the outer dense fibres and fibrous sheath during

spermiation was minimal, although the fibrous sheath appeared to increase in electron density (Figure 3.18).

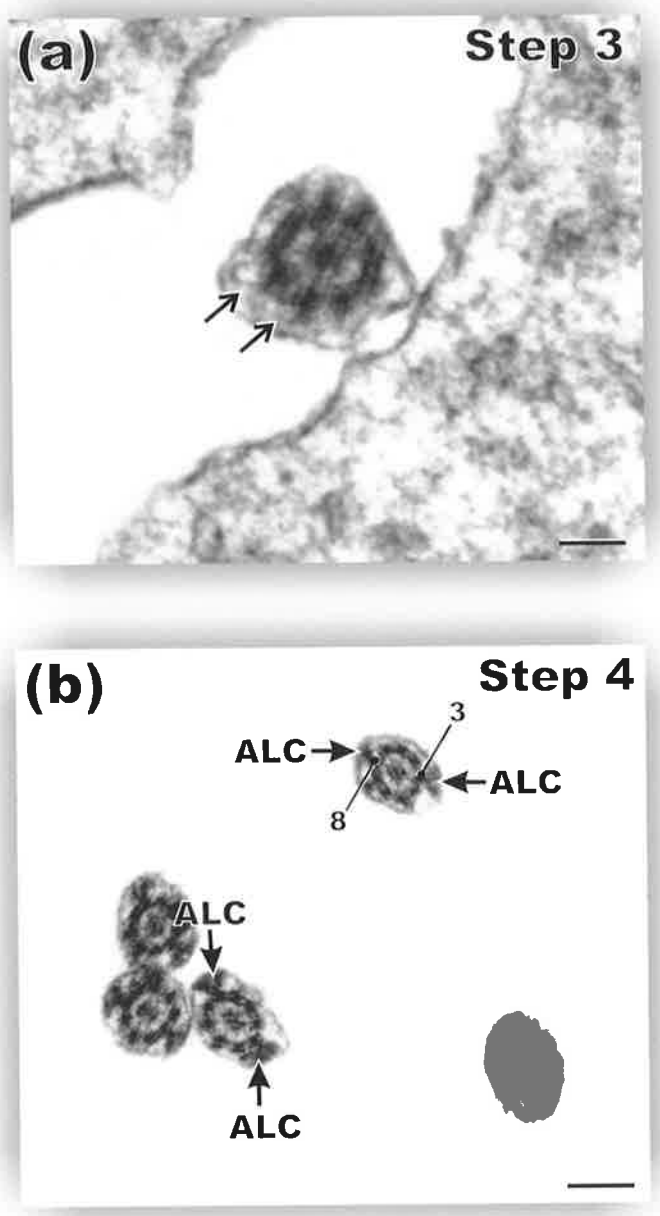

FIGURE 3.9 Transverse sections through the distal end of the flagella of (a) step 3 and (b) step 4 spermatids. (a) Electron dense material (arrows) is present between the axoneme and plasma membrane. (b) The anlagen of the longitudinal columns of the fibrous sheath (ALC) first appear as electron dense masses between outer microtubule doublets 3 and 8 of the axoneme and the plasma membrane.
Scale bars: (a) 0.1 μm, (b) 0.2 μm

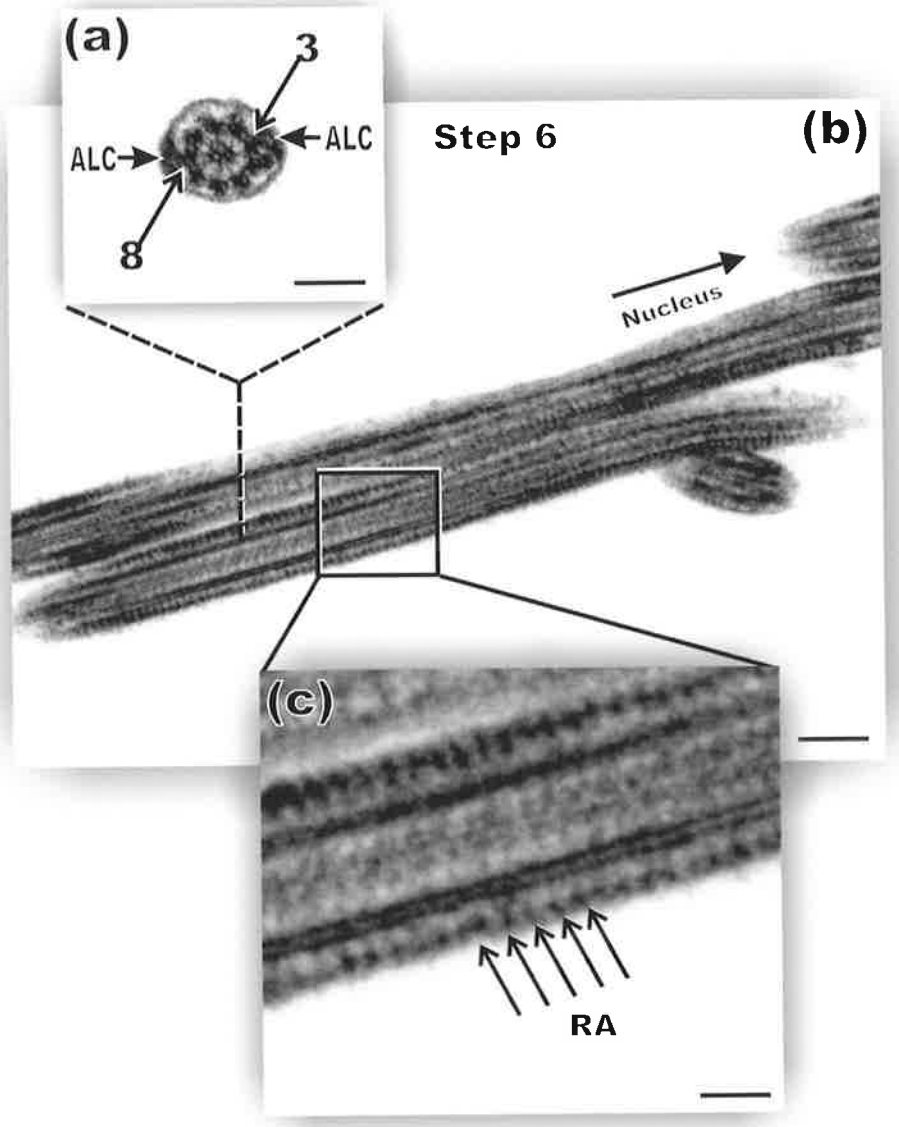

FIGURE 3.10 (a) Transverse and (b, c) longitudinal sections through the distal end of the flagellum of a step 6 spermatid within the lumen of a seminiferous tubule. (a) Electron dense material has accumulated immediately beneath the plasma membrane. (b, c) In longitudinal section the electron dense material can be identified as the anlagen of the circumferential ribs (RA) that are (c) composed of a series of evenly-spaced, circumferentially-orientated striations (arrows). *Scale bars: (a) 0.4 µm, (b) 0.3 µm, (c) 0.03 µm*

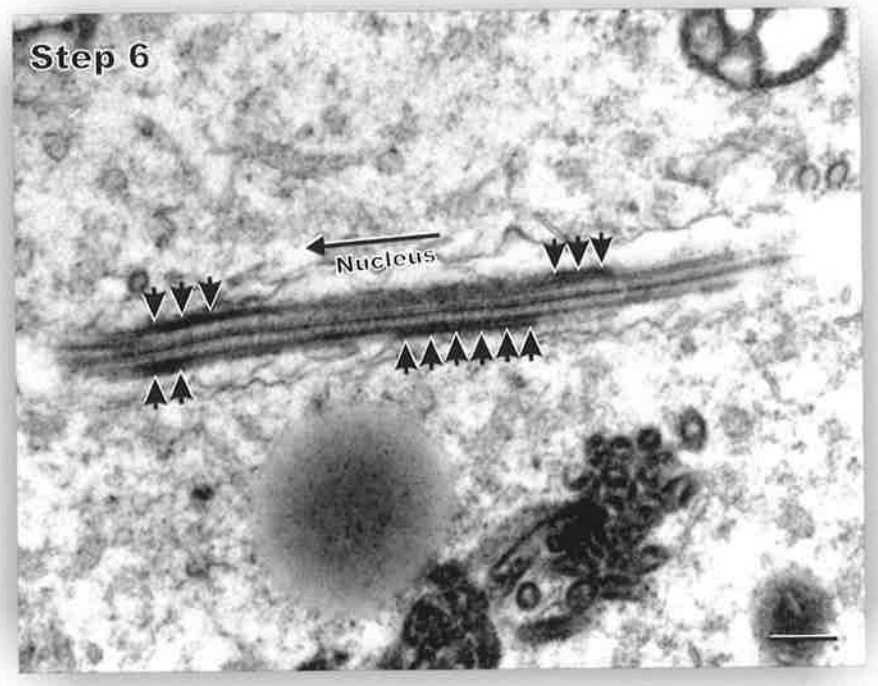

FIGURE 3.11 Longitudinal section through the proximal segment of the flagellum of a step 6 spermatid. The anlagen of the outer dense fibres appear as small, discontinuous, electron dense masses adjacent to the outer microtubule doublet of the axoneme (arrowheads).
Scale bar: (a) 0.3 µm

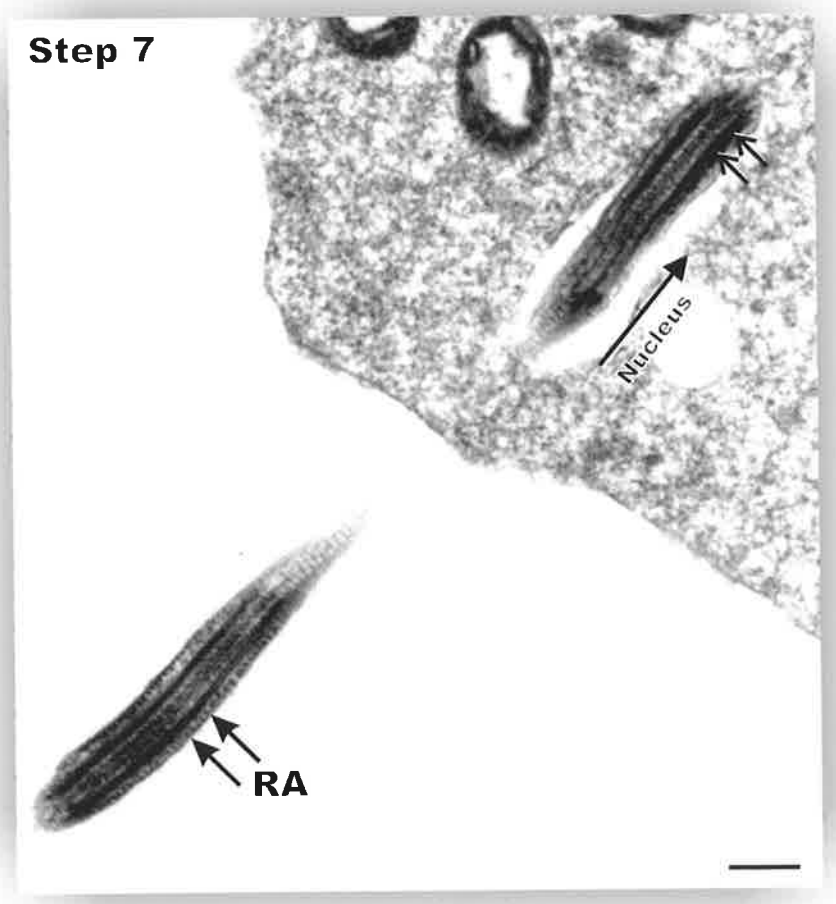

FIGURE 3.12 Longitudinal section through the flagellum of a step 7 spermatid. The anlagen of the circumferential ribs (RA) are now present within the proximal segment of the flagellum. The anlagen of the outer dense fibres (arrows) are extending toward the segment of the flagellum within the lumen of the seminiferous tubule.
Scale bar: (a) 0.2 µm

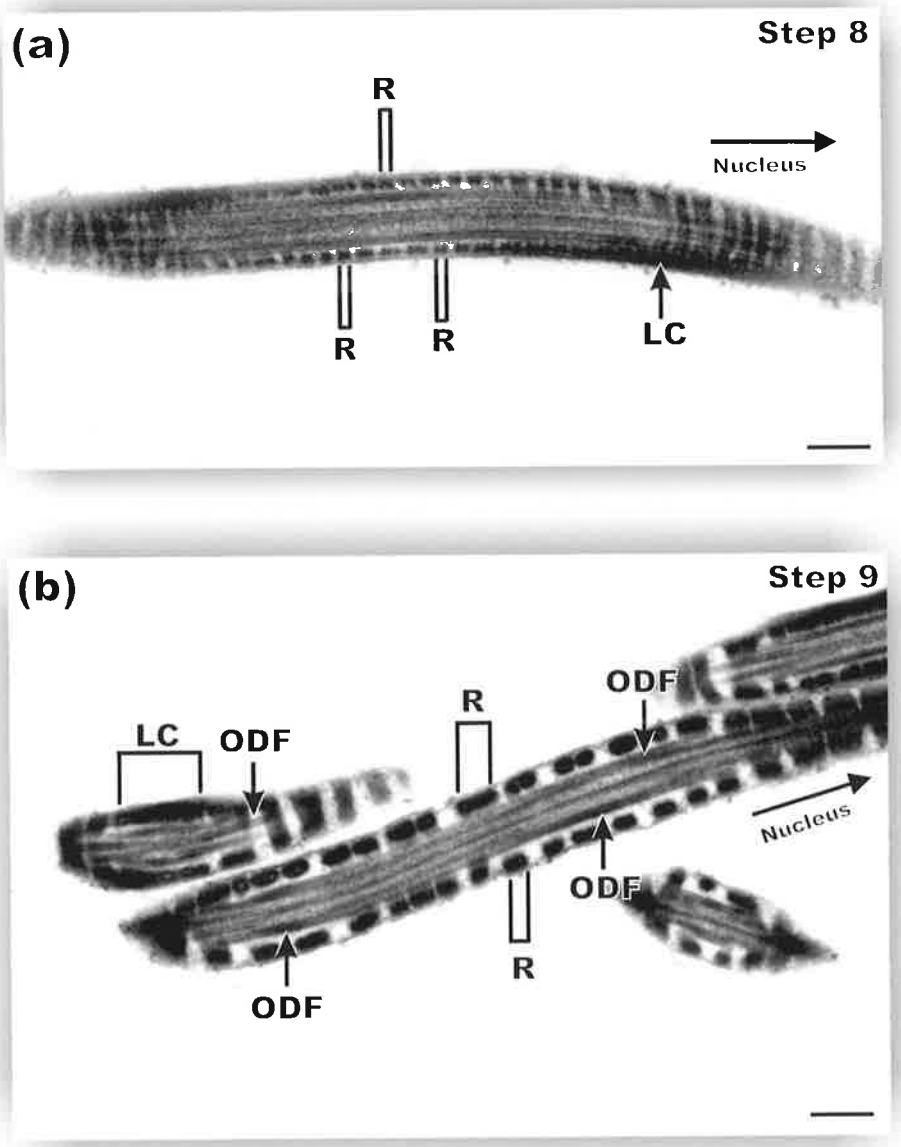

FIGURE 3.13 Longitudinal sections through the flagella of (a) step 8 and (b) step 9 spermatids within the lumen the seminiferous tubules. (a) The anlagen of the ribs and longitudinal columns thicken and coalesce to form the ribs (R) and columns (LC) respectively. (b) The ribs increase further in size during step 9 as adjacent ribs continue to coalesce. In addition, the outer dense fibres (ODF) also increase in size within this segment of the flagellum.
Scale bars: (a) 0.25 µm, (b) 0.25 µm

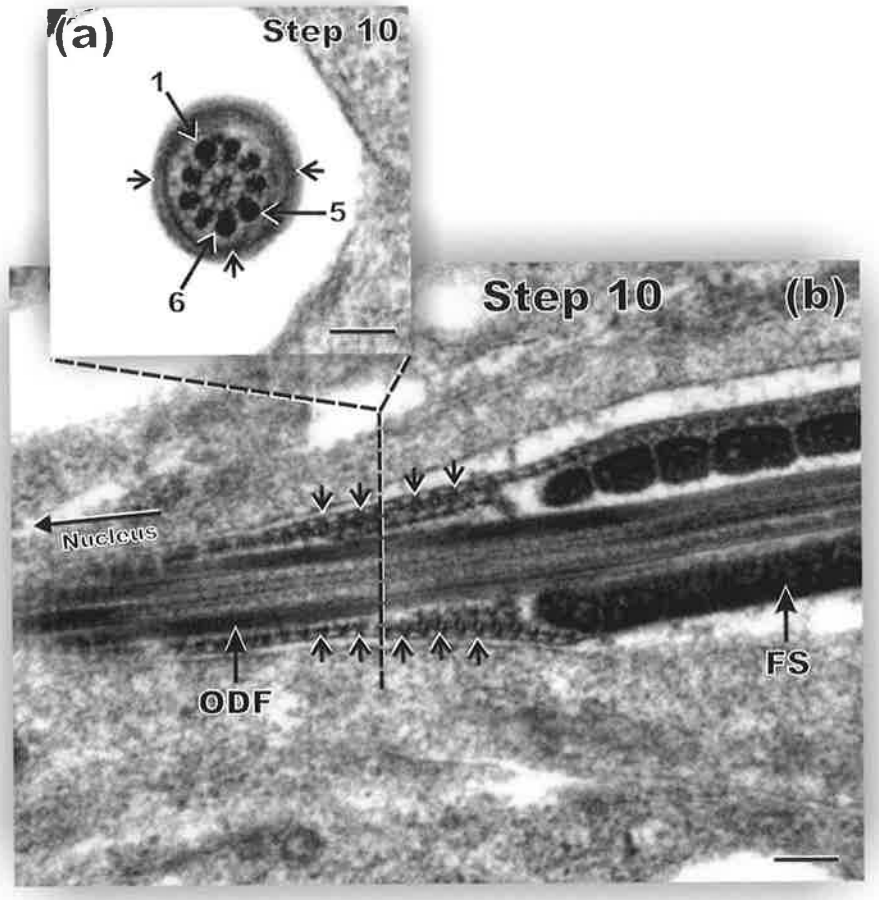

FIGURE 3.14 (a) Transverse and (b) longitudinal sections through the flagella of step 10 spermatids within the seminiferous tubule. (a) Each of the outer dense fibres has increased in size although fibres 1, 5 and 6 are consistently larger. (b) Within this region, what appear to be the rib anlagen (arrow heads) have developed in advance of the rudimentary longitudinal columns and assembled fibrous sheath (FS), giving the rib anlagen a 'zipper-like' appearance (arrowheads) in longitudinal section.
Scale bars: (a) 0.3 μm, (b) 0.3 μm

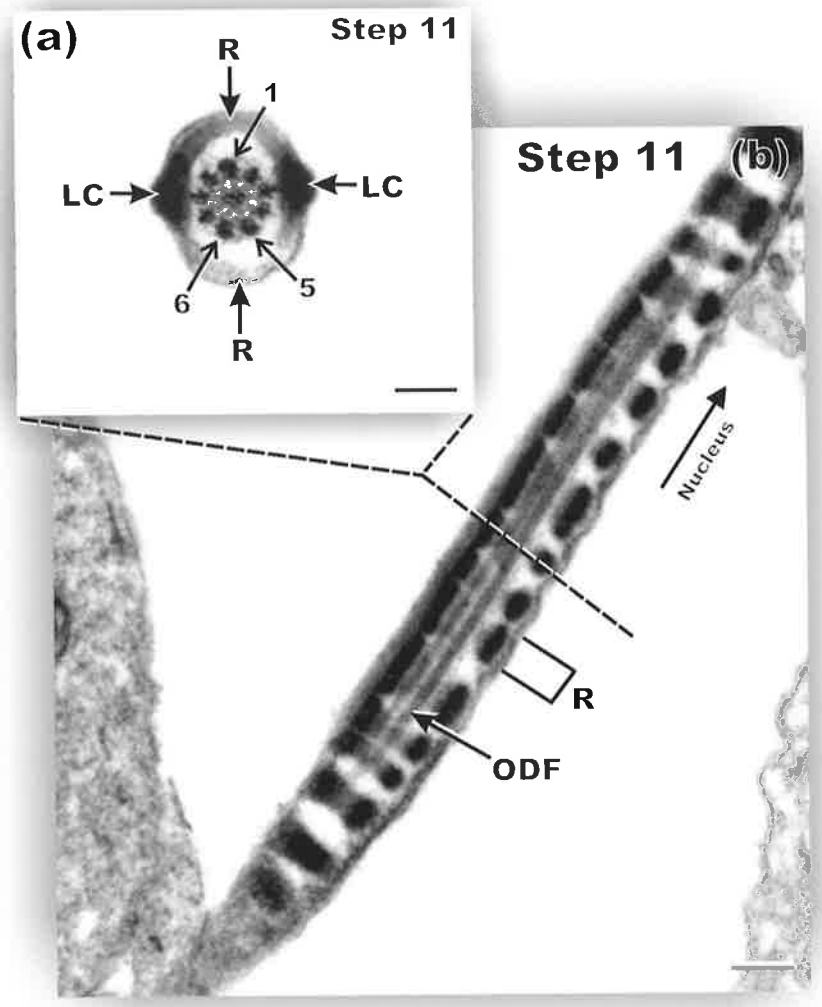

FIGURE 3.15 (a) Transverse and (b) longitudinal sections through the flagellum of step 11 spermatids within the lumen of the seminiferous tubules. (a) Outer dense fibres (ODF) within this segment of the flagellum are smaller than those within the flagellum closer to the spermatid nucleus, however fibres 1, 5 and 6 are the largest. The developing circumferential ribs (R) and longitudinal columns (LC) have increased in size but the ribs are less electron dense and project further away from the axoneme giving the flagellum an ovoid cross-sectional shape. (b) The ribs continue to coalesce and mature.
Scale bars: (a) 0.2 μm, (b) 0.25 μm

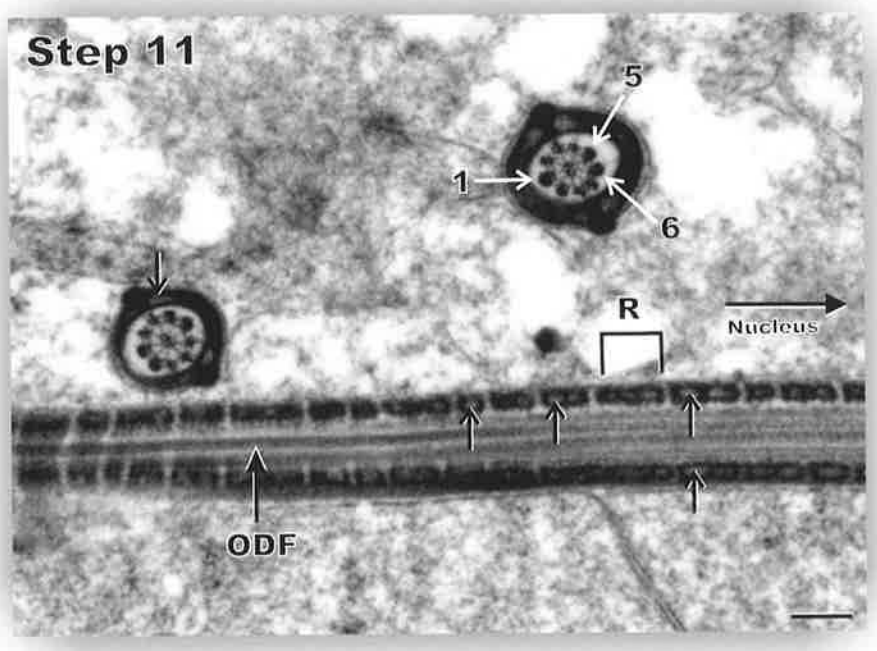

FIGURE 3.16 Transverse and longitudinal sections through the proximal segment of the principal piece of the flagellum of step 11 spermatids. As the fibrous sheath increases in electron density, small electron lucent spaces (arrows) develop in the region of contact between the circumferential ribs (R) and longitudinal columns. Outer dense fibres 1, 5 and 6 are the largest in size.
Scale bar: (a) 0.3 µm

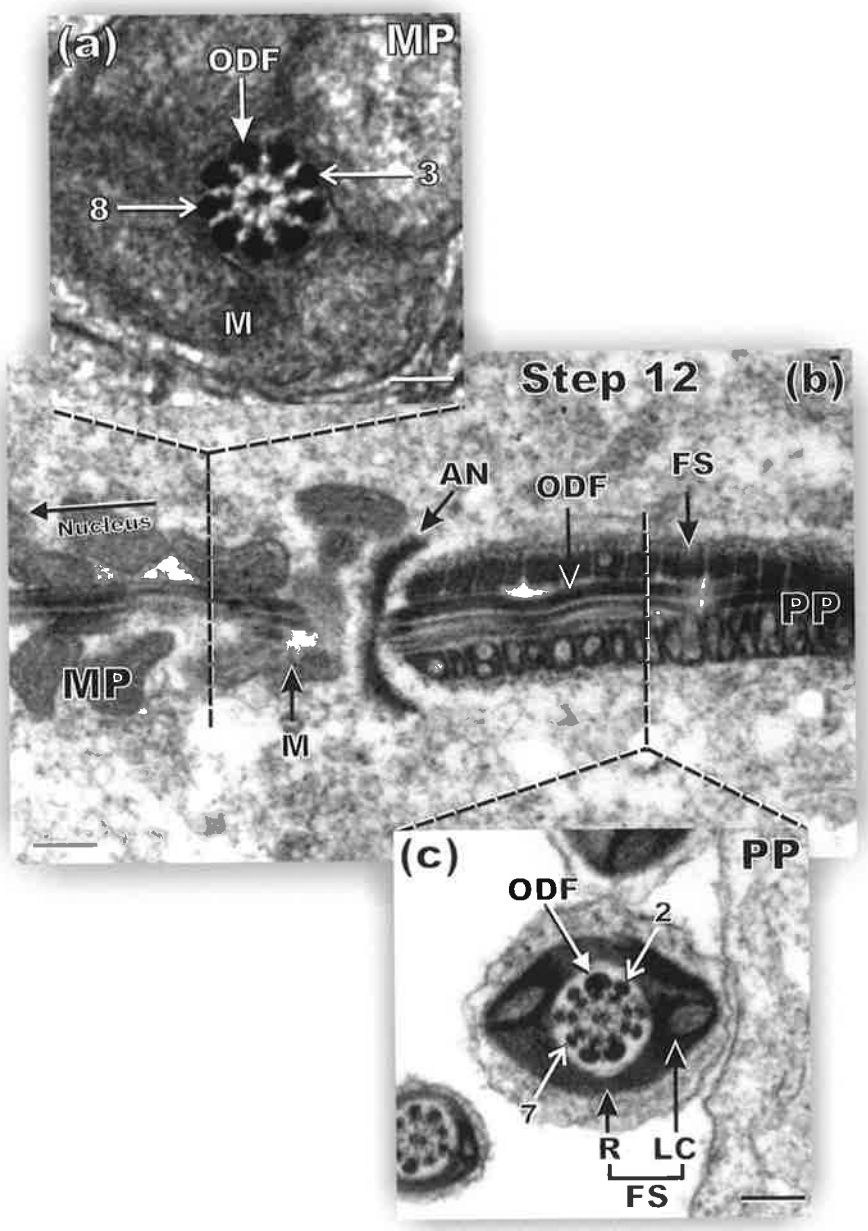

FIGURE 3.17 Transverse sections through the (a) midpiece (MP) and (c) principal piece (PP), and a (b) longitudinal section through the junction between the mid- and principal pieces of the flagellum of a step 12 spermatid. (a) In the midpiece, the outer dense fibres (ODF) have increased considerably in diameter and are approximately equal in size. (b, c) The fibrous sheath continues to gradually increase in size, as do the electron dense spaces present within them. Annulus (AN), Mitochondria (M).
Scale bars: (a) 0.15 µm, (b) 0.3 µm, (b) 0.2 µm

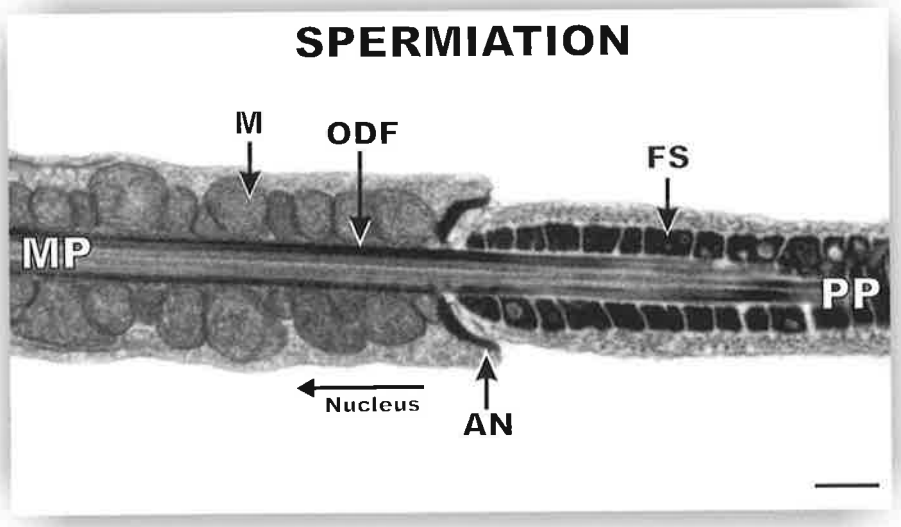

FIGURE 3.18 Longitudinal section through the junction between the midpiece (MP) and principal piece (PP) of a spermatozoa at spermiation. Further growth of the outer dense fibres (ODF) and fibrous sheath is minimal at this stage, although the fibrous sheath appears more electron dense and the number and size of the electron lucent vesicles within it have decreased considerably. Annulus (AN), Mitochondria (M).
Scale bar: (a) 0.3 µm

3.4 DISCUSSION

In this chapter, electron micrographs of developing possum spermatids were examined and classified into maturational 'steps' that were utilised to describe the formation of the outer dense fibres and fibrous sheath during spermiogenesis. By describing the general features underlying each step of spermiogenesis, it is possible to present a descriptive account of the morphogenesis of the outer dense fibres and fibrous sheath in an appropriate, chronological order.

3.4.1 Comparison of Spermiogenesis

The final sperm form develops as a result of the transformation of a small, round cell, the spermatid, which occurs after the completion of two meiotic divisions, into a highly polarised cell, the spermatozoon, that has a unique shape. This process, known as spermiogenesis, involves a remarkable morphogenetic transformation of the male gamete. During this process an acrosomal cap develops, the nuclear chromatin becomes highly compacted, and the nucleus assumes a species-specific, characteristic shape (Fawcett *et al.*, 1971). Spermiogenesis is one of the most complex processes of cellular differentiation known, as shown by electron microscopic investigations of this process in numerous eutherian species including the laboratory mouse (Gardner and Holyoke, 1964; Gardner, 1966, Russell *et al.*, 1990), human (de Krester, 1969), and laboratory rat (Roosen-Runge and Giesel, 1950; Clermont and Percy, 1957; Leblond and Clermont, 1952a,b; Clermont and Harvey, 1965; Lalli and Clermont, 1981; Ulvik *et al.*, 1982; Russell *et al.*, 1990). In the laboratory rat, spermiogenesis has been divided into four main phases and 19 spermatid steps (Leblond and Clermont, 1952a). The initial 'Golgi' phase (steps 1-3) is characterised by the formation of proacrosomal vesicles from the Golgi Apparatus. These coalesce to

form a single, spherical acrosomal vacuole, containing an electron dense granule, that adheres to the outer nuclear envelope to form the acrosome (Leblond and Clermont, 1952a; Lalli and Clermont, 1981; Russell *et al.,* 1990). During the subsequent 'cap' phase (steps 4-7), the acrosome gradually flattens over the surface of one pole of the nucleus whilst the axoneme of the flagellum begins to extend away from the nucleus. The 'acrosome' phase (steps 8-14) is characterised by the lateral flattening and recurving of the nucleus as the chromatin begins to condense. The acrosome also condenses during this phase and spreads over most of the ventral surface of the nucleus (Leblond and Clermont, 1952a; Lalli and Clermont, 1981; Russell *et al.,* 1990). In the final 'maturational' phase (steps 15-18), the volume of the nucleus diminishes as the chromatin is further condensed, and the nucleus is moulded into a more pronounced falciform shape (Leblond and Clermont, 1952a; Lalli and Clermont, 1981; Russell *et al.,* 1990).

The first detailed ultrastructural study of spermiogenesis in a marsupial species was conducted for the long-nosed bandicoot (*Perameles nasuta*) (Sapsford *et al.,* 1967, 1969, 1970). Although, in this study, bandicoot spermatids were not classified into developmental steps, spermiogenesis was nevertheless divided into six stages: (1) early spermatid, (2) nuclear protrusion, (3) nuclear flattening and condensation, (4) nuclear rotation, (5) early post-rotation and (6) late post-rotation (Sapsford *et al.,* 1969). The 'early spermatid' phase is similar to the 'Golgi' phase identified in the laboratory rat, however the bandicoot acrosomal vesicle does not contain an electron dense granule (Sapsford *et al.,* 1967). Diffuse granular material first appears within the bandicoot acrosomal vesicle during the subsequent 'nuclear protrusion' stage, at which time the vesicle flattens over the nucleus which elongates towards the developing acrosome (Sapsford *et al.,* 1967). In addition, during this stage the spermatid perinuclear cytoplasm begins to move towards the

flagellum, which develops and extends away from the longitudinal centriole (Sapsford *et al.*, 1967). The third stage of bandicoot spermiogenesis is characterised by the flattening and condensation of the spermatid nucleus in a plane at right angles to the axis of the flagellum so that the nucleus becomes rectangular in shape (Sapsford *et al.*, 1969). During the subsequent 'nuclear rotation' stage, the nucleus swivels about its point of attachment to the flagellum so that the angle between the nucleus and flagellum is reduced from 90° to approximately 45° (Sapsford *et al.*, 1969). As the spermatid nucleus rotates, its outline, which was smooth in previous stages, becomes increasingly irregular and the edges of the now plate-like nucleus curve around part of the flagellum (Sapsford *et al.*, 1969). This radical change in shape is accompanied by projections of the Sertoli cell cytoplasm into invaginations of the spermatid which, it has been suggested, act with the manchette to compress and help shape the spermatid nucleus (Sapsford *et al.*, 1969). These incursions, which are found mainly below the level of the distal border of the manchette in the proximal part of the spermatid, become less marked once nuclear rotation is complete. The final post-rotational stages of bandicoot spermiogenesis are largely characterised by movement of the spermatid nucleus towards the lumen of the tubule, and by the shedding of the residual cytoplasm, which is phagocytosed by the adjacent Sertoli cell (Sapsford *et al.*, 1969).

Following on from Sapsford's (1967, 1969, 1970) detailed investigation of bandicoot spermiogenesis several, albeit less detailed, ultrastructural studies of this process have been carried out on the following marsupial species: woolly opossum (*Caluromys philander*) (Phillips, 1970), American opossums (*Marmosa mitis* and *Didelphis virginiana*) (Rattner, 1972), brush-tail possum (Harding et al., 1976b), some dasyurids (Harding *et al.*, 1982), honey possum (*Tarsipes rostratus*) (Harding *et al.*, 1984), rock wallaby (*Petrogale*

assimilis) (Kim *et al.*, 1987), koala (*Phascolarctos cinereus*) (Harding *et al.*, 1987), tammar wallaby (*Macropus eugenii*) (Lin *et al.*, 1997) and southern hairy-nosed wombat (*Lasiorhinus latifrons*) (Ricci, 1997). Unfortunately, most of these studies, including that conducted for the brush-tail possum prior to the current investigation, were primarily focussed on the development of the acrosome or on post-testicular maturational events. Consequently, only general observations of spermiogenesis, and not detailed spermatid staging, were reported. Nevertheless, these studies did show that the main morphological events of marsupial spermiogenesis, with the exceptions of those in the koala and wombat, are very similar between species. Furthermore, they demonstrated that marsupial spermiogenesis is typically characterised by dorso-ventral nuclear flattening, as opposed to lateral flattening in eutherian species. Consequently, in most marsupials the acrosome is restricted to the dorsal side of the spermatid nucleus instead of covering the entire apical surface, and the flagellum inserts into the mid-ventral surface of the nucleus rather than into its trailing edge.

The description of brush-tail possum spermiogenesis presented in the current investigation is similar to that previously outlined for this species by Harding *et al.*, (1976b), and follows the pattern reported for most other marsupials. In the current investigation, however, possum spermiogenesis was divided into 12 maturational spermatid steps. This number compares favourably to the 14 spermatid steps were identified in the tammar wallaby (Lin *et al.*, 1997), but is less than the 19 and 16 steps identified respectively in the laboratory rat (Leblond and Clermont, 1952a; Lalli and Clermont, 1981; Russell *et al.*, 1990) and mouse (Oakberg, 1956; Gardner and Holyoke, 1964; Gardner, 1966, Russell *et al.*, 1990).

In the current study, steps 1-4 of possum spermiogenesis were characterised by the development of proacrosomal vesicles, from smaller Golgi vesicles, which merged to form a large electron lucent acrosomal vacuole that became apposed to, and then began to indent, one pole of the nucleus. The initiation of axoneme, and therefore flagellum, growth from the longitudinal centriole was also found to occur during this time. This initial period (steps 1-4) of possum spermiogenesis therefore correlates with the 'Golgi' and 'early spermatid' phases of bandicoot (Sapsford *et al.*, 1967) and laboratory rat spermiogenesis respectively, as well as steps 1-4 of tammar wallaby spermiogenesis (Lin *et al.*, 1997). The only major difference in this early phase of spermiogenesis between these species is the absence, in most marsupial species including the possum, of an acrosomal granule which is a typical feature of eutherian spermiogenesis. Electron lucent acrosomal vacuoles have similarly been found in a monotreme species, the platypus (*Ornithorhynchus anatinus*) (Lin and Jones, 2000). The functional significance of an acrosomal granule is unknown but it has been speculated that it could possibly related to the thickness and chemical composition of the egg coats (Guraya, 1971).

Subsequent ultrastructural differentiation of possum spermatids up until the stage of nuclear flattening, is generally similar to that reported for most other marsupial species (Phillips, 1970; Rattner, 1972; Harding *et al.*, 1976b; Harding *et al.*, 1982; Harding *et al.*, 1984; Harding *et al.*, 1987; Kim *et al.*, 1987; Lin *et al.*, 1997, Ricci, 1997), as well as for eutherian species such as the rat (Leblond and Clermont, 1952a; Lalli and Clermont, 1981; Russell *et al.*, 1990), mouse (Oakberg, 1956; Gardner and Holyoke, 1964; Gardner, 1966, Russell *et al.*, 1990), cat (Burgos and Fawcett, 1970), rabbit (Plöen, 1971), dog (Russell et al., 1990) and human (de Krester, 1969). The acrosomal vacuole collapses and flattens over the condensing nucleus and the axoneme extends into the lumen of the seminiferous

tubule. Beginning from step 7 of possum spermiogenesis, the spermatid nucleus, like those of all marsupials studied with the exception of the koala (Harding *et al.*, 1987) and wombat (Ricci, 1997), flattens in a distinctive dorso-ventral plane. This contrasts with the situation in eutherian mammals in which nuclear flattening occurs parallel to the long axis of the flagellum (for example, Leblond and Clermont, 1952a; Oakberg, 1956; Russell *et al.*, 1990) resulting in the spermatids having, upon release from the seminiferous epithelium, a streamlined appearance. As a result of the dorso-ventral mode of flattening, the possum acrosome comes to lie on the dorsal side of the spermatid nucleus, rather than over the entire apical surface, and the flagellum inserts into the mid-ventral side of the nucleus. Nuclear flattening in both marsupial and eutherian species appears to correspond with the period of maximal chromatin condensation leading to the suggestion that sperm nuclear, and therefore head, shape might largely be determined by the pattern of chromatin condensation (Fawcett *et al.*, 1971). Similar patterns of sperm head rotation and chromatin condensation have been reported for the bandicoot (Sapsford *et al.*, 1969) and wallaby (Lin *et al.*, 1997). Although the current study further demonstrates that, in general, the major features of spermiogenesis are similar across most marsupial species, some differences identified between marsupial and eutherian species were expected given the disparity in final sperm morphology between these two mammalian groups.

3.4.2 Comparison of Outer Dense Fibre Morphogenesis

Although numerous studies have analysed the mode of assembly of the connecting piece and axoneme (e.g., Fawcett and Phillips, 1969) of the mammalian sperm flagellum, relatively few detailed investigations have been conducted to ascertain how the outer dense fibres and fibrous sheath are assembled during spermiogenesis. Early ultrastructural studies of eutherian spermiogenesis made only passing references to the

development of the outer dense fibres (Challice, 1952; de Krester, 1969), but demonstrated that they first appeared alongside the outer microtubule doublets of the axoneme in the early stages of spermiogenesis and subsequently thickened (Challice, 1952). In an early ultrastructural study of human spermiogenesis, de Krester (1969) suggested that the outer dense fibres arise from the connecting piece, and that they may be closely associated with the segmented columns in this region (de Krester, 1969). This notion, although initially supported (see also Nicander and Bane, 1962, 1966) was, however, later disproved in more detailed ultrastructural investigations that clearly demonstrated that the outer dense fibres and segmented columns of the connecting piece are fundamentally different in both their fine structure and time and mode of origin (Fawcett and Phillips, 1969).

A subsequent, ultrastructural and radioautographic investigation of outer dense fibre morphogenesis in the laboratory rat showed the process is a lengthy, multi-step procedure extending from steps 8 to 19 of spermiogenesis, spanning approximately 13 days (Irons and Clermont, 1982a). Three distinct phases were identified: (1) the stage during which the anlagen of the outer dense fibres were formed (steps 8-14), (2) the period of growth of these fibres (stages 15-16), and (3) the stage during which the fibres assumed their definitive shape (steps 17-19) (Irons and Clermont, 1982a). During the initial phase, the anlagen of the outer dense fibres appeared as small, electron dense masses adjacent the outer microtubule doublets in the most proximal segment of the flagellum. Throughout steps 8-14 of spermiogenesis, these fibres gradually increased in length in a proximal-to-distal direction along the elongating flagellum, however during steps 15-16 there was a sudden increase in the diameter of the fibres especially within the midpiece of the flagellum (Irons and Clermont, 1982a). During the final phase (steps 17-19) the outer

dense fibres continued to enlarge, albeit slowly, and gradually projected away from the axoneme microtubules to which they are attached (Irons and Clermont, 1982a). Furthermore, radioautographic results suggested that the proteins that are rapidly incorporated into the outer dense fibres during step 16 of spermiogenesis are synthesised much earlier during spermiogenesis, suggesting that outer dense fibre proteins may be stored throughout the cytoplasm of these spermatids (Irons and Clermont, 1982a).

Although, prior to the current study, no specific investigation of outer dense fibre morphogenesis had been conducted for any marsupial species, Sapsford *et al.'s* (1970) ultrastructural study of bandicoot spermiogenesis did shed some light on this process in this species. In the bandicoot, the anlagen of outer dense fibres 3 and 8 only were first detected during the 'early spermatid' stage of spermiogenesis as small, electron dense masses adjacent the corresponding outer microtubule doublets of the axoneme (Sapsford *et al.,* 1970). During the subsequent 'nuclear flattening' phase of spermiogenesis, the anlagen of the remaining outer dense fibres appeared, however fibres 1 and 6 were most developed (Sapsford *et al.,* 1970). By the end of the subsequent 'nuclear rotation' phase, each of the outer dense fibres had increased in size, and soon after, each of the fibres, with the exception of 3 and 8, began to migrate away from the axoneme with connecting laminae forming to join these two structures (Sapsford *et al.,* 1970).

In the current study, possum outer dense fibre morphogenesis was found to be remarkably similar to that previously described for the laboratory rat (Irons and Clermont, 1982a) and bandicoot (Sapsford *et al.,* 1970), although some minor differences were noted. In each of these species, the anlagen of the outer dense fibres first appear adjacent the outer microtubule doublets of the axoneme at about the time that spermatid nuclear chromatin

begins to condense and the manchette appears (step 6 for the possum). In the possum and rat these fibres first develop within the most proximal segment of the flagellum adjacent the connecting piece and extend in a distal direction along the axoneme as spermiogenesis progresses. Sapsford *et al.*, (1970) did not comment on the direction of outer dense fibre morphogenesis in the bandicoot. In possum, rat and bandicoot, outer dense fibres 1, 5 and 6 are considerably larger than all others throughout most of spermiogenesis, suggesting that the other, smaller fibres (2, 3, 4, 7, 8 and 9) taper progressively at different levels along the flagellum whilst the largest fibres extend to the distal segment of the principal piece. It was only during the final stages of spermiogenesis (steps 11-12 and 16 in the possum and rat respectively, and during the 'post-rotational' phases of bandicoot spermiogenesis), that each of the outer dense fibres rapidly increased in size so that, within the midpiece at least, they were all approximately equal in diameter. This phenomenon has also been noted in ultrastructural studies of human spermiogenesis (de Krester, 1969). In the possum and rat, the mature outer dense fibres were closely apposed to the outer microtubule doublets of the axoneme around the time of spermiation, however this does not appear to be the case in the bandicoot as Sapsford *et al.*, (1970) found that the fibres settled some distance from axoneme with the two structures joined by long, electron dense 'connecting laminae'. In the bandicoot, it was hypothesized that these laminae may arise from electron dense material within the cytoplasm of the principal piece of the flagellum and/or from the cytoplasmic lobule of the spermatid (Sapsford *et al.*, 1970).

In the current study it has been possible to compare the ultrastructural features of possum outer dense fibre morphogenesis to that previously described for other marsupial and eutherian species. However the *timing* of the events in the formation of this structure cannot be compared because the length of each of the 12 developmental steps of possum

spermiogenesis has not yet been determined. Although the length of the cycle of the seminiferous epithelium for the possum had been previously calculated by radioautography and shown to be 15 days (Setchell and Carrick, 1973), only the length of the entire spermatogenic cycle, not the individual spermatid steps, were reported by these authors. Furthermore, Setchell and Carrick's (1973) investigation identified only 8 stages of spermatogenesis whereas 9 were found in the current study further complicating comparisons with their study.

(Please see 3.6 POSTSCRIPT)

3.4.3 Comparison of Fibrous Sheath Morphogenesis

Early ultrastructural studies of spermiogenesis usually made only passing, if any, reference to the assembly of the fibrous sheath, although in the human the anlagen of the circumferential ribs were found to first appear as a system of transversely orientated, microtubule-like structures arranged circularly around the axoneme (de Krester, 1969). As spermiogenesis progressed, granular, electron dense material accumulated within the spaces between these structures, and the anlagen of the longitudinal columns subsequently appeared (de Krester, 1969). The longitudinal columns were originally thought to develop as extensions of the outer dense fibres as they occupy the positions in the principal piece of the flagellum that outer dense fibres 3 and 8 reside in within the midpiece, however subsequent, more detailed ultrastructural investigations of spermiogenesis in other eutherian species (see below) demonstrated that this was not the case.

The first dedicated study of fibrous sheath morphogenesis in a eutherian species was, like that for the outer dense fibres, conducted by Irons and Clermont (1982b) for the laboratory

rat. In their electron microscopic and radioautographic investigation, the assembly of the rat fibrous sheath was found to be a lengthy, multi-step procedure that extended from steps 2-17 of spermiogenesis (Irons and Clermont, 1982b). Furthermore, the formation of the circumferential ribs and longitudinal columns occurred independently of each other with the development of the columns requiring approximately 15 days (steps 2-17), whereas deposition of the ribs was completed in approximately 4.5 days (steps 11-15) (Irons and Clermont, 1982b). In the rat, fibrous sheath formation began with the appearance of two longitudinally orientated, electron dense columns between the plasmalemma and outer microtubules 3 and 8 in the distal segment of the developing principal piece of the flagellum during step 3 of spermiogenesis (Irons and Clermont, 1982b). The anlagen of the columns gradually increased in length during steps 4-8 of spermiogenesis, eventually reaching the most proximal segment of the principal piece (Irons and Clermont, 1982b). The anlagen of the circumferential ribs appeared during step 11 of spermiogenesis, much later than the columns, as a series of circumferentially orientated, parallel striations within the distal segment of the principal piece of the flagellum (Irons and Clermont, 1982b). Fibrous sheath formation was subsequently completed in the final phase of spermiogenesis by the gradual thickening of the ribs and columns.

In the bandicoot, the anlagen of the longitudinal columns developed in a manner similar to that for the laboratory rat, although they appeared to be composed of alternating, poorly defined, dark and light bands that became more discernable as spermiogenesis progressed (Sapsford *et al.*, 1969, 1970). The anlagen of the circumferential ribs appeared much later as outgrowths, from each side of the longitudinal columns, of moderately electron dense, filamentous material which converged, and then condensed, to form the mature ribs of the fibrous sheath (Sapsford *et al.*, 1970). The controlling mechanism(s) of

this process was, however, difficult to comprehend as the number of filaments that converged to form each rib was variable within different segments of the flagellum (Sapsford *et al.*, 1970). During this period, an oval-shaped, filamentous body formed within the centre of the longitudinal columns and merged with the existing homogenous material of the columns, however in the final stages electron lucent vacuoles developed adjacent these bodies (Sapsford *et al.*, 1970).

In the current study, the mode of fibrous sheath assembly in the possum was found to be, in general, remarkably similar to that previously described for the laboratory rat and bandicoot. In each of the species, it was found that: (1) the anlagen of the longitudinal columns are the first components of the fibrous sheath to appear within the distal segment of the flagellum relatively early during spermiogenesis, (2) the rib anlagen arise from circumferential striations that gradually enlarge and coalesce to form the circumferential ribs, (3) the longitudinal columns and circumferential ribs of the fibrous sheath are assembled independently of each other, except for a period late in spermiogenesis when the development of both of these components occurs concurrently within the principal piece of the flagellum, and (4) the assembly of this fibrous sheath proceeds in a distal-to-proximal direction along the axoneme.

Despite these similarities, there are some differences in the development of the fibrous sheath between the human and possum/bandicoot/rat. In the human, de Krester (1969) claimed that the anlagen of the circumferential ribs develop prior to those of the longitudinal columns whereas the reverse is true in the possum, bandicoot (Sapsford *et al.*, 1970) and rat (Irons and Clermont, 1982b). Furthermore, in the human the anlagen of the ribs appear to consist of a series of 'microtubules' (de Krester, 1969) whereas filamentous

material has been observed in the other species. Whether there is some confusion over the nature of the material within the ribs, and hence the microtubules observed in human spermatids are in fact filaments, remains to be determined. Nevertheless, the functional significance of this difference, if it occurs, is difficult to comprehend as the final form of the fibrous sheath in the possum, human, bandicoot and rat is very similar. Whether the variations in fibrous sheath formation identified reflect differences in, for example, the protein composition of the fibrous sheath in these species, will be investigated in the subsequent chapter.

3.5 CONCLUSION

In the current study, electron micrographs of developing possum spermatids were analysed and classified into 12 maturational steps that were utilised to describe the formation of the outer dense fibres and fibrous sheath during spermiogenesis. By describing the general features underlying each step of spermiogenesis, it was possible to present a descriptive account of the morphogenesis of these cytoskeletal structures in an appropriate, chronological order. The modes of assembly of the outer dense fibres and fibrous sheath were then compared to those previously reported for a marsupial (bandicoot) and eutherian (laboratory rat), and were found to be remarkably similar. In the possum, outer dense fibre formation was found to proceed in a proximal-to-distal direction along the axoneme from step 6-12 of spermiogenesis, with maximal growth of the fibres occurring in the latter stages of this process. Fibres 1, 5 and 6 were most developed although each of the fibres taper off progressively within the flagellum. In comparison, formation of the fibrous sheath was found to occur in a distal-to-proximal direction over a longer period from steps 4-12 of spermiogenesis. The longitudinal columns develop prior to the circumferential ribs with their assembly occurring independently for most of

spermiogenesis. Unfortunately, in the current study it was not possible to determine the duration of each step of spermiogenesis, so the relative lengths of time of each phase of outer dense fibre and fibrous sheath assembly could not be ascertained. In Chapter 5 an immunocytochemical approach will be used to try to differentiate the site of formation of outer dense fibre and fibrous sheath proteins from their time of assembly during spermiogenesis.

3.6 POSTSCRIPT

Immediately prior to this thesis being printed, a report was published by Lin *et al.*, (2004), in Reproduction, Fertility and Development Volume 16, pp 307-313, in which the features and duration of the cycle of seminiferous epithelium in the brush-tail possum were described. In comparison to the 9 stages and 12 spermatid steps identified in the present chapter, Lin *et al.*, (2004) reported 10 stages of the seminiferous epithelium cycle and 14 steps of spermatid development. In comparison to the results of the current study, the additional spermatid steps identified by Lin *et al.*, (2004) were a step 1 spermatid in which no proacrosomal vesicles had yet arisen from the Golgi Apparatus, and a step 5 spermatid in which the nucleus began to bilaterally flatten but the acrosome remained round. As a result of these additional spermatid steps, 10, rather than 9, stages of the cycle of seminiferous epithelium were identified. In addition to these morphological findings, Lin *et al.*, (2004) also showed, by autoradiography, that the duration of one possum cycle is 13.5 days compared with 15 days as reported by Setchell and Carrick (1973). Moreover, Lin *et al.*, (2004) also demonstrated that the lifespan of possum spermatids is 21.4 days. These results suggest that the kinetics of possum spermatogenesis show a similar pattern to that of eutherians (Lin *et al.*, 2004). Further analysis of the specific duration of each spermatid

step is still required if the length of time required for assembly of the possum outer dense fibres and fibrous sheath is to be accurately determined.

Chapter 4

ISOLATION AND PROTEIN COMPOSITION OF THE OUTER DENSE FIBRES AND FIBROUS SHEATH

4.1 INTRODUCTION

In Chapter 3 the formation of the possum outer dense fibres and fibrous sheath were described, however to attempt to gain some insight into the function(s) of these cytoskeletal structures it is necessary to isolate and characterize the proteins contained therein. Baccetti *et al.*, (1973) employed two different techniques in their attempt to isolate bull sperm outer dense fibres: the first involved the use of sodium dodecylsulfate (SDS), whilst the second employed sperm head decapitation and sonication. Subsequent studies also used dithiothrietol (DTT) in conjunction with SDS (Olson and Sammons, 1980; Oko, 1988). The outer dense fibres were then separated by sucrose density gradient centrifugation, and the number and molecular weights of the proteins therein determined by SDS polyacrylamide gel electrophoresis (SDS-PAGE). Up to nine major protein bands have been described for the outer dense fibres of the laboratory rat (Olson and Sammons, 1980; Vera *et al.*, 1984; Oko, 1988; Kim *et al.*, 1999), but only three for the bull (Baccetti *et al.*, 1973, 1976a, b; Brito *et al.*, 1986) and human (Haidl *et al.*, 1991; Henkel *et al.*, 1994).

The proteins of the fibrous sheath was first isolated by treating sperm first with SDS and the non-ionic detergent Triton X-100 to solubilize the flagella membranes, and then Urea

and DTT to remove the outer dense fibres. The remaining fibrous sheath was then purified by density gradient centrifugation (Olson *et al.*, 1976). In the laboratory rat fibrous sheath up to 20 protein bands have been reported (Olson *et al.*, 1976; Oko, 1988; Kim *et al.*, 1995b), with 14 and 10 proteins identified respectively for the fibrous sheath in human (Jassim *et al.*, 1992) and rabbit (Kim *et al.*, 1997) sperm.

Prior to the present study, no known attempt had been made to extract and characterize the outer dense fibres and fibrous sheath of the sperm from any marsupial species. It was not even known whether the techniques developed to isolate and purify the eutherian sperm outer dense fibres and fibrous sheath could be used to extract these structures from sperm of marsupials. Characterizing the proteins of the marsupial outer dense fibres and fibrous sheath is fundamental to determining the functions of these sperm tail cytoskeletal components. Furthermore, knowledge of these structures for this group of extant mammals could indicate the extent of conservation of their proteins across all mammals and give some indication of the time of their evolution. The aim of this chapter is, therefore, to describe techniques for isolating and characterizing the outer dense fibres and fibrous sheath from sperm of the possum, and to determine their protein compositions by SDS-PAGE. These results will then be compared to those previously reported for eutherian mammals.

4.2 MATERIALS AND METHODS

4.2.1 Ruthenium Red Fixation of Spermatozoa

Possum cauda sperm were fixed in 3% glutaraldehyde containing 0.5% ruthenium red in 0.2 M cacodylate buffer, pH 7.4, for 4 h, washed in two changes of buffer containing 0.5% ruthenium red, and post-fixed in 1% osmium tetroxide in buffer containing 0.5% ruthenium

red. After washing in buffer, the sperm were processed as for routine transmission electron microscopy (see Chapter 2: General Materials and Methods).

4.2.2 Isolation of Sperm Flagella

Spermatozoa suspended in PBS-PMSF, pH 7.0 (see Chapter 2: General Materials and Methods), were first decapitated by sonication (Sanophon, Sydney). They were sonicated at 4°C for 15-second bursts separated by 30-second intervals. After each burst a drop of the sperm suspension was placed on a slide and viewed under a phase contrast microscope to determine the extent of sperm decapitation. The sperm were exposed to bursts of sonication until it was determined, by light microscopy, that at least 95% decapitation had been achieved. The decapitated spermatozoa were washed in PBS-PMSF, resuspended in 20 % (w/v) sucrose in PBS-PMSF, and layered over a sucrose gradient. Various sucrose gradient concentrations and centrifugation speeds were tested in an effort to determine the optimal ones for separating the sperm tails from the heads. Each experiment was conducted at least five times to ensure the results were repeatable and consistent. The sucrose gradient concentrations trialled were: 65%, 70% and 75%; 20, 30, 40 and 60%; 20, 40 and 60% (w/v) sucrose in PBS-PMSF. The decapitated sperm suspensions were layered over each of the above gradient systems in a 10 ml test tube and centrifuged at 4°C for 90 min in a Beckman TJ-6 swinging bucket rotor centrifuged at 3000 *g*. The material deposited at each sucrose interface and at the bottom of the test tubes was subsequently assessed by light microscopy. If the layer containing sperm tails was contaminated by more than 5% with sperm heads it was carefully removed, resuspended in 20% sucrose and centrifuged under identical conditions to remove most of the remaining heads. The purity of the isolated sperm tails was again assessed by light microscopy, and if there was less than 1% sperm head contamination the sperm tails were

diluted 1:1 with PBS and pelleted at 15 000 *g* for 15 min. A small amount of the material collected from each sucrose interface was also pelleted and fixed for routine transmission electron microscopy to further determine the efficiency of the separation techniques employed.

4.2.3 Isolation of Outer Dense Fibres

The procedure used to isolate the outer dense fibres from sperm tails was a modification of the technique originally developed by Olson and Sammons (1980). The isolated sperm tails were suspended in 5 ml of 1% sodium dodecyl sulfate (SDS), 2 mM dithiothrietol (DTT), in 25 mM Tris-HCl, pH 8, and shaken at room temperature for 30, 60, 90 or 120 min. The resultant suspensions were diluted with Tris-HCl, layered over a 20, 40 and 60% sucrose gradient and centrifuged at 3000 *g* for 60 min. The outer dense fibres were collected from the 40-60% sucrose interface, washed in Tris-HCl buffer, and pelleted at 15 000 *g* for 30 min. The pellet was either fixed for routine transmission electron microscopy or frozen at -70°C for later use (i.e. for solubilizing to run on a SDS gel).

4.2.4 Isolation of Fibrous Sheath

The procedure used to isolate the fibrous sheath from sperm tails was a modification of the technique originally developed by Olson *et al.*, (1976). The isolated sperm tails were suspended in 2% (v/v) Triton X-100, 5 mM DTT, in 50 mM Tris-HCl, pH 9, with shaking at 4°C for 15 min. The resultant suspension was centrifuged at 1000 *g* for 10 min, the supernatant discarded, and the procedure repeated. This was carried out to try to solubilise all membranous sperm tail components and was carefully monitored by Nomarski microscopy. The pellet was resuspended in 5 ml of 4.5 M Urea, 25 mM DTT, in 25 mM Tris-HCl, pH 8, at 4°C for either 3, 5 or 8 h with gentle shaking. The resultant

suspension was diluted with Tris-HCl and layered over a 20, 40, and 60% sucrose gradient and centrifuged at 3000 *g* for 60 min. The fibrous sheaths were collected from the 40-60% sucrose interface, washed in Tris-HCl buffer and pelleted at 15 000 *g* for 30 min. The pellet was either fixed for routine transmission electron microscopy or frozen at -70°C for later use.

4.2.5 SDS-Polyacrylamide Gel Electrophoresis (SDS-PAGE)

Isolated outer dense fibres and fibrous sheaths were solubilised in 2% SDS and 5% ß-mercaptoethanol for 5 min at 100°C, and any insoluble material was removed by centrifugation at 15 000 *g* for 20 min. Protein concentrations were determined using the Bio-Rad protein assay (Bio-Rad Laboratories, Hercules, CA), and the proteins were separated on linear gradient (7.5% - 15%) SDS-polyacrylamide gels. Up to 50 µg of protein per lane was used and the gels were stained with Coomassie Brilliant Blue. Broad range molecular weight standards (Bio-Rad) were used to determine the molecular weights.

All gels were repeated at least twice with samples from 5 different outer dense fibre and fibrous sheath incubations, and protein bands described consistently appeared in all gels.

4.3 RESULTS

4.3.1 Ruthenium Red Fixation of Sperm

Ruthenium red fixation of possum cauda sperm showed that, whilst the fibrous sheath is typically electron dense and homogeneous (Figure 4.1a), the outer dense fibres contain two distinct regions, a narrow, electron dense, outer C-shaped cortex, and a central, less electron dense medulla (Figure 4.1b, c).

4.3.2 Isolation of Sperm Flagella

In most cases, sonication of possum cauda spermatozoa for approximately six, 15-sec bursts at 100% output, resulted in the decapitation of approximately 95% of possum cauda sperm, however on rare occasions, fewer or additional bursts of sonication were required to separate the sperm heads from the tails; - this was determined on an individual basis for each case by careful examination of the spermatozoa by light microscopy after each sonication. The remaining 5% whole sperm were not sonicated further as this only resulted in the fragmentation of the already separated sperm tails which would presumably alter their density and therefore prevent a clear separation of heads and tails during the gradient centrifugation process.

The decapitated sperm in 20% (w/v) sucrose were initially layered over a 60%, 70% and 75% sucrose gradient and centrifugated in an attempt to separate the sperm tails (Calvin, 1976) (Figure 4.2a). This resulted in the sperm heads, plus the remaining whole sperm, being deposited at the bottom of the test tube, however the sperm tails, which settled at the 20-60% interface were contaminated with red blood cells and round masses of cytoplasmic, anuclear material which were probably cytoplasmic droplets (Figure 4.3). The red blood cells presumably originated from epididymal capillaries that were severed at the time of obtaining sperm from the cauda epididymides when the duct was cut into several pieces, whilst any cytoplasmic droplets would have been shed from spermatozoa during epididymal transit. As a result of this contamination, the decapitated sperm were subsequently layered either over (1) 30%, 40% and 60% sucrose gradients, or (2) 20%, 40% and 60% sucrose gradients in an attempt to obtain better separation of the sperm tails from the red blood cells and cytoplasmic droplets (Figure 4.2b, c). The 60% sucrose

layer was not removed from the gradient setup as it was found to act as a sufficient barrier to the sperm tails. In both of these gradient setups the sperm heads settled at the bottom of the test tube (Figure 4.2c) while an opaque layer of relatively pure sperm tails formed at the 40-60% interface (Figure 4.2b). The red blood cells and cytoplasmic droplets settled at the either 20-30% and 20-40% sucrose interfaces in the remaining gradient setups with no material present at the 30-40% interface in the former setup (Figure 4.2a). It was decided to use the 20%, 40% and 60% sucrose gradient to isolate the sperm tails in all subsequent experiments.

Transmission electron micrographs of material from each of the interfaces showed that the material present at the 20-40% interface was largely composed of red blood cells and spherical, anuclear masses which are assumed to be the cytoplasmic droplets (Figure 4.3), whereas sperm tails were present at the 40-60% interface (Figure 4.4a) and sperm heads at the bottom of the test tube (Figure 4.4b). These findings, therefore, confirm those obtained by light microscopy. It was found that, after sonication and centrifugation, most of the sperm tails had lost their plasma membranes and most of their midpiece fibre networks, however the mitochondrial sheath, outer dense fibres and fibrous sheath remained relatively intact (Figure 4.4a). The plasma membrane and most of the acrosomal material were similarly removed from the isolated sperm heads, although in some sperm heads, acrosomes with marked vacuolation of acrosomal material could be seen (Fig. 4.4b).

4.3.3 Isolation of Outer Dense Fibres

Incubation of the isolated sperm tails in 1% SDS and 2mM DTT for 30 min resulted in the solubilisation of the fibrous sheath, however the mitochondrial sheath persisted (Figure

4.5a). With further incubation (up to 60 min), the remnants of the mitochondrial sheath disappeared and only the outer dense fibre-connecting piece complexes remained (not shown). At this stage the individual outer dense fibres were splayed out from the connecting piece. Incubation of the tails for up to 90 min resulted in the solubilisation of the connecting pieces (Figure 4.5b). In addition, at this stage the appearance of some thin fibres, which appeared to arise from the main segments of the outer dense fibres and, therefore, could represent the cortex of the outer dense fibres, could be seen (Figure 4.5b). Incubation of this extract in SDS and DTT for an additional 30 min resulted in the complete solubilisation of the thin segments of the outer dense fibres and swelling of the remaining fibres, which may represent the medulla, although they retained their overall shape (Figure 4.6).

4.3.4 Isolation of Fibrous Sheath

Incubation of the possum cauda sperm tails in 2% TX-100 and 5 mM DTT for 2, 15 min periods resulted in the complete solubilisation of the mitochondrial sheath and remaining midpiece fibre network (Figure 4.7). Subsequent treatment of the sperm tails with 4.5 M Urea and 25 mM DTT for 3 h resulted in the complete solubilisation of the axoneme and the disruption and partial solubilisation of the outer dense fibres (Figure 4.8a). After 5 h the fibrous sheath remained, although minor remnants of the outer dense fibres persisted (Figure 4.8b). Prolonged exposure of sperm tails to Urea and DTT (up to 8 hr) to remove these outer dense fibre remnants resulted in the swelling and fragmentation of the fibrous sheath, however the few outer dense fibre remnants that remained still persisted (Figure 4.9). Consequently, all subsequent fibrous sheath incubations were terminated at 5 h.

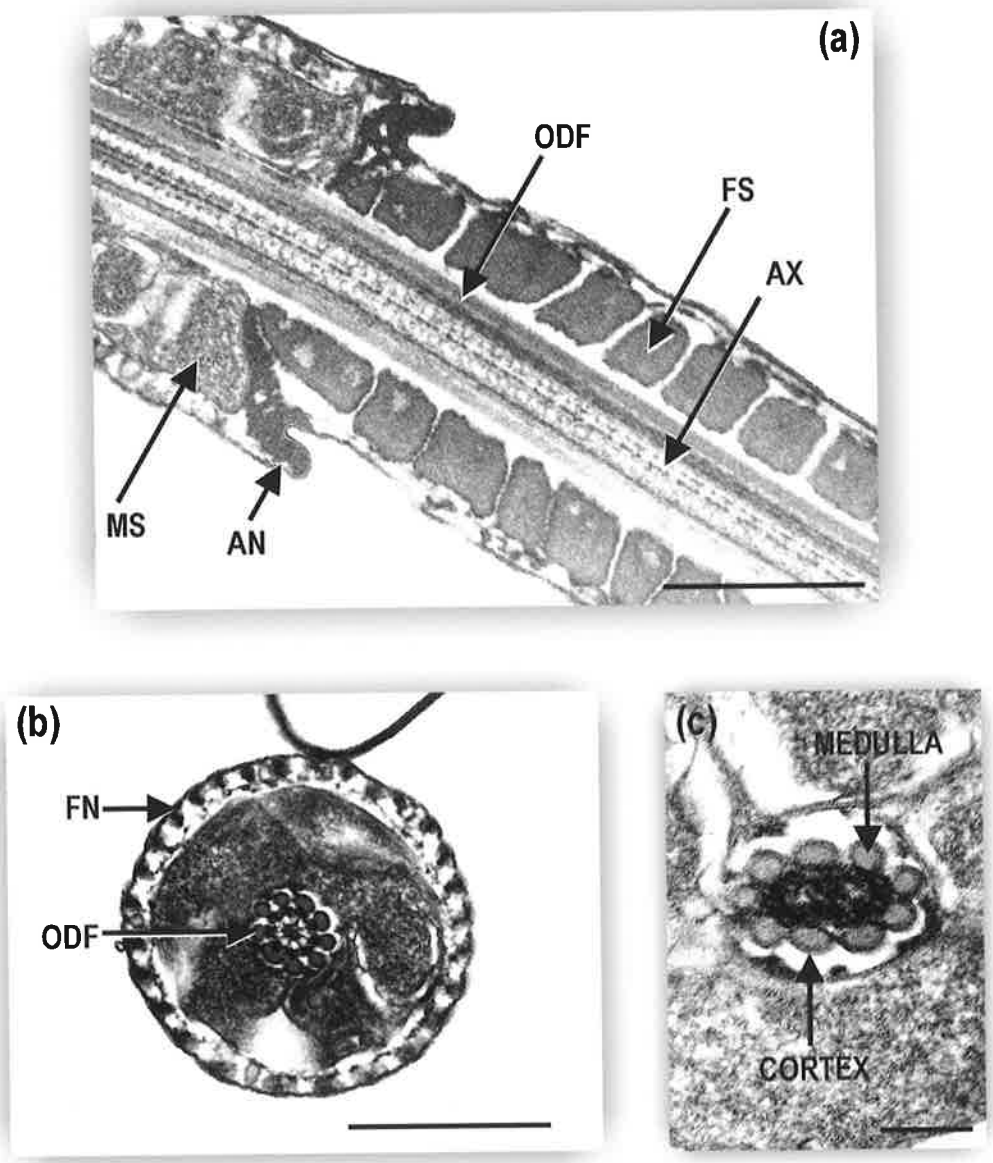

FIGURE 4.1 Transmission electron micrographs of (a) longitudinal and (b) transverse sections of possum cauda spermatozoa fixed with ruthenium red. (a) Staining of the fibrous sheath is homogeneous, however, (b) the outer dense fibres are composed of a narrow, electron dense peripheral C-shaped cortex and a central medulla that is less electron dense.
Scale bars: (a) 0.45 μm, (b) 0.5 μm, (c) 1.5 μm.

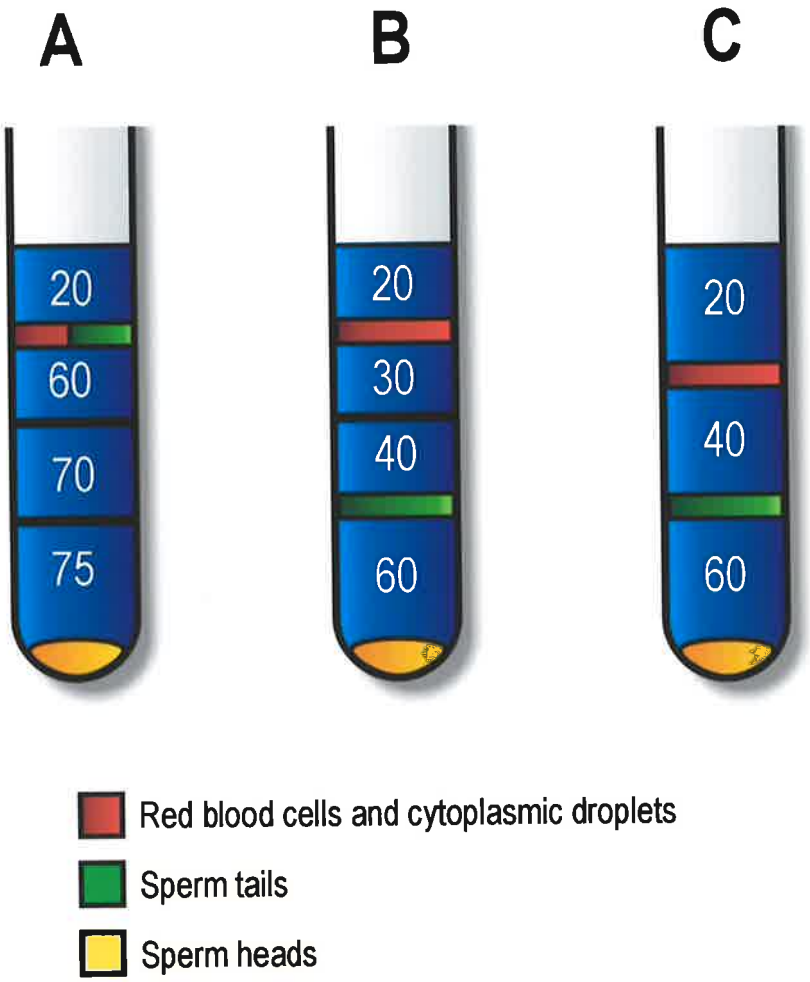

FIGURE 4.2 Diagrammatic illustration of the three different sucrose gradients trialled to obtain a relatively pure fraction of sperm tails. In each gradient system the sperm heads settled at the bottom of the test tube. (A) 20, 60, 70 and 75% sucrose gradient resulted in the deposition of red blood cells, cytoplasmic droplets and sperm tails at the 20-60% interface. In both (B) and (C) the sperm tails settled at the 40-60% interface, however the location of the red blood cells and cytoplasmic droplets varied.

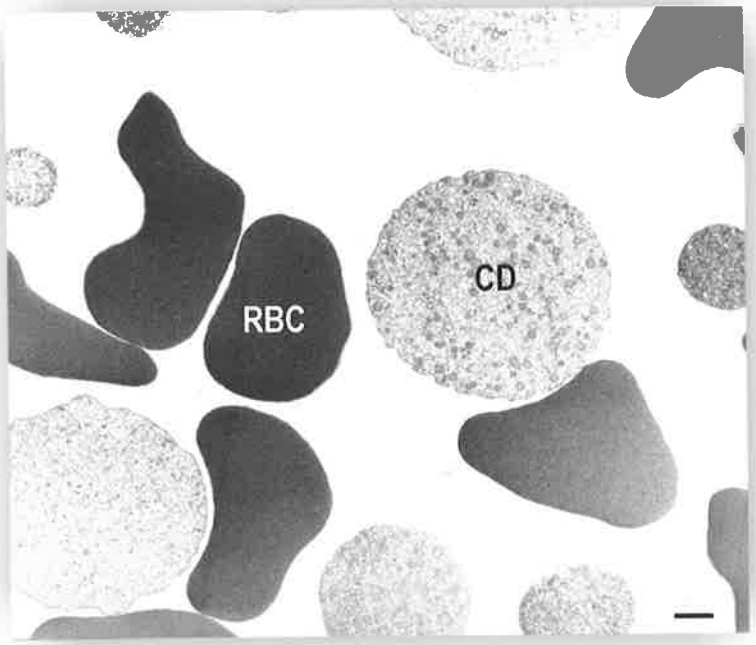

FIGURE 4.3 Transmission electron micrograph showing the red blood cells (RBC) and non-nucleated, spherical cytoplasmic masses, presumed to be cytoplasmic droplets (CD), present at the 20-40% interface of the sucrose density gradient.
Scale bar: 0.5 µm.

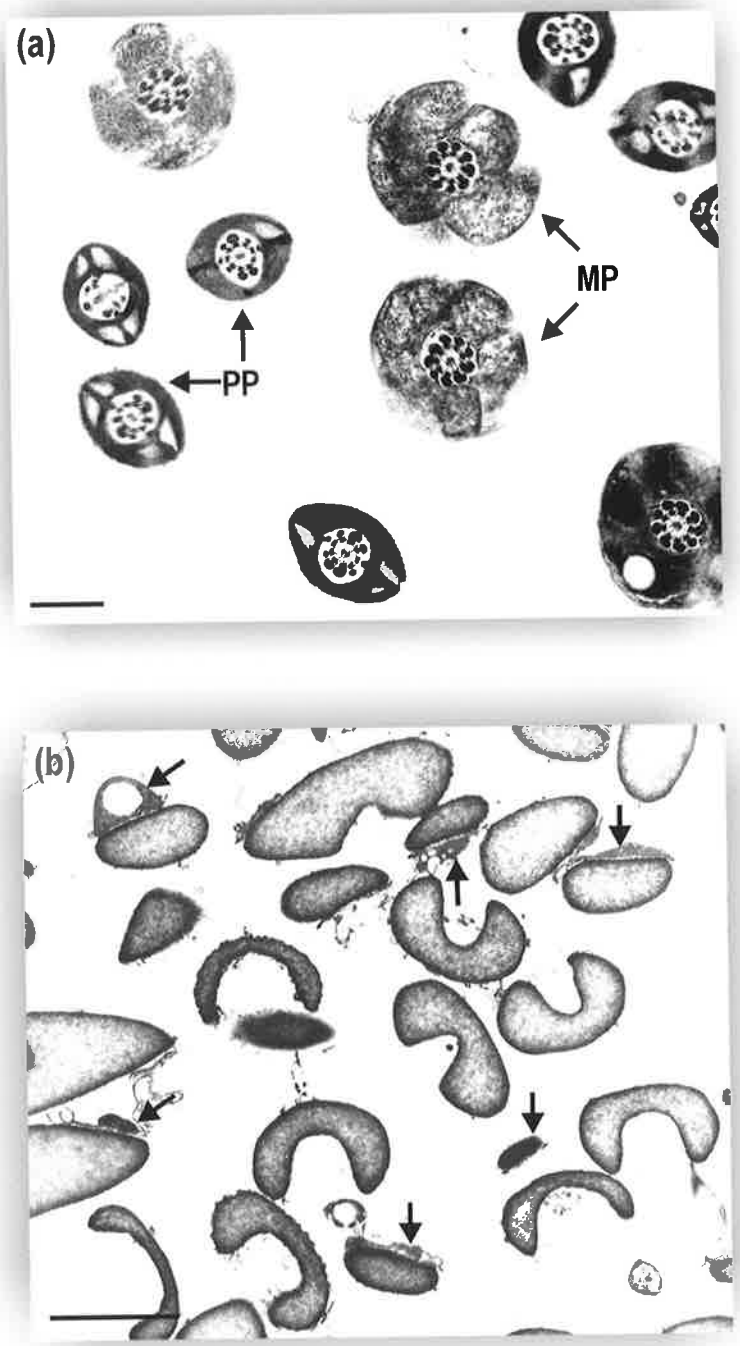

FIGURE 4.4 Sonication and sucrose density gradient centrifugation of possum cauda sperm resulted in the deposition of (a) largely intact sperm tails at the 40-60% interface, and (b) sperm heads at the bottom of the 60% sucrose layer. Acrosomes on the isolated sperm heads are vacuolated and/or their matrix is dispersed (arrowheads). Principal piece (PP), midpiece (MP).
Scale bars: (a) 0.5 μm; (b), 1 μm.

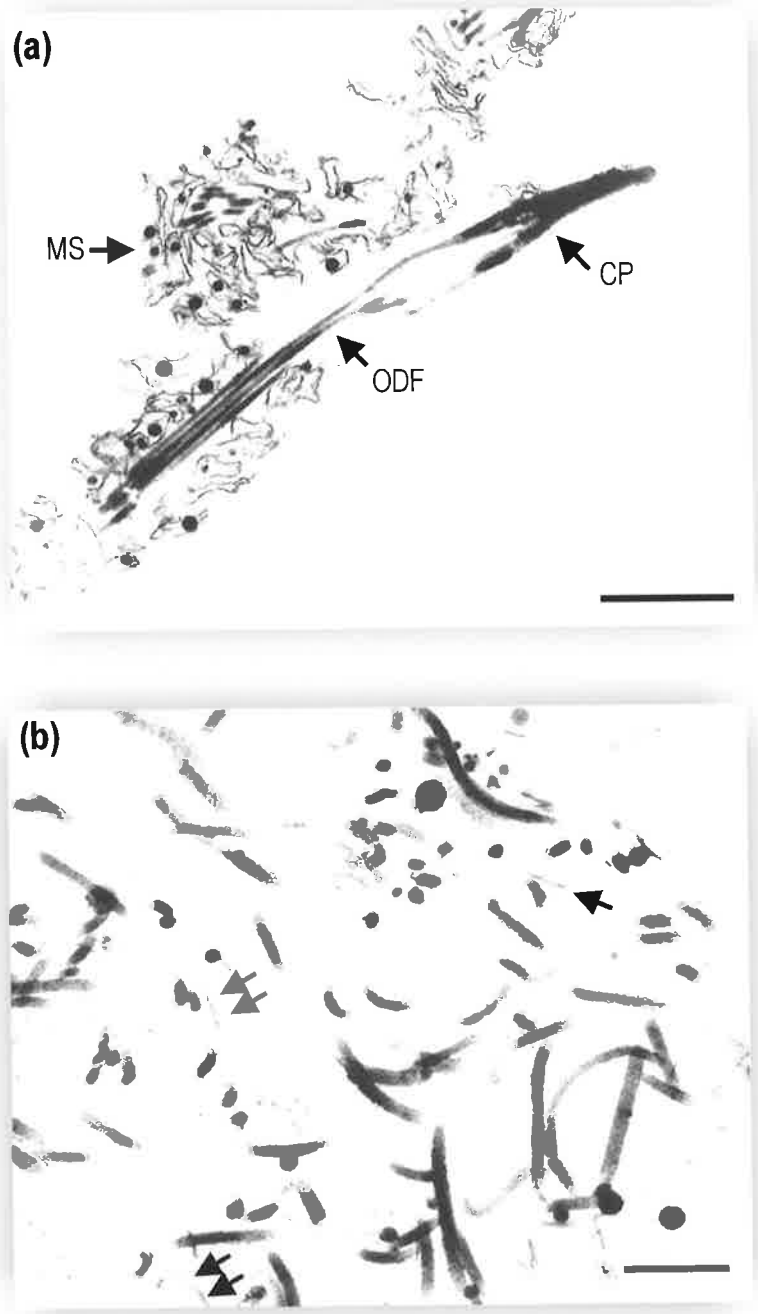

FIGURE 4.5 Electron micrographs showing that incubation of possum sperm tails in SDS-DTT for (a) 30 min resulted in the solubilisation of all sperm tail components with the exception of the outer dense fibres (ODF), connecting piece (CP) and fragments of the mitochondrial sheath (MS). (b) By 90 min, only the outer dense fibres remained and at this stage thin fibres of the outer dense fibres (arrowheads) were detached from its main portion.
Scale bars: (a) 0.5 μm; (b) 0.1 μm.

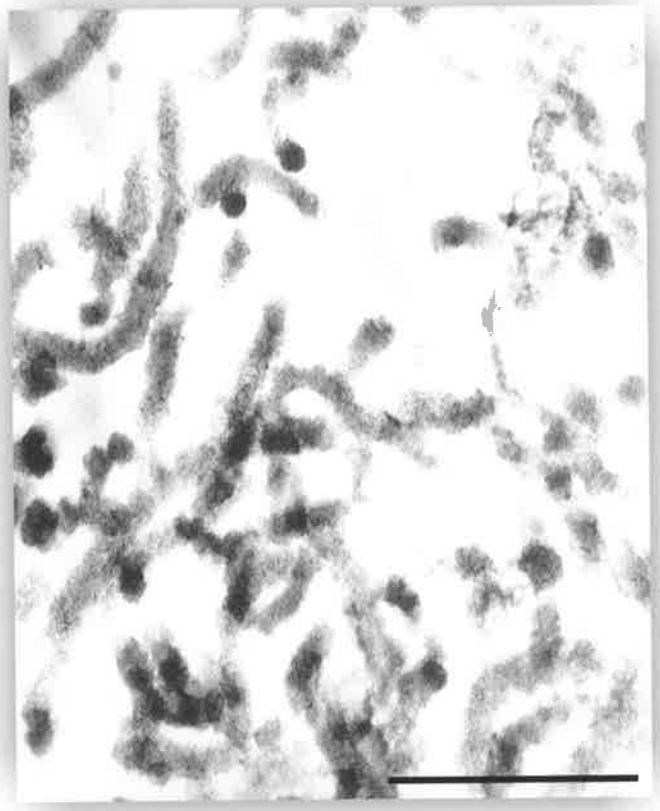

FIGURE 4.6 Electron micrograph of sperm tails incubated in SDS-DTT for 120 min. The thin fibres of the outer dense fibres have been solubilised and the larger fibres have swollen considerably.
Scale bar: 0.05 μm.

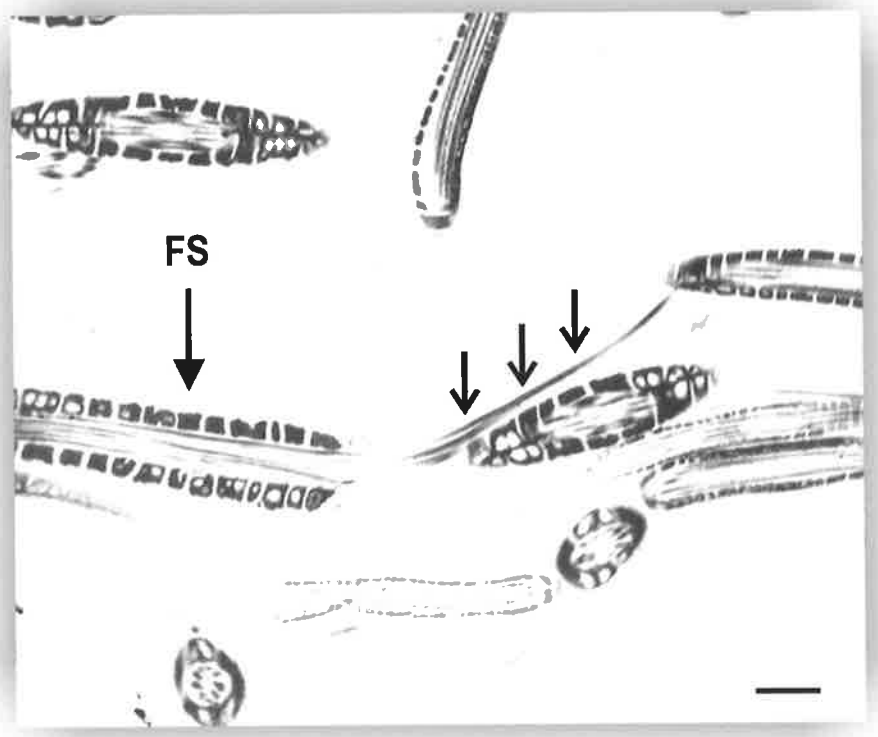

FIGURE 4.7 Incubation of possum sperm tails in Triton X-100–DTT resulted in the solubilisation of the mitochondrial sheath exposing the outer dense fibres (arrows) at their proximal, ends. Fibrous sheath (FS). *Scale bar: 0.5 μm.*

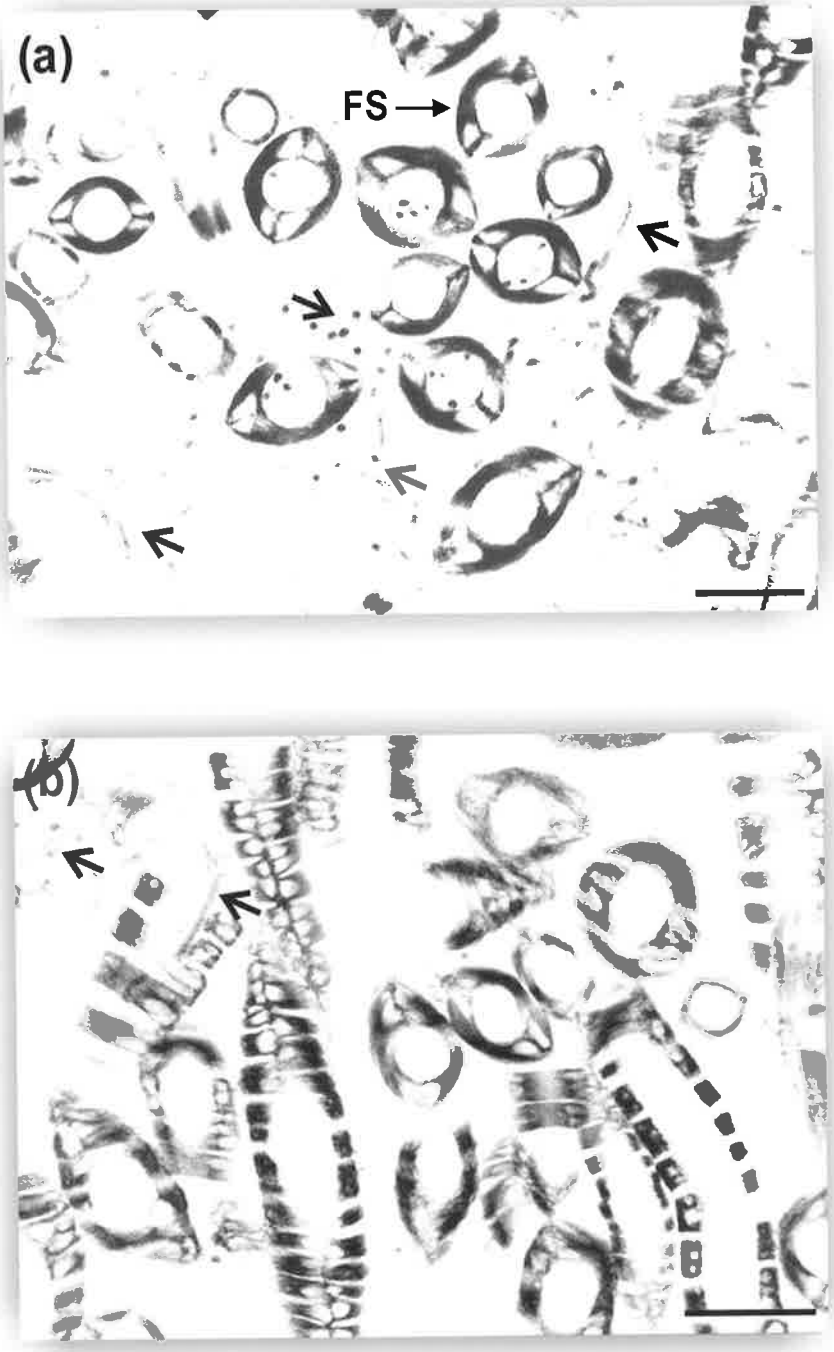

FIGURE 4.8 Electron micrographs showing the incubation of sperm tails in Urea-DTT for (a) 3 h resulted in the solubilisation of axoneme and disruption of the outer dense fibres (arrowheads), and (b) 5 h resulted in the solubilisation of most of the outer dense fibres (arrowheads) although the fibrous sheaths (FS) remained.
Scale bars: a, b, 0.5 μm.

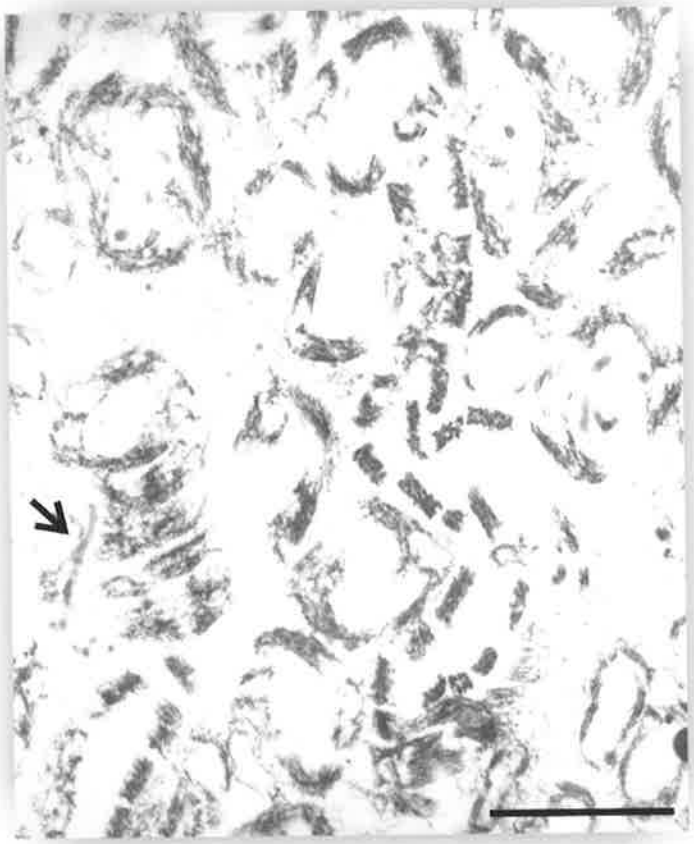

FIGURE 4.9 Electron micrograph showing that the incubation of sperm tails in Urea-DTT for 8 h resulted in the partial expansion and fragmentation of the fibrous sheath although small fragments of outer dense fibres still persisted (arrowhead).
Scale bar: 0.5 µm.

4.3.5 Protein Composition of Outer Dense Fibres

1D-SDS polyacrylamide gels of isolated outer dense fibres, after 90 min incubation, revealed the presence of seven major Coomassie Brilliant Blue-stained protein bands (Figure 4.10, Lane 1) (MWs: 73, 58, 55, 54, 52, 41 and 16 kDa). Subsequent silver staining of these ODF gels revealed an additional eleven minor bands (Fig. 4.10, Lane 2) (MWs: 106, 64, 43, 34, 32, 30, 29, 28, 26, 25 and 21 kDa). The 39-42 kDa and 15-17 kDa protein smears present after silver staining presumably originated from the 41 and 16 kDa outer dense fibre protein bands respectively, identified by Coomassie staining. The most prominent outer dense fibre protein bands had molecular masses of 73, 55, 41 and 16 kDa. SDS-polyacrylamide gels were also run of outer dense fibre fractions incubated in SDS-DTT for 120 min, at which stage the cortex-like fragments of the outer dense fibres had solubilised and only the medulla appeared to remain. Silver staining of these gels revealed that only two of the seven major possum outer dense fibre protein bands, the 41 and 16 kDa proteins, remained (Fig. 4.11).

4.3.6 Protein Composition of Fibrous Sheath

1D-SDS polyacrylamide gels of isolated fibrous sheath after 5 h incubation, revealed the presence of twelve major proteins bands stained by Coomassie Blue (MWs: 106, 76, 66, 62, 55, 53, 52, 46, 40, 30, 28, and 16 kDa) (Fig. 4.10, Lane 3). Subsequent silver staining revealed 3 additional minor bands (MWs: 35, 29 and 22 kDa) (Fig. 4.10, Lane 4). The most prominent fibrous sheath protein bands have molecular masses of 76, 66, 62, 52 and 40 kDa.

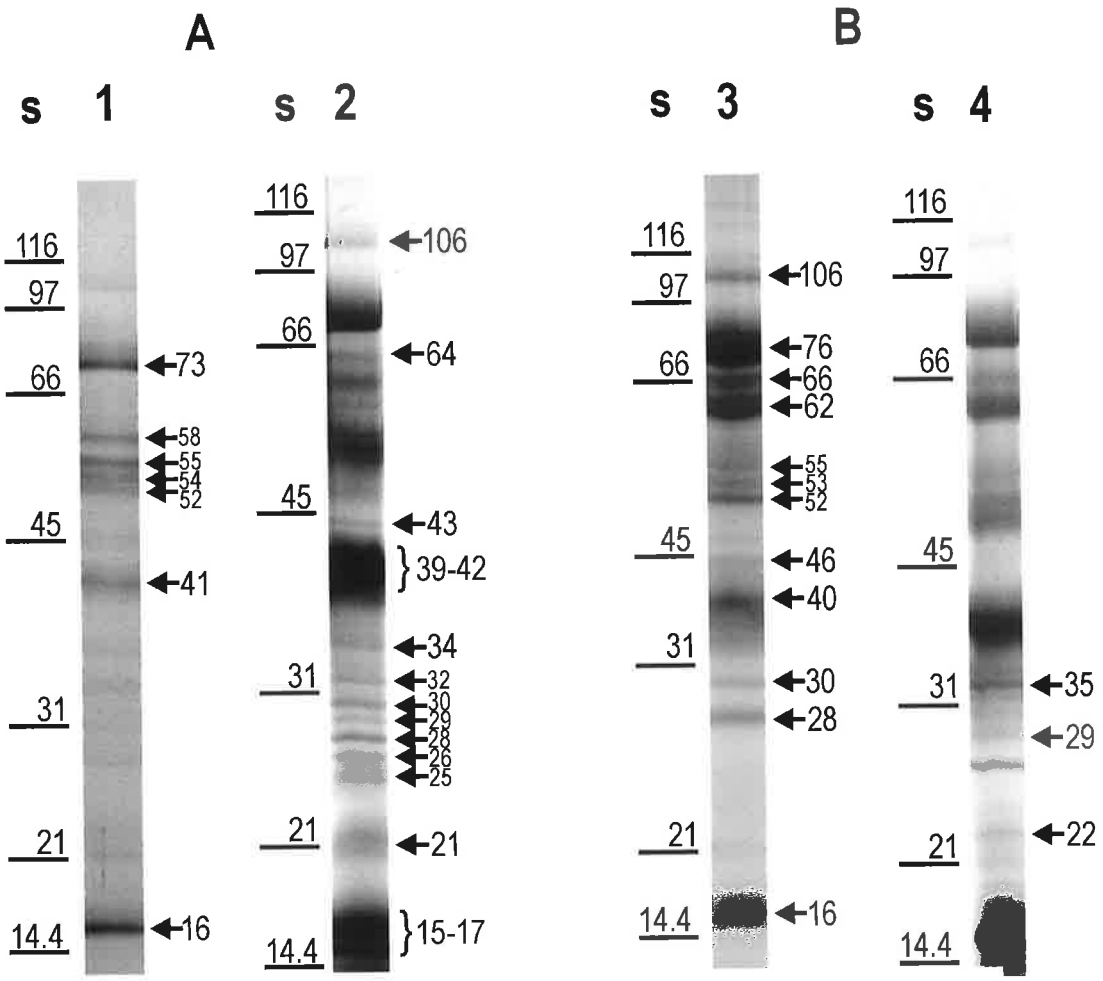

FIGURE 4.10 1D-SDS-PAGE of (A) total possum outer dense fibres stained with Coomassie Brilliant Blue (Lane 1) and silver (Lane 2), and (B) total possum fibrous sheath stained with Coomassie (Lane 3) and silver (Lane 4). Seven major and 11 minor outer dense fibre protein bands are present, and 12 major and 3 minor fibrous sheath protein bands are present (see text for details). Lanes *s*, molecular mass standards.

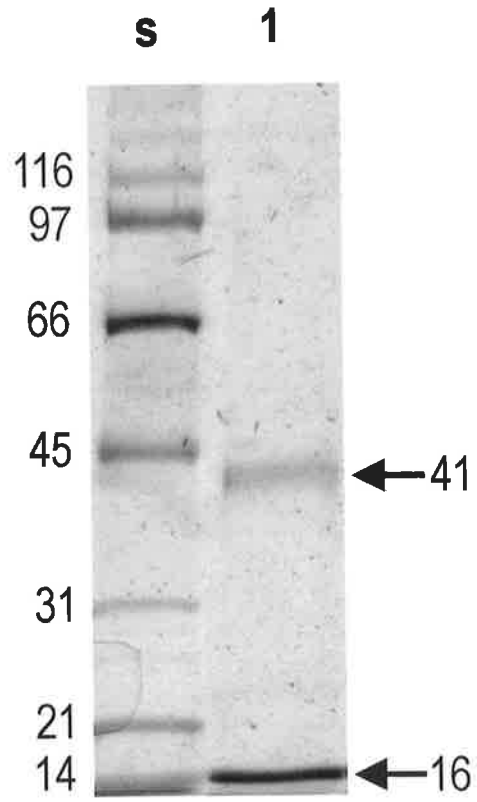

FIGURE 4.11 1D-SDS-PAGE of possum outer dense fibres, after 120 min incubation of sperm in SDS-DTT, stained with silver (Lane 1). Lane *s*, molecular mass standard.

4.4 DISCUSSION

4.4.1 Comparison of Sperm Decapitation and Sucrose Gradient Techniques

In this study, sperm tails were first removed from the sperm heads and then isolated into pure fractions before any specific incubations were carried out. This was done to try to ensure that there was no contamination of sperm head proteins in either the isolated outer dense fibre or fibrous sheath fractions. This is especially important considering that some of the laboratory rat outer dense fibre proteins have been shown to have similar molecular weights to those of, for example, the perforatorium (Oko and Clermont, 1988).

Early attempts at fractionating mammalian sperm often utilized chemical methods to dissociate the sperm heads from the tails. For example, spermatozoa of the mouse and rat were decapitated by incubation in endopeptidases, particularly trypsin (Edelman and Millette, 1971; Millette *et al.,* 1973). However, it was usually difficult to subsequently separate out relatively pure fractions of sperm heads and tails (Bradley *et al.,* 1981). In some of these studies, the pH of the incubating buffers was significantly altered from neutral, and/or reducing agents or detergents were also added (Millette *et al.,* 1973). This resulted in considerable damage and/or extraction of sperm components like the acrosome and mitochondrial sheath, which limited the usefulness of this procedure for experiments.

An alternative procedure of sperm fractionation, that of sonication, was developed. In cell biology, sonication involves the disruption of cellular components by either pulses or continuous waves of ultrasonic vibrations. This procedure was not commonly used in early experiments for it did not yield homogenous populations of sperm heads and tails.

However, by the mid-1970's, the sonication procedure was refined and relatively pure fractions of sperm heads and tails could now be isolated (Calvin *et al.,* 1975; Calvin, 1976; Calvin, 1979). In these studies, laboratory rat sperm were sonicated with continuous waves at 100% output for 10-sec bursts until the majority of the sperm tails were separated from the heads. The sperm tails were subsequently isolated from the heads by density gradient centrifugation with 1.8 M, 2.05 M and 2.2 M sucrose at 100 000 g for 60 min at 4°C (Calvin, 1976). Subsequent sperm fractionation studies that utilized sonication were largely modifications of this method and reported similar results, for example Oko (1988) demonstrated that four 15-sec bursts at 100% output were sufficient to decapitate laboratory rat sperm.

In the current study, the initial separation of possum sperm heads from tails was achieved with relatively shorter and fewer bursts of sonication than was reported in previous studies using laboratory rat (Oko, 1988; Kim *et al.,* 1995b, 1999) and tammar wallaby (Lin *et al.,* 1998) sperm. In the wallaby, decapitation was achieved with sonication using a Branson 450 Sonifier at 25 W with 0.6 pulses^{-1} for 2 x 10-sec on ice. This sonicator (25 W) is significantly more powerful than that used in the current study (10 W), which probably explains why up approximately 6 bursts of sonication was required to separate possum sperm heads from tails. It was suggested by Lin *et al.,* (1998) that the relative ease with which wallaby sperm heads separate from tails may be due to the mode of attachment of the tail to the fossa of the sperm head that occurs at the capitulum on the ventral surface of the marsupial sperm head (Lin *et al.,* 1998). Unlike placental mammals, where the sperm tail inserts into the base of the head, in most marsupial species the sperm tail inserts into the mid-ventral side of the head with the acrosome lying on the dorsal side and not forming a cap over the head (Rodger, 1991). This is because the sperm nucleus

flattens dorso-ventrally, rather than laterally, during spermiogenesis so that the sperm forms a 'T' shape. While this unique mode of sperm tail attachment is thought to allow the sperm head to rotate through various degrees during epididymal maturation (Rodger, 1991), it might also be related to the fact that there is less disulphide bonding in this region in marsupials compared to eutherians (Bedford and Hoskins, 1990; Lin *et al.,* 1998). This could reduce the strength of sperm head-tail attachment in marsupials, thereby resulting in reduced strengths and times of sonication being required to separate sperm heads from tails.

In the current study, the concentrations of sucrose, as well as force of centrifugation, required to separate possum sperm heads from tails were also different from those previously reported for eutherian species. In the laboratory rat, sperm heads and tails were separated by centrifugation at 100 000 *g* for 70 min through 65%, 70% and 75% sucrose gradients (Oko, 1988; Kim *et al.,* 1995b, 1999). However, for possum sperm, centrifugation at only 3000 *g* for 90 min through 20%, 40% and 60% sucrose gradients was necessary. Although, at this reduced speed, the centrifugation process sometimes had to be repeated to ensure a clean separation of possum sperm heads from tails, the final sperm tail extract was, nevertheless, consistently very pure using this technique. Moreover, it has been reported that repeating the centrifugation step also helps to purify sperm tail fractions in the laboratory rat (Calvin *et al.,* 1975). In the wallaby, it was also found that reduced centrifugation speeds, similar to those reported in the current study, were required to separate the sperm heads from the tails (Lin *et al.,* 1998), indicating that there are greater differences in density of the possum and wallaby sperm head and tail components compared to those of the rat.

In previous studies, particularly those utilising sperm from species other than the laboratory rat, separation of sperm heads from tails prior to extraction of the outer dense fibres and fibrous sheath was not always been carried out (Vera *et al.*, 1984; Brito *et al.*, 1986; Haidl *et al.*, 1991; Henkel *et al.*, 1994). In these studies, sperm heads are removed by chemical dissection means rather than by sonication and density centrifugation. To date, there is no clear consensus as to whether or not this method results in contamination of outer dense fibre and fibrous sheath extracts. Calvin *et al.*, (1975) found that it had no effect on the polypeptide composition of the rat outer dense fibres, however, Oko (1988) suggested that a protein ascribed to the outer dense fibres by Vera *et al.*, (1984) was in fact perforatorial protein resulting from sperm head contamination caused by this technique. In the current study, it was decided to separate sperm heads from tails prior to extraction of the cytoskeletal structures to avoid any risk of sperm head contamination.

4.4.2 Comparison of Outer Dense Fibre Isolation Techniques and Outer Dense Fibre Protein Compositions

A well-documented biochemical feature of the mammalian sperm tail is the marked insolubility of the outer dense fibres in denaturing chemicals (Calvin and Bedford, 1971; Bedford and Calvin, 1974). Based on this information, a protocol for extracting the outer dense fibres of laboratory rat sperm was developed by Calvin *et al.*, (1975) and involved incubating sperm tails in low concentrations of SDS and DTT overnight. Subsequent studies significantly increased the concentrations of SDS and DTT and consequently reduced the incubation time to less than 120 min (Oko, 1988; Kim *et al.*, 1999). In the current study, incubation of isolated possum sperm tails in 1% SDS and 2 mM DTT for 90 min resulted in the extraction of a relatively pure outer dense fibre fraction as determined transmission electron microscopy. The fact that the laboratory rat outer dense fibre

extraction protocol can be applied to a marsupial species suggests that possum outer dense fibre proteins are, like those from rat, cross-linked by disulphide bonding. It should be noted that reagents other than SDS and DTT have also been, and in some species continues to be, utilised to extract the mammalian outer dense fibres. For example, Olson and Sammons (1980) replaced the SDS for sodium lauroyl-sarcosine (SLS) and obtained identical results for the laboratory rat, while Vera *et al.*, (1984) replaced SDS-DTT with the cationic detergent cetyltrimethylammonium bromide (CTAB) and mercaptoethanol. This method has also been adapted to extract the outer dense fibres from human (Henkel *et al.*, 1992; Haidl, 1993) and bull spermatozoa (Brito *et al.*, 1986), as SDS, an anionic detergent, was shown to rapidly solubilize the entire sperm tail in these two species (Vera *et al.*, 1984; Henkel *et al.*, 1992). Although it is not clear why human and bull outer dense fibres resist solubilisation with CTAB but not SDS, Vera *et al.*, (1984) suggested that it may be related to the lower binding constant of CTAB compared with SDS. In the current study, substitution of SDS with a cationic detergent such as CTAB was not necessary as the SDS and DTT incubation proceeded at a reasonable rate and resulted in the extraction of a relatively pure, intact fraction of outer dense fibres. In the current study however, thin fibres of the possum outer dense fibres, perhaps segments from its cortex, were observed by TEM after 90 min of incubation in SDS and DTT. These thin fibres settled with the main segments of the outer dense fibre after density centrifugation and consequently the proteins contained therein were presumably observed in the polyacrylamide gels of this layer.

Solubilisation and 1D-PAGE of the isolated possum outer dense fibres stained with Coomassie consistently revealed seven major polypeptides with molecular masses of 73, 58, 55, 54, 52, 41 and 16 kDa. This is similar to the number of major rat outer dense fibre

proteins identified in studies in which the SDS-DTT extraction protocol was used (MWs: 84, 80, 32-26, 20 and 14.4 kDa (Oko, 1988); 84, 79, 66.2, 57.2, 32, 29, 26, 21 and 15.5 (Kim *et al.,* 1999)), although their molecular weights are somewhat different. The exception to this is the early Olson and Sammons (1980) study which also employed SDS-DTT but which identified only four polypeptides (MWs: 87, 25, 19 and 12 kDa), although the 25 kDa protein band was later found to be composed of two (Vera *et al.,* 1984; Oko, 1988) and then three (Kim *et al.,* 1999) proteins. Silver staining of the possum outer dense fibre gels revealed an additional eleven minor protein bands (MWs: 106, 64, 43, 34, 32, 30, 29, 28, 26, 25 and 21 kDa), compared to only five additional protein bands in silver stained gels of rat outer dense fibres (MWs: 190, 150, 54, 48.5 and 44.6 kDa (Kim *et al.,* 1999)). This suggests that either (1) there are significantly more minor proteins in the outer dense fibres of possum sperm than in rat, or (2) there may be minor contamination of the outer dense fibre fraction with, for example, proteins from remnants of the mitochondrial sheath not apparent by transmission electron microscopy.

In the studies in which CTAB-mercaptoethanol, rather than SDS and DTT, was used to extract the outer dense fibres, a similar number of major polypeptides were identified in the rat (MWs: 87, 30.4, 26, 18.4, 13 and 11.5 kDa (Vera *et al.,* 1984)), however just three proteins were reported in the bull (MWs: 85, 33 and 11 kDa) (Brito *et al.,* 1986), and human (MWs: 150, 67 and 55 kDa) (Haidl *et al.,* 1991). In the human and bull, however, the outer dense fibres were extracted using the CTAB-based protocol so it is possible that not all proteins were extracted and that additional proteins are present in their outer dense fibres. Regardless, it has been suggested that the rat outer dense fibres are comprised of a greater number of proteins than in human and bull because rat sperm tails are longer and, therefore, the outer dense fibres therein are thicker and, presumably, more complex

and so contain additional proteins (Henkel *et al.,* 1992). The correlation between sperm tail length and outer dense fibre size was first noted by Baltz *et al.,* (1990), who argued that it arises because sperm with longer tails undergo greater shear forces during epididymal transit and ejaculation and therefore require increased tensile strength from the outer dense fibres for protection. Whether or not rat outer dense fibres are biochemically more complex than their human and bull counterparts has yet to be determined, however this would seem unlikely for the outer dense fibres from each of these species appear morphologically very similar. Furthermore, in the current study possum outer dense fibres appear to be composed of a relatively large number of minor proteins, yet their flagella are significantly shorter than those of rat.

The most prominent possum outer dense fibre protein bands have molecular masses of 73 and 16 kDa. This compares to approximately 26-27 and 14-15 kDa for laboratory rat (Oko, 1988; Kim *et al.,* 1999), 85, 33 and 16 kDa for bull (Brito *et al.,* 1986) and 67 and 55 kDa for human (Henkel *et al.,* 1992; Haidl, 1993). With the exception of the human, the outer dense fibres of each of these other species are composed of a prominent low molecular weight protein between 16-14 kDa. Whether the 16 kDa possum outer dense fibre protein is homologous to the similarly-sized outer dense fibre proteins found in these eutherian species remains to be elucidated although, if this was shown to be the case, it would suggest a remarkable degree of conservation of this protein across eutherian and marsupial mammals. Little is known of the 16-14 kDa rat outer dense fibre protein as it remains the only major eutherian outer dense fibre to be sequenced and characterised in detail. In the current study, it would however appear that the possum 14 kDa outer dense fibre protein is a major component of the medulla of these fibres. This is because prolonged incubation of possum sperm tails in SDS-DTT (120 min) resulted in the

solubilisation of the thin fragments of the outer dense fibres, which are presumed to be the cortex of these fibres, and SDS-PAGE of the remaining medulla material revealed only two major proteins with molecular weights, 41 and 16 kDa, of which the latter predominates. In the bull, the major 11 kDa outer dense fibre protein has also been localised to the cortex of this structure (Schalles *et al.,* 1998).

4.4.3 Comparison of Fibrous Sheath Isolation Techniques and Protein Compositions

An important first step in characterising the marsupial fibrous sheath is to isolate it and then determine its protein composition. As with the outer dense fibres, the mammalian fibrous sheath is stabilised by disulphide bonds (Calvin and Bedford, 1971; Bedford and Calvin, 1974). Based on this property, Olson *et al.,* (1976) developed a technique for isolating the fibrous sheath from the other components of the sperm tail in the laboratory rat. Their procedure, which was subsequently also used by Olson *et al.,* (1976), Oko (1988), Brito *et al.,* (1989), Kim *et al.,* (1995b) and Jassim *et al.,* (1992), is a two-step process requiring, firstly, the solubilisation of the plasma membrane and mitochondrial sheath by incubation in Triton X-100 and DTT, and secondly, the gradual removal of outer dense fibres by prolonged incubation in Urea and DTT. Prior to Olson *et al's.,* (1976) study it had been shown that high concentrations of DTT and SDS could be used to solubilise the mitochondrial sheath (Calvin and Bedford, 1971; Millette *et al.,* 1973), however Olson *et al.,* (1976) were the first to demonstrate that a lower, and therefore less disruptive, concentration of DTT could also be used to solubilise the mitochondrial sheath if it is used in conjunction with Triton X-100 instead of SDS.

The next step in the sequential extraction procedure for isolating the fibrous sheath is the solubilisation of the remaining outer dense fibres by prolonged incubation of the sperm tails in 4.5 M Urea and 25 mM DTT, which results in the extraction of a relatively pure fibrous sheath fraction. In the possum, incubation of sperm tails in Urea and DTT for 5 h resulted in the extraction of the fibrous sheath from the remaining components of the flagellum. The concentrations of Urea and DTT used, as well as length of time of incubation, are comparable to those used in previous studies on laboratory rat sperm (Olson *et al.*, 1976; Oko, 1988, Brito *et al.*, 1989; Kim *et al.*, 1995b). In the rat, incubation of both whole (Olson *et al.*, 1976) and decapitated sperm (Oko, 1988) in Urea and DTT initially causes the outer dense fibres to coil in a helical fashion. However, this was not found to occur in the possum in the current study and also has not been reported for human (Jassim *et al.*, 1992; Kim *et al.*, 1997) and rabbit (Kim *et al.*, 1997) sperm. The functional significance of this coiling in rat sperm is unknown but it may indicate that individual possum, human and rabbit outer dense fibres might somehow be packaged differently within the sperm flagellum. Alternatively, they may already be packaged in their most favourable configuration in the possum, human and rabbit and hence do not need to unwind.

In addition to the initial coiling of the outer dense fibres, continued incubation of rat sperm tails in Urea and DTT also results in the appearance of fibrous material within the lumen of the fibrous sheath between the two longitudinal columns as determined by transmission electron microscopy (Olson *et al.*, 1976; Oko, 1988, Brito *et al.*, 1989; Kim *et al.*, 1995b). It has been suggested that this material, which is significantly reduced or eliminated by prolonged incubation (5 h) in Urea and DTT, represents the remnants of the outer dense fibres (Olson et al., 1976). The fact that the outer dense fibres and fibrous sheath,

therefore, appear to remain in close contact with each other even during this incubation process indicates that there may be a complex relationship between these two cytoskeletal structures. In the current study, incubation of possum sperm tails in Urea and DTT did not result in the appearance of fibrous material within the lumen of the fibrous sheath, however a very small number of the outer dense fibres were observed. These fibres persisted, even when the incubation was allowed to continue for 8 h. It would, therefore, seem that the outer dense fibres of at least possum sperm are more resistant to solubilisation than those of eutherian sperm. Residual outer dense fibres, as well as outer mitochondrial membranes, have also been detected in a similar study using ejaculated rabbit sperm, however when cauda sperm were substituted this material was no longer present suggesting that the outer dense fibres are stabilised during epididymal transit (Kim *et al.*, 1997). Unfortunately, this could not be tested for in the current study as ejaculated possum sperm could not be obtained. If the outer dense fibres are indeed stabilised as they pass through the epididymis it would not be the first example of such maturation of sperm components. In both marsupial and eutherian species, epididymal maturation is critical for sperm to acquire the ability to fertilise an oocyte (e.g. Harding *et al.*, 1979; Jones *et al.*, 1984; Jones and Murdoch, 1996; Lin *et al.*, 2000). It should be noted that, for the purposes of determining the protein composition of the possum fibrous sheath, incubation of sperm tails in Urea and DTT was terminated after 5 h, as opposed to 8 h, because the fibrous sheaths were very fragmented and appeared to be partly solubilised at 8 h.

Solubilisation and 1D SDS-PAGE of the possum fibrous sheath revealed twelve major proteins by Coomassie staining, with molecular masses of 106, 76, 66, 62, 55, 53, 52, 46, 40, 30, 28, and 16 kDa, with an additional three protein bands (MWs: 35, 29 and 22 kDa) identified by silver staining. In comparison, seventeen, fourteen and ten fibrous sheath

proteins have been identified by silver staining respectively in spermatozoa from the rat (Kim *et al.*, 1995b), human and rabbit (Kim *et al.* 1997). The significant increase in the number of proteins present in the fibrous sheath, compared to the outer dense fibres, in both the possum and eutherian species clearly reflects the increased complexity of the fibrous sheath with its distinct longitudinal columns and circumferential ribs. A possibilty exists that the minor 106, 55, 52 and 16 kDa possum fibrous sheath proteins are cross-contaminants from the outer dense fibres as proteins of identical molecular weights are present in gels of these fibres. For the 16 kDa fibrous sheath, this is more probable as it was found to be resistant to solubilisation (Figure 4.11) and, therefore would presumably be present in any outer dense fibre remnants present. Nevertheless, any outer dense fibre cross-contamination was found to be only very minor, suggesting that the 16 kDa protein can be attributed to the fibrous sheath. Furthermore, this 16 kDa protein was still present in gels of extracted fibrous sheaths after incubation of sperm tails in Urea and DTT for 8 h (not shown), at which time most of the outer dense fibre contaminants were no longer present, indicating that it is most likely a component of the fibrous sheath. Further supporting the notion that both the possum outer dense fibres and fibrous sheath contain distinct 16 kDa proteins is the fact that, in the laboratory rat, an ~14.4 kDa protein has been attributed to both the outer dense fibres and fibrous sheath, but antibodies affinity-purified to each of these proteins have been used to show that they are not cross-contaminants (Oko, 1988).

Previous to the current study, a 32 kDa protein, identified by a monoclonal antibody, PSA-10, had been claimed to occur in the possum and wallaby fibrous sheath (Harris and Rodger, 1998). This antibody was raised against possum acrosomal proteins, leading to the suggestion that fibrous sheath and acrosomal proteins might somehow be related. In

the current study, no 32 kDa protein was found in gels run of the possum fibrous sheath, although minor proteins with molecular masses of 28, 29 and 30 kDa were detected. It is possible that one of these proteins corresponds to the protein recognised by the PSA-10 antibody.

Although the molecular weights of most of the fibrous sheath proteins in each species are somewhat different, in the laboratory rat and rabbit the most prominent fibrous sheath proteins have molecular masses between 72 and 85 kDa (Olson *et al.*, 1976; Oko, 1988; Brito *et al.*, 1989; Kim *et al.*, 1995b; Kim *et al.*, 1997). In eutherian species, this protein has been sequenced and is referred to as AKAP4 (Carrera *et al.*, 1994; Johnson *et al.*, 1997). It is thought to play an important role in anchoring constituents required for sperm capacitation and movement (Mei *et al.*, 1997; Vijaraghaven *et al.*, 1997b). Interestingly, in the present study the most prominent possum fibrous sheath protein also has a molecular mass of 76 kDa, similar to that of AKAP4. A possibility, therefore, exists that this possum fibrous sheath protein may be the homologue of the AKAP4 eutherian protein.

4.5 CONCLUSION

The development of techniques to isolate the eutherian outer dense fibres and fibrous sheath from sperm of eutherian species was a fundamental first step in characterising the proteins contained therein and therefore gaining an understanding of the potential functions of these cytoskeletal structures. In the current study, it has been demonstrated that these techniques can be successfully applied, with minor modifications, to extract the outer dense fibres and fibrous sheath from a marsupial species, the brush-tail possum, and the proteins contained therein have now been identified. Although similar numbers of proteins are present in the possum and laboratory rat outer dense fibres and fibrous

sheath, the molecular weights of these proteins are somewhat different, with the notable exceptions of the major 16 kDa possum outer dense fibre protein and fibrous sheath proteins, and the major 76 kDa possum fibrous sheath protein. It is hypothesised that the 16 kDa protein is homologous to the 14-16 kDa rat outer dense fibre protein and, like this rat protein, may be a major component of the medulla of the possum outer dense fibres. Moreover, the 76 kDa protein may be homologous to the eutherian AKAP4 protein as these proteins are of very similar molecular weights. In subsequent chapters of this thesis, an immunocytochemical approach will be taken to determine whether or not there is conservation of the major outer dense fibre and fibrous sheath proteins across marsupial and eutherian mammals.

Chapter 5

IMMUNOCYTOCHEMICAL ANALYSIS OF FORMATION, AND MAJOR PROTEINS, OF THE OUTER DENSE FIBRES AND FIBROUS SHEATH

5.1 INTRODUCTION

In Chapter 4, a method for the extraction of the outer dense fibres and fibrous sheath from possum sperm was presented, and the number and molecular weights of the proteins contained therein determined by SDS-PAGE. Although the number of proteins identified in each structure, as well as the molecular weights of some of the major proteins, were similar to those previously reported for eutherian species such as the laboratory rat, the extent of homology of outer dense fibre and fibrous sheath proteins between marsupial and eutherian species is unknown. One approach to address this question is to ascertain whether antibodies raised against the proteins of the possum outer dense fibres and fibrous sheath cross-react to these cytoskeletal structures in other species. In previous studies using eutherian species, antibodies prepared against rat outer dense fibre and fibrous sheath proteins were found to bind to these cytoskeletal structures in several other eutherian species (Kim *et al.*, 1995b, 1999). Moreover, several of the major proteins in each of these cytoskeletal structures were found to share common epitopes (Oko, 1988).

Antibodies prepared against outer dense fibre and fibrous sheath proteins may also be used to determine their specific time and site of formation during spermiogenesis. In

Chapter 3, the major morphological changes during outer dense fibre and fibrous sheath formation were described at an ultrastructural level, however by this technique alone it was not possible to determine time and site of origin, developmental expression, and intracellular localisation of outer dense fibre and fibrous sheath proteins. In previous studies on the laboratory rat, it has been shown, with antibodies against proteins of the outer dense fibres and fibrous sheath, that outer dense fibre and fibrous sheath proteins appear within the spermatid cytoplasm prior to their assembly along the axoneme (Oko and Clermont, 1989; Clermont *et al.,* 1990). However, peak cytoplasmic immunoreactivity, and presumably maximum levels of translation, occur late in spermiogenesis. Furthermore, the proteins of the outer dense fibres appear to be stored in granulated cytoplasmic bodies prior to their assembly (Oko and Clermont, 1989; Clermont *et al.,* 1990).

In light of the fact that previous immunocytochemical studies have provided significant insight on the extent of conservation, as well as morphogenesis, of the outer dense fibres and fibrous sheath in the rat, the aim of the current chapter is to use polyclonal antibodies against the proteins of the possum outer dense fibres and fibrous sheath to (1) determine the extent of antigen cross-reactivity, and therefore possibly conservation, of these proteins between select marsupial species from several different families, as well as between the possum and the laboratory rat, and (2) re-examine the morphogenesis of the possum outer dense fibres and fibrous sheath in order to establish the precise time, and site of formation, of these proteins during spermiogenesis.

5.2 MATERIALS AND METHODS

5.2.1 Isolation of Outer Dense Fibre and Fibrous Sheath Proteins

The isolation of possum outer dense fibre and fibrous sheath proteins followed the protocols previously outlined in Chapter 4. Briefly, sperm tails were isolated by sonication and sucrose density gradient centrifugation and then incubated in either SDS-DTT or Urea-DTT to isolate the outer dense fibres and fibrous sheath respectively. These structures were subsequently solubilised in SDS-ß-mercaptoethanol.

5.2.2 Polyclonal Antibody Preparation

The denatured outer dense fibre and fibrous sheath fractions were emulsified in an equal volume of Freund's complete adjuvant (Sigma, St. Louise, MO). Approximately 50 µg of protein was injected either intraperitoneally or subcutaneously into either rabbits or Sprague-Dawley rats. Animals were boosted with 50 µg of solubilised protein in an equal volume of Freund's incomplete adjuvant at 2 week intervals for 6 weeks, and test bleeds were carried out 7 days after each boost. Serum was collected and stored at -70°C. Pre-immune sera were collected from all animals prior to immunization.

In the current study it was hoped that the polyclonal serum obtained could be affinity-purified in an attempt to separate antibodies reactive to only one possum outer dense fibre and fibrous sheath protein as described by Talian *et al.*, (1983). Unfortunately, however, attempts at affinity-purifying the sera obtained were unsuccessful, with no reactivity observed in western blots of possum fibrous sheath proteins. Limited quantities of sera precluded further attempts to affinity purify these antibodies.

5.2.3 Western Blotting

Spermatozoa from the cauda epididymides of the laboratory rat (Family: Muridae), wallaby (Family: Macropodidae), dunnart (Family: Dasyuridae) and koala (Family: Phascolarctidae) were solubilised in 4.5 M Urea, 2% SDS in 25 mM DTT for 5 h at room temperature, insoluble material was removed by centrifugation at 15 000 *g* for 20 min, and final protein concentration determined. Proteins were separated on 7 – 12% SDS-polyacrylamide mini gels (Bio-Rad) and up to 10 µg of protein was loaded per lane. Electrophoretic transfer of the proteins from the gels to the nitrocellulose was carried out in a Trans-blot cell (Bio-Rad) in 25 mM Na_2HPO_4 buffer at pH 6.4, 300 V, for 1 h. After removal from the transfer apparatus, the gels were stained with Coomassie Brilliant Blue and the nitrocellulose was stained temporarily with 0.2% Ponceau in 3% trichloracetic acid (TCA) to determine the effectiveness of the transfers. The blots were destained and blocked by incubating with 5% non-fat milk powder in TBS-Tween (25 mM Tris-HCl buffered saline, pH 7.4, containing 0.1% Tween-20), overnight at 4°C. They were washed in TBS-Tween and incubated with immune serum diluted 1:100 in TBS-Tween for 1 h at room temperature. The blots were subsequently rinsed in TBS-Tween 4 times at 5 min per time, and incubated with biotinylated goat anti-rat immunoglobulin antiserum (Zymed, San Francisco, CA), diluted 1:1000 in TBS-Tween for 1 h at room temperature. They were washed in TBS-Tween as described and incubated with strepavidin-alkaline phosphatase (SA-AP) (Amersham, Buckinghamshire, UK), diluted 1:3000 in TBS-Tween for a further 1 h. The blots were developed with 10 ml of 5'-bromo-4-chloro-3-indolyl phosphate/nitro blue tetrazolium (BCIP/NBT) liquid substrate system (Sigma). Controls consisted of replacing the primary antibody with pre-immune serum or buffer.

5.2.4 Indirect Immunofluorescence

Possum, koala, wallaby, dunnart and rat cauda epididymal sperm were washed in PBS, pH 7.4, and fixed in 3% paraformaldehyde, in PBS, at 4°C for 20 min. Reactive aldehyde groups were blocked by resuspending the fixed sperm in PBS containing 50 mM glycine for 20 min, and 100 µL aliquots were spotted on glass slides, pre-coated with 3-aminopropyltriethoxysilane (APES), for 2 h at 4°C. The slides were rinsed four times with PBS, pH 7.4, and spermatozoa permeabilised with ice-cold acetone for 5 min. The sperm were rinsed 4 times in PBS and incubated with 10% normal goat serum (NGS) in PBS for 20 min to reduce non-specific binding. They were then incubated overnight at 4°C with antiserum diluted 1:100 in PBS containing 0.1% BSA and 1% NGS. The slides were rinsed 4 times in PBS, incubated in PBS containing 10% NGS for 15 min, and then FITC-conjugated goat anti-rat IgG (Sigma) diluted 1:50 in PBS containing 0.1% BSA and 1% NGS for 45 min. Non-specific staining was determined by replacing the primary antiserum with pre-immune serum or PBS and autofluorescence was determined by omitting the second antibody.

5.2.5 Light Microscope Immunohistochemistry

Adult male possums were anaesthetized with isoflurane and testes and epididymides were fixed by perfusion for 20 min with Bouin's fixative. Testes were excised, cut into $1cm^3$ cubes and immersion-fixed in Bouin's fixative for 2 h. Tissue was cut into smaller, $5mm^3$ cubes, reimmersed in fixative for an additional 2 h, and dehydrated by passing through a graded series of ethanols. Tissue was infiltrated in paraffin wax, and 5µm sections were cut on a Leica microtome, and floated onto slides. The remaining steps in this protocol were adapted from that described by Oko and Clermont (1989). Deparaffinisation of these sections followed standard procedures with two notable exceptions: (i) during hydration

sections were immersed in 70% ethanol containing 1% (w/v) lithium carbonate to inactivate residual picric acid, and then (ii) endogenous peroxidase activity was eliminated by incubating sections in methanol containing 1% (v/v) hydrogen peroxide for 10 min. Hydrated sections were subsequently washed for 5 min in distilled H_20 containing 300 mM glycine to block any free aldehyde groups, and then rinsed in 20 mM Tris-HCl saline (TBS), pH 7.4.

Non-specific binding of IgG was blocked by incubating sections in 10% NGS in TBS for 30 min. Excess fluid was shaken off and sections were then incubated for 1 h with the primary antibody diluted 1:100 in TBS-Tween containing 1% NGS. Sections were washed 6 times for 5 min each in TBS-Tween containing 1% NGS, blocked with 10% NGS, and incubated with biotin-labelled goat anti-rat immunoglobulin (Sigma) diluted 1:25 in TBS for 1h. Sections were washed in TBS-Tween and incubated in SA-AP diluted 1:3000 in TBS for 1 h, washed again, and antibody-binding was visualised by incubating sections with diaminobenzidene tetrahydrochloride (Zymed, San Francisco). Sections were lightly counterstained with Haematoxylin, dehydrated by passing through a graded series of ethanols and mounted under glass coverslips with Pix mounting medium.

Pre-immune sera was used in place of primary antibody on all control slides. Immunostaining was repeated on sections of testes from four different animals to ensure that the results were reproducible.

5.2.6 Immunogold Electron Microscopy

Adult male possums were anaesthetized with isoflurane and testes and epididymides were fixed by perfusion for 20 min with 4% paraformaldehyde in 0.2 M PBS, pH 7.4. Tissue was

then dissected free and immersed in the same fixative for 2 h, washed in two changes of PBS and dehydrated by passing through a graded series of ethanols. The tissue was infiltrated in a 2:1 ratio of LR White:70% ethanol for 1 h, followed by two further incubations in pure LR White resin for 1 h and then overnight. The resin was again replaced just prior to polymerization in gelatin capsules at 60°C for 24 h. Ultrathin sections were cut on a Reichert Jung Ultracut microtome and mounted on nickel grids.

Sections on grids were blocked by incubating in 10% normal goat serum (NGS) in TBS for 30 min, and then incubating with the primary antibody diluted 1:100 in TBS-Tween containing 1% NGS for 1 h. The grids were washed 6 times for 5 min each in TBS-Tween, and further blocked in 10% NGS for 15 min before being incubated in 10 nm gold-conjugated goat anti-rat immunoglobulin (Sigma), diluted 1:20, for 1 h at room temperature. They were then washed 6 times for 5 min each, in TBS-Tween and 4 times for 5 min each in double distilled water. The grids were finally stained with uranyl acetate (3 min) and examined on a Phillips CM100 transmission electron microscope at 80 kV.

5.3 RESULTS

5.3.1 Immunoreactivity of Spermatozoa to Polyclonal Serum

No antibody responses were detected, by immunofluorescence or western blotting, in any of the rabbits immunised with either whole preparations of outer dense fibre or fibrous sheath proteins. As only very limited quantities of these proteins were available, it was decided that instead of merely repeating this experiment in rabbits, raising of antibodies would be attempted in an alternative species, the laboratory rat. It was hoped that outer dense fibre and fibrous sheath proteins would elicit a greater immune response in the rat compared to the rabbit. In the rat, either no or only a very weak antibody response was detected in animals immunised with outer dense fibre proteins. Consequently, it was not possible to further investigate outer dense fibre protein formation and conservation by immunocytochemical means. In contrast, a very strong antibody response was observed in each of the rats immunized with fibrous sheath proteins. As there were no differences in immunostaining with each of the anti-fibrous sheath antibodies, they will collectively be referred to, from this point onwards, as *PoTVFS* (*Polyclonal Trichosurus Vulpecula Fibrous* Sheath) serum.

The *PoTVFS* serum reacted strongly, and specifically, with proteins of the principal piece of permeabilised possum cauda sperm, with no staining observed over any of the proteins of the midpiece or sperm head (Figure 5.1a, b). Ultrastructural localization of *PoTVFS* to possum cauda sperm showed distinct immunogold labelling over the entire fibrous sheath, but no antibody reactivity was observed over the outer dense fibres, mitochondrial sheath, midpiece fibre network, acrosome or subacrosomal material (Figure 5.1c).

Intense immunofluorescence was also observed with *PoTVFS* over the principal piece in permeabilised cauda sperm from the koala (Figure 5.2a, b), dunnart (Figure 5.2c, d), and wallaby (Figure 5.2e, f), with intermittent fluorescence observed over the principal piece of laboratory rat sperm (Figure 5.2g, h). No staining of the sperm head or midpiece components was evident in any of these species. The same pattern of labelling was also observed over dunnart cauda sperm by immunoelectron microscopy (not shown). These dunnart sperm also have connecting laminae that occur between the outer dense fibres and axoneme; *PoTVFS* did not bind to proteins in these structures either.

In western blots, the *PoTVFS* serum reacted strongly with the major fibrous sheath polypeptides of molecular masses 106, 76, 62, 40 and 16 kDa (Figure 5.3, Lane 1). There was no cross-reactivity observed with the possum outer dense fibre proteins (Figure 5.3, Lane 2). In addition, the antibody cross-reacted with proteins from whole laboratory rat, wallaby, dunnart and koala cauda spermatozoa extracts (Figure 5.3, Lanes 3-6) (Table 5.1). The antibody cross-reacted with the 76 and 62 kDa proteins from all four species, as well as the 106 kDa proteins from rat, dunnart and koala, the 45 kDa proteins from rat and dunnart, and the 48 kDa proteins from tammar and koala (Figure 5.3, Lanes 3-6) (Table 5.1). Additional proteins were immunostained in each species, especially in wallaby sperm extracts (Table 5.1). No staining was observed when immune serum was replaced with pre-immune serum (Figure 5.3, Lanes 7-12).

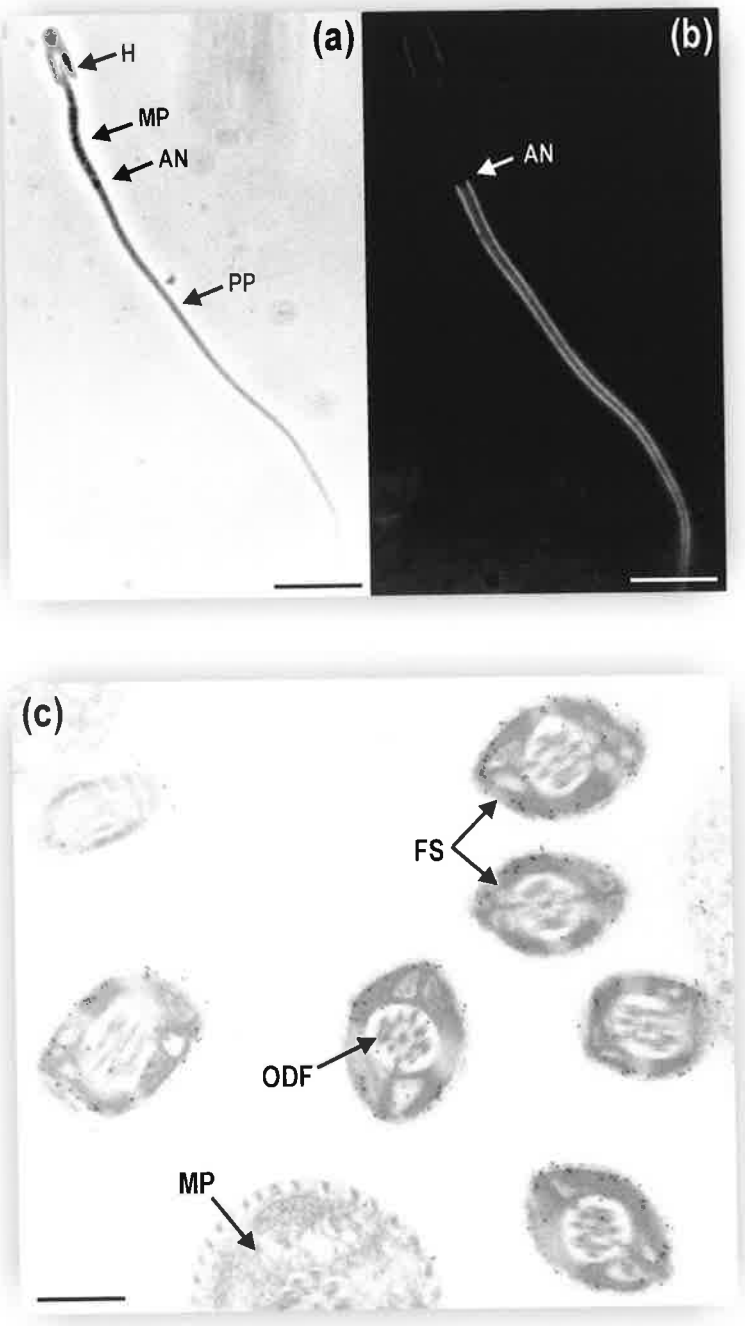

FIGURE 5.1 Immunocytochemistry of possum spermatozoa incubated with *PoTVFS* serum. (a) Phase contrast and (b) corresponding fluorescent micrographs of a possum spermatozoon probed with *PoTVFS* serum. There is positive staining of the principal piece (PP), but no cross-reactivity with the sperm head (H) or midpiece (MP); annulus (AN). (c) Transverse sections of sperm flagella showing immunogold localization of *PoTVFS* over the fibrous sheath (FS) with no specific labeling occurring over the outer dense fibres (ODF) and midpiece.
Scale bars: (a, b) 10 µm, (c) 0.5 µm.

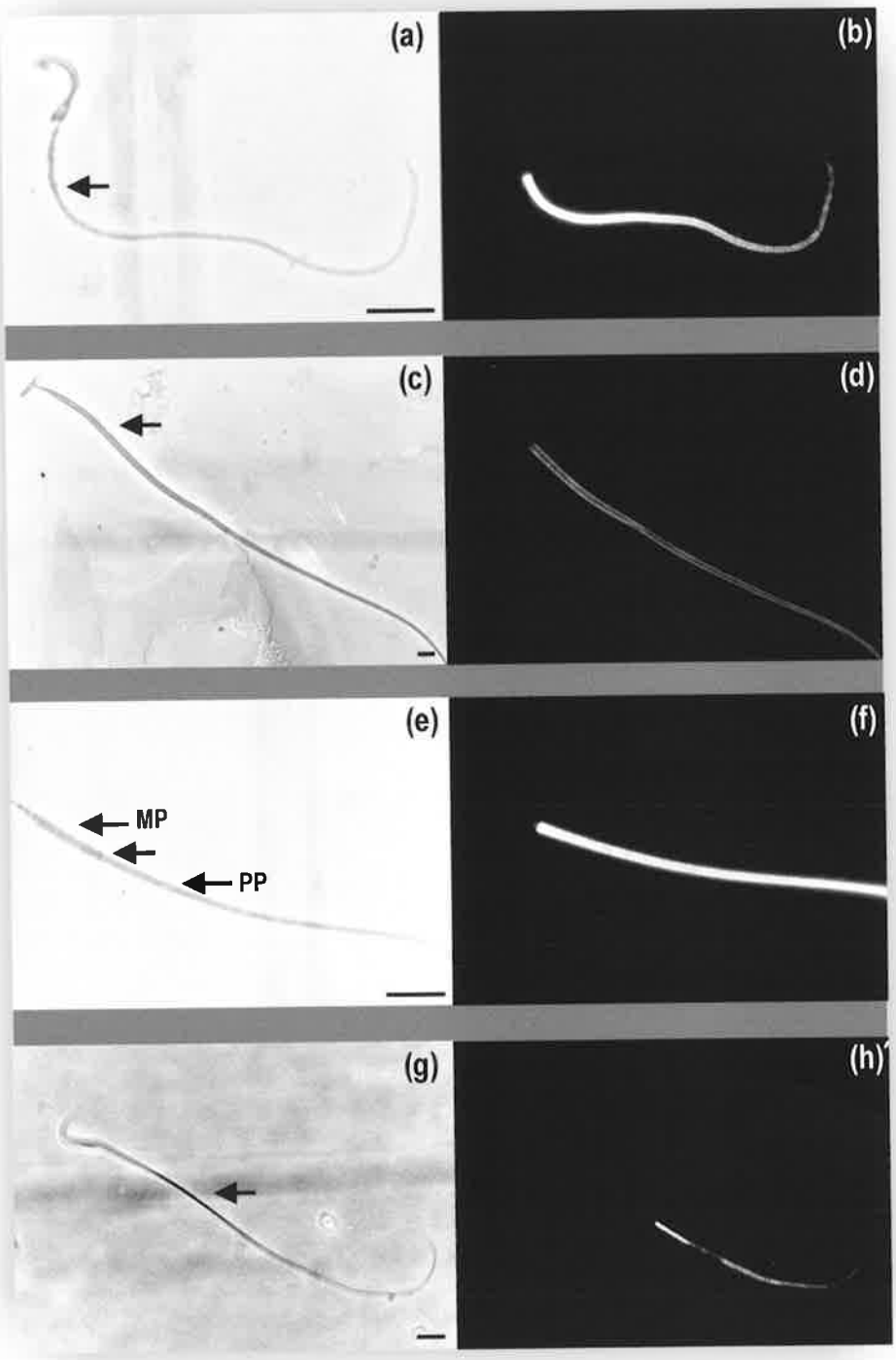

FIGURE 5.2 (a, c, e, g) Phase contrast and corresponding (b, d, f, h) immunofluorescent localization of *PoTVFS* serum to the principal piece of fixed, permeabilised cauda spermatozoa from the (a, b) koala, (c, d) dunnart, (e, f) wallaby and (g, h) laboratory rat. Strong fluorescence was observed over the principal piece (PP) of all species. Midpiece (MP), annulus (arrow).
Scale bars: 10 µm.

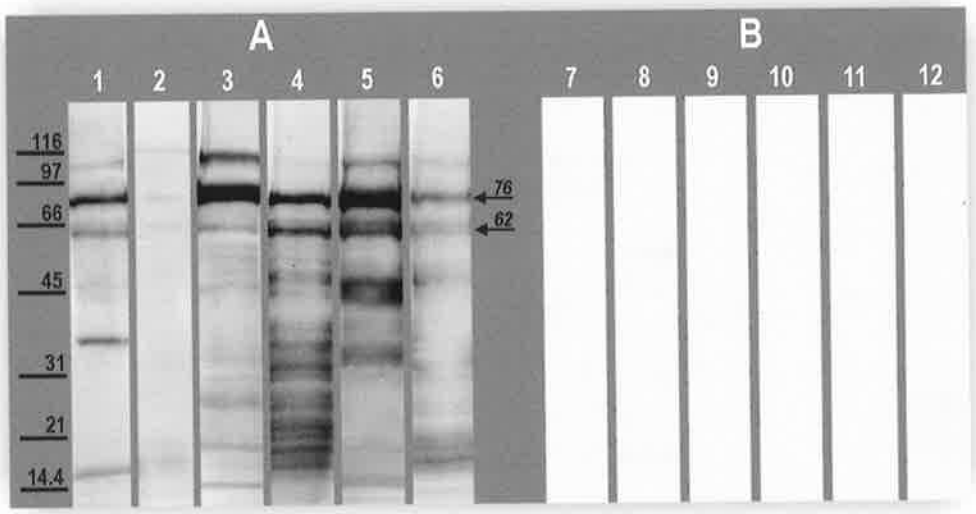

FIGURE 5.3 Western blot of possum fibrous sheath (Lane 1), possum outer dense fibres (Lane 2) and laboratory rat (Lane 3), wallaby (Lane 4), dunnart (Lane 5) and koala (Lane 6) whole sperm polypeptides, probed with the *PoTVFS* serum. *A* and *B* represent corresponding blots stained with immune and pre-immune sera respectively. The antibody recognized most of the major possum fibrous sheath proteins (Lane 1), but did not cross-react with the possum outer dense fibres (Lane 2). Numerous proteins from rat, wallaby, dunnart and koala spermatozoa were immunostained in the including the 76 and 62 kDa polypeptides in each species (Lanes 3-6). No immunoreactive bands were detected in blots probed with pre-immune sera controls (Lanes 7-12).

TABLE 5.1

Proteins Recognised* by *PoTVFS* Serum

Possum FS	Possum ODF	Rat Sperm	Wallaby Sperm	Dunnart Sperm	Koala Sperm
106	-	106	-	106	106
76#	-	**76**	**76**	**76**	**76**
62#	-	**62**	**62**	**62**	**62**
-	-	-	48	-	48
-	-	45	-	45	-
40	-	-	-	-	-
-	-	-	39	-	-
-	-	-	37	-	-
-	-	-	-	35	-
-	-	-	34	-	-
-	-	-	32	-	-
-	-	27	27	-	-
-	-	20	20	-	20
16	-	-	16	-	16
-	-	14	-	14	-

*Recognised by western blotting.
#The 76 and 62 kDa proteins are shown in bold as they are recognised in all species

5.3.2 Immunoreactivity of Spermatids to Fibrous Sheath Antibody

5.3.2.1 LM Immunohistochemistry

Immunohistochemical staining of the seminiferous tubules of possum testes with *PoTVFS* serum was found to be variable in different stages and step-specific. No reactivity was detected in any of the early, round spermatids (steps 1-6) treated with *PoTVFS* (Figures 5.4a-f), however the cytoplasm and developing flagellum of elongating spermatids (steps 7-12) (Figures 5.4g-i, a-c), as well as the flagella of spermatozoa at spermiation (Figure 5.4d), were immunoreactive. Faint immunostaining was first detected within the cytoplasm of step 7 spermatids (Figure 5.4g), however labelling rapidly increased in intensity in this region during steps 8 and 9, during which time the flagellum first appeared immunoreactive (Figures 5.4h, I arrows). Immunostaining was generally uniform throughout the cytoplasm of these spermatids. Peak cytoplasmic reactivity was found in step 10 cells (Figure 5.4a), during which time the entire flagellum was stained, and remained elevated during step 11 (Figure 5.4b), diminishing rapidly in the remaining step of spermiogenesis. In comparison, immunostaining of the spermatid flagellum, which began at step 8, increased steadily in intensity during steps 11-12 of spermiogenesis (Figures 5.4b, c), reaching a peak in spermatozoa at spermiation (Figure 5.4d). There was some minor staining of residual material within the seminiferous tubules during Stage IV (Figure 5.4d arrow).

No immunostaining was detected any of the seminiferous tubules incubated in pre-immune sera.

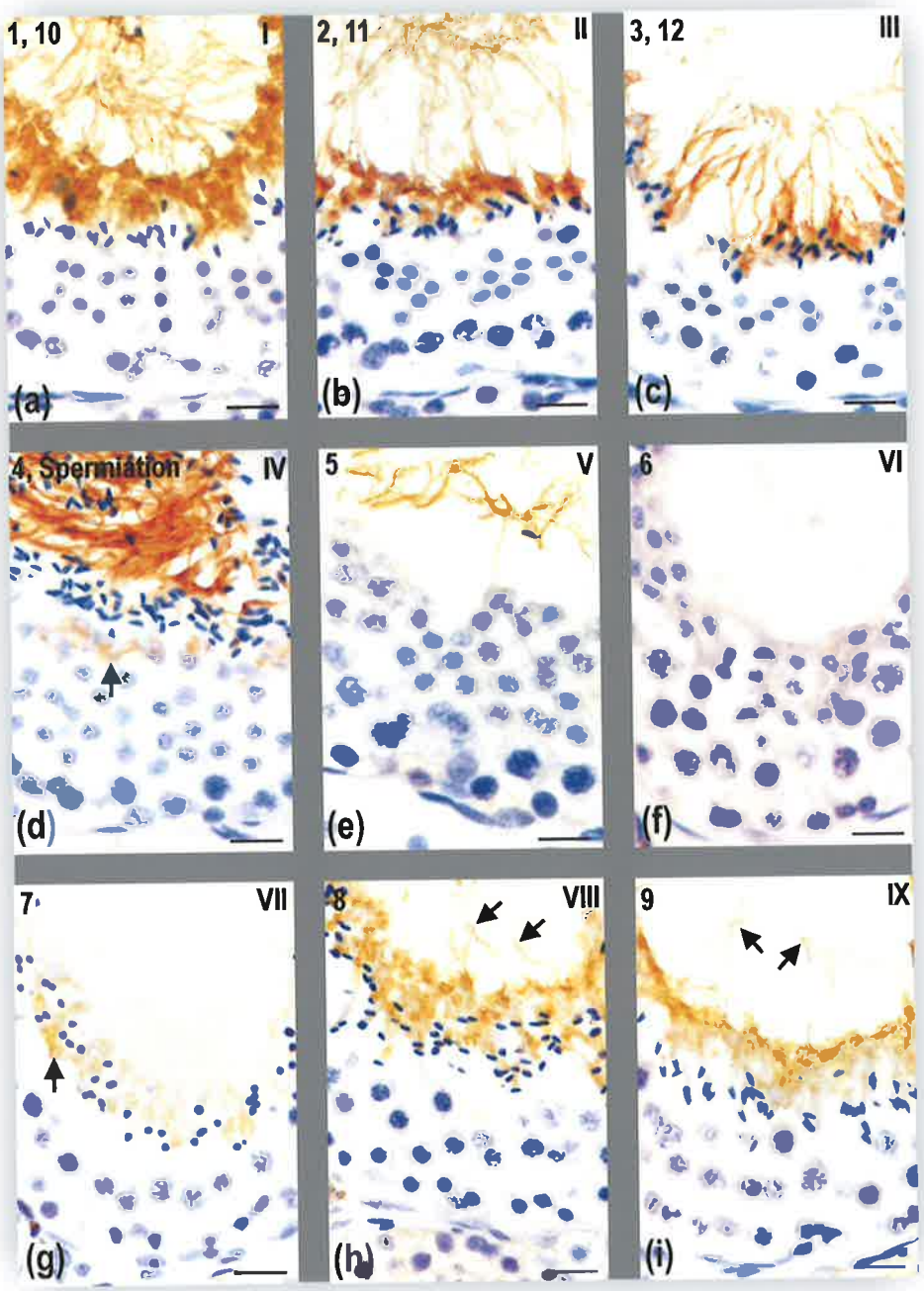

FIGURE 5.4 (a-i) Possum testicular sections immunostained with the *PoTVFS* serum. The stages (I–IX, top right corner of figures) of the cycle of seminiferous epithelium, and spermatid steps (1–12, top left corner of figures) of spermiogenesis, are indicated. Spermatid cytoplasmic staining extends from steps 7-12 of spermiogenesis but peaks in step 10 cells. Staining of the spermatid flagellum is first evident during step 8 of spermiogenesis (arrowheads) and peaks in spermatozoa at spermiation.
Scale bars: (a-i) 12 μm.

5.3.3.2 Immunogold Labelling

No immunogold labelling was detected in step 1-4 possum spermatids (distal flagellum of a step 4 spermatid shown in Figure 5.5a). During steps 5-9 of spermiogenesis, a small amount of labelling was detected over the spermatid flagellum, although it did not appear to be specifically localised to the anlagen of the longitudinal columns nor circumferential ribs of the fibrous sheath (Figure 5.5b; 5.6a, b, c; 5.7b; 5.8a, b). In step 10 spermatids, the fibrous sheath appeared, however, to be specifically, lightly labelled with the *PoTVFS* serum (Figure 5.9a); this labelling gradually increased in intensity in the remaining steps of spermiogenesis peaking at step 12 (Figure 5.9b; 5.10; 5.11a, b).

In contrast to labelling of the flagellum, labelling of the *PoTVFS* antiserum to the spermatid cytoplasm was found to occur from step 6 of spermiogenesis (Figure 5.6b), a step earlier than was found by immunohistochemistry. Gold labelling was initially diffuse (Figure 5.6b), but gradually increased in intensity (Figure 5.7a), peaking at step 10 (Figure 5.9b). In step 11 spermatids, there was a marked increase in immunogold labelling over the abaxial cytoplasm especially in the proximal segment of the flagellum (Figure 5.10). Immunogold labelling was restricted to the fibrous sheath of step 12 spermatids (Figure 5.11a, b).

No immunogold labelling was detected in any testicular sections incubated in pre-immune sera.

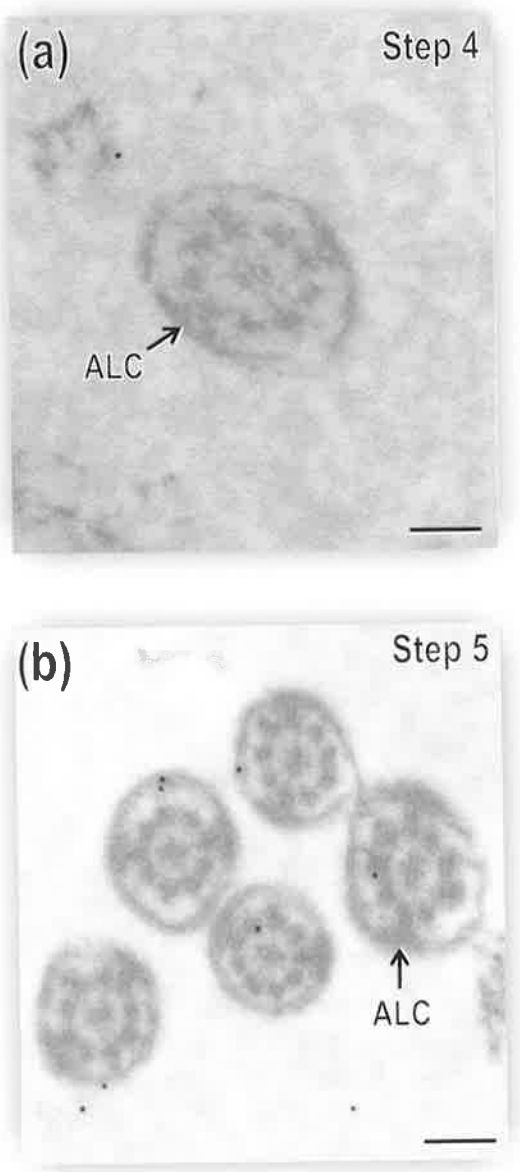

FIGURE 5.5 Transverse sections through the flagella of (a) step 4 and (b) step 5 possum spermatids treated with *PoTVFS* serum. Immunoreactivity is non-existent in the flagella of step 4 spermatids and only very weak and non-specific in step 5 cells. Anlagen of the longitudinal columns (ALC).
Scale bars: (a) 0.1 µm, (b) 0.15 µm

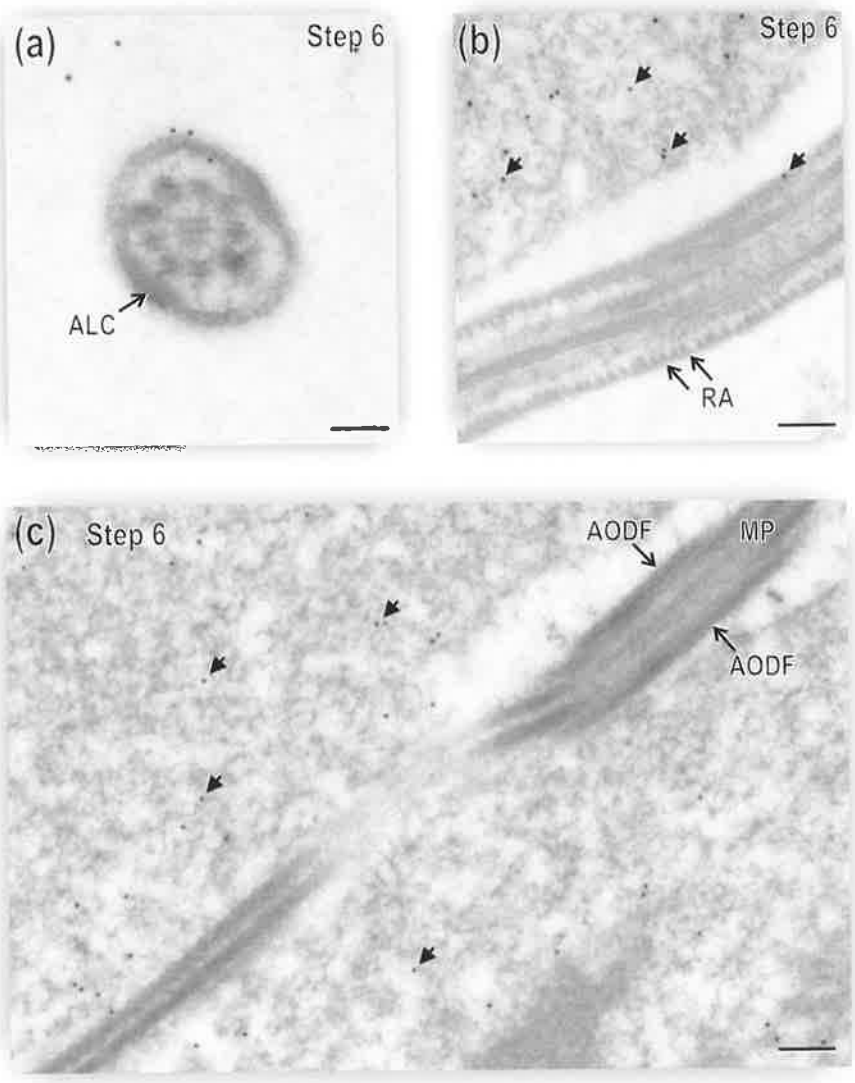

FIGURE 5.6 Transverse (a) and longitudinal (b, c) sections through step 6 possum spermatids treated with *PoTVFS* serum. Immunogold labelling of the flagellum is very weak in the (a) distal segment of the flagellum and (b) non-existent at its proximal end. There is uniform but relatively weak labelling of the spermatid cytoplasm (arrowheads). Anlagen of the longitudinal columns (ALC); anlagen of the circumferential ribs (RA); anlagen of the outer dense fibres (AODF); midpiece (MP).
Scale bars: (a) 0.1 μm, (b) 0.15 μm, (c) 0.2 μm

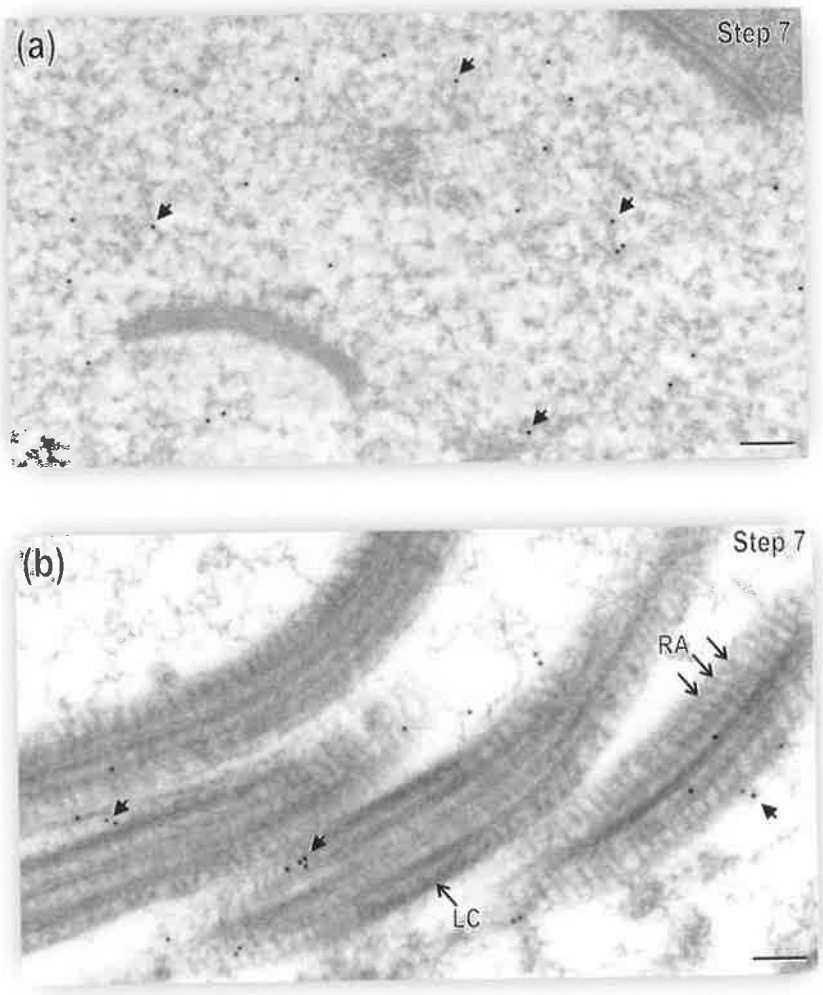

FIGURE 5.7 Sections through the (a) cytoplasm and (b) distal flagellum of a step 7 spermatid treated with *PoTVFS* serum. Labelling occurs over the spermatid cytoplasm (arrowheads), but is sparse over the anlagen of the longitudinal columns (ALC) and circumferential ribs (RA). *Scale bars: (a) 0.1 μm, (b) 0.1 μm*

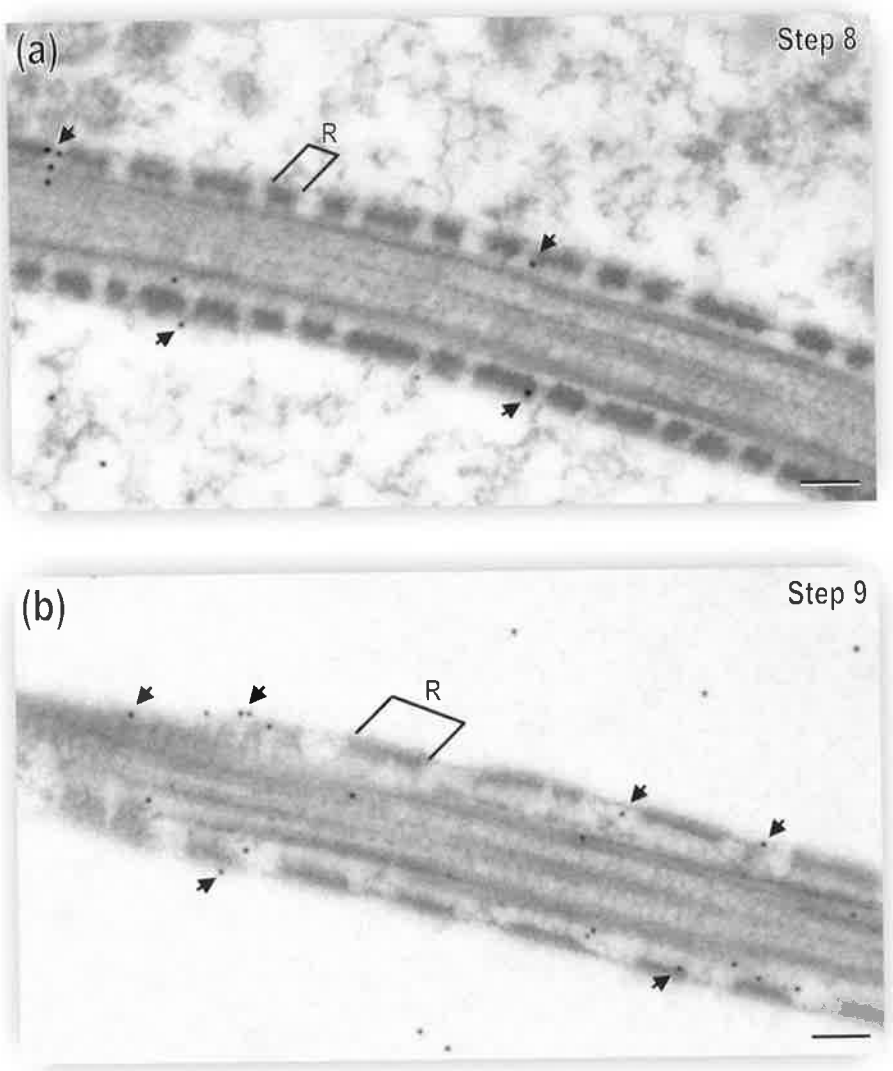

FIGURE 5.8 Longitudinal sections through the flagella of (a) step 8 and (b) step 9 spermatids treated with *PoTVFS* serum. There is weak, but non-specific labelling (arrowheads) over the flagellum. Circumferential ribs (R).
Scale bars: (a) 0.1 µm, (b) 0.1 µm

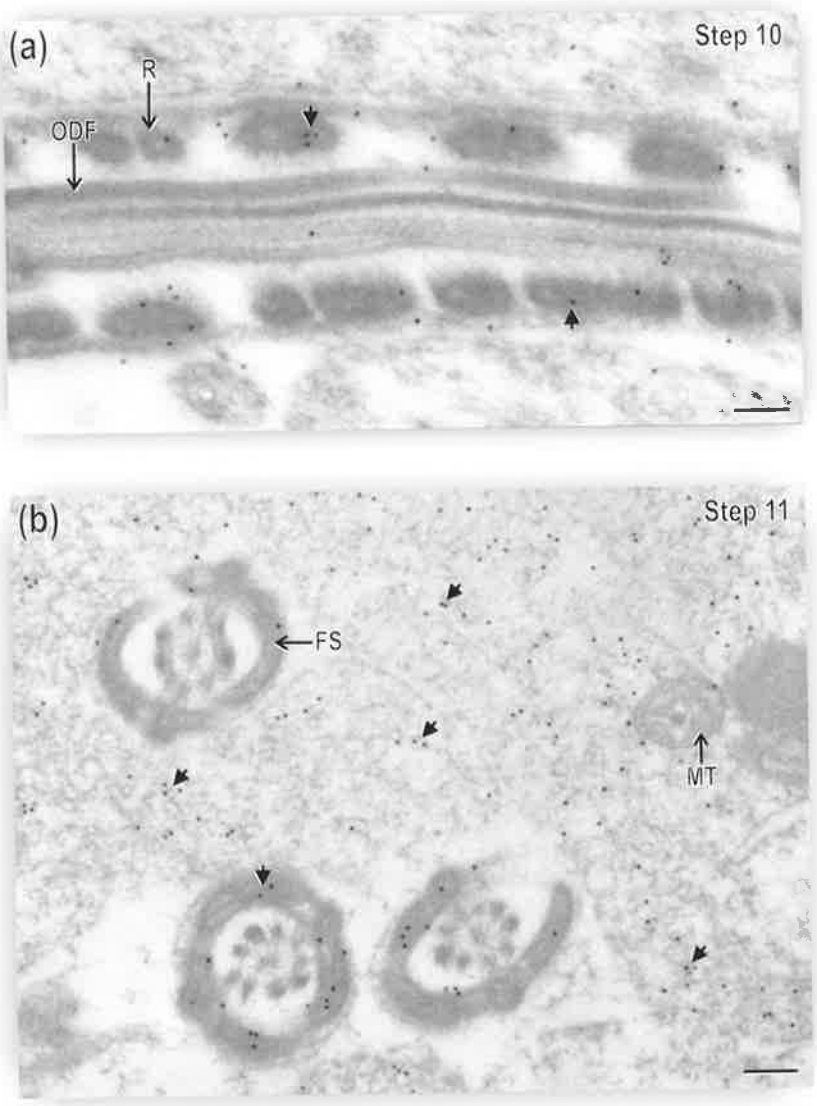

FIGURE 5.9 (a) Longitudinal and (b) transverse sections through the flagella of step 10 and 11 spermatids respectively treated with *PoTVFS* serum. The circumferential ribs (R) and longitudinal columns of the fibrous sheath (FS) are immunoreactive (arrowheads). In step 11 spermatids, the cytoplasmic lobule is also strongly labelled. No gold particles occur over the outer dense fibres (ODF) at either stage. Mitochondria (MT).
Scale bars: (a) 0.08 µm, (b) 1 µm

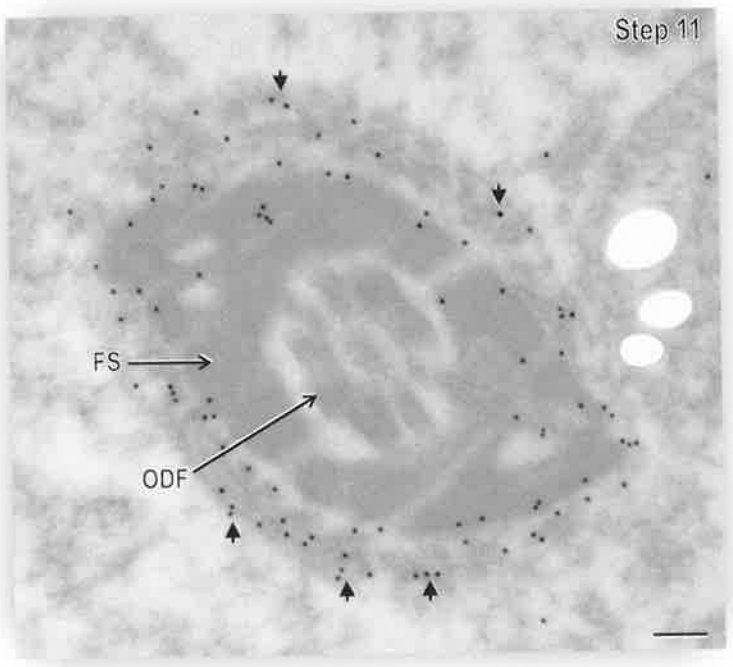

FIGURE 5.10 Transverse section through the proximal principal piece of the possum spermatid flagellum treated with *PoTVFS* serum. There is intense immunogold over the cytoplasm immediately beneath the plasmalemma (arrowheads) suggesting that these proteins migrate down the flagellum through this space before becoming incorporated into the fibrous sheath (FS). Outer dense fibres (ODF). *Scale bar: (a) 0.06 µm*

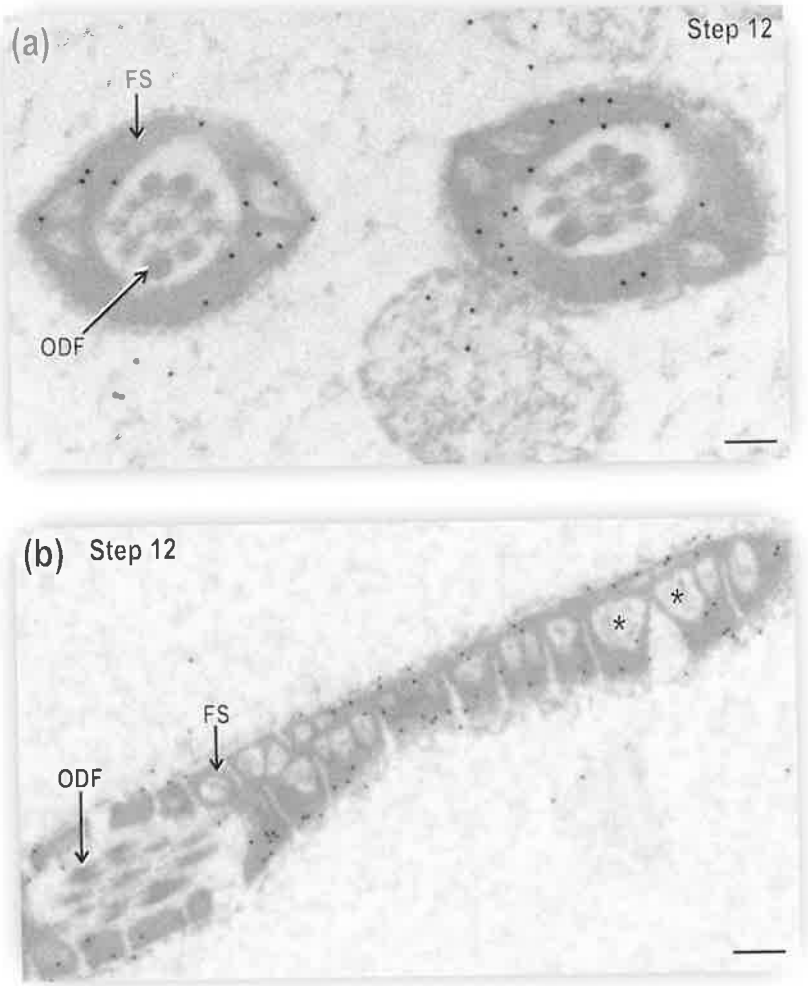

FIGURE 5.11 (a) Transverse and (b) longitudinal sections through the principal segment of the flagellum of a step 12 spermatid treated with *PoTVFS* serum. There is immunogold labelling over both the circumferential ribs and longitudinal columns of the fibrous sheath (FS) but not outer dense fibres (ODF).
Scale bars: (a) 0.08 µm, (b) 0.2 µm

5.4 DISCUSSION

In Chapter 4 it was found that several outer dense fibre and fibrous sheath proteins have molecular weights that are similar, or identical, to those previously reported for the laboratory rat. In the current chapter an anti-possum fibrous sheath serum was used to determine whether these proteins of similar molecular weight were homologous. In addition, an immunocytochemical approach was also undertaken to determine the time and site of formation of fibrous sheath proteins.

5.4.1 Antibodies to Outer Dense Fibre Proteins

Antibodies to eutherian outer dense fibre proteins were first prepared by immunising rabbits with solubilised, whole laboratory rat outer dense fibre extracts (Oko, 1988). The immune serum obtained was found to react strongly with not only the major rat outer dense fibre proteins (MWs: 84, 80, 27, 20 and 14.4 kDa), but also with the 14.4 kDa rat fibrous sheath protein, indicating that these proteins share common antigenic determinants and suggesting that at least one of the proteins of the outer dense fibres and fibrous sheath in this species may be homologous (Oko, 1988). More recently, Kim *et al.*, (1999) used similarly prepared outer dense fibre immune sera to demonstrate additional cross-reactivity with the 26 and 32 kDa rat fibrous sheath proteins. In addition to these standard polyclonal sera, antibodies have also been affinity-purified to the individual 20 kDa (Oko, 1998), 84 kDa (anti-ODF 84) (Oko, 1998; Schalles *et al.*, 1998), and 27 kDa (anti-ODF 27) (Oko and Clermont, 1989, Morales *et al.*, 1994) outer dense fibre proteins.

In the current study, possum outer dense fibres were found to be composed of seven major proteins with molecular masses of 73, 58, 55, 54, 52, 41 and 16 kDa (see Chapter 4). One of the most prominent possum proteins (16 kDa) was found to have a similar

molecular mass to the prominent laboratory rat outer dense fibre protein (either 14 kDa (Oko, 1988) or 15.5 kDa (Kim *et al.*, 1999)), and it was therefore suggested that these proteins might be conserved across these species. In the current chapter, this hypothesis was to be tested immunocytochemically using antibodies prepared against possum outer dense fibre proteins. Unfortunately, however, this was not successful as attempts to raise antibodies to possum outer dense fibre proteins, first in rabbits and then in laboratory rats, appeared to be unsuccessful. This was somewhat surprising given that similar techniques have previously yielded antibodies against outer dense fibre proteins from the laboratory rat (Oko, 1988; Perez-Ramirez and Castells, 1991; Kim *et al.*, 1999) and bull (Seefeldt-Schmidt *et al.*, 2003). Furthermore, in the current study it was possible to raise antibodies against possum fibrous sheath proteins and, in a previous investigation, immune serum was prepared against another marsupial sperm cytoskeletal protein, the 45 kDa wallaby subacrosomal protein (Lin *et al.*, 1998). In each of these studies, the protocols employed for raising polyclonal antibodies were either very similar, or identical, to that used in the current investigation, although the anti-subacrosomal serum was prepared in the laboratory mouse. Whether or not possum outer dense fibre proteins would exert a greater immunogenic response in mice or another species, as opposed to the poor response observed in rabbits and rats in the current study, remains unknown. Unfortunately the current study was already underway at the time of publication of Lin *et al.'s* (1998) findings, so it was not possible to replace rats with mice as the host species for the raising of antibodies. Alternatively, it may be possible that, regardless of the host species chosen, additional volumes/concentrations of possum outer dense fibres proteins are required (i.e. >100 µg for rabbits and >50 µg for rats) to initiate an immune response, although this would seem unlikely as the concentrations of antigen injected in the current study were similar to those used in previous, successful investigations. If this process is to be

repeated in a subsequent investigation, means of increasing the antigenicity of possum outer dense fibre proteins prior to immunisation will need to be investigated.

5.4.2 Cross-Reactivity of Fibrous Sheath Antibody

In previous studies, polyclonal and monoclonal antibodies have been prepared to proteins of whole fibrous sheath extracts and individual fibrous sheath proteins respectively. Polyclonal antibodies to the proteins of whole fibrous sheath extracts were first prepared against laboratory rat proteins by Oko (1988). This sera, obtained from rabbits, was found to react strongly with not just the major rat fibrous sheath proteins (MWs: 75, 27.5 and 14.4 kDa), but also with the 14.4 kDa rat outer dense fibre protein (Oko, 1988). Furthermore, antibodies affinity-purified to the 14.4 kDa rat fibrous sheath protein were found to cross-react with the 14.4 kDa rat outer dense fibre protein in immunoblots (Oko, 1988). Although these results initially suggested that the 14.4 kDa rat outer dense fibre and fibrous sheath proteins share some epitopes and therefore might be homologous, or even the same protein (Oko, 1988), this was not found to be the case in a subsequent cross-reactive study using a similarly prepared fibrous sheath polyclonal antibody (Kim *et al.*, 1995b). The exact nature of the relationship between the 14.4 kDa outer dense fibre and fibrous sheath proteins, therefore, remains unclear and will probably only be resolved at a molecular, rather than immunocytochemical, level.

Monoclonal, rather than polyclonal or affinity-purified, antibodies have also been constructed and used to further characterise the proteins of the fibrous sheath in the laboratory mouse (Sakai *et al.*, 1986; Fenderson *et al.*, 1988; Eddy *et al.*, 1991), human (Jassim, 1990, 1994, 1995; Jassim *et al.*, 1991a, b; 1992, 1993a, b; Jassim and Bottazzo, 1994; Jassim and Chen, 1994; Escalier *et al.*, 1997), and cockerel (Bozhurt and Holley,

1995). For example, a monoclonal antibody, *K32*, prepared against solubilised cauda mouse sperm, was found to bind to the longitudinal columns and circumferential ribs of the mouse fibrous sheath (Sakai *et al.*, 1986). Similarly, monoclonal antibody *ATC*, which was obtained by immunising mice with mechanically disassociated rat testicular cells and which was later found to bind to the GAPDS protein (see 1.4.3.4), labelled the entire fibrous sheath of mouse, rat and hamster flagella (Fenderson *et al.*, 1988), indicating that some fibrous sheath proteins are conserved across at least these eutherian species. An anti-somatic cell intermediate filament monoclonal antibody, *EBA 905*, was found to bind to the mouse 78 kDa fibrous sheath protein suggesting that they may be related (Eddy *et al.*, 1991). Similarly, an anti-human neurofilament monoclonal antibody, *RT97*, has also been localised to the outer surface of detergent-treated human sperm, and stains a phosphorylated epitope of 97 kDa protein in immunoblots (Jassim , 1991; Jassim *et al.*, 1991a). Numerous other monoclonal antibodies have been used to biochemically characterise the proteins that constitute the human fibrous sheath. For example, the *GDA-J/F3* monoclonal antibody, produced by immunising mice with ejaculated human sperm, was found to label the outer surface of detergent-treated human fibrous sheath (Jassim *et al.*, 1990). However, *GDA-J/F3* did not label the laboratory mouse and rat fibrous sheaths, suggesting that sequence divergence of this antigenic epitope may have evolved (Jassim *et al.*, 1990). Monoclonal antibodies *AJ-FS1* (Jassim and Chen, 1994) and *AJ-FS9* (Jassim, 1994), prepared specifically against human fibrous sheath proteins, have been found to label proteins on the outer surface of the human fibrous sheath. A monoclonal antibody, *CFS*, has also been prepared against the fibrous sheath proteins of an avian species, the domestic cock (*Gallus domesticus*), and was found to label both the longitudinal columns and circumferential ribs of the fibrous sheath in this species, as well as in the Japanese quail (*Coturnix coturnix*) (Bozkhurt and Holley, 1995). This suggests

that conservation of fibrous sheath proteins across species might not just relate to eutherian mammals but also to avian species as well.

In the current study, it was only possible, due to technical issues and time constraints, to raise polyclonal, rather than monoclonal, antibodies to possum fibrous sheath proteins. The sera, termed *PoTVFS*, was obtained from laboratory rats because initial attempts at raising antibodies in rabbits were unsuccessful. As was the case when trying to raise antibodies against outer dense fibre proteins, this may be because rabbits were not immunised with enough antigen in the current study. Alternatively, possum fibrous sheath proteins may simply be more naturally immunogenic in rodents than outer dense fibre proteins.

In Chapter 4, the possum fibrous sheath was shown to be composed of 12 major polypeptides (MWs: 106, 76, 66, 62, 55, 53, 52, 46, 40, 30, 28, and 16 kDa), however, because 106, 55, 52 and 16 kDa proteins are also found within the possum outer dense fibres, it is possible that these fibrous sheath proteins may be contaminants from the outer dense fibres. Based on the results of the current chapter, however, this would seem unlikely because the *PoTVFS* serum did not react with any outer dense fibre proteins by immunofluorescence, immunoelectron microscopy, or western blotting. This indicates that the 106, 55, 52 and 16 kDa possum fibrous sheath and outer dense fibres proteins are distinct. This is supported by Kim *et al.'s*, (1995b) findings that the similarly sized, 14.4 kDa laboratory rat outer dense fibre and fibrous sheath proteins are unrelated.

The extent of conservation of fibrous sheath proteins between both different marsupial species, and marsupial species and a eutherian species, was also investigated in the

current study. The *PoTVFS* serum cross-reacted with the principal pieces of cauda sperm from four different marsupial families: possum (Family: Phalangeridae), wallaby (Family: Macropodidae), dunnart (Family: Dasyuridae) and koala (Family: Phascolarctidae), as well as the principal piece of sperm from a eutherian species, the laboratory rat (Family: Muridae). In immunoblots, *PoTVFS* recognised numerous proteins from sperm of each of these marsupials species, as well as staining seven proteins from the rat with molecular masses of 106, 76, 62, 45, 27, 20 and 14 kDa corresponding roughly with the molecular weights of most of the previously reported major rat fibrous sheath proteins (Oko, 1988; Kim *et al.*, 1995b). Furthermore, in all of the species investigated, the 76 and 62 kDa sperm proteins are recognised by *PoTVFS*, suggesting that at least these proteins may be conserved in the fibrous sheaths of sperm from these marsupial and eutherian species. The recognition of the 76 kDa protein in each of these species is especially significant as this protein in the rat is referred to as AKAP4 and has an important role in eutherian sperm motility and capacitation (see 1.4.3.5). Based on their shared antigenicity, the current study indicates that sperm from at least five marsupial families might also each have a homolog of the eutherian AKAP4 protein.

In previous studies, the extent of conservation and specific location of individual fibrous sheath proteins has been examined using affinity-purified polyclonal antibodies prepared against the 76 kDa laboratory rat fibrous sheath protein (Oko, 1988; Oko and Clermont, 1989; Clermont *et al.*, 1990). This protein was found to be present throughout the entire length of the fibrous sheath in much the same pattern reported for standard polyclonal antibodies. In the current study attempts at extracting affinity-purified antibodies to individual possum fibrous sheath proteins from the *PoTVFS* serum were unsuccessful.

Consequently, the specific location and extent of homology of individual possum fibrous sheath proteins could not be determined in the current study.

Although monoclonal antibodies to possum fibrous sheath proteins were not prepared in the current study, in a previous investigation a monoclonal antibody, PSA-10, was found to react with a 32 kDa fibrous sheath and midpiece fibre network protein in both the possum and wallaby sperm (Harris and Rodger, 1998). This antibody was raised against possum acrosomal proteins, suggesting that a fibrous sheath and acrosomal protein may be related, however, in the present study there was no binding of *PoTVFS* to the possum acrosome nor to subacrosomal material. In Chapter 4, no 32 kDa protein was found in the polyacrylamide gels run of the possum fibrous sheath, although minor proteins with molecular masses of 28, 29 and 30 kDa were detected. It is therefore possible that one of these proteins corresponds to the 32 kDa protein recognised by the *PSA-10* antibody. In the current study, the *PoTVFS* serum did not bind to the midpiece fibre network of the possum sperm flagellum, suggesting that the proteins that constitute the fibrous sheath are unique in sperm and that a different suite of proteins constitute other cytoskeletal structures and the acrosome.

5.4.3 Comparison of Formation of Outer Dense Fibres

In Chapter 3, the morphogenesis of possum outer dense fibres was examined at an ultrastructural level and compared to that previously described for the laboratory rat by Irons and Clermont (1982a). Briefly, the stages of formation of the possum outer dense fibres during spermiogenesis were found to be very similar to those previously described in the rat. In both species the anlagen of the outer dense fibres were found to assemble adjacent the outer microtubule doublets of the axoneme in a proximal-to-distal direction.

This was followed by a sudden increase in the diameter of the outer dense fibres in the late stages of spermiogenesis. Despite these findings, a key question remains – what is the time and site of origin of outer dense fibre proteins during spermiogenesis.

One approach to addressing this question involves employing antibodies prepared against outer dense fibre proteins to try to localise these proteins within the cytoplasm of spermatids during spermiogenesis by both light and immunoelectron microscopy. In previous studies on the laboratory rat, antibodies to the proteins of whole outer dense fibre extracts, as well as affinity-purified antibodies to the 27 and 20 kDa proteins of this structure, were found to react with elongating spermatids from step 11 onwards, although peak cytoplasmic immunostaining was observed within the cytoplasm of step 16 spermatids (Oko and Clermont, 1989; Clermont *et al.,* 1990; Kim *et al.,* 1999). Furthermore, this immunolabelling was especially concentrated over specific "granulated bodies" during steps 10-14 (Clermont *et al.,*1990). These bodies appear to originate from the combination of fuzzy, fine filamentous, material (termed "puffs") that develop in association with the outer membrane of endoplasmic reticulum in the periaxonemal spermatid cytoplasm (Clermont *et al.,* 1990). The immunoreactivity of the granulated bodies suggested that they serve as the transitory storage sites for outer dense fibre proteins that are synthesised throughout the cytoplasm of step 9-17 spermatids (Clermont *et al.,* 1990). This is supported by the fact that there is a steady increase in size and number of these bodies between steps 10-17 of rat spermiogenesis which parallels the development of the outer dense fibres during this period (Clermont *et al.,* 1990). If, as has been suggested, the granulated bodies serve as storage sites for outer dense fibre proteins, no mechanisms have yet been postulated to explain how the synthesis, storage, release and transport of the proteins therein might be regulated. However, given that other

similar, complex processes must be occurring during spermiogenesis, it is possible to envisage that a process has been developed in spermatids to facilitate such functions.

In the current study, it was hoped that antibodies prepared against possum outer dense fibre proteins could be utilised in immunocytochemical experiments to determine both when, and where, these proteins are synthesised during spermatogenesis, as well as whether or not they are stored prior to their assembly along the axoneme. Unfortunately, this was not possible as current attempts at raising antibodies to these possum proteins were unsuccessful. Nevertheless, given the already established similarities in the morphology and formation of possum and rat sperm outer dense fibres, as determined by standard electron microscopy in Chapter 3, it is possible that possum outer dense fibre proteins are also stored in the spermatid cytoplasm prior to assembly. This will need to be investigated in a subsequent study.

5.4.4 Comparison of Formation of Fibrous Sheath

In Chapter 3, the formation of the possum fibrous sheath was described by routine transmission electron microscopy and found to be similar to that previously described for the laboratory rat (Irons and Clermont, 1982b) and bandicoot (Sapsford *et al.*, 1967, 1969, 1970). Briefly, in these species the longitudinal columns, and then circumferential ribs, of the fibrous sheath were found to develop independently of each other along the axoneme in a distal-to-proximal direction throughout most of spermiogenesis. Despite these findings, the precise time and site of origin of fibrous sheath proteins in the possum remained unknown. In the rat, such questions have previously been addressed by preparing antibodies against the proteins of whole fibrous sheath extracts, as well as the major 75 kDa and 14 kDa rat fibrous sheath proteins, and utilising them in immunocytochemical

experiments to ascertain specifically when and where these proteins are translated prior to their assembly during spermiogenesis (Oko and Clermont, 1989; Clermont *et al.*, 1990). In addition to confirming the earlier ultrastructural results, these immunocytochemical studies also clearly demonstrated that in the rat (1) immunostaining first occurs in the most distal segment of the flagellum but progresses in a proximal direction along the axoneme, (2) fibrous sheath proteins are dispersed relatively diffusely throughout the spermatid cytoplasm during spermiogenesis, and (3) peak cytoplasmic production of proteins occurs during step 15 of spermiogenesis (Oko and Clermont, 1989). Two additional, important findings of fibrous sheath formation have also been made by immunogold electron microscopy. Firstly, no organelles or cytoplasmic densities were immunoreactive to anti-fibrous sheath sera suggesting that fibrous sheath proteins are not stored prior to assembly, as is the case for outer dense fibre proteins. Instead, fibrous sheath proteins are distributed more widely in the cytoplasmic lobule prior to transport to the periaxonemal cytoplasm. Secondly, the anlagen of the longitudinal columns and circumferential ribs of the fibrous sheath in the rat are not reactive to anti-possum fibrous sheath serum, indicating that these structures may be composed of proteins different from those of the mature fibrous sheath, leading to the suggestion that the they might somehow act as organisers or triggers of fibrous sheath assembly (Clermont *et al.*, 1990; Oko, 1998).

Recently, antibodies to the laboratory mouse AKAP4 and AKAP3 proteins were used to shed additional light on the formation of the fibrous sheath in this species. By immunostaining, AKAP3 was first observed over the cytoplasm of round spermatids suggesting that translation of this protein begins soon after transcription (Brown *et al.*, 2003). However, a delay of more than four days occurs before AKAP3 is incorporated within the fibrous sheath of the flagellum, after the anlagen of the longitudinal columns has

begun, but concurrent with the first appearance of the precursors of the circumferential ribs (Brown *et al.*, 2003). This strongly suggested that AKAP3 is involved in the formation of the anlagen of the ribs. Furthermore, AKAP4 immunostaining was not observed until late in spermiogenesis, and was found to be promptly integrated into both the columns and ribs of the definitive fibrous sheath (Brown *et al.*, 2003). These results suggest that AKAP3 is involved in organising the basic structure of the fibrous sheath whereas AKAP4 has a major role in completing fibrous sheath assembly (Brown *et al.*, 2003).

In the current study, polyclonal antibodies were raised against the proteins of purified possum fibrous sheath fractions and used in immunocytochemical experiments in an attempt to distinguish the time of assembly of the components of the fibrous sheath (as described in Chapter 3) from the time and site of origin of fibrous sheath proteins within the spermatid cytoplasm. The immunolabelling data presented in the current study demonstrates that the formation of the fibrous sheath in the possum is very similar to that previously described for the laboratory rat (Oko and Clermont, 1989; Clermont *et al.*, 1990; Oko, 1998). Namely, in the possum, the *PoTVFS* serum was, like that prepared against rat fibrous sheath proteins, also found to initially label the cytoplasm of elongating spermatids. This immunoreactivity occurs in step 7 spermatids (stage VII) at which time the anlagen of the longitudinal columns and circumferential ribs of the fibrous sheath have already been laid down in a proximal direction along the flagellum. Cytoplasmic immunoreactivity with *PoTVFS* gradually increases, peaking at stage I, presumably because peak translation of fibrous sheath proteins occurs at this time, and remained elevated until the end of stage III. Flagellar reactivity to the *PoTVFS* serum began in step 8 spermatids (stage VIII) and was localised to this region until step 10 when the entire flagellum was lightly stained. Flagellar reactivity increased markedly during stages III and IV in step 12 spermatids and

spermatozoa respectively, and corresponded with a decline in cytoplasmic reactivity. A similar pattern of flagellar staining has been previously observed in the laboratory rat (Oko and Clermont, 1989), suggesting that most of the proteins destined for the fibrous sheath are incorporated into this structure quite late in spermiogenesis in both the possum and rat. If we presume that the *PoTVFS* serum reacts to a possum homologue of the AKAP4 (76 kDa) protein, as was argued in 5.4.2, one would therefore expect there to be an increase in immunolabelling over the fibrous sheath of the flagellum in the latter stages of spermiogenesis, as was found to occur in the mouse (Brown *et al.*, 2003). If a homologue to AKAP4 were found to occur in sperm from the possum, it would appear that its incorporation into the fibrous sheath of this species is also a major step in the completion of assembly of this cytoskeletal structure.

These light microscopic results were subsequently confirmed by immunogold electron microscopy. This technique demonstrated that, although the spermatid cytoplasm was diffusely, but evenly, labelled with the *PoTVFS* serum from step 6 of spermiogenesis, the fibrous sheath of the flagellum was only first clearly reactive in step 10 spermatids. During step 11, there was marked immunolabelling of the periaxonemal cytoplasm surrounding the fibrous sheath in the proximal principal piece, suggesting that many of the fibrous sheath proteins are somehow transferred from the cytoplasmic lobule to the fibrous sheath during this late stage of spermiogenesis. In the rat, it has been suggested that specialised microtubular translocator proteins may serve to transport both fibrous sheath and outer dense fibre proteins from the cytoplasmic to the axoneme during spermiogenesis in the rat (Oko, 1988).

The fact that, in the current study, the anlagen of the longitudinal columns and circumferential ribs of the fibrous sheath in the possum were either not, or only very weakly, immunoreactive with *PoTVFS*, indicates that the anlagen of the possum fibrous sheath may be composed of a different suite of proteins to those found in the mature fibrous sheath. This has been speculated to also be the case for the laboratory rat (Oko and Clermont, 1989; Clermont *et al.,* 1990). Moreover, it has been found that monoclonal antibodies reactive to fibrous sheath proteins from sperm of mouse (Sakai *et al.,* 1986; Fenderson *et al.,* 1988), human (Jassim, 1991) and cockerel (Bozkhurt and Holley, 1995) also do not label the proteins of the anlagen of the fibrous sheath in these species. An alternative reason why the *PoTVFS* serum does not recognise proteins of the anlagen of the fibrous sheath may be that the proteins of these structures are modified after they are assembled adjacent the axoneme and, hence, are antigenically 'immature'.

The fact that immunoreactivity of fibrous sheath proteins in both the possum and rat begins, and then peaks, well after chromatin condensation has begun (at which time transcription is believed to largely or even totally cease), suggests that these proteins are, like those of the outer dense fibres, translationally regulated in at least these two species. In the rat, this is supported by developmental northern blot analysis and in situ hybridisation of rat testes with a [H^3]-labelled probe for the 75 kDa (AKAP4) rat fibrous sheath protein, which demonstrated that the mRNA of this protein is first transcribed in the cytoplasm of round spermatids, prior to the appearance of the fibrous sheath (El-Alfy *et al.,* 1999). In the rat, outer dense fibre proteins are thought to be stored in transitory granulated bodies within the spermatid cytoplasm prior to their assembly along the axoneme, however no such bodies were found to occur for fibrous sheath proteins (Irons and Clermont, 1982a, b). As no potential storage sites for fibrous sheath proteins were,

likewise, detected in possum spermatids in the current study, one must presume that translation of these proteins is also regulated.

5.5 CONCLUSION

In the current chapter, polyclonal antibodies were utilised to determine the extent of conservation of fibrous sheath proteins, as well as to re-evaluate the formation of this structure during spermiogenesis. In summary, it was found that:

(1) No cross-reactivity exists between possum outer dense fibre proteins and antibodies to fibrous sheath proteins, indicating that, even though some of the proteins of these structures are of similar or identical molecular weights, they are nevertheless composed of different proteins.

(2) Anti-possum fibrous sheath sera cross-reacts with fibrous sheath proteins in the dunnart, koala, wallaby and even laboratory rat sperm, including the 76 and 62 kDa proteins in each of these species, suggesting that these proteins are highly conserved in the fibrous sheath of sperm of both marsupial and eutherian species.

(3) The production of possum fibrous sheath proteins is exclusive to elongating spermatids (steps 6-12 of spermiogenesis), with peak cytoplasmic immunoreactivity occurring in step 10 spermatids.

(4) Peak translation of possum fibrous sheath proteins occur well after chromatin condensation has begun, suggesting that these proteins are translationally regulated.

(5) Proteins of the anlagen of the possum fibrous sheath are, like those of the laboratory rat, antigenically dissimilar to those of the mature fibrous sheath, suggesting that either the precursor structure is composed of a different suite of proteins or that these proteins are somehow modified.

Chapter 6

CONSERVATION OF MAJOR OUTER DENSE FIBRE AND FIBROUS SHEATH PROTEINS

6.1 INTRODUCTION

In Chapter 5, an immunocytochemical approach was used to demonstrate that there is antigenic cross-reactivity, and hence conservation, of at least some fibrous sheath proteins in sperm between different marsupial families, as well as the laboratory rat. Unfortunately, however, it was not possible to test for conservation of individual fibrous sheath proteins as the *PoTVFS* serum used was a polyclonal antibody prepared against proteins of whole fibrous sheath extracts. Consequently, it was not possible to precisely determine which specific antibodies in the *PoTVFS* polyclonal mix were responsible for the cross-reactivity observed. For example, were the antibodies specific to the possum 76 kDa fibrous sheath protein responsible for the 76 kDa cross-reactive staining observed in western blots of sperm from other species, or could antibodies against other possum fibrous sheath proteins have been responsible? One approach to investigating this question is to utilise antibodies which have been prepared against specific fibrous sheath proteins to test for cross-reactivity. These could include affinity-purified polyclonal antibodies, monoclonal antibodies, or antibodies generated against specific cloned fibrous sheath proteins. Since it was not possible, in the current study, to prepare such antibodies against possum fibrous sheath proteins because of inadequate numbers of possums, it was necessary to procure antibodies previously prepared against individual eutherian fibrous sheath proteins. These

antibodies were then used in immunocytochemical cross-reactivity studies to ascertain whether or not fibrous sheath proteins are conserved.

To date, several of such antibodies have been prepared against specific eutherian fibrous sheath, as well as outer dense fibre, proteins (see Chapter 5). In the current study, antibodies generated specifically against the eutherian AKAP4 (76 kDa) and GAPDS (47.5 kDa) fibrous sheath, as well as to the ODF2 (84 kDa) outer dense fibre, proteins were used in immunocytochemical experiments to investigate whether or not sperm tail cytoskeletal proteins are conserved across eutherian and marsupial species. Any homology detected would have significant evolutionary and functional implications.

6.2 MATERIALS AND METHODS

6.2.1 Antibodies Utilised

The current study utilised antisera to the laboratory rat ODF2 (84 kDa) outer dense fibre protein, and laboratory mouse AKAP4 (73 kDa) and GAPDS (47.5 kDa) fibrous sheath proteins. The anti-rat ODF2 antibodies, termed *anti-ODF84* and *anti-111-450,* were generously donated by Professor Richard Oko from Queens University, Kingston, Ontario, Canada. *Anti-ODF84* is a polyclonal, affinity-purified antibody generated by screening Western blots of immobilised ODF2 protein with rabbit anti-whole outer dense fibre sera (Oko and Maravei, 1994). In contrast, the *anti-111-450* antibody was generated in a rabbit from a fusion protein of the 111-450 cDNA which encodes for the putative rat ODF2 protein (Shao *et al.,* 1997). *Anti-AKAP4* and *anti-GAPDS* sera were kindly donated by Professor Edward Eddy from the National Institute of Environmental Health Sciences, North Carolina, USA. *Anti-AKAP4* was generated by immunising rabbits with synthetic peptides against the 191-204 amino acid (aa) and 790-803 aa sequences of the cloned

laboratory mouse AKAP4 fibrous sheath protein (Brown *et al.*, 2003). The anti-GAPDS antibody was prepared in the rabbit against synthetic peptides corresponding to the 158-194 aa and 293-306 aa sequences of the cloned mouse GAPDS protein (Bunch *et al.*, 1998).

6.2.2 Indirect Immunofluorescence

Possum cauda epididymal sperm were washed in PBS, pH 7.4, and fixed in 3% paraformaldehyde, in PBS, at 4°C for 20 min. Reactive aldehyde groups were blocked by resuspending the fixed sperm in PBS containing 50 mM glycine for 20 min, and 100 µL aliquots were spotted on glass slides, pre-coated with 3-aminopropyltriethoxysilane (APES), for 2 h at 4ºC. The slides were rinsed four times with PBS, pH 7.4, and spermatozoa permeabilised with ice-cold acetone for 5 min. Sperm were rinsed 4 times in PBS and incubated with 10% normal goat serum (NGS) in PBS for 20 min to reduce non-specific binding. They were then incubated overnight at 4°C with primary antiserum (*anti-ODF2*, 1;500; *anti-AKAP4*, 1:1000; *anti-GAPDS*, 1:1000, as suggested by Professors Oko and Eddy) diluted in PBS containing 0.1% BSA and 1% NGS. The slides were rinsed 4 times in PBS, incubated in PBS containing 10% NGS for 15 min, and then FITC-conjugated goat anti-rabbit immunoglobulin (Sigma) diluted 1:50 in PBS containing 0.1% BSA and 1% NGS for 45 min. Non-specific staining was determined by replacing the primary antiserum with standard rabbit serum or PBS and autofluorescence was determined by omitting the secondary antibody.

6.2.3 Immunogold Electron Microscopy

Adult male possums were anesthetized with isoflurane and testes and epididymides were fixed by perfusion for 20 min with 4% paraformaldehyde in 0.2 M PBS, pH 7.4. Tissue was

then dissected free and immersed in the same fixative for 2 h, washed in two changes of PBS and dehydrated by passing through a graded series of ethanols. Tissue was infiltrated in a 2:1 ratio of LR White:70% ethanol for 1 h, followed by two further incubations in pure LR White resin for 1 h and then overnight. The resin was again replaced just prior to polymerization in gelatin capsules at 60°C for 24 h. Ultrathin sections were cut on a Reichert Jung Ultracut microtome and mounted on nickel grids.

Sections on grids were blocked by incubating in 10% normal goat serum (NGS) in TBS for 30 min, and then incubated with the primary antibody (*anti-ODF2*, 1;500; *anti-AKAP4*, 1:1000; *anti-GAPDS*, 1:1000, as suggested by Professors Oko and Eddy) diluted in TBS-Tween containing 1% NGS for 1 h. The grids were washed 6 times for 5 min each in TBS-Tween, and further blocked in 10% NGS for 15 min before being incubated in 10 nm gold-conjugated goat anti-rabbit immunoglobulin (Sigma), diluted 1:20, for 1 h at room temperature. They were then washed 6 times for 5 min each, in TBS-Tween and 4 times for 5 min each in ddH_2O. The grids were finally stained with uranyl acetate (3 min) and examined on a Phillips CM100 transmission electron microscope at 80 kV.

Non-specific staining was determined by replacing the primary antiserum with standard rabbit serum or PBS.

6.2.4 Western Blotting

Possum cauda sperm were solubilised in 4.5 M Urea, 2% SDS in 25 mM DTT for 5 h at room temperature, insoluble material was removed by centrifugation at 15 000 *g* for 20 min, and final protein concentration determined. Proteins were separated on 7–12% SDS-polyacrylamide mini gels (Bio-Rad) and up to 10 µg of protein was loaded per lane. Electrophoretic transfer of the proteins from the gels to the nitrocellulose was carried out in

a Trans-blot cell (Bio-Rad) in 25 mM Na_2HPO_4 buffer at pH 6.4, 300 V, for 1 h. After removal from the transfer apparatus, the gels were stained with Coomassie Brilliant Blue and the nitrocellulose was stained temporarily with 0.2% Ponceau in 3% trichloracetic acid (TCA) to determine the effectiveness of the transfers. The blots were destained and blocked by incubating with 5% non-fat milk powder in TBS-Tween (25 mM Tris-HCl buffered saline, pH 7.4, containing 0.1% Tween-20), overnight at 4°C. They were washed in TBS-Tween and incubated with primary antibody (*anti-ODF2*, 1;100; *anti-AKAP4*, 1:100; *anti-GAPDS*, 1:100, as suggested by Professors Oko and Eddy) for 1 h at room temperature. Blots were rinsed in TBS-Tween 4 times at 5 min per time, and incubated with biotinylated goat anti-rabbit immunoglobulin (Zymed, San Francisco, CA), diluted 1:1000 in TBS-Tween for 1 h at room temperature. They were washed in TBS-Tween as described and incubated with strepavidin-alkaline phosphatase (Amersham, Buckinghamshire, UK), diluted 1:3000 in TBS-Tween for a further 1 h. The blots were developed with 10 ml of 5'-bromo-4-chloro-3-indolyl phosphate/nitro blue tetrazolium (BCIP/NBT) liquid substrate system (Sigma).

Controls consisted of replacing the primary antibody with pre-immune serum or buffer.

6.3 RESULTS

In each of the immunocytochemical experiments outlined below, no labelling of cauda sperm by immunofluorescence, immunogold or immunoblotting was found to occur when the primary antibody was replaced with pre-immune serum.

6.3.1 *Anti-ODF2* (*anti-ODF84; anti-111-450*) Antibodies

Fixed possum cauda epididymal sperm incubated with the *anti-ODF84* affinity-purified antibody showed distinct, but intermittent, immunofluorescence over the principal piece of

the flagellum (Figure 6.1a, b, c). The variable nature of this staining was especially evident when flagella were viewed at high magnification (Figure 6.1c). By immunogold electron microscopy, weak labelling of this *anti-ODF84* was found to occur over both the cortex and medulla of the outer dense fibres within the middle and principal pieces of the flagellum (Figure 6.2a, b). In Western blots, *anti-ODF84* reacted strongly with the major 55 kDa and minor 28 kDa possum outer dense fibre proteins (Figure 6.3). Sperm incubated with the *anti-111-450* antibody showed either very weak or no labelling over the flagellum (not shown). Consequently, no further experiments were conducted using this particular serum.

6.3.2 *Anti-AKAP4* Antibody

There was no labelling of the principal piece of the possum sperm flagellum or head by immunofluorescence, however there was some relatively weak staining of the midpiece (Figure 6.4a, b). Fluorescence in this region was, however, the result of autofluorescence as it was also observed when sperm were treated with pre-immune serum (not shown). However, the principal piece of the laboratory rat sperm flagellum was labelled with the anti-AKAP4 antibody (Figure 6.4c, d). By immungold electron microscopy, labelling was found to occur over the mitochondrial sheath, but not over the fibrous sheath, outer dense fibres or any sperm head component (not shown). No possum fibrous sheath proteins were stained with the *anti-AKAP4* antibody by Western blotting (not shown), although only one attempt at this procedure could be carried out due to the very small amount of primary antibody available.

6.3.3 *Anti-GAPDS* Antibody

Immunofluorescence staining of possum cauda sperm with *anti-GAPDS* sera showed intense labelling over the principal piece of the flagellum. The midpiece and sperm head

were non-reactive (Figure 6.5a). By immunogold electron microscopy, the anti-AKAP4 antibody was found to label the fibrous sheath (Figure 6.5b) but not the axoneme, outer dense fibres or sperm head. No possum fibrous sheath proteins were stained with the *anti-GAPDS* antibody by Western blotting (not shown), although only one attempt at this procedure could be carried out due to the very small amount of primary antibody available.

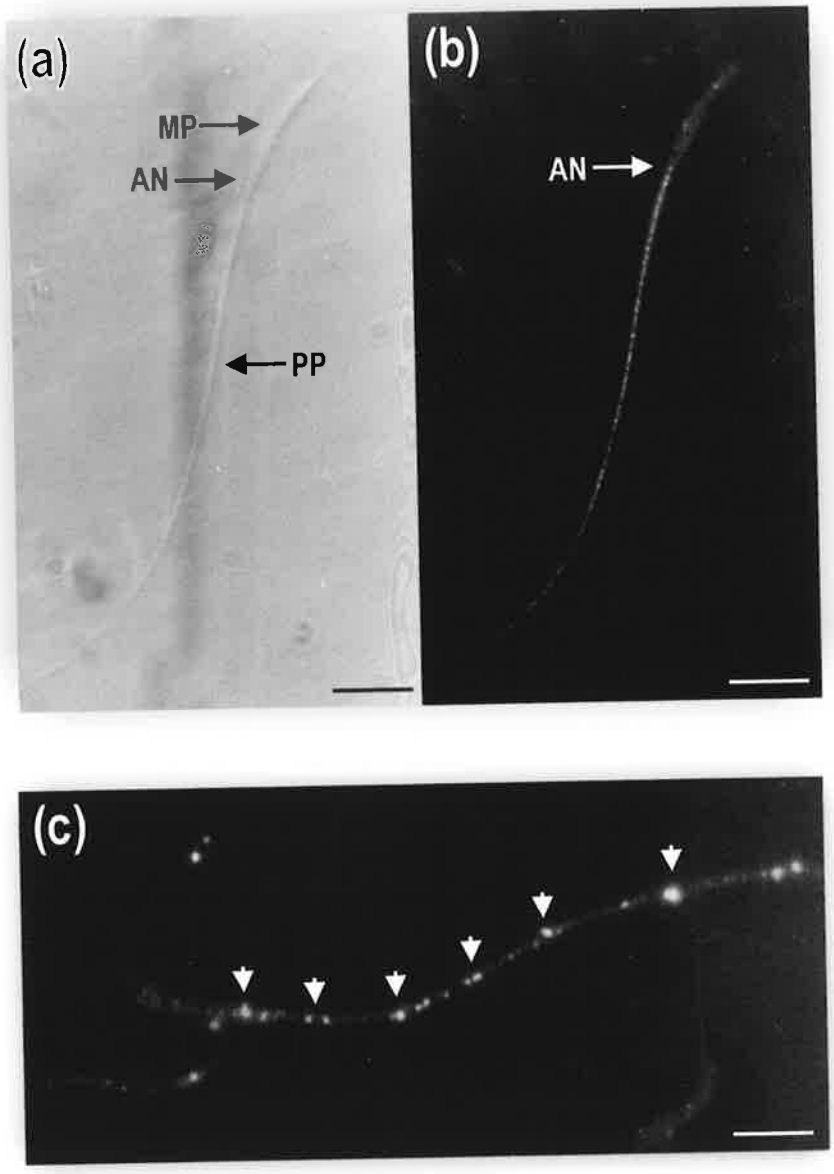

FIGURE 6.1 (a) Phase contrast and (b, c) fluorescent micrographs of possum cauda epididymal spermatozoa treated with *anti-ODF84* serum. (b) There is positive staining of the principal piece of the flagellum although (c) at higher magnification the labelling is variable along the flagellum (arrowheads).
Scale bars: (a) 0.5 µm, (b) 0.5 µm, (c) 0.8 µm

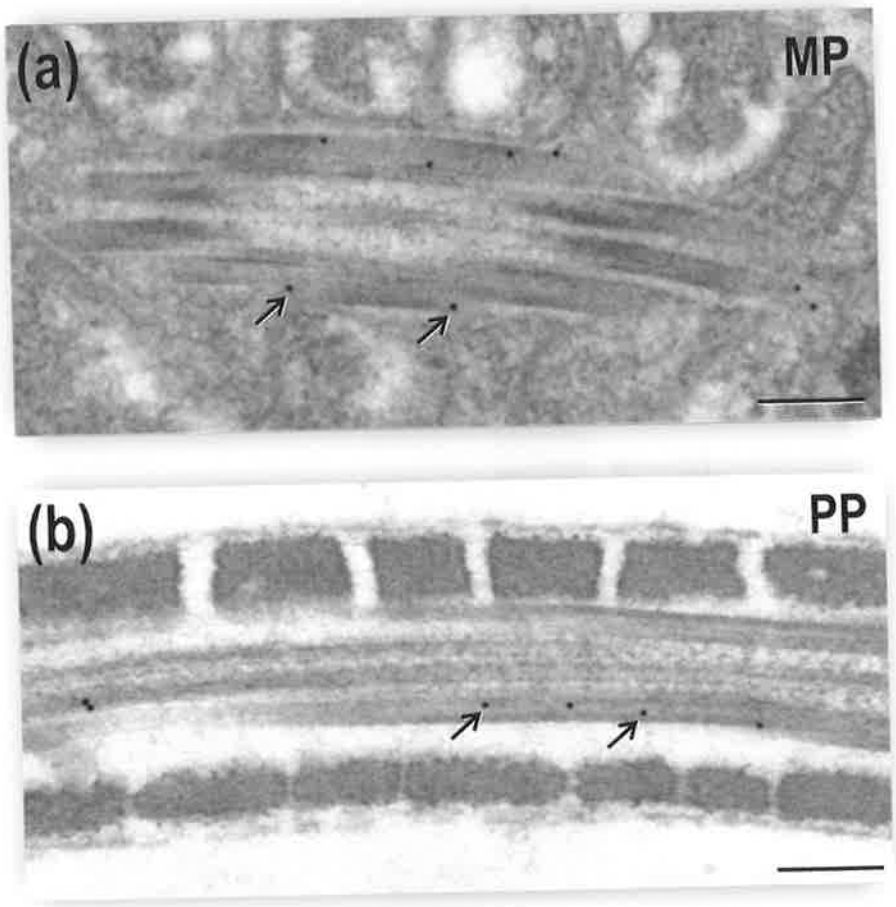

FIGURE 6.2 Longitudinal sections through the (a) midpiece (MP) and (b) principal piece (PP) of possum spermatozoa incubated in *anti-ODF84* serum. There is weak, but specific, immunogold labelling over the outer dense fibres (arrows).
Scale bars: (a) 0.2 µm, (b) 0.28 µm

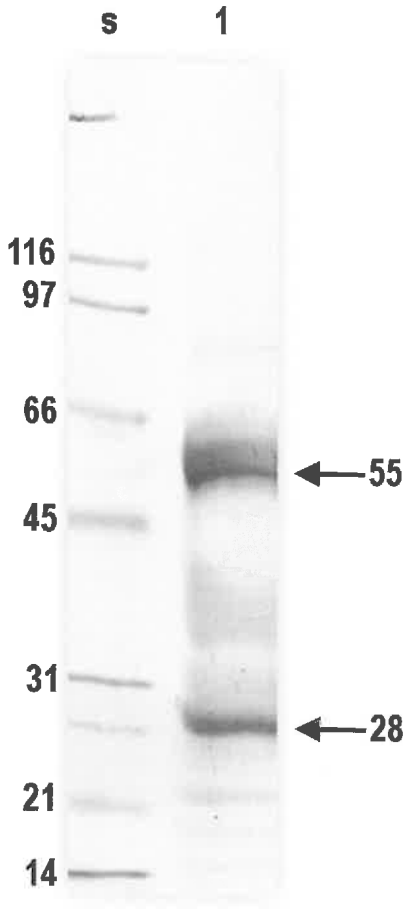

FIGURE 6.3 Western blot of possum sperm outer dense fibres (Lane 1) probed with *anti-ODF84* serum. The major 55 kDa and minor 28 kDa outer dense fibre proteins are recognised by this antibody. Lane *S*, molecular mass standard.

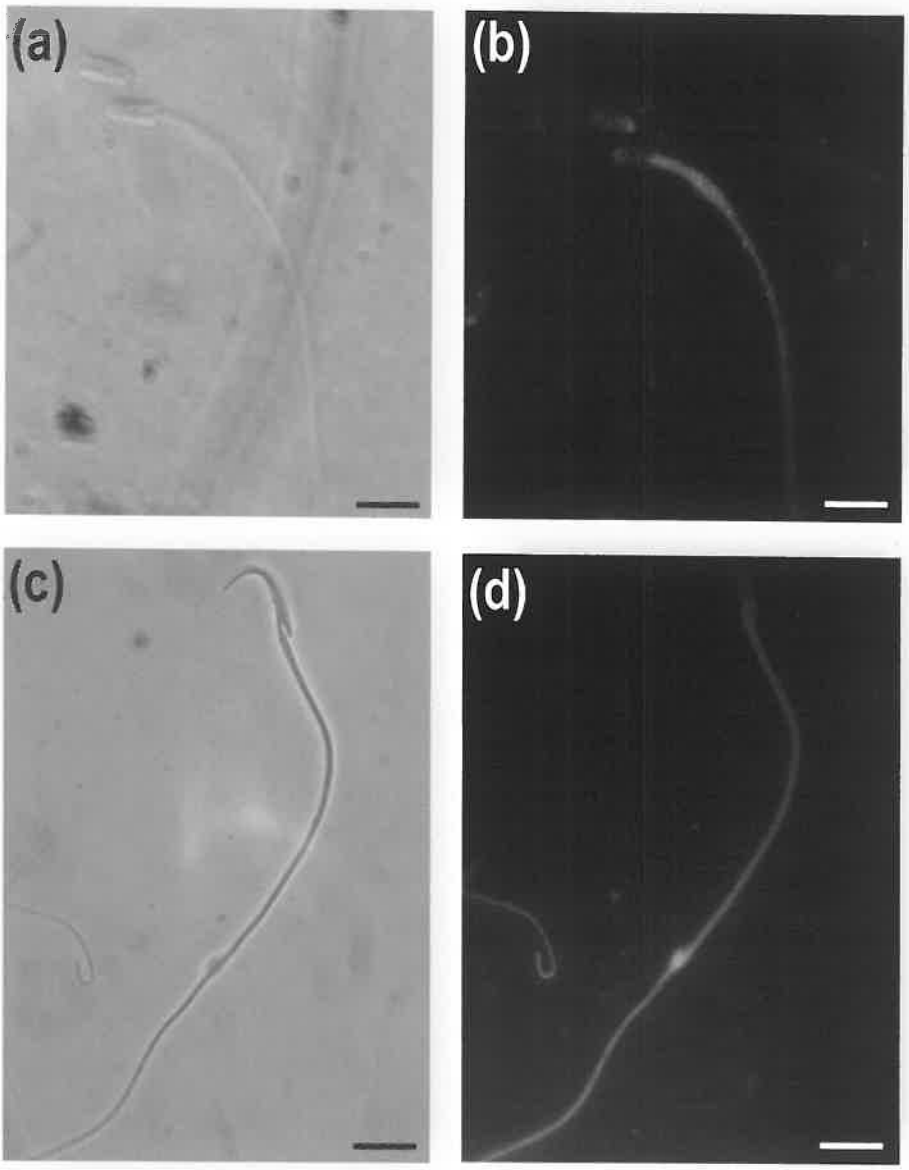

FIGURE 6.4 Phase contrast and corresponding fluorescent micrographs of (a, b) possum and (c, d) laboratory rat spermatozoa treated with *anti-AKAP4* serum. (b) There is weak staining of the midpiece of the possum flagellum, however (d) the principal piece of the rat sperm flagellum is reactive.
Scale bars: (a, b) 0.5 µm, (c, d) 0.35 µm

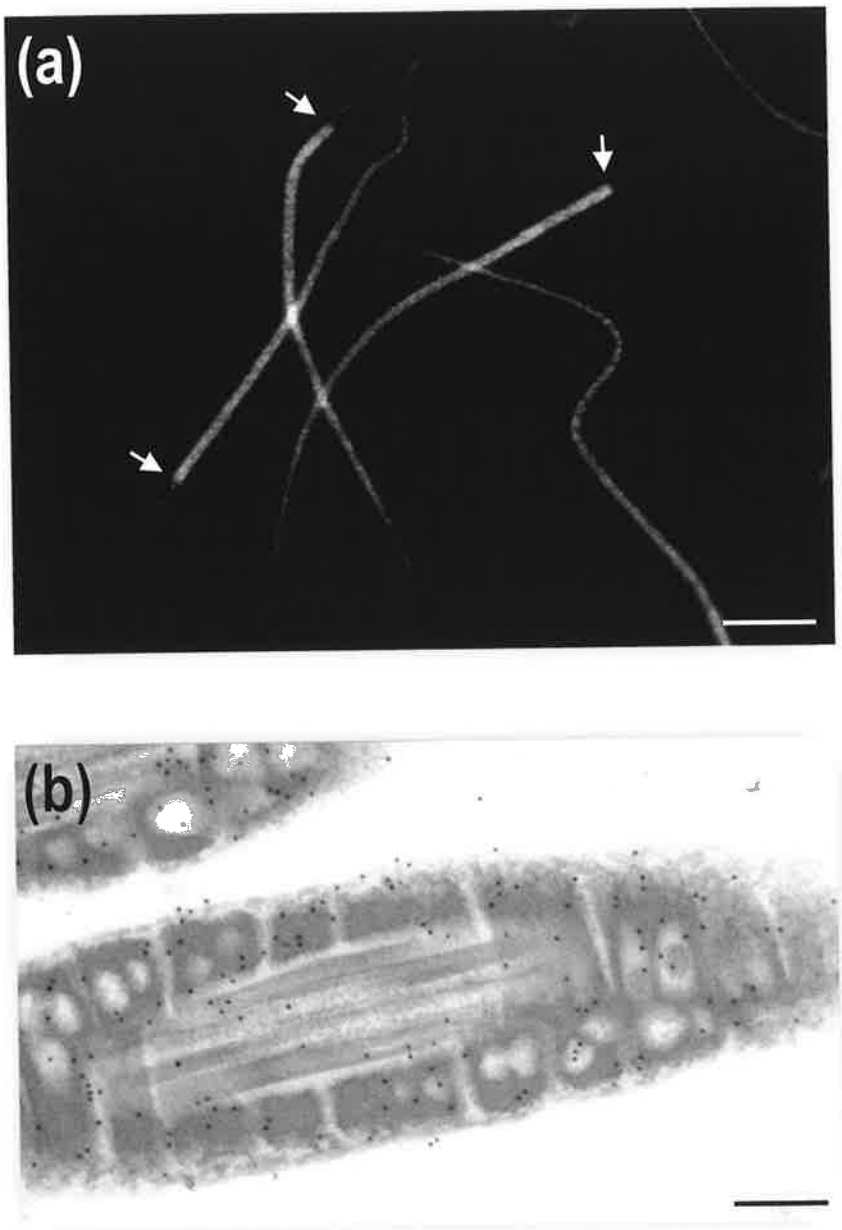

FIGURE 6.5 Immunocytochemistry of possum spermatozoa incubated with *anti-GAPDS* serum. (a) There is specific, strong staining of the principal piece of the flagellum. (b) Longitudinal section of the principal piece of the flagellum showing intense gold labelling over the fibrous sheath. Annulus (arrowheads).
Scale bars: (a) 0.5 µm, (b) 0.25 µm

6.4 DISCUSSION

Although the number and molecular weights of the major possum outer dense fibre and fibrous sheath proteins have been determined (see Chapter 4), and several fibrous sheath proteins were found to share antigenic determinants with those from the laboratory rat (see Chapter 5), the question of which specific proteins may be conserved across these species remained unknown. The objective of this chapter was, therefore, to address this question by incubating possum sperm with antibodies prepared against the eutherian ODF2, AKAP4 and GAPDS proteins with a view to ascertaining whether or not homologues of these proteins might occur in marsupial sperm.

6.4.1 Possible Conservation of the ODF2 Protein

In the current study, *anti-rat ODF84* serum was used in immunocytochemical experiments to determine whether or not there is a homologous protein to rat ODF2 in possum sperm. Although at least 14 proteins have been identified in rat outer dense fibres by polyacrylamide gel electrophoresis, including six major bands (Vera *et al.*, 1984, Oko, 1988; Kim *et al.*, 1999) (see Chapter 4 for further details), to date, nucleotide sequences encoding for only several of these proteins are known including the 27 (ODF1), 84 (ODF2), and 110 (ODF3) kDa laboratory rat outer dense fibre proteins (see 1.4.2.4). The most prominent of these proteins, ODF1, was cloned independently by three different groups employing different techniques. It was, therefore, originally referred to as RT7 (van der Hoorn *et al.*, 1990), rts 5/1 (Burfeind and Hoyer-Fender, 1991), and ODF27 (Morales *et al.*, 1994). Analysis of the predicted amino acid sequence of ODF1 revealed two putative domains; a conserved repetitive Cysteine-X-Proline (PCX) motif at the C-terminus, of which the majority are Cysteine-Glycine-Proline, and a leucine-zipper like motif at the N-terminal end of the protein (Van der Hoorn *et al.*, 1990). The presence of a leucine zipper,

which functions as a dimerization motif in the bZIP family of transcription factors (Glover and Harrison, 1995; Delmas *et al.*, 1993), is especially significant, ODF1 proteins have been found to be self-interact via the leucine zipper in this region (Shao and van der Hoorn, 1996). The cDNA clone encoding the ODF2 protein was isolated by utilising the leucine zipper of the ODF1 protein as "bait" in a yeast two-hybrid screening approach (Shao *et al.*, 1997). The ODF2 gene, which was initially referred to as 111-450, encodes a protein of 591 amino acids and contains two leucine zippers at its C-terminus, thereby indicating how it and the ODF1 protein are able to associate (Shao *et al.*, 1997). The predicted molecular weight of ODF2 was found to be 72 kDa, however, a polyclonal antibody, *anti-111-450*, generated against a fusion protein of the ODF2 cDNA, reacts with the 84 kDa rat outer dense fibre protein in Western blots indicating that this protein somehow migrates slower than expected by SDS-PAGE. The ODF2 protein was subsequently, and independently, also isolated by screening a rat testicular cDNA expression library with affinity-purified anti-ODF2 serum (*anti-ODF84* antibody) (Schalles *et al.*, 1998). In the current study, both the *anti-111-450* and *anti-ODF84* antibodies were utilised in immunocytochemical experiments to determine whether or not a homologous protein to ODF2 is present in possum sperm. Cross-reactivity to rat *anti-ODF84* serum was found to occur in possum caudal sperm by both immunofluorescence and immunoelectron microscopy. The *anti-ODF84* antibody stained all of the midpiece and most of the principal piece of the possum sperm flagellum, and labelled both the cortex and medulla of the outer dense fibres. In the laboratory rat, *anti-ODF84* similarly labels both the cortex and medulla of the outer dense fibres, however, additional labelling was also found to occur over the capitulum and striated columns in the neck region (Schalles *et al.*, 1998) strongly indicating the outer dense fibre proteins may be part of the substrate of the connecting piece. It has been suggested that the presence of ODF2 in the rat connecting piece-centriolar complex

may be important for fertilisation because it has been found that the ODF2 protein contains an epitope that, when phosphorylated, allows sperm-aster formation to occur (Long *et al.*, 1997). In the current study, *anti-ODF84* did not label the possum connecting piece, indicating that either accessibility to the epitopes of this structure are somehow blocked, or more likely that it is composed of a different suite of proteins and/or has distinct origins in eutherian and marsupial species.

In previous studies, *anti-ODF84* serum was found to react with not just the major 84 kDa, but also cross-react with the minor 71, 56, 40 and 25 kDa outer dense fibres in both the laboratory rat and bull sperm (Schalles *et al.*, 1998). In the possum, no 84 kDa outer dense fibre protein was found to exist in 1D SDS gels of outer dense fibres (see Chapter 4), however a 73 kDa protein is present which is extremely similar to the predicted 72 kDa molecular weight for the ODF2 protein based on its amino acid composition. In the current study, *anti-ODF84* did not recognise the 73 kDa outer dense fibre protein but rather stained the major 55 kDa, and minor 28 kDa, proteins instead. The fact that multiple, lower molecular weight possum outer dense fibre proteins are recognised by this antibody suggests that either: (1) different-sized proteins within the possum have similar antigenic epitopes to those of the 84 kDa rat protein, or (2) a similarly-sized protein (83 kDa) is present within the possum outer dense fibres but has cleaved into two smaller proteins (55 kDa and 28 kDa) prior to SDS-PAGE. The latter phenomenon has previously been reported for the laboratory rat by Kim *et al.*, (1999), who found that the 54 and 48.5 kDa rat outer dense fibre proteins appear to undergo spontaneous cleavage while in storage at -20°C, giving rise to an additional, minor 26 kDa protein band in polyacrylamide gels. Although the potential cause(s) of this phenomenon in the rat remain unknown, the fact that no other proteins appeared to degrade in Kim *et al.*,'s (1999) study suggests that it

may be unique to this protein in this species. In the current study, possum outer dense fibre proteins were similarly stored at -20°C prior to SDS-PAGE, however an 83 kDa protein band was not detected in any of the polyacrylamide gels run, indicating that either no such protein exists in the possum, or that if it does exist it is completely cleaved into 55 and 28 kDa proteins prior to SDS-PAGE. Further analysis of the possum proteins stained with *anti-ODF84* serum is, therefore, required if the nature of the relationship between, and extent of conservation of, the 84 kDa rat outer dense fibre protein and 55 and 28 kDa possum outer dense fibre proteins is to be determined.

With the exception of its potential role in sperm-aster formation, the function of the eutherian ODF2 protein, and therefore possibly the 55 and 28 kDa possum proteins, has yet to be definitively established. Nevertheless, in the rat, ODF2 has been found to specifically, and strongly, associated with the ODF1 protein via leucine zippers (Shao *et al.*, 1997). Together with the fact that ODF1 proteins also self-interact (Shao *et al.*, 1996), this may shed light on the molecular organisation of the outer dense fibre proteins. Two models have been proposed to explain how outer dense fibre proteins may be arranged. In the first, and favoured of these, ODF1 self-associates via its PCX repeat; one ODF1 interacts with ODF2 and the other with an unknown protein X, which can be ODF1, ODF2, or an as yet unknown leucine zipper-containing protein (Shao *et al.*, 1997) (Figure 6.6). In this model, ODF2 interacts, via its second leucine zipper, with another unknown protein, Y, which cannot be ODF1 or ODF2, suggesting that ODF2 acts as a structural link between these two regions (Shao *et al.*, 1997). This proposal gained further credence when immunolocalisation reports utilising affinity-purified antibodies to ODF1 and ODF2 showed that ODF2 is present in both the medulla and cortex of the outer dense fibre as apposed to the exclusive medullary localisation of ODF1 (Schalles *et al.*, 1998). More recently, the rat ODF3 (110 kDa) protein has been sequenced and secondary structure predictions indicate

that it has a coiled-coil structure and three leucine zippers (Petersen *et al.*, 2002). Coiled-coil proteins are formed by two or three alpha helices in parallel and in register (Lupas *et al.*, 1991). The ODF3 protein is, therefore, also likely to play an important structural role in the overall outer dense fibre framework and may form a 'fibrillar scaffold' onto which ODF1 and ODF2 associate (Petersen *et al.*, 2002). While further characterisation of the additional outer dense fibre proteins is required if the molecular structure, and consequently function, of the outer dense fibres is to be more definitively established, the presence of proteins in the possum that are antigenically similar to the eutherian ODF protein suggests that homologues of other outer dense fibre proteins, like ODF1 and ODF3, may eventually also be found in this marsupial species.

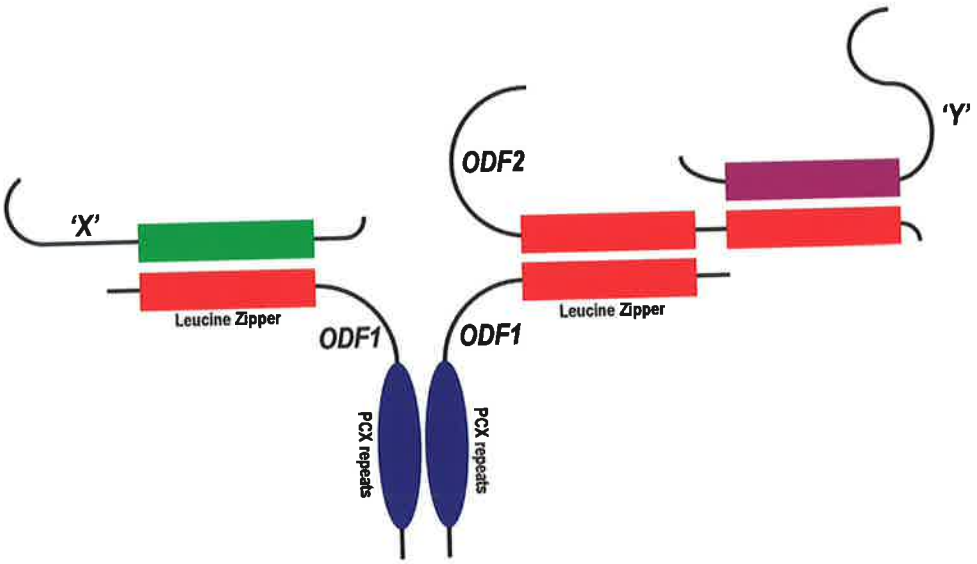

FIGURE 6.6 Model of protein interactions in the laboratory rat outer dense fibres. Two ODF1 proteins homodimerize mediated by their PCX repeats. One ODF1 protein associates with ODF2 via leucine zippers. The second ODF1 interacts with protein X. (For further details refer to text).
(Adapted from Shao *et al.*, 1997).

6.4.2 Possible Conservation of the AKAP4 Protein

In most eutherian species, the most abundant fibrous sheath protein, AKAP4, has a molecular mass, by ID PAGE, of between 73-80 kDa (Olson *et al.*, 1976; Oko, 1988; Brito *et al.*, 1989; Kim *et al.*, 1995b; Kim *et al.*, 1997). In the current study, the most abundant possum fibrous sheath protein has a similar molecular mass of 76 kDa (see Chapter 4). This raised the question of whether or not this possum fibrous sheath protein is, in fact, homologous to the eutherian AKAP4 protein.

The AKAP4 protein was independently sequenced by two research groups and, therefore, was initially referred to as p82 (Carrera *et al.*, 1994) and fibrous sheath component 1 (FSC1) (Fulcher *et al.*, 1995a). Carrera *et al.*, (1994) sequenced their protein by screening a mouse testis cDNA expression library with an antiserum generated against the mouse 82 kDa fibrous sheath protein. In contrast, Fulcher *et al.*, (1995a) utilised oligonucleotide probes designed from microsequenced fibrous sheath peptide fragments to probe a mouse round spermatid cDNA library to isolate their clone. The p82 and FSC1 cDNA clones are derived from the same gene but differ in their 5' untranslated regions as they are transcribed from different initiation sites (Turner *et al.*, 1998). Sequence analysis of these clones identified this fibrous sheath protein as an example of an A Kinase Anchoring Protein (AKAP); hence its name was changed firstly to AKAP82 (Carrera *et al.*, 1996) and then finally AKAP4 (Blake *et al.*, 2000). It has been shown that the AKAP4 protein is, in fact, synthesised during spermiogenesis as a precursor protein of ~97 kDa (840 aa) that is transported down the flagellum to the principal piece where it is proteolytically cleaved to a mature form of ~72 kDa (661 aa) (Carrera *et al.*, 1994; Johnson *et al.*, 1997; Brown *et al.*, 2003). Conserved homologues of the mouse AKAP4 protein were subsequently identified

in sperm from the human (76% aa identity) (Turner *et al.*, 1998), bovine (80% identity) (Moss *et al.*, 1999) and laboratory rat (93% identity) (El-Alfy *et al.*, 1999).

The function of AKAP4 has become somewhat clearer over the past few years. AKAPs tether Protein Kinase A (PKA) to particular cytoplasmic locations in cells. AKAP4 has two PKA-binding domains, domain A: aa 210-223 (Visconti *et al.*, 1997) and domain B: aa 326-345 (Miki and Eddy, 1998). These sites bind to either the RIα or RIIα subunits of PKA (domain A) (Miki and Eddy, 1998), or specifically to RIα (domain B) (Miki and Eddy, 1999). PKA is important in normal sperm functioning as it is thought to act as a downstream target for cyclic AMP (cAMP) which may be an important regulator of sperm capacitation (Visconti *et al.*, 1995) and motility (Tash, 1989; Lindemann and Kanous, 1989). The notion was supported by a study showing that sliding of the fibrous sheath is cAMP dependent (Si and Okuno, 1993). Moreover, targeted mutagenesis of the AKAP4 gene results in immotile sperm (Miki *et al.*, 2002).

In the current study, the potential conservation of AKAP4 in marsupials was tested by incubating possum sperm with an antibody raised against the mouse AKAP4 protein. This *anti-AKAP4* antibody used was not an affinity-purified polyclonal antibody, as was used to test for ODF2 conservation, but rather a polyclonal antibody generated against synthetic peptides corresponding to the 191-204 amino acid (aa) and 790-803 aa sequences of the mouse AKAP4 protein (Figure 6.7) (Brown *et al.*, 2003). *Anti-AKAP4* was found to weakly label the midpiece of the possum sperm flagellum by immunofluorescence, however no cross-reactivity over the principal piece, and therefore fibrous sheath, was detected. In contrast, studies in the laboratory mouse and rat have localised the AKAP4 protein to both the circumferential ribs and longitudinal columns of the fibrous sheath (Johnson *et al.*, 1997; El-Alfy *et al.*, 1999), as well as to the principal piece (and presumably also fibrous

sheath) of human (Turner *et al.*, 1998) and bovine (Moss *et al.*, 1999) sperm. In addition, no possum fibrous sheath proteins were recognised by the anti-*AKAP4* serum in Western blots. This finding was somewhat surprising, as (1) the major possum fibrous sheath protein and AKAP4 in the laboratory mouse have very similar molecular weights (76 and 73 kDa respectively), and (2) in Chapter 5, the *PoTVFS* serum was found to stain both the possum and rat 76 kDa fibrous sheath proteins. Moreover, conserved homologues of AKAP4 have been found in sperm from human (Turner *et al.*, 1998), bovine (Moss *et al.*, 1999) and laboratory rat (El-Alfy *et al.*, 1999).

There are several possible reasons why AKAP4 cross-reactivity was not found to occur in the possum. Firstly, assuming an AKAP4 gene is present in the possum, it is possible that the amino acid sequences (aa 191-204 and 790-803) of the AKAP4 protein to which the synthetic peptides, and therefore *anti-AKAP4* antibody, was generated (Brown *et al.*, 2003) may not be conserved in the possum. The *anti-AKAP4* antibody, which was used in the current study, was prepared against these specific amino acid sequences because a BLAST search indicated that they are not present in any other known mouse proteins (Brown *et al.*, 2003), thereby reducing the potential for false positive results in immuocytochemical experiments. The first sequence (aa 191-204), which is downstream the N-terminal end of the mature AKAP4 protein and adjacent a potential A-kinase anchoring domain, is relatively poorly conserved between mouse, rat, human and bovine sequences in comparison to the entire protein sequence (Figure 6.7). Consequently, it is possible that the *anti-AKAP4* serum may not have recognised any of the antigenic epitopes expressed on the possum AKAP4 protein, if indeed one does exist.

An alternative reason why no cross-reactivity was observed with the *anti-AKAP4* antibody is that no homologous protein exists in the possum. If this were the case, however, one would expect that an alternative kinase anchoring protein would be present within the possum sperm flagellum given the apparent importance of AKAPs in sperm. In several eutherian species, additional AKAPs, AKAP3 and TAKAP-80, have been identified. It may be that one, or both, of these proteins are present in the possum. AKAP3 was, like AKAP4, independently cloned by two separate groups (Vijayaraghavan *et al.*, 1997b, 1999; Mandal *et al.* 1999), and found to encode an 853-long amino acid protein with a calculated molecular weight of 94.6 kDa. In contrast to AKAP4, however, antisera prepared against the AKAP3 protein showed that it is localised to the circumferential ribs of the fibrous sheath (Mandal *et al.*, 1999) as well as, surprisingly, the acrosome (Vijayaraghavan *et al.*, 1999). To date, AKAP3 has been isolated and sequenced from sperm of the mouse, bovine (Vijayaraghavan *et al.*, 1999) and human (Mandal *et al.*, 1999; Vijayaraghavan *et al.*, 1999). Moreover, common Protein Kinase A (PKA)-binding domains were identified in each species, suggesting that this protein may have an important role to play in regulating sperm motility, as well as head-associated activities such as capacitation and the acrosome reaction (Vijayaraghavan *et al.*, 1999). However, it has not yet been possible to investigate whether this protein is present in the possum. More recently, two proteins that interact with the PKA-binding region of human AKAP3 were identified. One is ropporin, a spermatogenic cell-specific protein that interacts with the Rho signalling pathway (Fujita *et al.*, 2000), while the other is a novel AKAP-associated sperm protein (ASP) (Carr *et al.*, 2001). Less is known of the other fibrous sheath testis A-kinase anchoring protein, TAKAP-80, which was identified in laboratory rat sperm using a radiolabelled RII probe (Mei *et al.*, 1997). Although antisera raised against this protein recognised an 80 kDa protein on Western blots, the deduced 502 amino acid sequence of *TAKAP-80* predicts a

55.8 kDa fibrous sheath protein (Mei *et al.*, 1997). In the current study, it has not yet been possible to investigate whether any of these additional A Kinase Anchoring Proteins are present in possum sperm, however based on the fact that AKAP4 does not appear to be conserved, this warrants further investigation.

FIGURE 6.7 Comparison of amino acid sequences of bovine (bAKAP4) (Moss *et al.*, 1999), mouse (mAKAP4) (Carrera *et al.*, 1994; Fulcher *et al.*, 1995a), human (hAKAP4) and rat (rAKAP4) (El-Alfy *et al.*, 1999) AKAP4 proteins. The domains (aa 191-204 and aa 790-803) to which the *anti-AKAP4* serum has been prepared against are underlined in blue.

(next three pages)

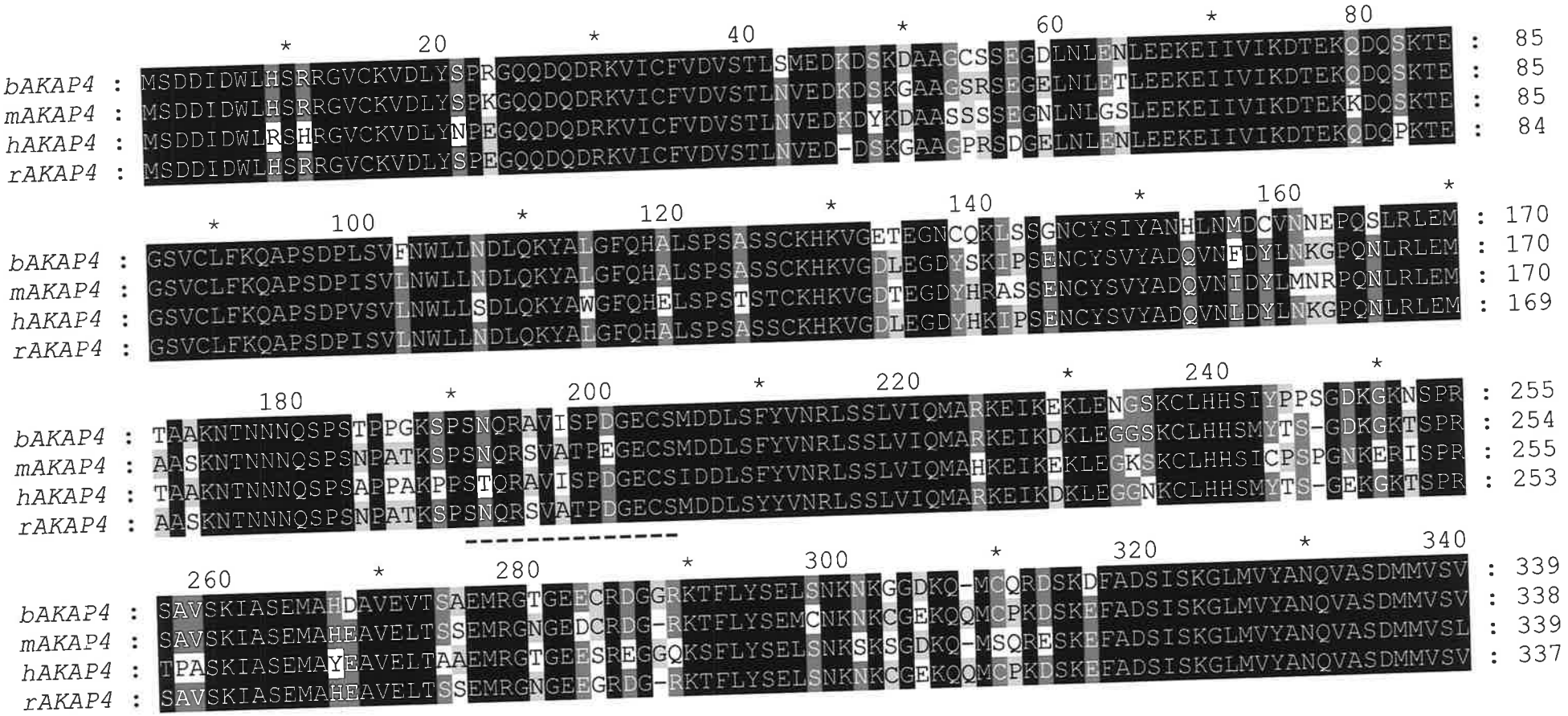
bAKAP4
mAKAP4
hAKAP4
rAKAP4

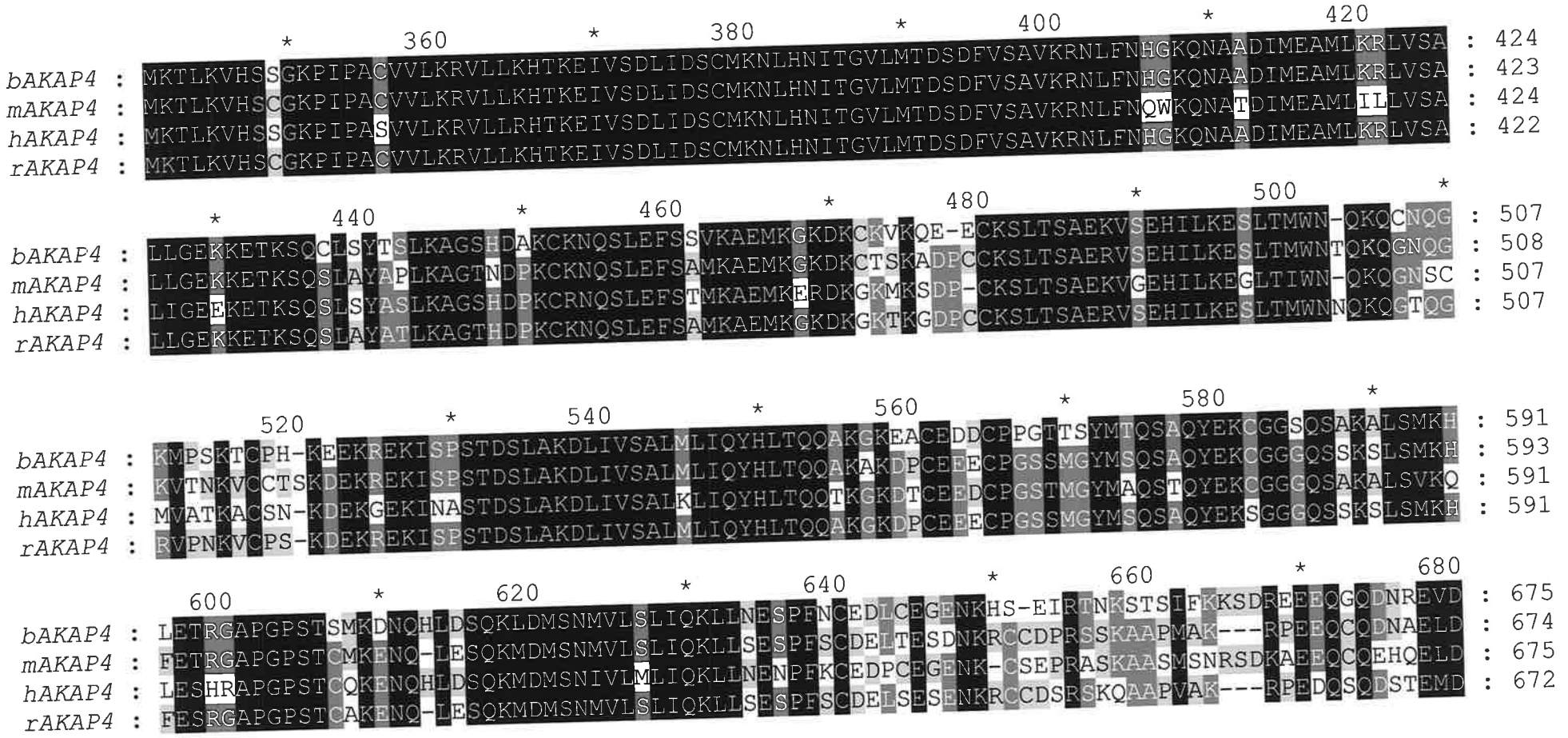
bAKAP4
mAKAP4
hAKAP4
rAKAP4

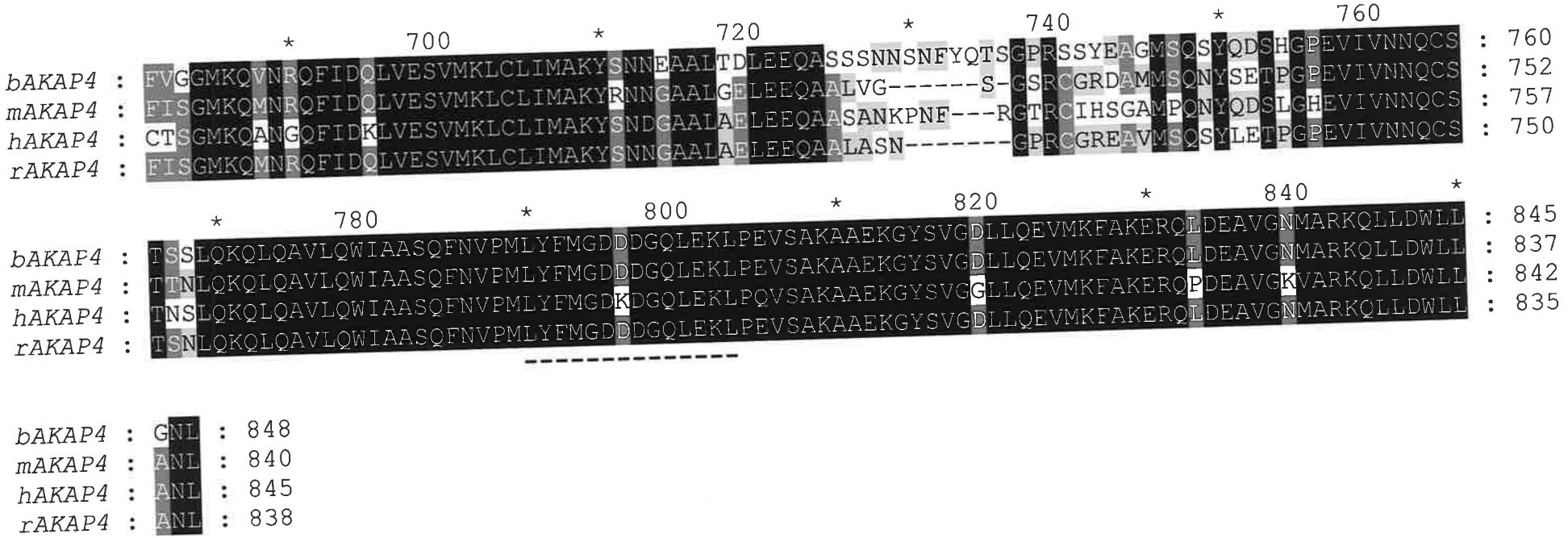
700
720
740
760
780
800
820
840
bAKAP4 : 760
mAKAP4 : 752
hAKAP4 : 757
rAKAP4 : 750
bAKAP4 : 845
mAKAP4 : 837
hAKAP4 : 842
rAKAP4 : 835
bAKAP4 : 848
mAKAP4 : 840
hAKAP4 : 845
rAKAP4 : 838

6.4.3 Possible Conservation of the GAPDS Protein

In somatic cells, Glyceraldehyde 3-phosphate dehydrogenase (*GAPD*) is an essential enzyme in the main pathway of glycolysis (the conversion of glucose to pyruvate, generating two ATP molecules). GAPD, therefore, serves a key role in providing the metabolic energy required to support many cellular functions (Welch *et al.*, 1992). For many years it was suspected that a GAPD enzyme is also involved in regulating glycolysis in rat spermatids (Nakamura *et al.*, 1986), and a unique GAPD enzyme that is expressed in spermatogenic cells, termed GAPDS, was subsequently found to occur in the laboratory mouse (Welch *et al.*, 1992). The mouse GAPDS gene was specifically isolated and sequenced by screening a mouse spermatogenic cell expression library with a monoclonal antibody, *ATC*, that was obtained by immunising mice with dissociated rat testis cells (Fenderson *et al.*, 1988). Antibody *ATC* recognises a 67 kDa fibrous sheath protein in the longitudinal columns and circumferential ribs of mouse, rat and hamster sperm, suggesting that this fibrous sheath protein is conserved in these species. However, antibody *ATC* does not recognise fibrous sheath proteins in guinea pig, rabbit and human sperm, indicating that this protein may not be conserved in all eutherian species (Fenderson *et al.*, 1988). Densitometry scans of gels indicated that the 67 kDa protein recognised by the *ATC* antibody represents approximately 16% of the total protein of the mouse fibrous sheath (Eddy *et al.*, 1991).

The mouse spermatogenic GAPDS gene identified encodes a protein of 438 aa compared to the GAPD protein expressed in somatic cells which is 333 aa in length, with the additional 105 aa of the GAPDS protein located on the N-terminus and composed predominately of proline residues (Welch *et al.*, 1992). The remaining GAPDS sequence has 71% identity with the somatic mouse GAPD gene (Welch *et al.*, 1992). The predicted

molecular weight of mouse the GAPDS protein is 47.5 kDa (Welch *et al.*, 1992), which is somewhat less than the 67 kDa fibrous sheath recognised by the ATC antibody. It has been suggested that the proline-rich N-terminus of the GAPDS protein is responsible for its slower than expected migration in SDS-gels (Bunch *et al.*, 1998). Northern blot analysis has found that GAPDS mRNA is present only in round and condensing spermatids (Welch *et al.*, 1992; Mori *et al.*, 1992). Recently, the human homologue of the mouse GAPDS protein was sequenced and found to have 83% identity to the mouse GAPDS gene. In addition, using the mouse GAPDS cDNA as a hybridization probe in Northern blots, GAPDS mRNA has also been found to occur in testis RNA samples of rat, rabbit and ram (Welch *et al.*, 1995). Furthermore, a 41.5 kDa fibrous sheath protein that is recognised by an anti-somatic GAPD antibody has been found to occur in the bull and may be the homologue of GAPDS in this species (Westhoff and Kamp, 1997).

The apparent conservation of the GAPDS enzyme in mouse, rat, human, hamster, rabbit, boar and, now, possum sperm suggests that this protein serves an important role in the sperm flagellum. In spermatids, it has been found that energy metabolism does not occur through glycolysis, as this process is inhibited in these cells, but rather depends mainly on the conversion of lactate to pyruvate for use in the citric acid cycle (Nakamura *et al.*, 1981; Mita and Hall, 1982; Jutte *et al.*, 1983; Grootegoed *et al.*, 1986). Incubation of round spermatids in the presence of glucose without any other energy substrates results in depletion of ATP and cell death (Grootegoed *et al.*, 1986; Nakamura *et al.*, 1982; Nakamura *et al.*, 1986). In contrast, in vitro studies indicate that rat and mouse spermatozoa are unable to utilise lactate or pyruvate as energy substrates (Fraser and Quinn, 1981; Mahadevan *et al.*, 1997). Instead, spermatozoa require glucose for hyperactivated motility of the flagellum (Fraser and Quinn, 1981) and fertilisation (Hoppe, 1976). Consequently, the glycolytic pathway is believed to be activated during the latter

stages of rat and mouse spermatid differentiation, at which time fibrous sheath morphogenesis reaches a peak, although the exact regulating mechanisms of this process are not yet fully understood (Bunch *et al.,* 1998). Glucose has also been found to be required for capacitation in sperm from human (Hoshi *et al.,* 1991), guinea pig (Mujica *et al.,* 1991) and macaque (Van deVoort and Overstreet, 1995).

Prior to the current study, a polyclonal antibody, termed anti-GAPDS, was raised against two synthetic peptides generated against the two domains of the mouse GAPDS protein (peptide A: aa 158-194; peptide B: 293-306) (Figure 6.8) (Bunch *et al.,* 1998). These sequences were chosen as they were found to differ substantially from those of the somatic GAPD enzyme. In the current study, the mouse *anti-GAPDS* antibody was used to test for antigenic cross-reactivity, and therefore potential conservation of the GAPDS gene, in possum sperm. In fixed and permeabilised possum cauda sperm, *anti-GAPDS* immunoreactivity was localised to the principal segment of the flagellum, with immunoelectron microscopy demonstrating that this protein is distributed throughout then entire fibrous sheath. Unfortunately, no specific fibrous sheath protein was found to stain with *anti-GAPDS* serum by Western blotting. However, only one attempt at this procedure could be undertaken due to the very small amount of primary antibody available. Given the intense labelling of the fibrous sheath by immunofluorescence and immunoelectron microscopy, one can only presume that the Western blotting technique used in the current study was not adequate or did not work and, therefore, requires adjustment if proteins are to be detected. For example, the concentration of the *anti-AKAP4* serum used may have been too low (1:100), or the incubation times may need to be increased. In the current study the possum fibrous sheath was found to contain major 66 and 46 kDa proteins (see Chapter 4), which are of similar molecular weights to the actual (67 kDa) and predicted (47.5 kDa) molecular weights of the mouse GAPDS protein respectively. The 66 kDa

possum protein was found to be one of the most prominent fibrous sheath proteins in this species. It is, therefore, possible that one of these proteins may be the homologue of the eutherian GAPDS protein. In the future, when additional quantities of the *anti-AKAP4* serum become available, it is hoped that the exact possum fibrous sheath protein(s) recognised by *anti-AKAP4* will be determined.

Although it has not been possible to definitively ascertain whether a GAPDS protein is located in possum sperm, it's presence is nevertheless suggested by the results of the current study. Consequently, it may be required by spermatogenic cells in this species. In marsupials, much less is known of the mechanisms by which spermatogenic cells derive their energy. To date, there are no published reports on the metabolism of testicular sperm, however several investigations have sought to explain energy metabolism of epididymal sperm. An early study showed that brush-tail possum sperm utilise *N*-acetyl-D-glucosamine (NAG) and glucose, and that their oxygen consumption is much greater than that of eutherian sperm (Rodger and Suter, 1978). More recently, it was found that tammar wallaby epididymal sperm metabolise glucose and NAG from the seminal plasma fluid, instead of fructose which is the major sugar present in semen of eutherian mammals (Murdoch and Jones, 1998). However, the rate of uptake of NAG is much greater than, and almost completely inhibits the oxidation of, glucose and any other substrates (Murdoch and Jones, 1998). In spite of this last finding, the likely detection of the GAPDS enzyme in possum epididymal sperm in the current study is still significant as – assuming possum and wallaby sperm metabolisms are similar – considerable amounts of glucose are liberated from NAG during metabolism (Murdoch and Jones, 1998), and this glucose fuels the glycolytic process in these cells.

FIGURE 6.8 Comparison of amino acid sequences of mouse (mGAPDS) (Welch *et al.*, 1992), and human (hGAPDS) (Welch *et al.*, 2000) GAPDS proteins. The domains (aa 158-194 and aa 293-306) to which the *anti-GAPDS* serum has been prepared against are underlined in blue.

(next page)

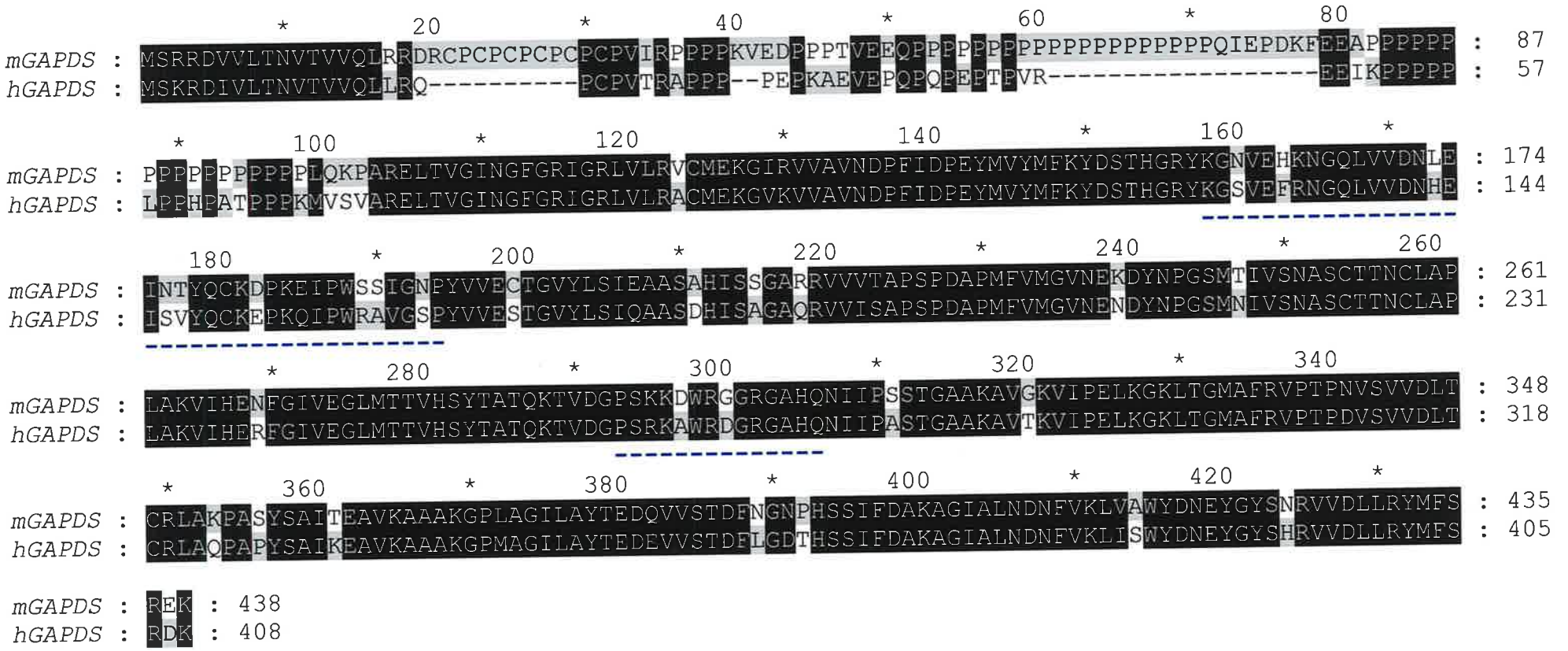
mGAPDS : MSRRDVVLTNVTVVQLRRDRCPCPCPCPCPCPVIRPPPPKVEDPPPTVEEQPPPPPPPPPPPPPPPPPPPQIEPDKFEEAPPPPPP : 87
hGAPDS : MSKRDIVLTNVTVVQLLRQ----------PCPVTRAPPP--PEPKAEVEPQPQPEPTPVR----------EEIKPPPPP : 57
mGAPDS : PPPPPPPPPPPLQKPARELTVGINGFGRIGRLVLRVCMEKGIRVVAVNDPFIDPEYMVYMFKYDSTHGRYKGNVEHKNGQLVVDNLE : 174
hGAPDS : LPPHPATPPPKMVSVARELTVGINGFGRIGRLVLRACMEKGVKVVAVNDPFIDPEYMVYMFKYDSTHGRYKGSVEFRNGQLVVDNHE : 144
mGAPDS : INTYQCKDPKEIPWSSIGNPYVVECTGVYLSIEAASAHISSGARRVVVTAPSPDAPMFVMGVNEKDYNPGSMTIVSNASCTTNCLAP : 261
hGAPDS : ISVYQCKEPKQIPWRAVGSPYVVESTGVYLSIQAASDHISAGAQRVVISAPSPDAPMFVMGVNENDYNPGSMNIVSNASCTTNCLAP : 231
mGAPDS : LAKVIHENFGIVEGLMTTVHSYTATQKTVDGPSKKDWRGGRGAHQNIIPSSTGAAKAVGKVIPELKGKLTGMAFRVPTPNVSVVDLT : 348
hGAPDS : LAKVIHERFGIVEGLMTTVHSYTATQKTVDGPSRKAWRDGRGAHQNIIPASTGAAKAVTKVIPELKGKLTGMAFRVPTPDVSVVDLT : 318
mGAPDS : CRLAKPASYSAITEAVKAAAKGPLAGILAYTEDQVVSTDFNGNPHSSIFDAKAGIALNDNFVKLVAWYDNEYGYSNRVVDLLRYMFS : 435
hGAPDS : CRLAQPAPYSAIKEAVKAAAKGPMAGILAYTEDEVVSTDFLGDTHSSIFDAKAGIALNDNFVKLISWYDNEYGYSHRVVDLLRYMFS : 405
mGAPDS : REK : 438
hGAPDS : RDK : 408

6.5 CONCLUSION

Notwithstanding the technical difficulties encountered, the current study has provided preliminary evidence that homologues of at least one eutherian outer dense fibre protein, ODF2, and one eutherian fibrous sheath proteins, GAPDS, occur in marsupial sperm. In future studies, one approach to more definitively establishing whether or not sperm tail cytoskeletal proteins are conserved across these two major groups of extant mammals would be to sequence the major possum outer dense fibre and fibrous sheath proteins and then compare the amino acid and/or nucleotide sequences with those for eutherians.

Chapter 7

FINAL DISCUSSION

7.1 INTRODUCTION

At the commencement of the studies reported in this thesis, it was hoped to (1) demonstrate how the outer dense fibres and fibrous sheath are formed during spermiogenesis, (2) identify the proteins that compose the outer dense fibres and fibrous sheath in a marsupial species and (3) elucidate the extent, if any, of homology of these proteins to those previously described for eutherian mammals. It was anticipated that this might shed further light on the possible functions of these sperm tail cytoskeletal structures, as well as aid in our understanding of the nature and extent of evolutionary conservation of these sperm proteins in mammals. To address these objectives, the morphological, biochemical and imunocytochemical properties of the marsupial outer dense fibres and fibrous sheath were described and compared with those of eutherian sperm. The brush-tail possum was used as model marsupial species.

7.2 MORPHOGENESIS OF THE OUTER DENSE FIBRES AND FIBROUS SHEATH

Prior to the current study, outer dense fibre and fibrous sheath morphogenesis had only been described in detail for the laboratory rat. In this species it was found that the assembly of these sperm tail cytoskeletal structures is a multi-step process extending over a significant portion of spermiogenesis (Irons and Clermont, 1982a, b). Moreover, outer dense fibre formation was found to proceed in a proximal-to-distal direction along the

axoneme, in an opposite direction to that for the fibrous sheath (Irons and Clermont, 1982a, b). In Chapter 3, possum spermiogenesis was divided into twelve maturational steps and the formation of the outer dense fibres and fibrous sheath were described in chronological order for each step. Outer dense fibre formation was found to occur during steps 6-12 of spermiogenesis, whereas fibrous sheath formation occurred during steps 4-12. The method of assembly of the possum outer dense fibres and fibrous sheath was found to be remarkably similar to that reported for the rat. Specifically, in both species: (1) the direction of assembly of the outer dense fibres and fibrous sheath along the axoneme is identical, (2) maximal growth of outer dense fibres occurs very late in spermiogenesis, with outer dense fibres 1, 5 and 6 largest in size and extending for the greatest distance within the flagellum, (3) formation of the longitudinal columns precedes, and for a significant portion of spermiogenesis is independent to, that of the circumferential ribs.

In Chapter 5, an antibody raised against proteins of whole possum fibrous sheath extracts was used to shed additional light on the formation of this structure. By immunohistochemistry, production of possum fibrous sheath proteins was found to occur in elongating spermatids (steps 6-12 of spermiogenesis), with peak cytoplasmic immunoreactivity observed in step 10 spermatids. However, the anlagen of the columns and ribs of the fibrous sheath were not recognised by this antibody, indicating that the proteins contained therein may be different to those of the mature structure or, alternatively, are modified after their initial assembly so that they appear antigenically different in the mature fibrous sheath. In the rat, where this phenomenon was also found to occur, it has been suggested that the anlagen of the columns and ribs may serve as a framework onto which the final fibrous sheath proteins are attached late in spermiogenesis. The fact that immunoreactivity of possum fibrous sheath proteins occurs

well after chromatin condensation has begun, at which time transcription is thought to cease, suggests that fibrous sheath proteins may be stored prior to their assembly along the axoneme. No evidence of concentrated storage within the spermatid was found, however the cytoplasm is diffusely immunoreactive from step 6 indicating that proteins reside at this location until they are required along the axoneme. This is supported by the fact that at step 11, just prior to the time at which the flagellum is maximally reactive to the anti-fibrous sheath serum, there is intense labelling over the periaxonemal cytoplasm. This indicates that proteins of the mature fibrous sheath are transported from the cytoplasm down the flagellum to the fibrous sheath at the period of maximal fibrous sheath growth. Incorporation of these proteins into the fibrous sheath late in spermiogenesis appears to be a major step in the completion of assembly of this structure.

7.3 PROTEIN COMPOSITION OF THE OUTER DENSE FIBRES AND FIBROUS SHEATH

The eutherian outer dense fibres and fibrous sheath are stabilised by abundant disulphide bonding and, therefore, are insoluble in a variety of high salt, detergent and acidic solutions (Calvin and Bedford, 1971; Bedford and Calvin, 1974; Calvin, 1975; Olson and Sammons, 1980). Based on these properties, techniques were developed to isolate the outer dense fibres (Olson and Sammons, 1980; Vera *et al.*, 1984; Oko, 1988; Kim *et al.*, 1999) and fibrous sheaths (Olson *et al.*, 1976; Oko, 1988; Kim *et al.*, 1995b) from the sperm flagellum. Prior to the current study, almost nothing was known of the protein composition of the outer dense fibres and fibrous sheath for any marsupial species. In Chapter 4, techniques were developed, based on those used for the laboratory rat, to isolate and then purify the outer dense fibres and fibrous sheath from the possum sperm flagellum. By 1D SDS-PAGE, it was found that the outer dense fibres are composed of

seven major proteins (MWs: 73, 58, 55, 54, 52, 41 and 16 kDa), with the 41 and 16 kDa proteins found to occur in, but perhaps not exclusive to, the medulla of the fibres. In contrast, the fibrous sheath is composed of twelve major proteins (MWs: 106, 76, 66, 62, 55, 53, 52, 46, 40, 30, 28, and 16 kDa) reflecting its greater structural complexity. Although similar numbers of proteins are present in possum and rat sperm, their molecular weights differ somewhat, with the exception of the 16 kDa outer dense fibre protein and 76 and 16 kDa fibrous sheath proteins which occur in both species. This suggested potential conservation of at least these sperm tail cytoskeletal proteins across both eutherians and marsupials.

7.4 CONSERVATION OF OUTER DENSE FIBRE AND FIBROUS SHEATH PROTEINS

In Chapter 5, an anti-possum fibrous sheath polyclonal serum (*PoTVFS*) was used to show, by immunocytochemical means, that whilst the possum outer dense fibres and fibrous sheaths contain several proteins of identical or very close molecular weights, these proteins are, in fact, antigenically dissimilar and therefore presumably distinct. Moreover, the *PoTVFS* serum did not bind to any other sperm structure, like, for example, the sperm head, outer dense fibres and midpiece fibre network, indicating that fibrous sheath proteins are unique.

In the current study evidence was also presented, using the *PoTVFS* serum, of conservation of fibrous sheath epitopes in sperm from four different marsupial families (possum, koala, wallaby and dunnart) as well as a eutherian species (laboratory rat). In particular, the 76 and 62 kDa proteins are recognised in each of these species suggesting that homologues of these proteins might occur. The apparent conservation of the 76 kDa

fibrous sheath protein is especially significant as a similar-sized protein has also been found to be a major component of the fibrous sheath in the laboratory mouse (Carrera *et al.*, 1994; Fulcher *et al.*, 1995a), human (Turner *et al.*, 1998), bull (Moss *et al.*, 1999) and laboratory rat (El-Alfy *et al.*, 1999). In these eutherian species this protein is an example of an A Kinase Anchoring Protein and hence has been named AKAP4. The possibility that a homologue of AKAP4 might be present in possum sperm was subsequently tested by incubating possum sperm in anti-mouse AKAP4 serum. No cross-reactivity with this antibody was, however, observed. Given the apparent importance of AKAP4 in eutherian sperm (discussed further in 7.5.2), one must presume that either (1) the *anti-AKAP4* serum was either not prepared against a conserved domain of the AKAP4 protein, or (2) that an alternate AKAP is found in possum sperm. Alternatively, one cannot rule out the possibility that no examples of AKAPs are found in possum sperm. As it was only possible to carry out cross-reactivity tests with *anti-AKAP4* serum once, due to the small quantity of serum available, one cannot rule out the possibility that, with further refinement of the protocols used, cross-reactivity might have eventually been observed.

Although it remains unclear whether a homologue of AKAP4 occurs in marsupial sperm, the current study did provide evidence that a homologue of the laboratory mouse spermatogenic glyceraldehyde 3-phosphate dehydrogenase (GAPDS) protein is present within the possum fibrous sheath. In Chapter 6, anti-mouse GAPDS serum was found to bind specifically and intensely over the principal piece and fibrous sheath of possum sperm by immunofluorescence and immunoelectron microscopy respectively. Unfortunately, a limited volume of *anti-GAPDS* serum meant that, once again, it was not possible to carry out repeated immunoblots to determine which possum fibrous sheath protein(s) is responsible for the cross-reactivity observed. Nevertheless, given the predicted and actual

molecular weights of the mouse GAPDS protein are 47.5 kDa and 67 kDa respectively, one can only speculate, at this stage, that either the major 46 kDa or 66 kDa possum fibrous sheath protein is responsible for the cross-reactivity observed and, therefore, is the homologue of the eutherian GAPDS enzyme. The functional significance of the GAPDS enzyme in the sperm flagellum will be discussed in 7.5.2.

With regards to possible conservation of outer dense fibre proteins in eutherian and marsupial mammals, the current study provides evidence that a homologue of the laboratory rat ODF2 protein occurs in the possum. In Chapter 6, anti-rat ODF2 serum was found to label the principal piece and outer dense fibres of possum sperm by immunofluorescence and immunoelectron microscopy respectively. In the rat, ODF2 has a predicted and actual molecular weight of 72 kDa and 84 kDa respectively (Shao *et al.*, 1997; Schalles *et al.*, 1998), however, whilst a major 73 kDa protein was found to occur in the possum outer dense fibres, it was not stained by the anti-ODF2 serum in Western blots. Instead, the major 55 kDa and minor 28 kDa possum fibrous sheath proteins were recognised, suggesting that either (1) different-sized proteins within the possum have similar antigenic epitopes to those of the rat ODF2 protein, or (2) that a similarly-sized ODF2 protein is present in the possum outer dense fibres but has been cleaved into two smaller proteins (55 kDa and 28 kDa) prior to SDS-PAGE. Alternatively, one cannot rule out the possibility that the 55 and 28 kDa possum outer dense fibres share antigenic epitopes with ODF2 but are unrelated. The functional significance of the possible conservation of ODF2 in marsupials will be discussed in 7.5.1.

7.5 FUNCTION OF SPERM TAIL CYTOSKELETON

The fact that in the current study, the morphogenesis, and some of the proteins of, the outer dense fibres and fibrous sheath have been found to be remarkably similar in sperm from both a marsupial and eutherian species, leads to the question of whether or not these cytoskeletal structures have similar functions in both of these lineages of extant mammal.

7.5.1 Possible Functions Of The Outer Dense Fibres

To date, most studies have suggested that the outer dense fibres have an important structural/mechanical role(s) only, largely because of the close physical relationship between these fibres and the axoneme microtubules. The fact that mammalian outer dense fibre proteins are stabilised by abundant disulphide bonding (Calvin and Bedford, 1971; Bedford and Calvin, 1974; Calvin, 1975; Olson and Sammons, 1980) lead, early on, to the hypothesis that these structures act to stiffen the axoneme (Phillips and Olson, 1974). Calvin and Bedford (1971) and Calvin *et al.*, (1975) suggested that, because of their insolubility in a variety of high salt and detergent solutions, the outer dense fibres might contain sperm keratins. Very recently, several cytokeratins were identified, by immunoblotting using anti-cytokeratin antibodies, in bovine sperm outer dense fibre fractions, including cytokeratin 19 (*CK19*), suggesting that they may play an important structural or tension-bearing role in sperm flagella (Hinsch *et al.*, 2003). Moreover, it has been shown that a 57 kDa sperm-associated keratin, *Sak57*, in rat spermatids migrates along the microtubules of the manchette to the outer dense fibres and fibrous sheath suggesting that keratins are also involved in the assembly of these cytoskeletal structures. In the current study, it was not possible to specifically test for whether or not outer dense fibre proteins are examples of keratins, largely because the lack of quantity of possum

material restricted the number of experiments that could be carried out. Nevertheless, evidence has been presented in the current study that, at least some, eutherian and marsupial outer dense fibre proteins are biochemically and antigenically similar and, therefore, may be closely related.

Previously, it has been suggested that outer dense fibres may function to stabilise the mammalian sperm flagellum. This is because comparative, high-speed kinematography studies of sperm motility indicated that flagella of species with relatively small outer dense fibres, for example mouse, human and rabbit, are quite flexible, forming arcs with a small radius of curvature as they beat (Phillips, 1972). However, in laboratory rat and Chinese hamster sperm, which have unusually large outer dense fibres, the sperm tails have bending waves of lower amplitude and appear to be stiffer (Phillips, 1972). The outer dense fibres, therefore, are thought to have become necessary in order to stabilise, and hence sustain, the long flagella observed in most mammalian sperm. This notion was subsequently supported by a study in which the relative tensile strengths of sperm from seven mammalian species was investigated by measuring the minimum shear force necessary to 'kill' (make immotile) sperm suspended in a viscous fluid (Baltz *et al.*, 1990). It was found that longer sperm flagella are not as fragile as would be expected from theoretical predictions, possibly because the outer dense fibres confer increasing tensile strength to protect sperm from shear forces encountered during epididymal transit and especially during ejaculation (Baltz *et al.*, 1990).

In the current study, the pattern of possum sperm motility was not specifically examined, however previous investigations have shed light on motility in representatives from several marsupial families, including Dasyuridae, Peramelidae and the American didelphids

(Taggart and Temple-Smith, 1990; Taggart *et al.*, 1993, 1995a, b; Moore and Taggart, 1995). In addition, observations on the movement of sperm from several diprotodontan species and several macropodids (Clulow *et al.*, 1992; Taggart *et al.*, 1995a) have been made. In many of these species, active progressive motility was observed in mature sperm from the cauda epididymides *in vitro,* however, in those species in which the outer dense fibres are extremely radially displaced, such as the brown marsupial mouse (*Antechinus stuartii*) (a dasyurid) (Taggart and Temple-Smith, 1990) and northern (*Isoodon macropus*) and southern (*Isoodon obesulus*) brown bandicoots (peramelids) (Taggart *et al.*, 1995b), snake-like sinusoidal progressive motility was instead observed in viscous media. Ultrastructural studies of sperm from numerous marsupial groups have shown that the only feature common to flagella of dasyurids and peramelids is the extreme radial displacement of the outer dense fibres, hence it was hypothesised that they may play an integral role in the occurrence of a sinusoidal mode of sperm movement in these species (Taggart *et al.*, 1995a). In the possum, as well as in macropods, no evidence of such sperm movement has previously been reported (Taggart *et al.*, 1995a) or even observed informally in the current study. Interestingly, possum and macropod sperm flagella are relatively short (~106–124 µm) (Cummins and Woodall, 1985) compared with those of dasyurids and peramelids (~250-270 µm and ~170 µm respectively) (Cummins and Woodall, 1985; Taggart and Temple-Smith, 1990), indicating that radial displacement of the outer dense fibres might also be related to the length of the sperm flagellum. It has been proposed that the radial displacement of the outer dense fibres reflects the least ancestral marsupial condition (Temple-Smith, 1987), suggesting that the possum flagellum has undergone least adaptive change.

On a somewhat related note, a hypothesis has been presented in an attempt to explain the functional significance of the attachment of the outer dense fibres to both the outer microtubule doublets of the axoneme and the connecting piece (Lindemann, 1996). In the current study, the attachment of the outer dense fibres to the connecting piece was evident when possum sperm were incubated in SDS-DTT for 60 mins (Figure 4.5a). The hypothesis developed was based on the premise that forces produced by interdoublet sliding are transferred to the outer dense fibres, and suggests that the fibres not only provide stiffness, but also provide a means to proportionally raise the bending torque (rotation) of the flagellum to overcome its additional flexural rigidity (Lindemann, 1996). This is because torque is the product of force times lever arm length (diameter) and the effective diameter of the outer dense fibres is greater than that of the outer microtubule doublets. Consequently, energy from more dynein cross-bridges can be consolidated into the production and propagation of flagella bends in long sperm (Lindemann, 1996). In the possum, any additional bending torque resulting from an increase in the effective diameter would be relatively small as the outer dense fibres are located immediately adjacent the outer microtubule doublets. Furthermore, the length of the possum flagellum is relatively small compared to that of the laboratory rat on which Lindemann's (1996) notion was based.

Further evidence of the potential role of the outer dense fibres in sperm motility comes from investigations of malformed sperm from asthenoteratozoospermic men. In these individuals, incomplete development of the outer dense fibres has been strongly linked with motility disorders (Haidl *et al.*, 1991), although it should be noted that any underlying genetic defect in these individuals might give rise to alternate, less obvious, malformations/abnormalities that could be influencing sperm behaviour.

More recently, molecular characterisation of some of the major eutherian outer dense fibre proteins has shed new light on the underlying molecular organisation of this structure. For example, the nucleotide sequences of the 27 kDa (ODF1) (Burfeind *et al.*, 1993; Higgy *et al.*, 1994; Burmester and Hoyer-Fender, 1996), 84 kDa (ODF2) (Shao *et al.*, 1997) and 110 kDa (ODF3) (Petersen *et al.*, 2002) laboratory rat outer dense fibre proteins are known. Interestingly, the ODF1, ODF2 and ODF3 proteins, as well as two additional outer dense fibre-interacting proteins Spag4 (Shao *et al.*, 1999) and Spag5 (Shao *et al.*, 2001), contain, and are thought to interact with one another, by leucine zippers. Moreover, ODF1 can also self-interact via its leucine zipper, indicating that it may act as the framework protein onto which other outer dense fibre proteins associate (Shao *et al.*, 1997; 1999; 2001). In the current study, evidence has been presented to suggest that a homologue to the ODF2 protein is found in the outer dense fibres of possum sperm. If this is definitively shown to be the case, for example by sequencing the possum homologue, it would indicate that marsupial outer dense fibre proteins may be organised in a manner similar to that described for the rat.

7.5.2 Possible Functions Of The Fibrous Sheath

In early studies, it was shown that the mammalian fibrous sheath is highly resistant to acid solubilisation, indicating that the proteins of this structure are, like those of the outer dense fibres, stabilised by disulphide bonds (Calvin and Bedford, 1971; Bedford and Calvin, 1974). Therefore, it was hypothesised that the fibrous sheath might also be involved in stiffening the flagellum (Calvin and Bedford, 1971; Bedford and Calvin, 1974). Ultrastructural investigations of fibrous sheath morphology have shown that its longitudinal columns appear to be attached to outer microtubule doublets 3 and 8 of the axoneme

(Fawcett and Phillips, 1969; Fawcett, 1975). Consequently, it has been proposed that the fibrous sheath might also serve to modulate the plane of the flagellar beat by restricting the participation of microtubules 3 and 8 in microtubule sliding and axoneme bending during flagellar movement (Eddy and O'Brien, 1994). In addition, the longitudinal columns themselves might limit bending in the plane of the central pair of microtubules of the axoneme (Fawcett, 1975). It has also been suggested that the longitudinal columns of the fibrous sheath may, in association with the central pair of microtubules of the axoneme, outer microtubule doublets 3 and 8, and the outer dense fibres, provide an underlying structural and organising framework for the flagellum (Lindemann *et al.*, 1992). This is because these sperm tail structures together form a tightly connected 'I'-beam-like partition extending most of the length of the flagellum that does not actively participate in sliding (Lindemann *et al.*, 1992). In a related theory, it has been argued that the apparent connection of the fibrous sheath to the annulus at its proximal end means that the fibrous sheath is confined to a restricted space within the flagellum. Consequently, any microtubular sliding thrusts of the axoneme are likely to be transmitted to the fibrous sheath, forcing it to bend and thereby converting the linear movements of the microtubules into bending waves (Jassim, 1995).

To date, only a few experimental studies have been able to specifically investigate the role of the fibrous sheath, largely because of the difficultly in isolating it from adjacent tail structures. In one such investigation, motile mouse sperm were carefully treated to remove the plasmalemma and mitochondrial sheath (Si and Okuno, 1993). Following the addition of Mg-ATP and trypsin to induce the sliding disintegration of microtubules from the axoneme, the outer microtubule doublet-outer dense fibre (doublet-ODF) complexes were found to loop outward between the annulus and connecting piece. When doublet-ODF

extrusion was complete, the fibrous sheath was pulled proximally toward the sperm head (Si and Okuno, 1993). It was subsequently shown that doublet-ODF extrusion occurs in a specific sequence and that the doublet-ODFs adjacent outer microtubules 3 and 8 are responsible for fibrous sheath sliding (Si and Okuno, 1995). This would appear to demonstrate that doublet-ODFs and the fibrous sheath are connected and provides evidential support for Lindemann's *et al.,* (1992) theory of fibrous sheath function.

Additional evidence that the fibrous sheath has a mechanical role in sperm flagellar bending comes from studies of infertile men. Dysplasia of the fibrous sheath (DFS), which is characterised by hyperplasia and disorganisation of the fibrous sheath, has been described as a syndrome of infertile men and results in 95-100% sperm immotility (Chemes *et al.,* 1987). In these patients, the sperm flagella appear rigid, short, and thick and there is often associated displacement of the axoneme microtubules. The familial incidence of DFS – it has been found in brothers – indicates a genetic component in some patients (Chemes *et al.,* 1987; Olmedo *et al.,* 1997).

In the current study, the possum fibrous sheath was found to be both morphologically and chemically similar to that of the laboratory rat and mouse. As it is similarly bordered by the annulus and also appears to be closely associated with outer microtubule doublets 3 and 8 of the axoneme, it is also presumably restricted in its movement within the principal piece, thereby possibly affecting flagella movement. Moreover, the possum fibrous sheath is also resistant to solubilisation as evidenced by the fact that it was unaffected by prolonged incubation in relatively high concentrations of Triton X-100, DTT and Urea. Given these similarities, it is possible that the aforementioned theories developed for the eutherian

fibrous sheath espousing its mechanical role in normal sperm functioning, are likely to be applicable to marsupial sperm.

While the classical view is that the fibrous sheath has a passive, structural role, recent molecular studies have indicated that the fibrous sheath may also be involved in signal transduction. This is because three of the proteins of the mouse fibrous sheath, including the most abundant protein, AKAP4, are examples of A-Kinase Anchoring Proteins (Carrera *et al.*, 1994, 1996; Fulcher *et al.*, 1995a; Vijayaraghavan *et al.*, 1999). Such proteins are responsible for binding, and therefore compartmentalising within the cytoplasm, the regulatory subunit of Protein Kinase A (PKA), thereby placing it in proximity to proteins immediately downstream the signal transduction pathways (Colledge and Scott, 1999; Miki *et al.*, 2002). PKA responds rapidly to cyclic AMP (cAMP) (Colledge and Scott, 1999) and intracellular levels of cAMP are known to rise in the epididymis (Lewis and Aitken, 2001) and female reproductive tract (Tash and Means, 1983; Visconti *et al.*, 1995). The cAMP-signalling pathway has, therefore, been implicated in the regulation of sperm maturation, motility, capacitation, hyperactivation and the acrosome reaction (Eddy and O'Brien, 1994; Yanagimachi, 1994). Therefore, by anchoring cAMP-dependent PKA, the AKAP proteins of the fibrous sheath may enable these processes, which are fundamental for fertilisation, to occur. In support of this notion, it has been found that incubation of bovine sperm in PKA-anchoring inhibitory peptides disrupts sperm motility, suggesting that PKA-AKAP interactions, and not PKA catalytic activity, is required for motility (Vijayaraghavan *et al.*, 1997a). It should be noted, however, that in RIIα knockout mice (RIα and RIIα are subunits of PKA onto which AKAP anchors), sperm motility and fertility are unaffected even though the majority of PKA is not anchored to the flagellum (Burton *et al.*, 1999). It has been suggested that in these animals, PKA may, instead, bind to the less common RIα domain

of PKA (Miki and Eddy, 1998), although testing this with knockout animals is impossible as it is embryonically lethal (Eddy *et al.*, 2003). More recently, targeted disruption of the AKAP4 gene in mice was found to result in immotile sperm and infertility (Miki *et al.*, 2002). In the current study, no evidence of conservation of AKAP4 in possum sperm was presented, however it is possible that alternate AKAP, like AKAP3 and TAKAP80, may be present in sperm from this mammalian group.

In the current study evidence was, however, presented that suggests a homologue of the eutherian GAPDS protein is present in the fibrous sheath of marsupial sperm. This has significant implications for possum sperm metabolism as this protein is thought to anchor enzymes for the glycolytic pathway that provide the energy hyperactivated sperm require to penetrate the egg coats (Fraser and Quinn, 1981; Travis *et al.*, 1998).

In addition to serving a structural role in flagellar bending, these results indicate that the possum fibrous sheath also acts, at the very least, as a scaffold onto which proteins required for the glycolytic pathway are anchored.

7.6 EVOLUTION OF SPERM TAIL CYTOSKELETON

In the current study, evidence has been presented indicating that the formation and at least some of the proteins of the outer dense fibres and fibrous sheath are remarkable similar in the two major mammalian groups. This indicates that, prior to divergence into eutherians and marsupials, an increased complexity of the cytoskeleton of the sperm tail evolved.

In studies examining the evolution of sperm, it has been shown that the (1) acrosome, (2) elongated appearance of the nucleus, and (3) orderly arrangement of the mitochondria in the midpiece, are progressively acquired during evolution and, consequently, are examples of advanced sperm traits (Afzelius, 1979; Baccetti, 1982). Conversely, the sperm basic 9+2 flagellum appears to be a primitive feature present from the beginning of the male germ cell phylogeny (Afzelius, 1979). The structure of the flagellum, however, varies depending on whether internal or external fertilisation occurs. Sperm tails from all aquatic phyla, in which external fertilisation occurs, display a simple 9+2 microtubule axoneme, as is found in somatic cell cilia. Conversely, internal fertilisation, which has evolved in association with terrestrial life, results in sperm flagella displaying a 9+9+2 pattern as a result of acquiring additional, accessory proteins/structures adjacent the outer microtubule doublets (Franzen, 1956; Nicander, 1970; Baccetti, 1982; van der Horst *et al.*, 1989). These accessory flagellar structures vary considerably in appearance and composition. In the Insects and Onychophorans, nine additional microtubules surround the basic axoneme and, in the case of Insects, they have arms with ATPase activity and, therefore, may have an active role in flagellar movement (Baccetti, 1986). However, in sperm from most other internal fertilisers, nine fibre-like accessory structures are instead present adjacent the outer microtubule doublets of the axoneme. These structures vary in form from quite short and thick in Pogonophora, Cyclostomata, Elasomobranchia, some Teleostea, most of the Annelida and some Chelicerata, to relatively thick and almost as long as the flagellum in Gastropoda, Cephalopoda and terrestrial vertebrates (Baccetti, 1982, 1986). In mammalian species, these structures are the nine outer dense fibres. Additional periaxonemal cytoskeletal structures have also developed in sperm from some groups. For example, in Insects, crystalline 'accessory bodies' made of prekeratin are present in some species (Baccetti, 1972) presumably to sustain the very long sperm flagella typical of this

group (Baccetti, 1978; Baccetti, 1982). Periaxonemal structures are most prominent, however, in sperm from mammals, some reptiles and most passerine birds where they form the fibrous sheath or fibrous sheath-like structures. The reptilian fibrous sheath generally appears as a thick, amorphous rib-like, electron-dense coat around the axoneme of both the midpiece and principal piece of the flagellum (Harding *et al.*, 1995; Ismail and Dehlawi, 1995; Scheltinga *et al.*, 2001). The fibrous sheath of non-passerine birds has been described as an amorphous, irregularly-beaded, filamentous mesh (Baccetti and Afzelius, 1976; Burgess *et al.*, 1991; Jones and Lin, 1993; Lin and Jones, 1993); hence in some species it is said to have transformed into an 'amorphous sheath' (Thurston and Hess, 1987). Rudimentary longitudinal columns and circumferential ribs occur in the ostrich (Soley, 1994), whilst the fibrous sheath of Tinamou and Rhea, the most ancient groups of bird, have semicircular ribs (Asa *et al.*, 1986; Baccetti *et al.*, 1991).

In the current study, the outer dense fibres and fibrous sheath were characterised for a marsupial species and found to be similar to those of eutherian species, namely the laboratory rat. Precisely when marsupials and eutherians, the two largest mammalian groups, diverged from a common ancestor is still open to debate (Woodburne *et al.*, 2003). Nevertheless, the balance of paleontological and morphological data suggests that the split between Metatheria (marsupials plus fossil relatives) and Eutheria (eutherians plus fossil relatives) probably occurred after the beginning of the Cretaceous, approximately 144 million years ago (Luo *et al.*, 2001, 2002; Cifelli and Davis, 2003). Molecular data, however, has yielded conflicting results, with dates for the timing of this split ranging from 163 – 190 million years ago (for review see Cifelli and Davis, 2003). The fact that results of the current study indicate that the method of assembly and composition of the outer dense fibres and fibrous sheath are remarkably similar, if not highly conserved, across marsupials

and eutherians, indicates that these cytoskeletal structures developed prior to the divergence of these two major lineages of extant mammals. In fact, the appearance of the fibrous sheath-like structures in some birds and reptiles indicates that their evolutionary origins are likely much older. It would be interesting to see whether or not the apparent conservation of mammalian ODF2 and GAPDS reported in this thesis is extended across to outer dense fibre and fibrous sheath proteins from sperm of reptiles and non-passerine birds. Regardless of such findings, the sheer presence of these sperm tail cytoskeletal structures in such diverse groups indicates that they have developed to serve a crucial function(s) in sperm.

7.7 CONCLUDING REMARKS

The findings reported in this thesis are the result of the first detailed investigation of the morphogenesis, chemical properties and protein compositions of the outer dense fibres and fibrous sheath from sperm of a marsupial species. Previously, all knowledge of these elements had come from studies on eutherian species, most notably the laboratory rat and mouse. The fact that significant similarities were demonstrated between the outer dense fibres and fibrous sheath of sperm from a marsupial and eutherian species suggests that they developed prior to the divergence of these lineages of extant mammals from a common ancestor and indicates that they play crucial roles in the sperm flagellum. The discovery of possible homologues of the ODF2 and GAPDS eutherian proteins in a marsupial species supports this notion and provides insight into some of the functions of the outer dense fibres and fibrous sheath in marsupial sperm.

It is hoped that the current study will provide the preliminary framework on which to base future investigations of the marsupial sperm tail cytoskeleton. In particular, subsequent

characterisation of the proteins of the outer dense fibres and fibrous sheath at a molecular level will hopefully not only shed definitive light on whether or not homologues of eutherian proteins occur in marsupials, but may also indicate how such proteins are organised within these structures. This information would supplement the expanding pool of molecular data that has been accumulated in recent years for marsupials and aid in our understanding of the evolution of sperm from in this major mammalian group.

Chapter 8

REFERENCES

Afzelius BA (1979) Sperm structure in relation to phylogeny in lower metazoa. In *The Spermatozoon: Maturation, Motility and Surface Properties*. Eds DW Fawcett and JM Bedford, Urban and Schwarzenberg, Baltimore, pp 243-251

Afzelius BA (1988) Microtubules in the spermatids of stick insects. *Journal of Ultrastructure and Molecular Structure Research*. **98**:94-102

Anberg A (1957) The ultrastructure of the human spermatozoon; an electronmicroscopic study of spermatozoa from sperm samples and the epididymis including some observations of the spermatid. *Acta obstetricia et gynecologica Scandinavica* **36**:1-133

Arora KK, Fanciulli M and Pedersen PL (1990) Glucose phosphorylation in tumour cells: cloning, sequencing and overexpression of an active form of a full length cDNA encoding a mitochondrial bindable form of hexokinase. *Journal of Biochemistry* **265**:6481-6488

Asa C, Phillips DM and Stover J (1986) Ultrastructure of spermatozoa of the Crested Tinamou. *Ultrastructure and Molecular Structure Research* **94**:170-175

Aul RB and Oko R (2002) The major subacrosomal occupant of bull spermatozoa is a novel histone H2B variant associated with the forming acrosome during spermiogenesis. *Developmental Biology* **242**:376-387

Baccetti B (1972) Insect sperm cells. *Advances in Insect Physiology* **9**:315-397

Baccetti B (1978) L'evoluzione dello spermatozoo. *Accademia Nazionale dei Lincei* **4**:95-127

Baccetti B (1982) The evolution of the sperm tail. In *Prokaryotic and Eukaryotic Flagella.* Eds WB Amos and JG Duckett, Cambridge University Press, London, pp 521-532

Baccetti B (1984) The human spermatozoon. In *Ultrastructure of reproduction.* Eds J Van Blerkom and PM Motta, Martinus Nijhoff, Boston, pp 110-126

Baccetti B (1986) Evolutionary trends in sperm structure. *Comparative Biochemistry and Physiology* **85**:29-36

Baccetti B and Afzelius BA (1976) The biology of the sperm cell. *Monographs in Developmental Biology* **10**:1-254

Baccetti B, Burrini AG and Falchetti E (1991) Spermatozoa and relationships in Palaeognath birds. *Biology of the Cell* **71**:209-216

Baccetti B, Dallai R, Pallini V, Rosati F and Azfelius BA (1977) Protein of insect sperm mitochondrial crystals. Crystallomitin. *Journal of Cell Biology* **73**:594-600.

Baccetti B, Pallini V and Burrini AG (1973) The accessory fibres of the sperm tail. I. Structure and chemical composition of the bull coarse fibres. *Journal of Submicroscopic Cytology* **5**:237-256

Baccetti B, Pallini V and Burrini AG (1976a) The accessory fibres of the sperm tail. II. Their role in binding zinc in mammals and cephalopods. *Journal of Submicroscopic Cytology* **54**:261-275

Baccetti B, Pallini V and Burrini AG (1976b) The accessory fibres of the sperm tail. I. High-sulphur and low-sulphur components in mammals and cephalopods. *Journal of Submicroscopic Cytology* **57**:289-308

Baltz JM, Williams PO and Cone RA (1990) Dense fibres protect mammalian sperm against damage. *Biology of Reproduction* **43**:485-491

Bawa SR (1963) Outer coarse fibres of the mammalian sperm tail – an electron microscope study. *Journal of Ultrastructure Research* **9**:475-483

Bedford JM (1991) The coevolution of mammalian gametes. In *A comparative overview of mammalian fertilization*. Eds BS Dunbar and MG O'Rand, Plenum Press, New York, pp 3-36

Bedford JM and Calvin HI (1974) Changes in -S-S- linked structures of the sperm tail during epididymal maturation, with comparative observations in sub-mammalian species. *Journal of Experimental Zoology* **187**:181-204

Bedford JM and Hoskins DD (1990). The mammalian spermatozoon: morphology, biochemistry and physiology. In *Marshall's physiology of reproduction*. Ed GE Lamming, Churchill Livingstone, New York, pp 379-568

Bishop MWH and Austin CR (1957) Mammalian spermatozoa. *Endeavour* **16**:137-150

Bishop AL and Hall A (2000) Rho GTPases and their effector proteins. *Journal of Biochemistry* **348**:241-255

Blake JA, Epping JT, Richardson JE and Davisson MT (2000). The mouse genome database (MGD): expanding genetic and genomic resources for the laboratory mouse. *Nucleic Acids Research* **28**:108-111

Bloom W and Fawcett DW (1975) *A textbook of histology 10th Ed.* WB Saunders, London

Bozkurt HH and Holley MC (1995) Identification of a 53-kDa antigen in the fibrous sheath of avian spermatozoa. *Journal of Reproductive Immunology* **29**:149-160

Bradfield JRG (1955) Fibre patterns in animal flagella and cilia. *Symposium of the Society of Experimental Biology* **9**:306-334

Bradley FM, Meth BM and Bellve AR (1981) Structural proteins of the mouse spermatozoan tail: an electrophoretic analysis. *Biology of Reproduction* **24**:691-701

Breed WG, Idriss D and Oko RJ (2000) Protein composition of the ventral processes on the sperm head of Australian hydromyine rodents. *Biology of Reproduction* **63**:629-34

Breed WG and Leigh CM (1988) Morphological observations on sperm-egg interactions during in vivo fertilization in the dasyurid marsupial, *Sminthopsis crassicaudata*. *Gamete Research* **19**:131-149

Breed WG and Leigh CM (1992) Marsupial fertilization: some further ultrastructural observations on the dasyurid, *Sminthopsis crassicaudata*. *Molecular Reproduction and Development* **32**:277-292

Brito M, Figueroa J, Maldanado EU, Vera JC and Burzio LO (1989) The major component of the rat sperm fibrous sheath is a phosphoprotein. *Gamete Research* **22**: 205-217

Brito M, Figueroa J, Vera JC, Cortés P and Hott R (1986) Phosphoproteins are structural components of bull sperm outer dense fiber. *Gamete Research* **15**: 327-336.

Brokaw CJ (1987) Regulation of sperm flagellar motility by calcium and cAMP-dependent phosphorylation. *Journal of Cell Biochemistry* **35**:175-184

Brown PR, Miki K, Harper DB and Eddy EM (2003) A-kinase anchoring protein 4 binding proteins in the fibrous sheath of the sperm flagellum. *Biology of Reproduction* **68**:2241-2248

Bunch DO, Welch JE, Magyar PL, Eddy EM and O'Brien DA (1998) Glyceraldehyde 3-phosphate dehydrogenase-S protein distribution during mouse spermatogenesis. *Biology of Reproduction* **58**:834-841

Burfeind P, Belgardt B, Szpirer C and Hoyer-Fender S (1993) Structure and chromosomal assignment of a gene encoding the major protein of rat sperm outer dense fibers. *European Journal of Biochemistry* **216**:497-505

Burfeind P and Hoyer-Fender S (1991) Sequence and developmental expression of mRNA encoding a putative protein of rat sperm outer dense fibres. *Developmental Biology* **148**:195-204

Burgess SA, Dover SD and Woolley DM (1991) Architecture of the outer arm dynein ATPase in an avian sperm flagellum, with further evidence for the B-link. *Journal of Cell Science* **98**:17-26

Burgos MH and Fawcett DW (1970) Studies on the fine structure of the mammalian testis. I. Differentiation of the spermatids in the cat (*Felis domestica*). *The Journal Of Biophysical and Biochemical Cytology*. **1**:287-300

Burgos MH, Vitale-Calpe R and Aoki A (1970) Fine structure of the testis and its functional significance. In *The testis, volume I, development, anatomy and physiology.* Eds AD Johnson, WR Gomes and NL Vandemark, Academic Press, New York, pp 551-649

Burmester S and Hoyer-Fender S (1996) Transcription and translation of the outer dense fiber gene (odf1) during spermiogenesis in the rat. A study by in situ analysis and polysome fractionation. *Molecular Reproduction and Development* **45**:10-20

Burton KA, Treash-Osio B, Muller CH, Denphy EL and McKnight GS (1999) Deletion of type II alpha regulatory subunit delocalizes protein kinase A in mouse sperm without affecting motility of fertilization. *Journal of Biological Chemistry* **272**:24131-24136

Calvin HI (1975) Keratinoid proteins in the heads and tails of mammalian spermatozoa. In *Biology of the male gamete*. Eds JG Duckett and PA Racy, Academic Press, London, pp 257-273

Calvin HI (1976) Isolation and subfractionation of mammalian sperm heads and tails. In *Methods of cell biology, volume XIII*. Ed DM Prescott, Academic Press, New York, pp 85-104

Calvin HI (1979) Isolation of stable structures from rat spermatozoa. In *The spermatozoon*. Eds DW Fawcett and JM Bedford, Urban and Schwarzenberg, Baltimore, pp 387-390

Calvin HI and Bedford JM (1971) Formation of disulphide bonds in the nucleus and accessory structures of mammalian spermatozoa during epididymal maturation. *Journal of Reproduction and Fertility (Supplement)* **13**:65-75

Calvin HI and Bleau G (1974) Zinc-thiol complexes in keratin-like structures of rat spermatozoa. *Experimental Cell Research* **86**:280-284

Calvin HI, Hwang FH and Wohlrab H (1975) Localisation of zinc in a dense fiber-connecting piece fraction of rat sperm tails analogous chemically to hair keratin. *Biology of Reproduction* **13**:228-239

Carr DW, Fujita A, Stentz CL, Liberty GA, Olson GE and Narumiya S (2001) Identification of sperm-specific proteins that interact with A-kinase anchoring proteins in a manner similar to the type II regulatory subunit of PKA. *Journal of Biological Chemistry* **276**:17332-17338

Carrera A, Gerton GL and Moss SB (1994) The major fibrous sheath polypeptide of mouse sperm: structural and functional similarities to the A-kinase anchoring protein. *Developmental Biology* **165**:272-284

Carrera A, Moss J, Ning XP, Gerton GL, Kopf GS and Moss SB (1996) Regulation of protein tyrosine phosphorylation in human sperm by a calcium/calmodium-dependent mechanism: identification of A kinase anchor proteins as major substrates for tyrosine phosphorylation. *Developmental Biology* **180**:284-296

Catalano RD, Hillhouse EW and Vlad M (2001) Developmental expression and characterization of FS39, a testis complementary DNA encoding an intermediate filament-related protein of the sperm fibrous sheath. *Biology of Reproduction* **65**:277-287

Catalano RD, Vlad M and Kennedy RC (1997) Differential display to identify and isolate novel genes expressed during spermatogenesis. *Molecular Human Reproduction* **3**:215-221

Challice CE (1952) Some observations on the morphology of spermatozoa by electron microscopy. *Proceedings of the Society for the Study of Fertility* **4**:21-26

Chemes HE, Brugo S, Zanchetti F and Carrere C (1987) Dysplasia of the fibrous sheath: an ultrastructure defect of human spermatozoa associated with sperm immotility and primary sterility. *Fertility and Sterility* **48**:664-669

Cifelli RL and Davis BM (2003) Marsupial origins. *Science* **302**:1899-1900

Cleland KW and Rothschild FRS (1959) The bandicoot spermatozoon: an electron microscope study of the tail. *Proceedings of the Royal Society of London* **150**:24-42

Clermont Y and Harvey SC (1965) Duration of the cycle of the seminiferous epithelium of normal, hypophysectomized and hypophysectomized-hormone treated albino rats. *Endocrinology* **76**:80-89

Clermont Y, Oko R and Hermo L (1990) Immunocytochemical localization of proteins utilized in the formation of outer dense fibres and fibrous sheath in rat spermatids: an electron microscope study. *The Anatomical Record* **227**:447-457

Clermont Y and Percy B (1957) The stages of the cycle of the seminiferous epithelium of the rat: practical definitions in PA-Schiff-hematoxylin and hematoxylin-eosin stained sections. *Revue Canadienne de Biologie* **16**:451-462

Clermont Y and Rambourg A (1978) Evolution of the endoplasmic reticulum during rat spermiogenesis. *American Journal of Anatomy* **151**:191-212

Clulow J, Jones RC and Murdoch RN (1992) Maturation and regulation of the motility of spermatozoa in the epididymis of the tammar wallaby (*Macropus eugenii*). *Journal of Reproduction and Fertility* **94**:295-303

Colledge M and Scott JD (1999) AKAPs: from structure to function. *Trends in Cell Biology* **9**:216-221

Courtens JL, Courot M and Flechon JE (1976) The perinuclear substrate of boar, bull, ram and rabbit spermatozoa. *Journal of Ultrastructure Research* **57**:54-64

Cummins JM (1976) Epididymal maturation of spermatozoa in the Marsupial Trichosurus vulpecula: Changes in motility and gross morphology. *Australian Journal of Zoology* **24**:449-511

Cummins JM and Woodall PF (1985) On mammalian sperm dimensions. *Journal of Reproduction and Fertility* **75**:153-175

Curry MR and Watson PF (1995) Sperm structure and function. In *Gametes: The spermatozoon.* Eds JG Grudzinskas and JL Yovich. Cambridge University Press, Cambridge, pp 45-69

de Krester DM (1969) Ultrastructural features of human spermiogenesis. *Zeitschriff für Zellforschung und mikroskopische Anatomie* **98**:477-505

Delmas V, van der Hoorn F, Mellstrom B, Jegou B and Sassone-Corsi P (1993) Induction of CREM activator proteins in spermatids: down-stream targets and

implications for haploid germ cell differentiation. *Molecular Endocrinology* **7**:1502-1514

Diekman AB, Olson G and Goldberg E (1998) Expression of the human antigen SPAG2 in the testis and localization to the outer dense fibers in spermatozoa. *Molecular Reproduction and Development* **50**:284-93

Dooher GB and Bennett D (1973) Fine structural observations on the development of the sperm head in the mouse. *American Journal of Anatomy* **136**:339-362

Eddy EM and O'Brien DA (1994) The spermatozoon. In *The physiology of reproduction*. Eds E Knobil and JD Neill, Raven Press, New York, pp 29-77

Eddy EM, O'Brien DA, Fenderson BA and Welch JE (1991) Intermediate filament-like proteins in the fibrous sheath of the mouse sperm flagellum. *Annals of the New York Academy of Sciences* **637**:224-239

Eddy EM, Toshimori K and O'Brien DA (2003) Fibrous sheath of mammalian spermatozoa. *Microscopy Research and Technique* **61**:103-115

Eddy EM, Welch JE, Mori C, Fulcher KD and O'Brien DA (1994) Role and regulation of spermatogenic cell-specific gene expression: enzymes of glycolysis. In *Function of somatic cells in the testis*. Ed A Bartke, Springer, New York, pp 362-372

Edelman GM and Millette CF (1971) Molecular probes of spermatozoan structures. *Proceedings of the National Academy of Sciences USA* **68**:2436-2440

Einarsson S and Nicander L (1968) Fine structure of the fibrous sheath of stallion sperm tails. *Journal of Reproduction and Fertility* **16**:295-296

El-Alfy M, Moshonas D, Morales CR and Oko R (1999) Molecular cloning and developmental expression of the major fibrous sheath protein (FS 75) of rat sperm. *Journal of Andrology* **20**:307-318

Escalier D, Gallo JM and Schrevel J (1997) Immunocytochemical characterisation of a human sperm fibrous sheath protein, its developmental expression pattern, and morphogenetic relationships with Aactin. *The Journal of Histochemistry and Cytochemistry* **45**: 909-922

Espevik T and Elgsaeter A (1978) A freeze-etch study of dense fibres in rat spermatozoa. *Journal or Reproduction and Fertility* **54**:203-204

Farrell KW (1982) Purification and reassembly of tubulin from outer doublet microtubules. *Methods in Cell Biology* **24**:61-78

Fawcett DW (1970) A comparative view of sperm ultrastructure. *Biology of Reproduction (Supplement 2)* **2**:90-127

Fawcett DW (1975) The mammalian spermatozoon. *Developmental Biology* **44**:394-436

Fawcett DW, Anderson WA and Phillips DM (1971) Morphogenetic factors influencing the shape of the sperm head. *Developmental Biology* **26**:220-251

Fawcett DW and Phillips DM (1969) The fine structure and development of the neck region of the mammalian spermatozoon. *The Anatomical Record* **165**:153-184

Fenderson BA, Toshimor K, Muller CH, Lane TF and Eddy EM (1988) Identification of a protein in the fibrous sheath of the sperm flagellum. *Biology of Reproduction* **38**:345-357

Franke W, Grund WC and Scmid E (1979) Intermediate filament proteins present in Sertoli cells are of vimentin type. *European Journal of Cell Biology* **19**:269-275

Franzen A (1956) On spermiogenesis, morphology of the spermatozoon, and biology of fertilization among invertebrates. *Zoologiska Bidrag fran Uppsala* **31**:355-482

Fraser LR and Quinn PJ (1981) A glycolytic product is obligatory for initiation of the sperm acrosome reaction and whiplash motility required for fertilization in the mouse. *Journal of Reproduction and Fertility* **61**:25-35

Fujita FA, Nakamura K, Kato T, Watanabe N, Ishizaki T, Kimura K, Mizoguchi A and Narumiya S (2000) Ropporin, a sperm-specific binding protein of rhophilin, that is localized in the fibrous sheath of sperm flagella. *Journal of Cell Science* **113**:103-12

Fulcher KD, Mori C, Welch JE, O'Brien DA, Klapper DG and Eddy EM (1995a) Characterization of Fsc1 cDNA for a mouse sperm fibrous sheath component. *Biology of Reproduction* **52**:41-49

Fulcher KD, Welch JE, Klapper DG, O'Brien DA and Eddy EM (1995b) Identification of a unique μ-class glutathione S-transferase in mouse spermatogenic cells. *Molecular Reproduction and Development* **42**:415-424

Gagnon C (1995) Regulation of sperm motility at the axonemal level. *Reproduction, Fertility and Development* **7**:847-855

Gardner PJ (1966) Fine structure of the seminiferous tubule of the Swiss mouse. The spermatid. *The Anatomical Record* **155**:235-249

Gardner PJ and Holyoke EA (1964) Fine structure of the seminiferous tubule of the swiss mouse. I. The limiting membrane, Sertoli cell, spermatogonia, and spermatocytes. *The Anatomical Record* **150**:391-404

Gastmann C, Burfeind P, Günther E, Hameister H, Szpirer C and Hoyer-Fender S (1993) Sequence, expression, and chromosomal assignment of a human sperm outer dense fiber gene. *Molecular Reproduction and Development* **36**:407-418

Gibbons IR (1981) Cilia and flagella of eukaryotes. *Journal of Cell Biology* (Supplement) **91**:107-124

Gibbons IR (1989) Microtubule-based motility: an overview of a fast moving field. In *Cell movement, volume 1, the dynein ATPase*. Eds FD Warner, P Satir and IR Gibbons, Alan and Liss, New York, pp 3-22

Gibbons BH and Gibbons IR (1973) The effect of partial extraction of dynein arms on the movement of reactivated sea urchin sperm. *Journal of Cell Science* **13**:337-357

Glover JN and Harrison SC (1995) Crystal structure of the heterodimeric bZIP transcription factor c-Fos-c-Jun bound to DNA. *Nature* **373**:257-261

Gordon M and Bensch KG (1968) Cytochemical differentiation of the guinea pig sperm flagellum with phosphotungstic acid. *Journal of Ultrastructure Research* **24**:33-50

Griffin LD, Geib BD, Wheeler DA, Davision D, Adams V and McCabe ERB (1991) Mammalian hexokinase 1: evolutionary conservation and structure to function analysis. *Genomics* **11**:1014-1024

Grootengoed JA and Den Boer PJ (1989) Energy metabolism of spermatids: a review. In *Cellular and molecular events in spermiogenesis as targets for fertility regulation.* Eds DW Hamilton and GMH Waites. Cambridge University Press, Cambridge, pp 193-215

Grootegoed JA, Jansen R and van der Molen HJ (1986) Effect of glucose on ATP dephosphorylation in rat spermatids. *Journal of Reproduction and Fertility* **77**:99-107

Guraya SS (1971) Comparative histochemical observations on the contributions of the acrosomal vesicle and granule to the acrosomal cap in the spermatozoon of mammals. *Zeitschrift zelltorsch* **114**:321-330

Haidl G (1993) Outer dense fibres: functional or structural elements? *Andrologia* **25**:13-17

Haidl G and Becker A (1991) Elektronenmikroskopische befunde an menschlichen spermatozoen mit flagellumdefekten. *Hautarzt* **42**:242-246

Haidl G, Becker A and Henkel R (1991) Poor development of the outer dense fibres as a major cause of tail abnormalities in the spermatozoa of astherotertozoospermic men. *Human Reproduction* **6**:1431-1438

Harding HR (1977) Reproduction in male marsupials: a critique, with additional observations on sperm development and ultrastructure. PhD Thesis. The University of New South Wales, Australia

Harding HR, Aplin KP and Mazur M (1995) Ultrastructure of spermatozoa of Australian blindsnakes, Ramphotyphlops spp. (Typhlopidae, Squamata): First observations on the mature spermatozoon of Scolecophidian snakes. In *Advances in spermatozoal phylogeny and taxonomy*, Eds BG Jamieson, J Ausio and J-L Justine, *Memoires Du Museum National D'Histoire Naturelle* **166**: 385-396

Harding HR, Carrick FN and Shorey CD (1975) Ultrastructural changes in spermatozoa of the brush-tailed possum, *Trichosurus vulpecula* (Marsupialia), during epididymal transit. Part I: The flagellum. *Cell Tissue Research* **164**:121-132

Harding HR, Carrick FN and Shorey CD (1976a) Ultrastructural changes in spermatozoa of the brush-tailed possum, *Trichosurus vulpecula* (Marsupialia), during epididymal transit. Part II: The acrosome. *Cell and Tissue Research* **171**:61-73

Harding HR, Carrick FN and Shorey CD (1976b) Spermiogenesis in the brush-tailed possum, *Trichosurus vulpecula* (Marsupialia). The development of the acrosome. *Cell and Tissue Research* **171**:75-90

Harding HR, Carrick FN and Shorey CD (1979) Special features of sperm structure and function in marsupials. In *The spermatozoon*. Eds DW Fawcett and JM Bedford, Urban and Schwarzenberg, Baltimore, pp 289-303

Harding HR, Carrick FN and Shorey CD (1984) Sperm ultrastructure and development in the honey possum, Tarsipes rostratus. In *Possums and gliders*. Eds AP Smith and ID Hume, Australian Mammal Society and Surrey Beatty and Sons, Sydney, pp451-461

Harding HR, Carrick FN and Shorey CD (1987) The affinities of the koala *Phascolarctus cinerus* (Marsupialia: Phascolarctidae) on the basis of sperm ultrastructure and development. In *Possums and opossums: studies in evolution*, Ed M Archer, Surrey, Beatty and Royal Zoological Society of New South Wales, Sydney, pp 353-364

Harding HR, Woolley PA, Shorey CD and Carrick FN (1982) Sperm ultrastructure, spermiogenesis and epididymal sperm maturation in dasyurid marsupials: phylogenetic implications. In *Carnivorous marsupials*, pp 659-673, Ed M Archer, Royal Zoological Society of New South Wales, Sydney

Harris MS and Rodger JC (1998) Characterisation of fibrous sheath and midpiece fibre network polypeptides of marsupial spermatozoa with a monoclonal antibody. *Molecular Reproduction and Development* **50**:461-473

Hayes JD and Pulford DJ (1995) The glutathione S-transferase supergene family: regulation of GST and the contribution of the isoenzymes to cancer chemoprotection and drug resistance. *Critical Reviews in Biochemistry and Molecular Biology* **30**:445-600

Hecht NB (1987) Gene expression during spermatogeneis. *Annals of the New York Academy of Sciences* **513**:90-101

Henkel R, Stalf T, Mertens N, Miska W and Schill WB (1994) Outer dense fibres of human spermatozoa: partial characterization and possible physiological functions. *International Journal of Andrology* **17**:68-73

Henkel R, Stalf T and Miska W (1992) Isolation and partial characterization of the outer dense fibre proteins from human spermatozoa. *Journal of Biological Chemistry* **373**:685-689

Higgy NA, Pastoor T, Renz C, Tarnasky HA and van der Hoorn FA (1994) Testis-specific RT7 protein localises to the sperm tail and associates with itself. *Biology of Reproduction* **50**:1357-1366

Hinsch E, Boehm JG, Groeger S, Muller-Schloesser and Hinsch K-D (2003) Identification of cytokeratins in bovine sperm outer dense fibre fractions. *Reproduction in Domestic Animals* **38**:155-160

Hofferbert S, Burfeind P, Hoyer-Fender S, Lange R, Haidl G and Engel W (1993) A homozygous deletion of 27 base pairs in the coding region of the human outer dense fibre protein gene does not result in a pathologic phenotype. *Human Molecular Genetics* **2**:2167-2170

Holstein AFC and Roosen-Runge EC (1981) *Atlas of human spermatogeneis*. Grosse Verlag, Berlin

Hoppe PC (1976) Glucose requirement for mouse sperm capacitation in vitro. *Gamete Research* **15**:39-45

Horowitz JM, Toeg H and Orr GA (1984) Characterization and localization of cAMP-dependent protein kinases in rat caudal epididymal sperm. *Journal of Biological Chemistry* **259**:832-838

Hoshi K, Tsukikawa S and Sato A (1991) Importance of Ca2+, K+ and glucose in the medium for sperm penetration through the human zona pellucida. *Tohoku Journal of Experimental Medicine* **165**:99-104

Hoyer-Fender S, Burfeind P and Hameister H (1995) Sequence of mouse Odf1 cDNA and its chromosomal localization: extension of the lineage group between human chromosome 8 and mouse chromosome 15. *Cytogenetics and Cell Genetics* **70**:200-204

Huang B, Piperno G and Luck D (1979) Paralysed flagella mutants of Chlamydomonas reinhardtie: defective for axonemal doublet microtubule arms. *Journal of Biochemistry* **254**:3091-3099

Hughes RL (1965) Comparative morphology of spermatozoa from five marsupial families. *Australian Journal of Zoology* **13**:533-543

Irons MJ and Clermont Y (1982a) Formation of the outer dense fibres during spermiogenesis in the rat. *The Anatomical Record* **202**:463-471

Irons MJ and Clermont Y (1982b) Kinetics of fibrous sheath formation in the rat spermatid. *American Journal of Anatomy* **165**:121-130

Ishmail MF and Dehlawi GY (1995) Ultrastructure of spermiogenesis of Saudian reptiles. Sperm tail differentiation in *Stenodacetylus selvini*. *Journal of Environmental Sciences* **10**:97-106

Jassim A (1990) GDA-J/F7 monoclonal antibody: a new marker for sperm cell precursors in human semen. *Journal of Reproductive Immunology* **18**:123-137

Jassim A (1991) AJ-p97: a novel antigen of the human sperm tail fibrous sheath detected by a neurofilament monoclonal antibody. *Journal of Reproductive Immunology* **20**:15-26

Jassim A (1994) AJ-FS9 monoclonal antibody detects masked antigens within the human sperm tail fibrous sheath. *Human Reproduction* **9**:1836-1844

Jassim A (1995) Molecular and ontogenic analysis of the human sperm tail fibrous sheath. In *Advances in spermatozoal phylogeny and taxonomy*. Eds BG Jamieson, J Ausio and J-L Justine, Mémoires Du Muséum National D'Histoire Naturelle, Paris,**166**:431-436

Jassim A, al-Zuhdi Y and Gray A (1993a) Antigenic determinants of human sperm tail fibrous sheath proteins. *Journal of Reproductive Immunology* **23**:281-295

Jassim A, Auger D, Oliver T and Sachs J (1990) GDA-J/F3 Monoclonal antibody as a novel probe for the human sperm tail fibrous sheath and its anomalies. *Human Reproduction* **5**:990-996

Jassim A and Bottazzo GF (1994) The target antigen for GDA-J/F3 monoclonal antibody in the human sperm tail fibrous sheath is a non-collagenous asialo-glycoprotein: implications and significance. *Human Reproduction* **9**:1452-1458

Jassim A and Chen YL (1994) AJ-FS1 monoclonal antibody detects a novel group of non-glycosylated antigens within the human sperm tail fibrous sheath. *Human Reproduction* **9**:1459-1465

Jassim A, Foxon R, Purkis P, Gray A and al-Zuhdi Y (1993b) AJ-p90: a novel protein of the perinuclear theca in human sperm subacrosome. *Journal of Reproductive Immunology* **23**:169-188

Jassim A, Gillot DJ and Al-Zuhdi Y (1991a) Human sperm tail fibrous sheath undergoes phosphorylation during its development. *Human Reproduction* **6**:1135-1142

Jassim A, Gillot DJ, Al-Zuhdi Y, Gray A, Foxton R and Bottazzo GF (1992) Isolation and biochemical characterization of the human sperm tail fibrous sheath. *Human Reproduction* **7**:86-94

Jassim A, Schofield O, Whitehead P, Purkis P, Heagerty AH, Sachs JA, Eady RA and Leigh IM (1991b) Detection of a novel basement membrane antigen by GDA-J/F3 anti-human sperm fibrous sheath monoclonal antibody. *British Journal of Dermatology* **125**:101-107

Johnson LR, Foster JA, Haig-Ladewig L, VanScoy H, Rubin C, Moss SB and Gerton GB (1997) Assembly of AKAP82, a protein kinase A anchor protein, into the fibrous sheath of mouse sperm. *Developmental Biology* **192**:340-350

Jones RC, Hinds LA and Tyndale-Biscoe CH (1984) Ultrastructure of the epididymis of the tammar, *Macropus eugenii*, and its relationship to sperm maturation. *Cell and Tissue Research.* **237**:525-35

Jones RC and Lin M (1993) Spermatogenesis in birds. *Oxford Review of Reproductive Biology* **15**:233-264

Jones RC and Murdoch RN (1996) Regulation of the motility and metabolism of spermatozoa for storage in the epididymis of eutherian and marsupial mammals. *Reproduction, Fertility and Development* **8**:553-68

Jutte NH, Jansen R, Grootegoed JA, Rommerts FF and van der Molen HJ (1983) FSH stimulation of the production of pyruvate and lactate by rat Sertoli cells may be involved in hormonal regulation of spermatogenesis. *Journal of Reproduction and Fertility* **68**:219-226

Kadlubowski M, Hughes RA, Gregson NA. (1980) Experimental allergic neuritis in the Lewis rat: characterization of the activity of peripheral myelin and its major basic protein, P2. *Brain Research* **184**:439-454

Kierszenbaum AL, Rivkin E, Fefer-Sadler S, Mertz JR and Tres LL (1996) Purification, partial characterisation and localisation of Sak57, an acidic intermediate filament keratin present in rat spermatocytes, spermatids, and sperm. *Molecular Reproduction and Development* **44**:382-394

Kim JW, Harding HR and Shorey CD (1987) Electron-microscopic studies on the spermiogenesis and spermatozoa of the allied rock wallaby (*Petrogale assimilis*). *Korean Journal of Electron Microscopy* **17**:1-15

Kim YH, Adham IM, Haack T, Kremling H and Engel W (1995a) Molecular cloning and characterisation of the bovine and porcine outer dense fibers cDNA and organization of the bovine gene. *Journal of Biological Chemistry* **376**:431-435

Kim YH, deKrester DM, Temple-Smith PD, Hearn MTW and McFarlane JR (1997) Isolation and characterization of human and rabbit sperm tail fibrous sheath. *Molecular Human Reproduction* **3**:307-313

Kim YH, McFarlane JR, Almahbobi G, Stanton PG, Temple-Smith PD and deKrester DM (1995b) Isolation and partial characterization of rat sperm tail fibrous sheath proteins and comparison with rabbit and human spermatozoa using a polyclonal antiserum. *Journal of Reproduction and Fertility* **104**:107-114

Kim YH, McFarlane JR, O'Bryan MK, Almahbobi G, Temple-Smith PD and deKrester DM (1999) Isolation and characterization of rat sperm tail outer dense fibres and comparison with rabbit and human spermatozoa using a polyclonal antiserum. *Journal of Reproduction and Fertility* **116**:345-353

Kuhn R, Schäfer U and Schäfer M (1988) Cis-acting regions sufficient for spermatocyte-specific transcriptional and spermatid-specific translational control of the *Drosphila melanogaster* gene mst(3)gl-9. *EMBO Journal* **7**:447-454

Lalli M and Clermont Y (1981) Structural changes of the head components of the rat spermatid during late spermiogenesis. *American Journal of Anatomy* **160**:419-434

Leblond CP and Clermont Y (1952a) Definition of the stages of the cycle of the seminiferous epithelium in the rat. *Annals of the New York Academy of Science* **55**:548-573

Leblond CP and Clermont Y (1952b) Spermiogenesis of rat, mouse, hamster, and guinea pig as revealed by the 'periodic acid-fuchsin sulfurous acid' technique. *The American Journal of Anatomy* **90**:167-215

Lewin B (1997) *Genes VI*. Oxford University Press, New York

Lewis B and Aitken RJ (2001) Impact of epididymal maturation on the tyrosine phosphorylation patterns exhibited by rat spermatozoa. *Biology of Reproduction* **64**:1545-1556

Lin M, Harman A and Fletcher TP (2004) Cycle of the seminiferous epithelium in a marsupial species, the brushtail possum (*Trichosurus vulpecula*), an estimation of its duration. *Reproduction, Fertility and Development* **16**:307-313

Lin M, Harman A and Rodger JC (1997) Spermiogenesis and spermiation in a marsupial, the tammar wallaby (*Macropus eugenii*). *Journal of Anatomy* **190**:377-395

Lin M and Jones RC (1993) Spermiogenesis and spermiation in the Japanese quail (*Coturnix coturnix japonica*). *Journal of Anatomy* **183**:525-35

Lin M and Jones RC (2000) Spermiogenesis and spermiation in a monotreme mammal, the platypus, *Ornithorhynchus anatinus*. *Journal of Anatomy* **196**:217-232

Lin M, Zhang X, Murdoch R and Aitken RJ (2000) In vitro culture of brushtail possum (*Trichosurus vulpecula*) epididymal epithelium and induction of epididymal sperm maturation in co-culture. *Journal of Reproduction and Fertility* **119**:1-14

Lin M, Zhang X, Wade M, Harris M and Nickel M (1998) Isolation of proteins from subacrosomal region of spermatozoa from a marsupial, the tammar wallaby (*Macropus eugenii*). *Journal of Reproduction and Fertility* **113**:257-267

Lin RY, Moss SB and Rubin CS (1995) Characterization of S-AKAP, a novel developmentally regulated A kinase anchoring protein of male germ cells. *Journal of Biological Chemistry* **270**:27804-27811

Lindemann CB (1996) Functional significance of the outer dense fibers of mammalian sperm examined by computer simulations with the geometric clutch model. *Cell Motility and the Cytoskeleton* **34**:258-270

Lindemann CB, Fentie I and Rikmenspoel R (1980) A selective effect of Ni2+ on wave initiation in bull sperm flagella. *Journal of Cell Biology* **87**:420-426

Lindemann CB and Kanous KS (1989) Regulation of mammalian sperm motility. *Archives of Andrology* **23**:1-22

Lindemann CB, Orlando A and Kanous KS (1992) The flagellar beat of rat sperm is organized by the interaction of two functionally distinct populations of dynein bridges with a stable central axonemal partition. *Journal of Cell Science* **102**:249-260

Long CR, Duncan RP and Rabl JM (1997) Isolation and characterisation of MPM-2 reactive sperm proteins: homology to components of the outer dense fibers and segmented columns. *Biology of Reproduction* **57**:246-254

Longo FJ, Krohne G and Franke WW (1987) Basic proteins of the perinuclear theca of mammalian spermatozoa and spermatids. A novel class of cytoskeletal elements. *Journal of Cell Biology* **105**:1105-1120

Luo, ZX, Cifelli RC and Kielan-Jaworowska Z (2001) Dual evolution of tribosphenic mammals. *Nature* **409**:53-57

Luo, ZX, Kielan-Jaworowska Z and Cifelli RL (2002) In quest for a phylogeny of mesozoic mammals. *Acta Palaeontologica Polonica* **47**:1-78

Lupas A, Van Dyke M and Stock J (1991) Predicting coiled coils from protein sequences. *Science* **252**:1162-1164

Mackenbach P, Den Boer PJ and Jong JW (1990) Effects of glucose and adenosine on the ATP content of hamster spermatids. *Reproduction, Fertility and Development* **2**:145-152

Mahadevan MM, Miller MM and Moutos DM (1997) Absence of glucose decreases human fertilization and sperm movement characteristics in vitro. *Human Reproduction* **12**:119-123

Mandal A, Naaby-Hansen S, Wolkowicz MJ, Klotz K, Shetty J, Retief JD, Coonrod SA, Kinter M, Sherman N, Cesar F, Flickinger CJ and Herr JC (1999) FSP95, a testis-specific 95-kilodalton fibrous sheath antigen that undergoes tyrosine phosphorylation in capacitated human spermatozoa. *Biology of Reproduction* **61**:1184-1197

Mate KE and Rodger JC (1991) Stability of the acrosome of the brush-tailed possum (*Trichosurus vulpecula*) and tammar wallaby (*Macropus eugenii*) in vitro and after exposure to conditions and agents known to cause capacitation or acrosome reaction of eutherian spermatozoa. *Journal of Reproduction and Fertility* **91**:41-48

Mei X, Singh IS, Erlichman J and Orr GA (1997) Cloning and characterization of a testis-specific, developmentally regulated A-kinase-anchoring protein (TAKAP-80) present on the fibrous sheath of rat sperm. *European Journal of Biochemistry* **246**:425-432

Miki K and Eddy EM (1998) Identification of tethering domains for protein kinase A type I alpha regulatory subunits on sperm fibrous sheath protein Fsc1. *Journal of Biological Chemistry* **273**:34384-34390

Miki K and Eddy EM (1999) Single amino acids determine specificity of binding of protein kinase A regulatory subunits by protein kinase A anchoring proteins. *Journal of Biological Chemistry* **274**:29057-29062

Miki K, Willis WD, Brown PR, Goulding EH, Fulcher KD and Eddy EM (2002) Targeted disruption of the Akap4 gene causes defects in sperm flagellum and motility. *Developmental Biology* **15**:331-342

Millette CF, Spear PG, Gall WE and Edelman GM (1973) Chemical dissection of mammalian spermatozoa. *The Journal of Cell Biology* **58**:662-675

Miranda-Vizuete A, Tsang K, Yu Y, Jimenez A, Pelto-Huikko M, Flickinger CJ, Sutovsky P and Oko R (2003) Cloning and development analysis of murid

spermatid-specific thiredoxin-2 (SPTRX-2), a novel sperm fibrous sheath protein and autoantigen. *The Journal of Biological Chemistry* **278**:44874-44885

Mita M and Hall PF (1982) Metabolism of round spermatids from rats: lactate as the preferred substrate. *Biology of Reproduction* **26**:445-455

Monesi V, Geremia A, D'Agostino D and Boitoni C (1978) Biochemistry of male germ cell differentiation in mammals: RNA synthesis in meiotic and postmeiotic cells. *Current Topics in Developmental Biology* **12**:11-36

Moore HD and Taggart DA (1995) Sperm pairing in the opossum increases the efficiency of sperm movement in a viscous environment. *Biology of Reproduction* **52**:947-53

Morales CR, Oko R and Clermont Y (1994) Molecular cloning and developmental expression of an mRNA encoding the 27 kDa outer dense fibre protein of rat spermatozoa. *Molecular Reproduction and Development* **37**:229-240

Mori C, Nakamura N, Welch JE, Gotoh H, Goulding EH, Fajioka M and Eddy EM (1998) Mouse spermatogenic-cell specific type 1 hexokinase (mHk1-s) transcripts are expressed by alternative splicing from the mHk1 gene and the HK1-S protein is localized mainly in the sperm tail. *Molecular Reproduction and Development* **49**:374-385

Mori C, Welch JE, Fulcher KD, O'Brien DA and Eddy EM (1993) Unique hexokinase messenger ribonucleic acids lacking the porin-binding domain are developmentally expressed in mouse spermatogenic cells. *Biology of Reproduction* **49**:191-203

Mori C, Welch JE, Sakai Y and Eddy EM (1992) In situ localization of spermatogenic cell-specific glyceraldehyde 3-phosphate dehydrogenase (Gapd-s) messenger ribonucleic acid in mice. *Biology of Reproduction* **46**:859-868

Moss SB, Turner RMO, Burkert KL, Vanscoy H and Gerton GL (1999) Conservation and function of a bovine sperm A-kinase anchor protein homologous to mouse AKAP82. *Biology of Reproduction* **61**:335-342

Mujica A, Moreno-Rodriguez R, Naciff J, Neri L and Tash JS (1991) Glucose regulation of guinea-pig sperm motility. *Journal of Reproduction and Fertility* **92**:75-87

Murdoch RN and Jones RC (1998) The metabolic properties of spermatozoa from the epididymis of the tammar wallaby, *Macropus eugenii*. *Molecular Reproduction and Development* **49**:92-99

Nakamura K, Fujita A, Murata T, Watanabe G, Mori C, Fujita J, Watanabe N, Ishizaki T, Yoshida O and Narumiya S (1999) Rhophilin, a small GTPase Rho-binding protein, is abundantly expressed in the mouse testis and localized in the principal piece of the sperm tail. *Federation of European Biochemical Societies Letters* **445**:9-13

Nakamura M, Fujiwara A, Yasamasu I, Okinaga S and Arai K (1982) Regulation of glucose metabolism by adenine nucleotides in round spermatids from rat testes. *Journal of Biological Chemistry* **257**:13945-13950

Nakamura M, Hino A, Yasumasu I and Kato J (1981) Stimulation of protein synthesis in round spermatids from rat testes by lactate. *Journal of Biochemistry* **89**:1309-1315

Nakamura M, Okinaga S and Arai K (1986) Studies of metabolism of round spermatids: glucose as unfavourable substrate. *Biology of Reproduction* **35**:927-935

Nakamura Y, Tanaka H, Koga M, Miyagawa Y, Iguchi N, de Carvalho CE, Yomogida K, Nozaki M, Nojima H, Matsumiya K, Okuyama A and Nishimune Y (2002) Molecular cloning and characterization of oppo 1: a haploid germ germ cell-specific complementary DNA encoding sperm tail protein. *Biology of Reproduction* **67**:1-7

Nelson L (1958) Cytochemical studies with the electron microscope. I. Adenosine triphosphate in rat spermatozoa. *Biochemica et Biophysica Acta* **27**:634-641

Nelson L (1962) Cytochemical aspects of spermatozoan motility. In *Spermatozoan motility*. Ed DW Bishop, American Association for the Advancement of Science, Washington, pp 171-187

Nicander L (1962) Development of the fibrous sheath of the mammalian sperm tail. *Proceedings of the 5th International Conference for Electron Microscopy*, M4

Nicander L (1970) Comparative studies on the fine structure of vertebrate spermatozoa. In *Comparative Spermatology*. Ed B Baccetti, Academic Press, New York, pp 47-56

Nicander L and Bane A (1962) New observations on the fine structure of spermatozoa. *International Journal of Fertility* **7**:339-344

Nicander L and Bane A (1966) Fine structure of the sperm head in some mammals with particular reference to the acrosome and the subacrosomal substance. *Zeitscrift fur Zellforschung und Mikroskopische Anatomie* **72**:496-515

O'Bryan MK, Loveland KL, Herszfeld D, McFarlane JR, Hearn MTW and de Krester DM (1998) Identification of a rat testis-specific gene encoding a potential rat outer dense fiber protein. *Molecular Reproduction and Development* **50**:313-322

O'Bryan MK, Sebire K, Meinhardt A, Edgar K, Keah HH, Hearn MT and de Kretser DM (2001) Tpx-1 is a component of the outer dense fibers and acrosome of rat spermatozoa. *Molecular Reproduction and Development* **58**:116-125

Ochs D, Wolf DP and Ochs RL (1986) Intermediate filaments in human sperm heads. *Experimental Cell Research* **167**:495-504

Oko R (1988) Comparative analysis of proteins from the fibrous sheath and outer dense fibres of rat spermatozoa. *Biology of Reproduction* **39**:169-182

Oko R (1995) Developmental expression and possible role of perinuclear theca proteins in mammalian spermatozoa. *Reproduction Fertility and Development* **7**:777-797

Oko R and Clermont Y (1988) Isolation, structure and protein composition of the perforatorium of rat spermatozoa. *Biology of Reproduction* **39**:673-687

Oko R and Clermont Y (1989) Light microscopic immunocytochemical study of fibrous sheath and outer dense fibre formation in the rat spermatid. *The Anatomical Record* **225**:46-55

Oko R and Maravei D (1994) Protein composition of the perinuclear theca of bull spermatozoa. *Biology of Reproduction* **50**:1000-1014

Oko R and Morales CR (1994) A novel testicular protein, with sequence similarities to a family of lipid binding proteins, is a major component of the rat sperm perinuclear theca. *Developmental Biology* **166**:235-245

Olmedo SB, Nodar F, Chillik C and Chemes HE (1997) Successful intracytoplasmic sperm injection with spermatozoa from a patient with dysplasia of the fibrous sheath and chronic respiratory disease. *Human Reproduction* **12**:1497-1499

Olson GE (1980) Changes in intramembranous particle distribution in the plasma membrane of *Didelphis virginiana* spermatozoa during maturation in the epididymis. *The Anatomical Record* **197**:471-488

Olson GE, Hamilton DW and Fawcett DW (1976) Isolation and characterization of the fibrous sheaths of rat epididymal spermatozoa. *Biology of Reproduction* **14**:517-530

Olson GE, Lifsics M, Fawcett DW and Hamilton DW (1977) Structural specializations in the flagellar plasma membrane of opossum spermatozoa. *Journal of Ultrastructure Research* **59**:207-221

Olson GE and Sammons DW (1980) Structural chemistry of outer dense fibers of rat sperm. *Biology of Reproduction* **22**:319-332.

Pedersen H (1972) The post-acrosomal region of the spermatozoa of man and Macaca arctoides. *Journal of Ultrastructure Research* **40**:366-377

Pedersen H (1974) The human spermatozoon. *Danish Medical Bulletin* **21**:3-26

Perez-Ramirez B and Castells M (1991) In vitro biosynthesis of rat sperm outer dense fiber components. *Life Sciences* **49**:1549-1554

Petersen C, Aumuller G, Bahrami M and Hoyer-Fender S (2002) Molecular cloning of Odf3 encoding a novel coiled-coil protein of sperm tail outer dense fibres. *Molecular Reproduction and Development* **61**:102-112

Phillips DM (1969) Exceptions to the prevailing pattern of tubules (9 + 9 + 2) in the sperm flagella of certain insect species. *Journal of Cell Biology* **40**:28-43

Phillips DM (1970) Ultrastructure of spermatozoa of the woolly opossum, *Caluromys philander*. *Journal of Ultrastructure Research* **33**:381-397

Phillips DM (1972) Comparative analysis of mammalian sperm motility. *Journal of Cell Biology* **53**:561-573

Phillips DM and Olson G (1974) Mammalian sperm motility - structure in relation to function. In *The functional anatomy of spermatozoon.* Ed BA Afzelius, Permagon Press, Oxford, pp 117-126

Pihlaja DJ and Roth LE (1973) Bovine sperm fractionation. II. Morphology and chemical analysis of tail segments. *Journal of Ultrastructure Research* **44**:293-309

Ploen L (1971) A scheme of rabbit spermateleosis based upon electron microscopical observations. *Zeitschrift fur Zellforschung und mikroskopische Anatomie.* **115**:553-564

Price JM (1973) Biochemical and morphological studies of outer dense fibres of rat spermatozoa. *Journal of Cell Biology* **59**:272

Rattner JB (1972) Nuclear shaping in marsupial spermatids. *Journal of Ultrastructure Research* **40**:498-512

Retzius G (1906) Die spermine der marsupialier. *Biologica Unters* **13**:77-86

Ricci M (1997) A study of spermiogenesis and epididymal sperm maturation in the wombat (*Lasiorhinus latifrons*) with special reference to nuclear morphogenesis. Honours Thesis. The University of Adelaide, Australia

Rodger JC (1991) Fertilization in marsupials. In *A comparative overview of mammalian fertilization*. Eds BS Dunbar and MG O'Rand, Plenum Press, New York, pp 117-135

Rodger JC and Bedford JM (1982) Separation of sperm pairs and sperm-egg interactions in the opossum, *Didelphis virginiana*. *Journal of Reproduction and Fertility* **64**:171-179

Rodger JC and Suter DAI (1978) Respiration rates and sugar utilization by marsupial spermatozoa. *Gamete Research* **1**:111-116

Roosen-Runge EC and Giesel LO (1950) Quantitative studies on spermatogenesis in the albino rat. *American Journal of Anatomy* **87**:1-30

Rowe JD, Patskovsky YV, Mastokovska LN, Novikova E and Listowsky I (1998a) Rationale for reclassification of a distinctive subdivision of mammalian class Mu glutathione S-transferases that are primarily expressed in testis. *Journal of Biological Chemistry* **273**:9593-9601

Rowe JD, Tchaikovskaya T, Shintani N and Listowsky I (1998b) Selective expression of a glutathione S-transferase subclass during spermatogenesis. *Journal of Andrology* **19**:558-567

Russell LD, Ettlin RA, Sinha AP, and Clegg ED (1990) *Histological and histopathological evaluation of the testis*. Cache River Press, Clearwater

Sakai Y, Koyama YI, Fujimoto H, Nakamoto T and Yamashina S (1986) Immunocytochemical study on fibrous sheath formation in mouse spermiogenesis using a monoclonal antibody. *The Anatomical Record* **215**:119-126

Sapsford CS, Rae CA and Cleland KW (1967) Ultrastructural studies on spermatids and Sertoli cells during early spermiogenesis in the bandicoot *Perameles nasuta* Geoffroy (Marsupialia). *Australian Journal of Zoology* **15**:881-909

Sapsford CS, Rae CA and Cleland KW (1969) Ultrastructural studies on maturing spermatids and on Sertoli cells in the bandicoot *Perameles nasuta* Geoffroy (Marsupialia). *Australian Journal of Zoology* **17**:195-292

Sapsford CS, Rae CA and Cleland KW (1970) Ultrastructural studies on the development and form of the principal piece sheath of the bandicoot spermatozoon. *Australian Journal of Zoology* **18**:21-48

Satir P (1974) How cilia move. *Scientific American* **231**:44

Satir P (1979) Basis of flagellar motility in spermatozoa: current status. In *The spermatozoon.* Eds DW Fawcett and JM Bedford, Urban and Schwarzenberg, Baltimore, pp 85-90

Schäfer M, Börsch D, Hulster A and Schäfer U (1993) Expression of a gene duplication encoding conserved sperm tail proteins is translationally regulated in *Drosophila melanogaster. Molecular and Cellular Biology* **13**:1708-1718

Schalles U, Shao X, van der Hoorn FA and Oko R (1998) Developmental expression of the 84-kDa ODF sperm protein: localization to both the cortex and medulla of outer dense fibers and to the connecting piece. *Developmental Biology* **199**:250-260

Scheltinga DM, Jamieson BG, Espinoza RE and Orrell KS (2001) Descriptions of the mature spermatozoa of the lizards *Crotaphytus bicinctores*, *Gambelia wislizenii*

(Crotaphytidae), and *Anolis carolinensis* (Polychrotidae) (Reptilia, Squamata, Iguania). *Journal of Morphology* **247**:160-171

Schnall MD (1952) Electronmicroscopic study of human spermatozoa. *Fertility and Sterility* 3:62-82

Schultz-Larsen J (1958) The morphology of the human sperm; electron microscopic investigations of the ultrastructure. *Acta pathologica et microbiologica Scandinavica* **44**:1-121

Seefeldt-Schmidt B, Henkel R, Schill WB and Miska W (2003) Localization of a new polypeptide in mammalian outer dense fibres. *Andrologia* **35**:2-12

Serres C, Escalier D and David G (1983) Ultrastructural morphometry of human spermatozoa flagellum with a stereological analysis of the lengths of the outer dense fibres. *Biology of the Cell* **49**:153-162

Serres C, Feneux D and Jounnet I (1986) Abnormal distribution of the periaxonemal structures in a human sperm flagellar dyskinesia. *Cell Motility and the Cytoskeleton* **6**:68-76

Setchell BP and Carrick FN (1973) Spermatogenesis in some Australian marsupials. *Australian Journal of Zoology* **21**:491-499

Shao X, Tarnasky HA, Lee JP, Oko R and van der Hoorn FA (1999) Spag4, a novel sperm protein, binds outer dense fibre protein Odf1 and localises to microtubules of manchette and axoneme. *Developmental Biology* **211**:109-123

Shao X, Tarnasky HA, Schalles V, Oko R and van der Hoorn FA (1997) Interactional cloning of the 84 kDa major outer dense fiber protein Odf84 – leucine zippers mediate associations of Odf 84 and Odf 27. *Journal of Biological Chemistry* **272**:6105-6113

Shao X and van der Hoorn FA (1996) Self-interaction of the major 27-kilodalton outer dense fiber protein is in part mediated by a leucine zipper domain in the rat. *Biology of Reproduction* **55**:1343-1350

Shao X, Xue J and van der Hoorn FA (2001) Testicular protein Spag5 has similarity to mitotic spindle protein Deepest and binds outer dense fiber protein Odf1. *Molecular Reproduction and Development* **59**:410-416

Si Y and Okuno M (1993) The sliding of the fibrous sheath through the axoneme proximally together with microtubule extrusion. *Experimental Cell Research* **208**:170-174

Si Y and Okuno (1995) Extrusion of microtubule doublet outer dense fibres 56 associating with fibrous sheath sliding in mouse sperm flagella. *Journal of Experimental Zoology* **273**:355-362

Soley JT (1994) Centriole development and formation of the flagellum during spermiogenesis in the ostrich (*Struthio camelus*). *Journal of Anatomy* **185**:301-313

Taggart DA, Leigh CM and Breed WG (1995a) Ultrastructure and motility of spermatozoa in the male reproductive tract of perameloid marsupials. *Reproduction, Fertility and Development* **7**:1141-1156

Taggart DA, Leigh CM, Schultz D and Breed WG (1995b) Ultrastructure and motility of spermatozoa in macropodid and potoroidid marsupials. *Reproduction, Fertility and Development* **7**:1129-1140

Taggart DA, O'Brien HP and Moore HDM (1993) Ultrastructural characteristics of in vivo and in vitro fertilization in the grey short-tailed opossum, *Monodelphis domestica*. *The Anatomical Record* **237**:21-37

Taggart DA and Temple-Smith (1990) An unusual mode of progressive motility in spermatozoa from the dasyurid marsupial, *Antechinus stuartii. Reproduction, Fertility and Development* **2**:107-114

Takai Y, Sasaki T and Matozaki T (2001) Small GTP-binding proteins. *Physiological Review* **81**:153-208

Talian JC, Olmsted JB and Goldman R (1983) A rapid procedure for preparing fluorescin-labeled specific antibodies from whole antiserum: Its use in analysing cytoskeletal architecture. *Journal of Cell Biology* **97**:1277-1282

Tash JS (1989) Protein phosphorylation: the second messenger signal transducer of flagellar motility. *Cell Motility and the Cytoskeleton* **14**:332-339

Tash JS and Bracho GE (1994) Regulation of sperm motility: emerging evidence for a major role for protein phosphatases. *Journal of Andrology* **15**:505-509

Tash JS and Means AR (1983) Cyclic adenosine 3',5' monophosphate, calcium and protein phosphorylation in flagellar motility. *Biology of Reproduction* **28**:75-104

Telkka A, Fawcett DW and Christensen AK (1961) Further observations on the structure of the mammalian sperm tail. *The Anatomical Record* **141**:231-246

Temple-Smith PD (1981) Redistribution of intramembranous particles in the midpiece plasma membrane of the brush-tailed possum spermatozoon during epididymal transit. *Journal of Anatomy* **132**:310

Temple-Smith PD (1984) Phagocytosis of sperm cytoplasmic droplets by a specialized region in the epididymis of the brush-tailed possum, *Trichosurus vulpecula. Biology of Reproduction* **30**:707-729

Temple-Smith PD (1987) Sperm structure and marsupial phylogeny. In *Possums and opossums: studies in evolution*. Ed M Archer, The Royal Zoological Society of New South Wales and Surrey Beatty and Sons, Sydney, pp 171-193

Temple-Smith PD (1994) Comparative structure and function of marsupial spermatozoa. *Reproduction, Fertility and Development* **6**:421-435

Temple-Smith PD and Bedford JM (1976) The features of sperm maturation in the epididymis of a marsupial the brush-tailed possum *Trichosurus vulpecula*. *American Journal of Anatomy* **147**:471-500

Temple-Smith PD and Bedford JM (1980) Sperm maturation and the formation of sperm pairs in the epididymis of the opossum, *Didelphis virginiana*. *Journal of Experimental Zoology* **214**:161-171

Thurston RJ and Hess RA (1997) Ultrastructure of spermatozoa from domesticated birds: comparative study of turkey, chicken and guinea fowl. *Scanning Microscopy* **1**:1829-1838

Trapp BD, Dubois-Daleq M and Quaries RH (1984) Ultrastructural localization of P2 protein in actively myelinating rat Schwann cells. *Journal of Neurochemistry* **43**:944-948

Trapp BD, Itoyama Y, MacIntosh TD and Quaries RH (1983) P2 protein in oligodendrocytes and myelin of the rabbit central nervous system. *Journal of Neurochemistry* **40**:47-54

Travis AJ, Foster JA, Rosenbaum NA, Visconti PE, Gerton GL and Moss SB (1998) Targeting of a germ cell-specific type 1 hexokinase lacking a porin-binding domain to the mitochondria as well as to the head and fibrous sheath of murine spermatozoa. *Molecular Biology of the Cell* **9**:263-276

Turner RMO, Johnson LR, Haig-Ladewig L, Gerton GL and Moss SB (1998) An X-linked gene encodes a major human sperm fibrous sheath protein, hAKAP82. *Journal of Biological Chemistry* **27**:32135-32141

Ulvik NM, Dahl E and Hars R (1982) Classification of plastic-embedded rat seminiferous epithelium prior to electron microscopy. *International Journal of Andrology* **5**:27-36

van de Voort CA and Overstreet JW (1995) Effects of glucose and other energy substrates on the hyperactivated motility of Macaque sperm and the zona pellucida-induced acrosome reaction. *Journal of Andrology* **16**:327-333

van der Hoorn FS, Tarnasky HA and Nordeen SK (1990) A new rat gene RT7 is specifically expressed during spermatogenesis. *Developmental Biology* **142**:147-154

van der Horst G, van der Merwe L and Visser J (1989) Fertilization pattern and sperm tail structure. *Electron Microscopy Society of Southern Africa Proceedings* **19**:151-152

van Vorstenbosch CJ, Colenbrander B, Wensing CJ, Ramaekers FC and Vooijs GP (1984) Cytoplasmic filaments in fetal and neonatal pig testis. *European Journal of Cell Biology* **34**:292-299

Vera JC, Brito M and Burzio LO (1987) Biosynthesis of rat sperm outer dense fibres during spermiogenesis: In vivo incorporation of [^{3}H]leucine into the fibrillar complex. *Biology of Reproduction* **36**:193-202

Vera JC, Brito M, Zuvic T and Burzio LO (1984) Polypeptide composition of rat sperm outer dense fibers – a simple procedure to isolate the fibrillar complex. *Journal of Biological Chemistry* **259**:5970-5977

Vijayaraghaven S, Goueli SA, Davey MP and Carr DW (1997a) Protein kinase A-anchoring inhibitor peptides arrest mammalian sperm motility. *Journal of Biological Chemistry* **272**:4747-4752

Vijayaraghaven S, Liberty G, Mohan J, Winfrey V, Olson G and Carr D (1999) isolation and molecular characterization of AKAP1110, a novel, sperm-specific protein kinase A-anchoring protein. *Molecular Endocrinology* **13**:705-717

Vijayaraghaven S, Olson GE, Nagdas S, Winfrey VP and Carr DW (1997b) Subcellular localization of the regulatory subunits of cyclic adenosine 3'5'-monophosphate-dependent protein kinase in bovine spermatozoa. *Biology of Reproduction* **57**:1517-1523

Virtanen I, Badley RA, Paasivuo R and Lento VP (1984) Distinct cytoskeletal domains revealed in sperm cells. *Journal of Cell Biology* **99**:1083-1091

Visconti PE, Johnson LR, Oyaski M, Fornes M, Moss SB, Gerton GL and Kopf GS (1997) Regulation, localization, and anchoring of protein kinase A subunits during mouse sperm capacitation. *Developmental Biology* **192**:351-363

Visconti PE, Moore GD, Bailey JL, Leclerc P, Connors SA, Pan D, Olds-Clarke P, and Kopf GS (1995) Capacitation of mouse spermatozoa. II. Protein tyrosine phosphorylation and capacitation are regulated by a cAMP-dependent pathway. *Development* **121**:1139-1150

Welch JE, Brown PR, O'Brien DA and Eddy EM (1995) Genomic organization of a mouse glyceraldehyde 3-phosphate dehydrogenase gene (Gapd-s) expressed in post-meiotic spermatogenic cells. *Developmental Genetics* **16**:179-189

Welch JE, Brown PR, O'Brien DA, Magyar PL, Bunch DO and Eddy EM (2000) Human glyceraldehyde 3-phosphate dehydrogenase-2 gene is expressed specifically in spermatogenic cells. *Journal of Andrology* **21**:328-338

Welch JE and O'Rand MG (1985) Identification and distribution of actin in spermatogenic cells and spermatozoa of the rabbit. *Developmental Biology* **109**:411-417

Welch JE, Schatte EC, O'Brien DA and Eddy EM (1992) Expression of a glyceraldehyde 3-phosphate dehydrogenase gene specific to mouse spermatogenic cells. *Biology of Reproduction* **46**:869-878

Westoff D and Kamp G (1997) Glyceraldehyde 3-phosphate dehydrogenase is bound to the fibrous sheath of mammalian sperm. *Journal of Cell Science* **110**:1821-1829

Woolley DM (1971) Striations in the peripheral fibers of rat and mouse spermatozoa. *Journal of Cell Biology* **49**:936-939

Woodburne MO, Rich TH and Springer MS (2003) The evolution of tribospheny and the antiquity of mammalian clades. *Molecular Phylogenetics and Evolution* **28**:360-385

Yanagimachi R (1994) Mammalian fertilization. In *The physiology of reproduction*. Eds E Knobil and J Neill, Raven Press, New York, pp 189-317

Yano Y and Miki-Noumura T (1981) Sliding velocity between outer doublet microtubules of sea-urchin sperm axonemes. *Journal of Cell Science* **44**:169-186

Yasuzumi G (1956) Spermatogenesis in animals as revealed by electron microscopy. I. Formation and submicroscopic structure of the middlepiece of the albino rat. *Journal of Biophysical and Biochemical Cytology* **2**:445-450

Yasuzumi G, Shiraiwa S and Yamamoto H (1972) Spermatogenesis in animals as revealed by electron microscopy. XXVII. Development of the neck region and flagellum of the cat spermatozoon. *Zeitschrift fur Zellforschung und mikroskopische Anatomie* **125**:497-505

Zarsky HA, Cheng M and van der Hoorn FA (2003) Novel RING finger protein OIP1 binds conserved amino acid repeats in sperm tail protein ODF1. *Biology of Reproduction* **68**:543-552

Ricci, M. and Breed, W.G. (2001). Isolation and partial characterization of the outer dense fibres and fibrous sheath from the sperm tail of a marsupial: the brushtail possum (Trichosurus vulpecula). *Reproduction*, 121(3), 373-388.

Formerly the *Journal of Reproduction and Fertility* and *Reviews of Reproduction* Abstract Series No 27 July 2001

Reproduction

The official journal of the Society for the Study of Fertility

Society for the Study of Fertility

Annual Conference

University of Cambridge

July 2001

Abstracts of Papers

www.journals-of-reproduction.org.uk
ISSN 0954-0725

Ricci, M. and Breed, W.G. (2001). Immunocytochemical investigation of fibrous sheath morphogenesis in a marsupial: the brush-tail possum. In *Abstract of papers: Society for the Study of Fertility, Annual Conference,* 4th-6th July, Sheffield: England, 1990.

ABSTRACT SERIES NUMBER 25 JULY 2000

Journal of REPRODUCTION and fertility

Society for the Study of Fertility
British Fertility Society
British Andrology Society
JOINT MEETING

ISSN: 0954–0725

Ricci, M. and Breed, W.G. (2000). Isolation and partial characterization of the outer dense fibres and fibrous sheath from the sperm tail of a marsupial. In *Fertility 2000: Society for the Study of Fertility, British Andrology Society, British Fertility Society: Joint Summer Meeting, University of Edinburgh,* July 2000, Edinburgh, Scotland.

AUSTRALIAN SOCIETY FOR REPRODUCTIVE BIOLOGY

PROGRAM AND MINIPOSTERS

THIRTIETH
Annual Conference

26th - 29th September 1999

Hilton-on-the-Park, Melbourne

ISSN 0812-7662

Ricci, M. and Breed, W.G. (1999). Isolation of the outer dense fibres and fibrous sheath from brush-tailed possum spermatozoa. In *Proceedings of the thirtieth Annual Conference: Australian Society for Reproductive Biology,* 26-29 September 1999, Melbourne, Victoria.